Analysis and Improvement of an Existing University District Energy System

Analyse und Verbesserung eines bestehenden Energiesystems an einem Universitätscampus
Zur Erlangung des akademischen Grades Doktor-Ingenieur (Dr.-Ing.)
Genehmigte Dissertation von Johannes Julius Oltmanns aus Stuttgart
Tag der Einreichung: 10. August 2020, Tag der Prüfung: 15. Dezember 2020

1. Gutachten: Prof. Dr.-Ing. Peter Stephan
2. Gutachten: Prof. Dr. Sven Werner
Darmstadt – D 17

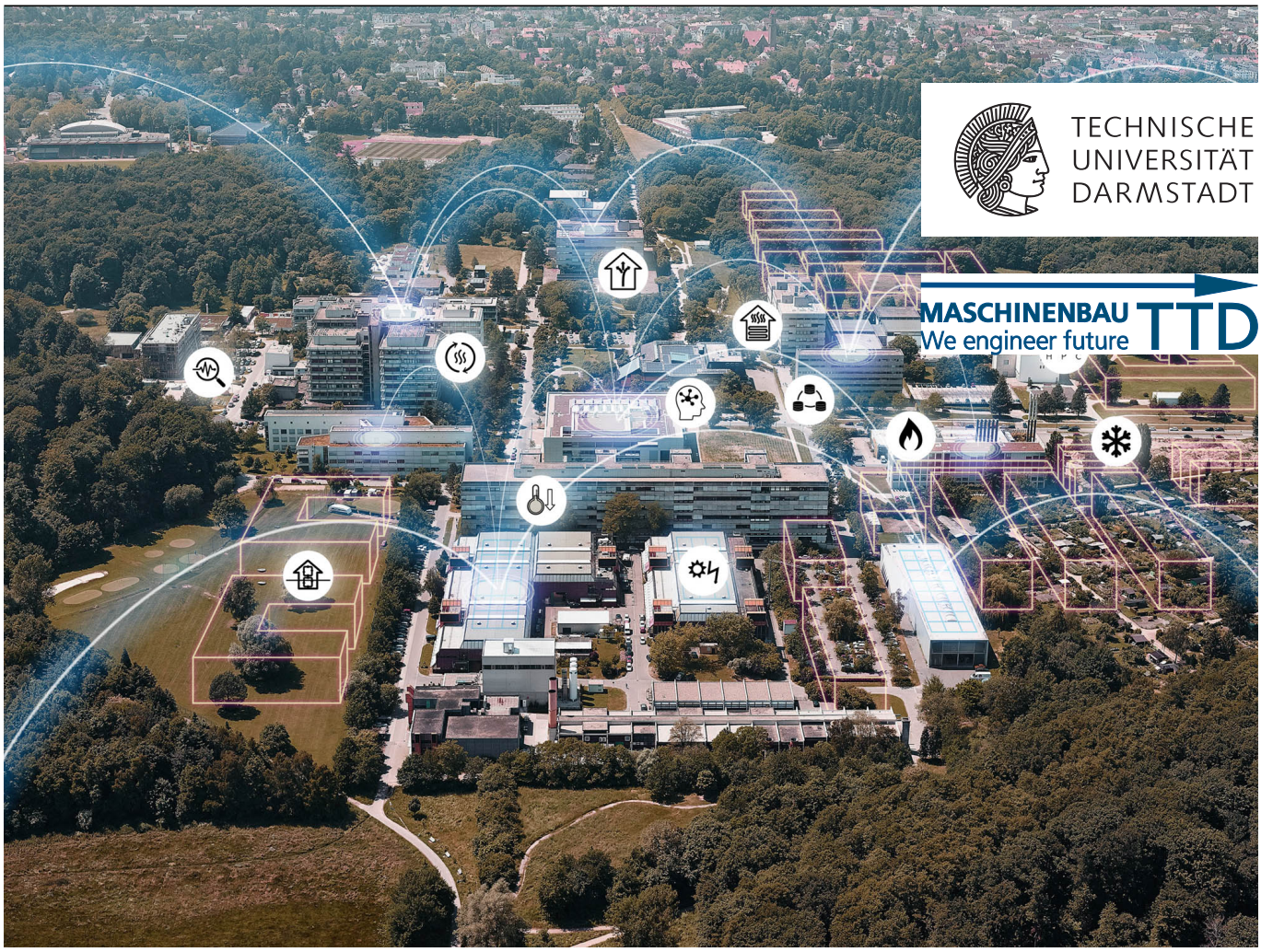

Analysis and Improvement of an Existing University District Energy System
Analyse und Verbesserung eines bestehenden Energiesystems an einem Universitätscampus

Accepted doctoral thesis by Johannes Julius Oltmanns

1. Review: Prof. Dr.-Ing. Peter Stephan
2. Review: Prof. Dr. Sven Werner

Date of submission: 10. August 2020
Date of thesis defense: 15. Dezember 2020

Darmstadt – D 17

Bitte zitieren Sie dieses Dokument als:
URN: urn:nbn:de:tuda-tuprints-173672
URL: http://tuprints.ulb.tu-darmstadt.de/id/eprint/17367

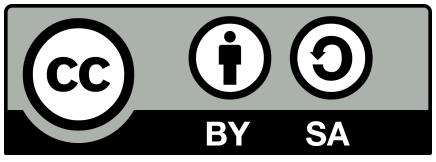

Erklärungen laut Promotionsordnung

§8 Abs. 1 lit. c PromO

Ich versichere hiermit, dass die elektronische Version meiner Dissertation mit der schriftlichen Version übereinstimmt.

§8 Abs. 1 lit. d PromO

Ich versichere hiermit, dass zu einem vorherigen Zeitpunkt noch keine Promotion versucht wurde. In diesem Fall sind nähere Angaben über Zeitpunkt, Hochschule, Dissertationsthema und Ergebnis dieses Versuchs mitzuteilen.

§9 Abs. 1 PromO

Ich versichere hiermit, dass die vorliegende Dissertation selbstständig und nur unter Verwendung der angegebenen Quellen verfasst wurde.

§9 Abs. 2 PromO

Die Arbeit hat bisher noch nicht zu Prüfungszwecken gedient.

Darmstadt, 10. August 2020

J. Oltmanns

Danksagung

Diese Dissertation entstand im Rahmen meiner Tätigkeit als wissenschaftlicher Mitarbeiter am Institut für Technische Thermodynamik der TU Darmstadt, während der ich das Projekt ”EnEff:Stadt Campus Lichtwiese” bearbeiten durfte. Mein Dank gilt zuallererst meinem Gruppenleiter Frank Dammel, der mich in diesem Prozess sehr unterstützt hat, jederzeit für Fragen zur Verfügung stand und viele wichtige Impulse für die erfolgreiche Umsetzung der Arbeit gegeben hat. Großer Dank gilt Prof. Peter Stephan, der es mir mit der Betreuung dieser Arbeit ermöglicht hat, mich beruflich mit meinen Herzensthemen Energieeffizienz und Klimaschutz zu beschäftigen.

Bedanken möchte ich mich bei allen aktuellen und ehemaligen Kollegen am Institut. Der kollegiale Zusammenhalt am TTD war ein wichtiger Faktor dafür, dass ich immer gerne zur Arbeit gegangen bin, und stets offene Türen für Fragen haben es mir ermöglicht, mich fachlich weiterzuentwickeln. Besonderer Dank gilt meinen Bürokollegen, insbesondere Paul Michael Falk und Kai Schweikert, mit denen ich stets über fachliche und nicht-fachliche Fragen diskutieren konnte.

Großer Dank gilt meinem Projektteam, besonders David Sauerwein und Christopher Ripp, für die enge und erfolgreiche Zusammenarbeit im Rahmen von ”EnEff:Stadt Campus Lichtwiese”. Als wir das Projekt begannen hatte ich gehofft, damit einen konkreten Beitrag zur Absenkung der Treibhausgasemissionen der TU Darmstadt liefern zu können. Ich bin sehr dankbar, dass uns dies mit der Realisierung der Abwärmenutzung des Hochleistungsrechners, der Temperaturabsenkung im Gebäude der Architektur und der umfassenden Erweiterung des Energiemonitorings am Campus Lichtwiese gelungen ist. Dies war nur durch die enge Zusammenarbeit mit dem Baudezernat der TU Darmstadt möglich, besonders mit den Energiemanagern Ulrich Mehlstäubl und Karsten Kutschera sowie den Referats- und Dezernatsleitern Michael Förster und Edgar Dingeldein. Ihnen kommt nun auch die Aufgabe zu, die im Rahmen des Projekts und dieser Arbeit entwickelten Vorschläge aufzunehmen und umzusetzen.

Danken möchte ich außerdem meinen Kollegen des IEA Annex TS2 für den sehr wertvollen Austausch. Sie haben mich für das Thema 4. Generation der Fernwärme begeistert und damit einen wesentlichen Grundstein für meine Arbeit gelegt. Besonderer Dank gilt in diesem Zusammenhang Prof. Sven Werner, der nicht nur aufgrund seiner umfangreichen Erfahrung ein sehr wertvoller Ansprechpartner war, sondern sich auch bereit erklärt hat, das Koreferat für meine Dissertation zu übernehmen.

Einen wichtigen Beitrag zum Erfolg meiner Arbeit wurde durch die vielen Studenten gelegt, die ich im Rahmen von Abschlussarbeiten betreuen durfte. Stellvertretend nennen möchte ich hier Peter Warsow, der mir auch weiterhin als kompetenter Ansprechpartner zur Verfügung steht.

Nicht vergessen möchte ich meine Familie sowie meine Freundin Mariana, die mich immer darin bestärkt hat, mir anspruchsvolle Ziele zu setzen und mich gleichzeitig daran erinnert hat, wie wichtig es ist, zwischendurch auch Ruhepausen einzulegen, um langfristig produktiv sein zu können.

Zusammenfassung

Der Klimawandel gehört zu den größten Krisen der Menschheit im 21. Jahrhundert. Es handelt sich dabei um eine komplexe Herausforderung, die Auswirkungen auf alle Ebenen der Gesellschaft hat, von der persönlichen bis zur internationalen Ebene. Nur wenn alle Teile der Weltgemeinschaft an einem Strang ziehen, wird es möglich sein, die im Pariser Klimaschutzabkommen von 2015 vereinbarte Begrenzung der Klimaerwärmung auf 1.5 °C gegenüber vorindustrieller Zeit zu erreichen. Einen wichtigen Beitrag dazu müssen die lokalen Ebenen der Stadt bzw. des Quartiers liefern, die aufgrund der weltweit fortschreitenden Urbanisierung immer wichtiger werden. Innerhalb des Quartiers hat der Energiebedarf der Gebäude großen Einfluss auf die CO_2-Emissionen.

Eine zentralisierte Versorgung mit thermischer Energie via Fernwärme und Fernkälte ermöglicht eine hocheffiziente Energiebereitstellung über Kraft-Wärme- bzw. Kraft-Wärme-Kälte-Kopplung sowie die Einbindung lokal vorhandener Abwärmequellen aus Industriebetrieben oder Rechenzentren. Mittels kosteneffizienten thermischen Speichern können Erzeugung und Bedarf voneinander entkoppelt und Laufzeiten von Kraft-Wärme-Kopplungsanlagen verlängert werden. Außerdem können fluktierend zur Verfügung stehende regenerative Quellen wie solarthermische Energie effizienter genutzt werden.

Grundlage dieser Arbeit bildet ein dynamisches Simulationsmodell des Energiesystems des Campus Lichtwiese der Technischen Universität Darmstadt, das die Erzeugungsanlagen, die thermischen Netze sowie die Gebäude als Verbraucher darstellt und miteinander verbindet. Aufbauend auf Zeitreihen des aktuellen bzw. des zukünftigen Energiebedarfs an Wärme, Kälte und elektrischer Energie können damit sowohl die Netzverluste und die Energieerzeugung des Gesamtsystems, als auch die resultierenden CO_2-Emissionen und Kosten berechnet werden. Durch einen Vergleich verschiedener Szenarien im Rahmen von Jahressimulationen wird anhand des Campus Lichtwiese aufgezeigt, wie bestehende Energiesysteme auf Quartiersebene auf eine lokale Energiewende vorbereitet werden können. Forschungsschwerpunkte bilden die Optimierung der Auslegung und des Betriebs bestehender Energiesysteme mit Fernwärmenetzen der 3. Generation, die Absenkung der Temperaturen zur Überführung der Netze in die 4. Generation der Fernwärme, sowie die Integration von Rechenzentrumsabwärme. Alle vorgeschlagenen Maßnahmen werden energetisch, ökologisch und wirtschaftlich mit dem Ist-Zustand des Systems verglichen.

Die Ergebnisse zeigen, dass das Energiesystem der TU Darmstadt für den aktuellen Bedarf gut ausgelegt ist und betrieben wird, dass aber gleichzeitig großes Potential zur Verringerung der Temperaturen und Energiebedarfe durch Maßnahmen innerhalb der Gebäude besteht. Außerdem kann gezeigt werden, dass eine Einbindung von Rechenzentrumsabwärme in eine Fernwärmeversorgung ökologisch sinnvoll ist, sogar ohne dass vorher die Netztemperaturen abgesenkt werden. Durch eine Umsetzung der entwickelten Maßnahmen können die CO_2-Emissionen des Quartiers reduziert werden.

Wichtiger ist allerdings, dass die Maßnahmen die Voraussetzung schaffen, um die Energieversorgung am Campus, insbesondere in Bezug auf Wärme und Kälte, mittelfristig auf erneuerbare Quellen umzustellen. Die am Beispiel des Campus Lichtwiese entwickelten Maßnahmen lassen sich auch auf andere Quartiere übertragen. Entscheidend dafür ist ein umfangreiches Energiemonitoring, das dem Betreiber ein gutes Verständnis seines

Systems ermöglicht und es erlaubt, Fehler mit geringem Aufwand zu identifizieren und die entsprechenden Maßnahmen einzuleiten.

Summary

Climate change is one of the greatest crises facing humanity in the 21st century. It is a complex challenge that affects all levels of society, from the personal to the international level. Only if all parts of the international community work together, it will be possible to limit global warming to 1.5 °C above pre-industrial levels, as agreed in the Paris Agreement on Climate Change in 2015. An important contribution to this must be made in cities and districts, which are becoming increasingly more important due to the worldwide progress of urbanization. Within the district, energy demand of buildings has a great influence on the CO_2 emissions.

A centralized supply of thermal energy via district heating and cooling enables highly efficient generation via combined heat and power or combined heat, power and cooling as well as the integration of locally available waste heat sources from industrial plants or data centers. By means of cost-efficient thermal storage, generation and demand can be decoupled from each other, and operating times of combined heat and power plants can be extended. In addition, renewable sources such as solar thermal energy can be used more efficiently.

The basis of this work is a dynamic simulation model of the energy system of campus Lichtwiese of the Technical University of Darmstadt, which represents and connects the generation plants, the thermal networks and the buildings as consumers. Using time series of the current and future energy demand of the buildings for heat, cooling, and electric energy, the energy production of the entire system and the resulting CO_2 emissions and costs can be calculated. By comparing different scenarios via annual simulations within the model, the example of campus Lichtwiese shows how existing energy systems can be prepared for a local energy transition at the district level. Research focuses on the optimization of the design and operation of existing energy systems with 3rd generation district heating networks, the reduction of temperatures to transfer the networks to 4th generation district heating, and the integration of data center waste heat. All proposed measures are be compared energetically, ecologically and economically with the current state of the system.

The results show that the energy system of the TU Darmstadt is well designed and operated for the current demand, while at the same time there is great potential for reducing temperatures and energy demands by measures within the buildings. Furthermore, it can be shown that the integration of data center waste heat into district heating is already ecologically reasonable today, even without a prior reduction of network temperatures. By implementing the developed measures, the CO_2 emissions of the district can be reduced.

More important, however, is that the measures presented are a prerequisite to decarbonize the TU Darmstadt campus Lichtwiese energy system in the medium term, especially regarding heating and cooling. The measures developed for campus Lichtwiese can be transferred to other districts. The decisive factor here is comprehensive energy monitoring, which enables the operator to gain a good understanding of his system, to identify faults with little effort and to take corresponding measures to improve their system.

Contents

Nomenclature

Latin Letters

Letter	Description	Unit
A	Annuity	€/a
A_{ref}	energy reference area buildings	m^2
C	costs	€
c_{cap}	specific capacity costs	€/MW
c_{CO2}	specific CO_2 emissions price	€/t_{CO2}
$c_{\text{CO2,gas}}$	specific CO_2 emissions costs gas	€/MWh
$c_{\text{CO2,gas}}$	specific CO_2 emissions costs electric energy	€/MWh
c_{E}	specific demand-related (energy) costs	€/MWh
c_{gen}	specific investment costs generation units	€/MW
c_p	specific heat capacity exhaust gas	kJ/kgK
c_{TES}	specific investment costs thermal energy storage	€/MWh
c_{W}	specific heat capacity water	kJ/kgK
CFL	Courant number	–
ΔCO_2	CO_2 emissions savings	t_{CO2}/a
d	outer pipe diameter	m
D	outer insulation diameter	m
E	energy	MWh
E_{TES}	maximum energy content thermal energy storage	MWh
$\dot{E}$	power	MW
$\dot{E}_{\text{max}}$	Annual maximum 15 minutes average power supply	MW
Ex	exergy	MWh
f_{a}	annuity factor	1/a
f_{b}	price-dynamic cash value factor	a
$f_{\text{CHP,el}}$	allocation factor of CO_2 emissions and costs to CHP electric energy generation	–
$f_{\text{CHP,th}}$	allocation factor of CO_2 emissions and costs to CHP heat	–
f_{CO2}	CO_2 emissions factor	t_{CO2}/a
f_{dn}	regression dummy variable to distinguish between day and night operation	–

$f_{\text{el,TUD}}$	factor between electric energy demand Lichtwiese and TU Darmstadt	–
f_j	share of heat demand substation j in district heat demand	–
$f_{\dot{M}_{\text{vent}},j}$	factor between minimum and maximum mass flow	–
f_{op}	cost factors of operation-related costs for maintenance, servicing and inspection	–
$f_{\dot{Q}_{\text{vent}},j}$	factor between minimum and maximum heat flow	–
f_{short}	proportion of shortcut flow in total measured mass flow Lichtwiese west	%
$\overline{f}_{\text{TES}}$	average charging level thermal storage	–
f_{w}	regression dummy variable to distinguish between weekday and weekend operation	–
f_{winter}	regression dummy variable to distinguish between summer and winter operation	–
h	distance between pipe centers and ground surface	m
H_{i}	inferior heating value natural gas	kJ/m^3
Δh	specific enthalpy difference	kJ/kg
L	route length of the pair of pipes (half the pipe length)	m
n	counting variable	
$\dot{M}$	mass flow	kg/s
p	pressure	bar
P_{gen}	capacity generation facilities	MW
P_{TES}	capacity storage tanks	MWh
q	interest rate factor	–
q_j	specific heat demand of building j	–
Q	heat	MWh
$\dot{Q}$	heat flow	MW
r	price change factor	–
r_{TES}	radius thermal energy storage	m
R	thermal resistance	m^{2}K/W
R^2	coefficient of determination	–
R^2_{adj}	adjusted coefficient of determination	–
s	distance between pipe centers	m
S	scenario	–
t	observation period	a
T	temperature	°C
u	flow velocity in district heating pipes	m/s
V	volume	m^3
$\dot{V}$	volume flow	m^3/h
w	wind speed	m/s
Δx	length of volume section in district heating pipes	m

Greek Letters

Letter	Description	Unit
β_0	intercept	kW
β_1	regression coefficient T_{amb}^3	$\text{kW}/(\text{°C})^3$
β_2	regression coefficient T_{amb}^2	$\text{kW}/(\text{°C})^2$
β_3	regression coefficient T_{amb}	kW/°C
β_4	regression coefficient w^2	$\text{kW}/(\text{m/s})^2$
β_5	regression coefficient w	$\text{kW}/(\text{m/s})$
β_6	regression coefficient ψ	kW
β_7	regression coefficient $T_{\text{amb,24}}$	kW/K
β_8	regression coefficient $T_{\text{amb,48}}$	kW/K
β_9	regression coefficient $T_{\text{amb,72}}$	kW/K
β_{10}	regression coefficient f_{dn}	–
β_{11}	regression coefficient $T_{\text{amb,24}}$	kW
$\gamma_{\text{ex,gas}}$	exergy coefficient gas	–
Δ	difference	–
ϵ	regression residual	kW
η	efficiency	%
$\eta_{\text{el,100\%}}$	electric efficiency at full load	%
$\eta_{\text{th,100\%}}$	thermal efficiency at full load	%
λ	heat conductivity	W/mK
ξ_0	intercept	kW
ξ_1	regression coefficient $T_{\text{R,vent}}$	kW/°C
ρ_{W}	water density	kg/m^3
σ	standard deviation	–
τ	time-averaged	–
$\Delta\tau$	fixed time step size simulation model	s
ψ	humidity	%

Subscripts

Symbol	Description
0	initial state
1	current state
amb	ambient
bottom	storage bottom
build	buildings

cap	capacity
chg	storage charge
co	coinciding temperatures
contr	contractor
cool	cooling
dem	demand
dis	storage discharge
el	electric
exh	exhaust gas
g	ground
grid	electric grid
i	counting variable time steps
I	primary side
II	secondary side
in	incoming
ins	insulation
inv	investment costs
j	counting variable subsystems
k	counting variable volume sections of thermal storage tanks
lin	linear design optimization
Liwi	campus Lichtwiese
loss	losses
m	number of substations with reduced temperatures
$\dot{M}$	mass-averaged
meas	measured
op	operation
out	outgoing
rmf	reduced mass flow
R	return
red	return temperature reduction
reg	regression
rel	relative deviation
RH	room heating
S	supply
sat	saturation
SH	space heating
short	shortcut flow
sim	simulated
stor	stored energy thermal storage

sub	substation
target	target return temperature
th	thermal
thesis	sum of measures proposed in this thesis
top	storage cover
ts	time steps
use	useful energy thermal storage
vent	ventilation
wall	storage wall
west	Lichtwiese west heating circuit

Abbreviations

Acronym	**Description**
3GDH	3rd generation district heating
4GDH	4th generation district heating
AGFW	Energy Efficiency Association for heating, cooling and CHP
AC	absorption cooling
BHS	buffer heat storage
BS	buffer storage
CHP	combined heat and power
CC	compression cooling
CS	cooling storage
CSI	center of smart interfaces
DC	district cooling
DH	district heating
DHN	district heating network
DWD	Deutscher Wetterdienst (German weather service)
EER	energy efficiency ratio
HC	hybrid cooler
HOB	heat-only boiler
HP	heat pump
HPC	high performance computer
HPS	heat and power station
HR	heat recovery
HW	hot water
HWC	hot water cooling
HX	heat exchanger
IPCC	Intergovernmental Panel on Climate Change

LHV	lower heating value
LMTD	logarithmic mean temperature difference
LP	linear programming
MILP	mixed integer linear programming
PV	photovoltaic cells
RTD	resistance temperature detector
SHS	seasonal heat storage
TES	thermal energy storage
TRY	test reference year
TU	Technical University
TUD	Technical University of Darmstadt
VAT	value-added tax
WHU	waste heat utilization

List of Figures

List of Tables

1 Introduction

As I am writing this introduction to my PhD thesis, the world encounters itself in the middle of a global crisis: The COVID-19 pandemic deeply affects the lifestyle our society has known for the past decades and challenges truths long thought unchangeable such as the European integration process and the freedom of movement within the European Union. In the midst of this imminent crisis, people are fast to forget about another global crisis: Climate change is no longer a future threat, but a present reality, affecting humanity as a whole. Climate change, along with secondary effects, such as climate-induced migration, cannot be solved by developing a vaccine that might be available in a couple of months or years, and will consequently be the major challenge for humanity for the remainder of the 21st century. Avoiding and mitigating climate change is a complex task that has to be tackled from a personal to the global level. Small gradual steps will no longer be sufficient, but it is rather necessary to question our lifestyle and to redesign the way our economy works, equally to what we currently see in times of COVID-19.

In the future, an ever growing percentage of the world's population is expected to live in cities, making the local level a priority for tackling climate change. Residential and commercial buildings account for 26 % of the energy demand and 36 % of the CO_2 emissions in the European Union [1]. In district energy system, heating, cooling and electric energy demand are among the main sources of greenhouse gas emissions. District heating and cooling are mature technologies to supply a substation with heat or cooling energy from sources located outside the perimeter of the building. The first district heating system was built in 1877 in Lockport, NY, and several others followed soon after all across the north-eastern United States [2]. The first European district heating systems were erected in Germany in the 1920s [3]. Nowadays, about 80 000 district heating systems are operating globally, with roughly 6000 located in Europe [4]. District heating is most common in northern and central Europe as well as in former communist countries such as eastern Europe, Russia and China. District cooling is a comparatively new technology with the first networks being built in the 1960s in the United States, Germany and France [3]. Although, nowadays, district cooling energy demands are much smaller than district heating demands, they are likely to grow significantly in the future as a reaction to increased cooling demands due to rising standards of living and increased ambient temperatures in times of climate change [5]. The construction of a district energy system comes with high investment costs and the life time of its components is long, reaching from 10-20 years for combined heat and power plants to more than 50 years for the network pipes and over 100 years for the buildings connected. While guidelines and measures to be taken in newly developed districts are essential, it is also important to find ways to decarbonize existing district heating and cooling systems. In the following, measures to prepare a decarbonization of the TU Darmstadt campus Lichtwiese energy system are presented. The university has committed itself to achieving the national climate protection goals locally, by reducing its area-specific CO_2 emissions by 80 % until 2050 compared to the 1990 level [6]. This thesis proposes an approach to the first steps on this way. The measures presented here can be applied to any existing district energy system, as long as energy monitoring is available.

Outline of the work

The remainder of this thesis is organized as follows: First, the state of the art is presented and the aim of the thesis is deduced (chapter 2). Subsequently, the TU Darmstadt campus Lichtwiese energy system is introduced (chapter 3), and an overview of its monitoring infrastructure is given (chapter 4). The target variables and evaluation methods are explained in chapter 5, and an introduction to the energy system model is given in chapter 6. Chapters 7-9 describe the proposed measures to prepare TU Darmstadt campus Lichtwiese for decarbonization. Even though these measures result in some reductions of CO_2 emissions, they will not be sufficient to reach TU Darmstadt's own climate protection goals. Thus, chapter 10 quantifies necessary future CO_2 emissions reductions. The thesis is closed with a conclusion and outlook (chapter 11).

2 State of the art and aim of this thesis

This chapter first gives an overview of research activities on district energy systems and derives additional research needs that will be addressed in this thesis.

2.1 State of the art

Thermal district energy systems consist of three major sections [1]: The first section is composed of the supply units and storage, which may also include electric energy supply in the case of cogeneration. The second section represents the district heating or district cooling network itself, which consists of pipes and pumps circulating water in the pipes. The third section are the users, which can be residential or commercial buildings as well as industrial facilities. Heat or cooling energy is transmitted from the network to the user at a substation and distributed inside the building, to serve for space heating, domestic hot water preparation, ventilation pre-heating, air-conditioning or for process heat or cooling applications. Improving the energy efficiency and decarbonization of district energy systems has been an important issue in recent research. Measures to realize this task include improving the design and operation of the supply facilities and thermal storage in current fully or partly fossil based district energy systems, and the reduction of temperatures in district heating systems, which is a prerequisite for an increase in the use of renewable heat sources. Using waste heat from low-temperature heat sources such as data centers primarily eliminates mechanical cooling demand to dissipate the heat into the environment, and also makes it possible to replace fossil heat generation.

Numerous studies have been published on the **optimization** of the design and operation of district heating systems including multiple heat sources as well as storage. They differ in terms of their objectives. Olsthoorn et al. [7] present a review on studies regarding the optimization of the operation of district heating systems as well as the integration of heat storage technologies and renewable sources. They identify exergy efficiency, cost, exergo-economic, greenhouse gas and multi-objective approaches as typical objective criteria.

Combined heat and power (**CHP**) plants are a very effective way to reuse the waste heat of a turbine or a motor generating electric energy for heating purposes. Therefore, they represent a core technology in many district heating systems. At the same time, operating a CHP plant is a complex task, because heat and electric energy are necessarily generated simultaneously. In CHP based district energy systems, an important issue is to make the CHP operation more dependent on the electric energy instead of the heat demand, because electric energy is usually more cost intensive. To avoid a dissipation of unused heat to the environment, alternative heat sinks have to be found to continue operating CHP plants during summer months. To increase the CHP operating hours, absorption chillers can be integrated in district energy systems with cooling demands, because cooling loads are usually highest during the summer [8].

A very common approach to optimize the operation of a district energy system is to disconnect supply and demand via **thermal storage**. They represent a cheap and effective solution to increase operating hours of CHP plants and to make it possible to cope with an increased share of fluctuating renewable sources. Thus,

thermal storage is part of virtually any study on operation optimization of thermal district energy systems (e.g. [9–13]). Thermal storage comes in different sizes and designs with different purposes, such as stratified tank storage, mostly used for daily or weekly charging cycles, or pit storage for seasonal energy storage. Thermal storage in district energy systems usually store hot water for district heating and cold water for district cooling purposes. An overview of different storage technologies is given in [14–16]. Guelpa and Verda [17] perform a review of different storage technologies and their performance in district heating and cooling systems. In addition to using external storage solutions, the heat capacity of buildings [18–20] and the network itself [21, 22] can be used as thermal storage. The results reveal that the storage capacity of such solutions is much smaller than for external storage [23]. Vandermeulen et al. [24] provide a review of control strategies for district heating and cooling networks, including different types of storage. In addition to the optimization of the system operation, some studies take into account the size and location of the generation units such as CHP plants [25] or storage [26] when performing a system optimization. Other studies optimize the network structure and pipe sizing [27–29].

The **optimization algorithms** applied are using linear [30] and non-linear programming [31] including or not discrete variables (mixed-integer) [32]. Important variables such as heat demand are uncertain and vary over time, which is why stochastic optimization is a commonly used approach to determine operation strategies [33, 34]. Another approach to account for uncertainties are sensitivity analyses [35]. Some studies apply multi-objective optimization algorithms. Buoro et al. [36] formulate a multi-objective optimization model for the optimal design and operation of a district heating system including cogeneration, a solar thermal plant and long term heat storage using Mixed Integer Linear Programming (MILP). Fazlollahi et al. [37, 38] present a multi-objective mixed integer non-linear programming approach to optimize the operation of a district energy system regarding energetic, economic and environmental aspects. When integrating storage in district heating networks, reliable predictions of future energy demands are necessary to develop efficient operation strategies for the storage facilities. Bavière and Vallée [39] compare various heat flow prediction models and include the impact of the network heat capacity on the required supply. Dahl et al. [40] use weather predictions and an auto-regressive forecasting model for district heating load forecasting. Fang and Lahdelma [41] compare a linear regression and a time series approach to forecast district heating demand and conclude that the linear approach with a weekly forecasting horizon yields the best results. Johansson et al. [42] use online machine learning algorithms to realize demand forecasting.

The **reduction of network temperatures** has been a priority for operators since the early days of district heating. While the first networks were supplied with steam at up to 200 °C, temperatures have been reduced continuously over the past century. Based on the temperature level, district heating networks are categorized in different generations. The current standard are 3rd generation district heating systems (3GDH) at supply temperatures close to 100 °C, where heat is supplied mostly via fossil and biomass based CHP plants, heat-only boilers (HOB) or high temperature waste heat sources, such as waste incineration plants [43–45]. In recent years, extensive research has been carried out on how to realize a transition from this standard towards a future 4th generation of district heating (4GDH). A detailed introduction to 4GDH at temperatures well below 100 °C can be found in [43], while the current status of research on 4GDH is described in [46].

The main benefits of **4GDH** heating are improved possibilities to integrate renewable heat sources and waste heat, as well as higher efficiencies for heat pumps and for conventional CHP plants [47]. Decreases in network heat losses represent another, though minor, advantage of low-temperature district heating [48]. Schmidt et al. [49] give an overview of the characteristics and advantages of 4GDH. To reduce district heating temperatures, several adaptations in different parts of a district heating system are necessary. Averfalk and Werner [50] describe seven different barriers to reduce district heating network temperatures in different parts of the system and recommendations on how to overcome those, including the introduction of three-pipe distribution systems, apartment substations and enhanced heat exchangers. In another paper, the same authors focus on

measures to decrease return temperatures from residential buildings and investigate possible ways to reduce temperatures [51].

In the network itself, both the **layout** and the **design of the pipes** have to be reconsidered in 4GDH systems. Assymetrical pipe insulation and twin pipes can help to minimize heat losses within the network [52]. Triple pipe systems can further decrease network temperatures by moving recirculation to an additional small pipe, thereby reducing the temperature in the return pipe [51, 53]. Brange et al. [54] study bottlenecks, i.e. locations with low differential pressure, which can arise when heat demand in an existing network increases or supply temperatures are lowered without simultaneously decreasing return temperatures. Possible solutions include higher supply temperatures, bigger pipe diameters, increased pumping capacities and more efficient substations to lower return temperatures. In an economic analysis of the same measures, the authors conclude that increasing the supply temperature, though easy to realize, is the most costly option in the long run. Lowering return temperatures in the substations can be very advantageous, but this measure is not applied frequently [55, 56]. Best et al. [57] analyze the impact of pipe diameters on the total distribution costs and conclude that smaller pipe diameters lead to reduced total costs due to lower heat losses, even though it comes with the disadvantage of high pressure losses during peak heat demand. Typically, district heating networks are designed with a tree structure suited best for heat supply with a central heat source. In 4GDH, where decentrally located renewable heat sources play an ever more important role, such structures may be limited in capacity. Instead, a ring structure offers more flexibility for the future integration of new heat sources at any location in the system [58].

To realize 4GDH in an existing district, also **adaptations inside the connected buildings** are necessary. Some studies identify high radiator design temperatures as a main barrier for low return temperatures [59, 60], while others say that in most buildings, existing radiators are designed for the worst case of a very cold winter and are hence capable of providing the necessary heat at low temperatures for most of the year [61]. Yang et al. [62] evaluate different substation configurations for domestic hot water preparation. Since supply temperatures in 4GDH systems can be below the minimum required hot water temperatures to avoid legionella growth [63], additional booster heat sources such as heat pumps [64] or direct electric heaters [65] are necessary.

Low-temperature district heating makes it possible to use many **new heat sources** that were not feasible before, due to their low temperature level. A lot of research has been performed on the integration of solar thermal energy in district heating systems (e.g. [66–69]). Since solar radiation is not equally distributed throughout the year, seasonal heat storage and complex control strategies are necessary to operate a solar district heating system efficiently [70]. Geothermal heat represents a safe and adaptive renewable source [71], though investments in drilling are high and risky [72]. Østergaard and Lund [73] carry out a case study on integrating geothermal energy in the Danish city of Frederikshavn, concluding that, while available, geothermal heat can be a major factor to reduce the use of other heat sources such as fossil fuels or biomass. Many studies have been conducted on integrating waste heat in district heating systems using heat pumps, both as a central heat source as well as in decentral locations, to make use of low temperature heat sources and excess electric energy from renewable sources such as wind and photovoltaic cells (PV) [74–76]. Waste heat sources can be industrial plants, sewage water plants or supermarkets.

A new and emerging waste heat source are **data centers**, because data center energy demand is rising steeply [77] and waste heat temperatures are increasing, due to modern hot-water cooling technologies [78, 79]. Several examples for data center waste heat integration in district heating systems exist mainly in Nordic countries. A recent study presents an overview of different waste heat utilization projects from large data centers in Denmark, Sweden and Finland [80], making it evident that energy efficiency is a pressing issue for data center operators nowadays. In Stockholm, the local district heating company Stockholm Exergi has

launched a program called ”Open District Heating”, offering data center operators to buy their waste heat at a price depending on the respective outdoor temperature [81]. Wahlroos et al. [82] carried out a study on the impact of data center waste heat integration in the district heating system of the city of Espoo, Finland. They conclude that waste heat utilization in district heating is favorable even in large quantities, as energy-related costs can be decreased considerably. In 2018, the Scandinavian telecommunications company Telia opened a data center with a maximum electric power of 24 MW in Helsinki, Finland, supplying 200 GWh/a of heat to the nearby city of Espoo [83]. As early as 2014, the Russian internet company Yandex set up a data center in Mäntsälä, Finland. The current power demand of this facility is 10 MW, one third of which is being utilized in the local district heating system. In the future, this demand is expected to grow up to 40 MW with a utilization rate of 50 % of the available waste heat [84]. In this facility, the cooling air heats up water to 30-45 °C, which is then boosted up to 55-60 °C by a heat pump to become useful in the nearby district heating network [85]. In Braunschweig, Germany, the utility company Veolia integrates heat from a data center in a low-temperature district heating network, supplying heat to a recently developed residential and commercial area with 600 homes [86]. Examples for waste heat utilization in a single building are the data center of Eurotheum in Frankfurt am Main, Germany, which supplies office spaces and a hotel within the building [87, 88] and Wallotstraße in Dresden, Germany, where 56 residential units in an apartment building are supplied by 20 racks with a total thermal power of 30 kW [89]. TU Darmstadt is currently implementing its own data center waste heat utilization project, integrating the heat into the return flow of the university’s district heating network [79] (see chapter 9).

Barriers to a successful **transition from 3GDH to 4GDH** can be of both technical or economic nature. Pellegrini et al. [90] present different barriers for transforming an existing district heating network to low-temperature heat supply in Italy. The identified barriers include market conditions, investment uncertainty and technical issues. Other barriers are a lack of trust between district heating companies and consumers when it comes to remote substation control, insufficient cooperation between generation and distribution companies and legislation not yet adapted to future realities [91].

Technical issues are often faults in different parts of a district heating system, including the network, the substations and the buildings, making it difficult to lower temperatures. Gadd and Werner [92, 93] present faults in district heating substations, such as low temperature differences between supply and return as well as poor substation control. They propose a method called ”Temperature Difference Signature” to detect faulty temperature differences, plotting the daily average temperature difference over the outdoor temperature and defining an area of three standard deviations around the average value as correct functioning and everything outside this area as a temperature fault. Månsson et al. [94] share experiences on typical faults in Swedish substations, identifying heat exchangers, control systems and controllers, actuators, control valves as well as the internal heating system of the customer as the most common sources of faults. The authors conclude that the most important aspect regarding fault elimination in substations is physical access to the substation for the utility. To gain this access, a good relationship between the utility and the customers has to be maintained. The level of cooperation of the customers will be higher if easily understandable incentives are offered by the utility. To detect and eliminate faults efficiently, more detailed monitoring is necessary, both in the network as well as at the substations [90]. To process metering data efficiently, modern data analysis tools, such as data mining [95] or machine learning [96], are used.

On the economic side, **new business models** are a prerequisite for successful implementation of 4GDH, sharing the profits of lower temperatures between the network operator and the customers. At the same time, business models are difficult to change, as long as existing business models remain profitable [97]. Lygnerud [98] presents the cases of six district energy systems in the process of lowering their district heating network temperatures. She concludes that in the cases presented, business models are not adapted at the same time as network temperatures are reduced, resulting in unexplored economic potentials. In another paper, Lygnerud

et al. [99] present barriers for investing in low-temperature waste heat integration in district heating systems, namely the absence of a district heating network in the vicinity of the heat source, different perceptions towards the value of the waste heat between the district heating operator and the waste heat provider and uncertainties about the future availability of the waste heat source.

Several **case studies on the transformation of university district energy systems** have been carried out in the past. Erhorn-Kluttig et al. [100] present an overview of energy transition projects on four campuses of different sizes and different building characteristics in Germany. The projects take into account both measures inside the buildings and in the generation facilities and networks, but focus on planning and simulation, while only small measures, such as a refurbishment of lightning, are actually implemented. Coccolo et al. [101] develop an energy transition roadmap for the campus of the Swiss Federal Institute of Technology in Lausanne (EPFL) until 2050, proposing a strategy for the refurbishment of the buildings. Pagliarini and Rainieri [102] use the example of the campus of the University of Parma to carry out a study on optimal sizing of a heat storage in a CHP based district heating system. Oltmanns et al. [8, 103] carry out two studies on decreasing the temperatures and the CO_2 emissions of the TU Darmstadt campus Lichtwiese district energy system. These studies serve as pre-studies for this thesis.

2.2 Aim of this thesis

As presented in chapter 2.1, extensive research on improving the energy efficiency and decreasing the CO_2 intensity of district energy systems has been carried out in the past. Nevertheless, a lot of questions remain unanswered.

When optimizing the design of a district energy system including storage using a linear programming approach, the storage energy content and capacity depends on the reference temperature, which can be chosen in different ways, depending on whether the useful energy or the total stored energy is of interest. Similarly, a design optimization needs a long-term forecast of the energy demand occurring in the system, while, in reality, heat demands are difficult to foresee for more than a week in advance, because they highly depend on weather conditions. The same is true for other variables of the system such as network heat losses, which have to be defined as exogene variables in the linear model, while they depend both on ambient conditions and the network temperature at each time step. Therefore, the results of a linear optimization algorithm highly depend on the assumptions made by the researcher and have to be validated using a more detailed model.

The characteristics, benefits, barriers, and necessary measures to implement 4GDH have been described in detail in the literature, but little knowledge is available on how to define where to implement which measure most efficiently. Since a transformation from 3GDH to 4GDH is capital intensive, it is important to know which buildings in a system lead to high supply or return temperatures and why, so investments can be made where the highest leverage can be created. In the district energy system of a university campus such as the one under consideration here, ventilation systems are a major source of high temperatures, both due to issues in the ventilation control system and a lack of heat recovery. Ventilation temperature faults have received little attention in 4GDH research so far, because most studies carried out in the past focus on districts of primarily residential buildings, where natural ventilation is predominant and ventilation pre-heating plays a subordinate role.

Data centers represent an important source of waste heat in many district energy systems especially at universities, though in most cases, the potential remains unused, because the waste heat temperature level is too low to be used as a heat source for the district heating network. All known implementation projects

regarding waste heat integration in district heating have in common that they still rely on traditional air cooling for the data center itself, leading to rather low waste heat temperatures and a high temperature difference between waste heat and district heating that has to be overcome by a heat pump. Better results are reached when data center waste heat utilization is combined with hot water server cooling, making it possible to extract the heat at higher temperatures than in the case of traditional air cooling. This approach yields high efficiencies for the heat pump and makes it possible to utilize the waste heat in both 3GDH and 4GDH systems.

This thesis was prepared in the context of the research project ”EnEff:Stadt Campus Lichtwiese”, which serves to support the operations department at TU Darmstadt in its quest to realize an energy transition on the local level at campus Lichtwiese. This task is being realized by an interdisciplinary team, consisting of architects, electrical as well as mechanical engineers. The project has been running since 2016 and will continue until the end of 2022. So far, outputs of the project consist of an enhancement of the energy monitoring infrastructure at campus Lichtwiese, as well as the realization of different implementation projects, such as data center waste integration in district heating presented in chapter 9 and a field study on temperature reduction and demand side management in the Architecture institute building. The final deliverable of the project will be an energy concept for the future development of campus Lichtwiese after 2030. This concept will set a path for the decarbonization of the campus energy system, including generation, distribution and consumption of heat, cooling and electric energy. The aim of this thesis is to identify measures necessary to prepare the campus to become an energy efficient and low-emissions energy system in the future. With the help of extensive energy monitoring, a detailed understanding of the setup and operation of the current system is created, facilitating the process of defining concrete measures to decarbonize the campus district energy system.

In a more general context, TU Darmstadt campus Lichtwiese can serve as an exemplary case for other district energy systems, and the tools and measures developed in this thesis can be applied by operators willing to realize an energy transition in their district. A prerequisite to applying the approaches and methods developed here is a comprehensive understanding of the system functioning through energy monitoring.

Based on the research needs identified during the literature review and the specific needs of the TU Darmstadt campus Lichtwiese energy system, three main research tasks were identified:

- Development of a two-stage optimization algorithm for the design and operation of a district energy system including 3rd generation district heating, cooling, and electric energy demand.
- Definition of metrics to identify measures that are critical to reduce network temperatures. The metrics serve to determine where to apply which measure to decrease the network temperature most efficiently.
- Development of a concept for an efficient utilization of data center waste heat, combining hot-water server cooling with waste heat integration in the adjacent district heating network.

The three different research tasks build upon each other: While it is important for any operator of a district energy system to optimize the design and operation of its system regarding the current energy demands and temperature requirements, it is also necessary to identify and invest in improvements of the efficiency of the connected buildings and the required temperatures. When taking decisions regarding future investments in new generation facilities and storage, future retrofitting of the buildings should be taken into consideration, as this can have a substantial influence on heat demand and network temperatures. In future energy systems, waste heat from different local sources will become ever more important and lowering district heating temperatures increases the feasibility of waste heat utilization, as in the case of TU Darmstadt’s own data center.

In the following chapters, the methodology for each of the research tasks will be developed and applied to the TU Darmstadt campus Lichtwiese, presenting results regarding final energy supply, CO_2 emissions, and costs.

3 The TU Darmstadt campus Lichtwiese energy system

Technical University of Darmstadt is one of the leading technical universities in Germany. In 2018, almost 26.000 students were studying in one of 113 programs, with Computer Science, Mechanical Engineering and Business Engineering being the most popular fields. The university is divided into four main sites (Lichtwiese, Stadtmitte, Botanischer Garten, Hochschulstadion) with a total usable area of 310 000 m^2 in 164 buildings [104]. TU Darmstadt has pledged to fulfill the German national climate protection goals at the local level of its campus areas, namely a reduction of the area-specific CO_2 emissions by 80 %, compared to the 1990 level, until 2050 [6].

Campus Lichtwiese is one of TU Darmstadt's principal sites. It is a typical university campus, built on the outskirts of Darmstadt starting in the late 1960s, once an expansion of the original campus in the city center was not possible anymore. It unites different use cases such as lecture halls, laboratory buildings, office buildings, and the university dining hall in a self-contained area outside the city, representing a very good object for a case study to demonstrate how to realize the energy transition on a local level. The campus comes with several unique characteristics compared to other districts, such that all buildings are non-residential, leading to low hot water demands and a high need of ventilation, especially in laboratory buildings. A big advantage of the campus is that all buildings belong to the same entity, facilitating communication processes to implement the necessary measures. Likewise, generation units, storages and networks are also part of the university's property, but currently operated by an external company in the context of a contracting agreement. This agreement is renegotiated every 15 years and the current contracting period ends in 2030. Table 3.1 gives an overview of the most important facts about the Lichtwiese energy system.

Table 3.1: Key facts campus Lichtwiese.

Total land area	245 000 m^2
Total heated floor area	155 000 m^2
Number of buildings connected to district heating	32
Number of buildings connected to district cooling	12
Trench length district heating network	4.2 km
Average outer diameter district heating network	240 mm
Trench length district cooling network	1.5 km
Annual final energy supply heat (2018)	25 200 MWh_{th}/a
Annual final energy demand heat (2018)	22 600 MWh_{th}/a
Annual final energy demand cooling energy (2018)	8000 MWh_{th}/a
Annual electric energy demand (2018)	31 300 MWh_{el}/a
Annual average supply temperature district heating (2017-2019)	88 °C
Annual average return temperature district heating (2017-2019)	58 °C
Annual average outdoor temperature (2017-2019)	11.1 °C

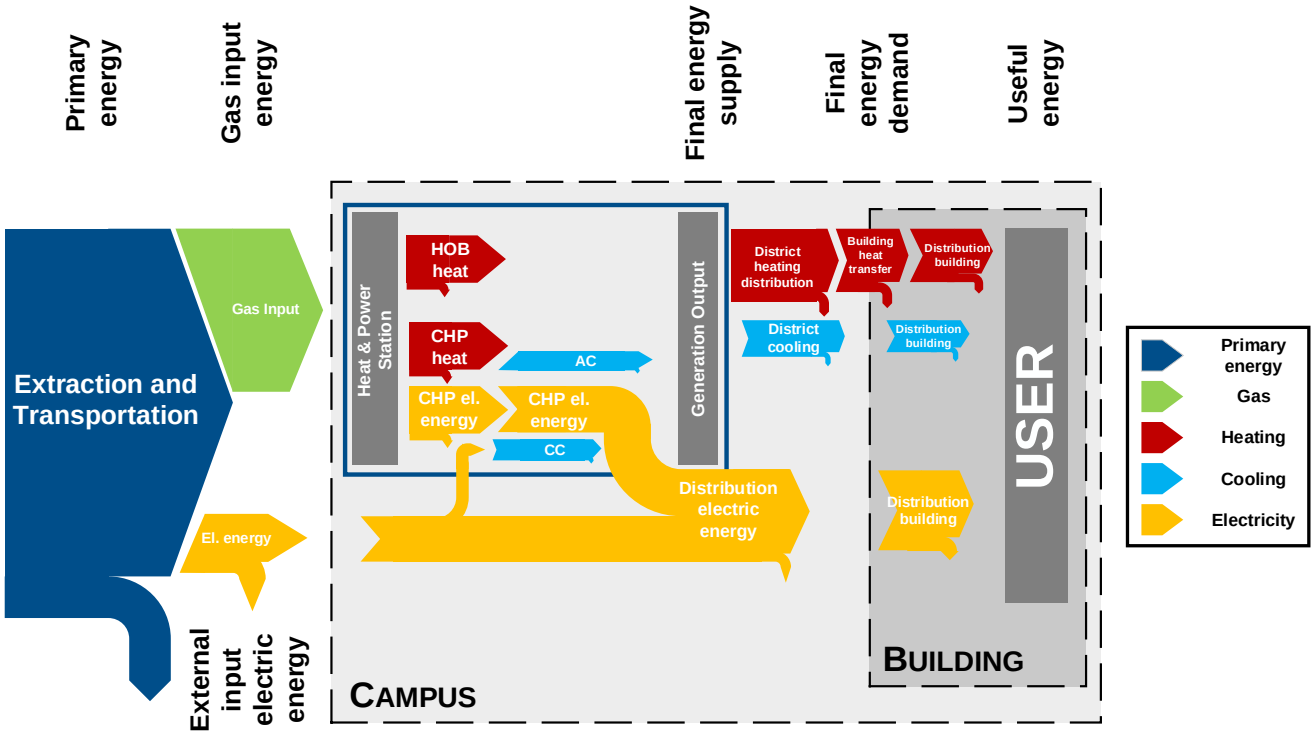

Fig. 3.1: Energy flow diagram campus Lichtwiese (2018).

A district energy system consists of generation, distribution and consumption. Fig. 3.1 shows the energy flow diagram of TU Darmstadt for the reference year. The input to the system are gas used in the CHP plants and HOB as well as grid electric energy. The gas is transformed to heat and electric energy. A part of the CHP heat is used to generate cooling energy via absorption chillers (AC). Additional cooling energy is generated via compression chillers (CC) supplied with grid electric energy. The final energy supply consisting of electric energy, heat and cooling energy is then transmitted to the buildings in the respective networks, transferred from the network to the building in a substation (thermal energy) or a transformer (electric energy) and provided to the users in their offices, lecture halls or laboratories. Every one of these transformation or transportation processes comes with certain efficiencies, losses and changes in temperature or voltage. This chapter introduces the relevant components of the campus energy system, namely generation, networks and buildings.

3.1 Generation

Electric, heating and cooling energy for the four main campus areas of TU Darmstadt are generated at the heat and power station (HPS) located on campus Lichtwiese. The electric energy generated at the HPS serves campus Lichtwiese and can be fed into the public grid and accounted for the demand of the other campus areas, as long as the generation is not higher than the university's total demand of electric power. The university is not allowed to sell excess electric energy to the public grid and electric energy storage are neither available in the university energy system nor within the scope of this thesis. Therefore, the maximum electric

power output of the CHP plants is always restricted by the total demand of the university. When the demand of electric power exceeds the local generation, additional electric energy is purchased from the electric grid.

The HPS was renovated in recent years. Until 2016, it was made up of three CHP gas engines, each of which yielding a thermal and electric capacity of $P_{\text{th,CHP}} = 2.0\,\text{MW}_\text{th}$ / $P_{\text{el,CHP}} = 1.95\,\text{MW}_\text{el}$ and a thermal and electric efficiency at full load ($\eta_{\text{th,100\%}}$ / $\eta_{\text{el,100\%}}$) of $\eta_{\text{th,100\%}} = 42.7\,\%$ / $\eta_{\text{el,100\%}} = 40.2\,\%$. In 2017 and 2018, the HPS was expanded with a new building and an additional CHP ($P_{\text{th,CHP}} = 3.0\,\text{MW}_\text{th}$ / $P_{\text{el,CHP}} = 3.25\,\text{MW}_\text{el}$, $\eta_{\text{th,100\%}} = 42.4\,\%$, $\eta_{\text{el,100\%}} = 45.6\,\%$). Two out of the three existing CHP plants were overhauled and equipped with new engines (now $P_{\text{th,CHP}} = 2.0\,\text{MW}_\text{th}$ / $P_{\text{el,CHP}} = 2.0\,\text{MW}_\text{el}$, $\eta_{\text{th,100\%}} = 43.6\,\%$, $\eta_{\text{el,100\%}} = 43.8\,\%$ each). The third existing plant was not overhauled and serves now as a backup plant that only goes into operation when the other plants are not functioning properly. CHP plants can be operated in partial load mode, but not below 50 % of the electric capacity of the plant. Below this value, the electric efficiency decreases significantly and it becomes better to generate heat and power separately using HOB and grid electric energy. To supply peak heat demand in the winter months, six HOB with a heat capacity of $P_{\text{th,HOB}} = 9.3\,\text{MW}_\text{th}$ each are available at the HPS. HOB are more flexible than CHP plants and can be operated at any partial load operating point.

In the former setup, about two thirds of the university's electric energy demand was generated by the CHP plants. Due to the increased CHP capacity, local electric energy generation was increased to more than three quarters of the total demand of TU Darmstadt. Likewise, the share of CHP heat in total heat supply was increased from 50 % in 2016 to 55 % in 2018. In the future, additional heat will be supplied by the university's own high-performance computer (HPC) "Lichtenberg Hochleistungsrechner" (see chapter 9). The waste heat from the HPC will be integrated into the district heating network via a heat pump (HP/HPC).

Central cooling serves to fulfill cooling demands for the university's own data center as well as laboratory cooling and air-conditioning of lecture halls where necessary. For the time being, air-conditioning for office spaces is neither available nor foreseen to be installed in the future. Central cooling only exists at campus Lichtwiese, where the buildings with the highest cooling demand within the university are located. Cooling energy is supplied by an AC with a maximum load of $P_{\text{cool,AC}} = 1\,\text{MW}_\text{th}$. The heat necessary for the AC comes from CHP plants and makes it possible to extend the operation period of these plants into the summer season. Before the AC was installed in 2017, three CC with a capacity of $P_{\text{cool,CC}} = 1\,\text{MW}_\text{th}$ each were used to cool the data center and to supply a local cooling network connecting the buildings of the chemistry department. To reduce the impact of daily demand peaks in both heating and cooling, stratified water storage tanks were erected (2x 125 m^3 for heating, 2x 150 m^3 for cooling). Since the storage capacity is low compared to the university's heat and cooling demand, the CHP plants run on a heat-guided operation mode.

3.2 Networks

The energy generated at the HPS is distributed via a local medium voltage electric grid, a district heating as well as a district cooling network. The focus of this thesis lies on the thermal energy supply. Therefore, electric energy is taken into account in the context of generation (combined heat and power as well as additional electric energy demand from the electric grid), but local distribution and its associated losses are not analyzed.

All four main campus areas of TU Darmstadt are connected by a district heating network with a total length of 14 km, 4.2 km of which are located on campus Lichtwiese. Additionally, several public buildings in the city of Darmstadt are supplied with heat from the HPS, increasing the total heat demand by about 13 % compared to the university buildings' heat demand. The district heating network at campus Lichtwiese is made up of a main ring pipe and sub-networks in the different faculty areas (Mechanical Engineering,

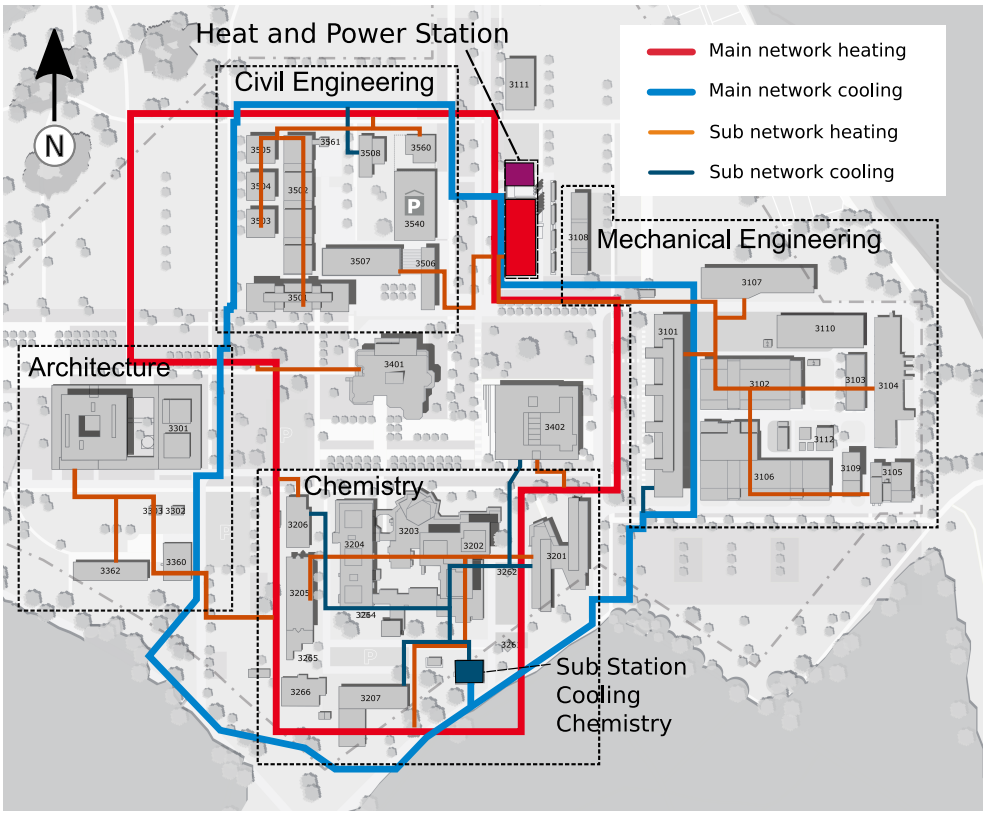

Fig. 3.2: TU Darmstadt campus Lichtwiese district heating and district cooling networks (2018).

Chemistry, Architecture and Civil Engineering). The sub-network supplying the department of Mechanical Engineering is connected directly to the heat and power station, while all other sub-networks go off the main ring. In addition to the district heating network for Campus Lichtwiese shown in Fig. 3.2, each of TU Darmstadt's remaining campuses has its own district heating pipes directly connected to the HPS. In total, five heating circuits are connected at the HPS: Lichtwiese west, Lichtwiese east, Mechanical Engineering, Hochschulstadion and Stadtmitte/Botanischer Garten. TU Darmstadt's district heating network is a classic 2-pipe hot water system typical for 2$^{\text{nd}}$ and 3$^{\text{rd}}$ generation district heating systems [4]. The district heating supply temperature fluctuates throughout the year between $T_{\text{S,DH}} = 65\,°\text{C}$ and $T_{\text{S,DH}} = 110\,°\text{C}$, the return temperature between $T_{\text{R,DH}} = 45\,°\text{C}$ and $T_{\text{R,DH}} = 75\,°\text{C}$. Table 3.2 shows the pipe lengths for different pipe diameters at Campus Lichtwiese. Based on the outer diameters for the different pipe sizes indicated in the data sheet of the pipe supplier [105], the average outer diameter of the campus Lichtwiese district heating network can be calculated to be 240 mm.

Table 3.2: Pipe length for different pipe diameters.

Pipe diameter	**DN300**	**DN250**	**DN200**	**DN150**	**DN125**	**DN80**	**DN65**
Pipe length in m	2090	135	260	885	413	356	55

A district cooling network with a length of 1.5 km was constructed together with the acquisition of the absorption cooling machine and only connects campus Lichtwiese. The temperatures in the district cooling network are designed to be $T_{\text{S,DC}} = 6\,°\text{C}$ (supply temperature) and $T_{\text{R,DC}} = 12\,°\text{C}$ (return temperature) [8]. Fig. 3.2 illustrates the campus and the setup of the thermal networks.

3.3 Buildings

Campus Lichtwiese was inaugurated in the late 1960s and has been expanded repeatedly ever since. Nowadays, it comprises 35 buildings (32 of which are connected to district heating and 12 to district cooling) and a total heated floor area of 155 000 m^2 for different purposes such as lecture halls, offices and laboratories. Campus Lichtwiese is home to five out of 13 faculties at TU Darmstadt: Architecture, Mechanical Engineering, Civil Engineering, Chemistry and Material Science. 20 buildings date back to the first construction phase in the 1960s and 1970s, while newer buildings were added since the mid-1990s. Construction activity has been high in the last decade and new buildings are added continuously. As the university keeps growing, more buildings are expected to be constructed in the coming decades and projections suggest that the total heated space might reach up to 300 000 m^2 by 2050. Fig. 3.3 shows the heated floor area of each building and the years of their construction. It can be seen that most of the larger buildings exceeding 10 000 m^2 were built in the first construction phase of the campus in the 1960s and 1970s. Many of those buildings have a poor energetic performance and need to be renovated in the near future. The numbering refers to the internal building numbering used at TU Darmstadt and will be used throughout this thesis. Table 3.3 lists the principal buildings on campus, not including unheated utility buildings such as garages that are not relevant for an analysis of the energy system. Not all buildings are connected to district heating (DH) or district cooling (DC). Therefore, it is indicated which buildings are connected to which system. The presented annual heat demand represents the average heat demand between April 1st, 2017 and March 31st, 2019.

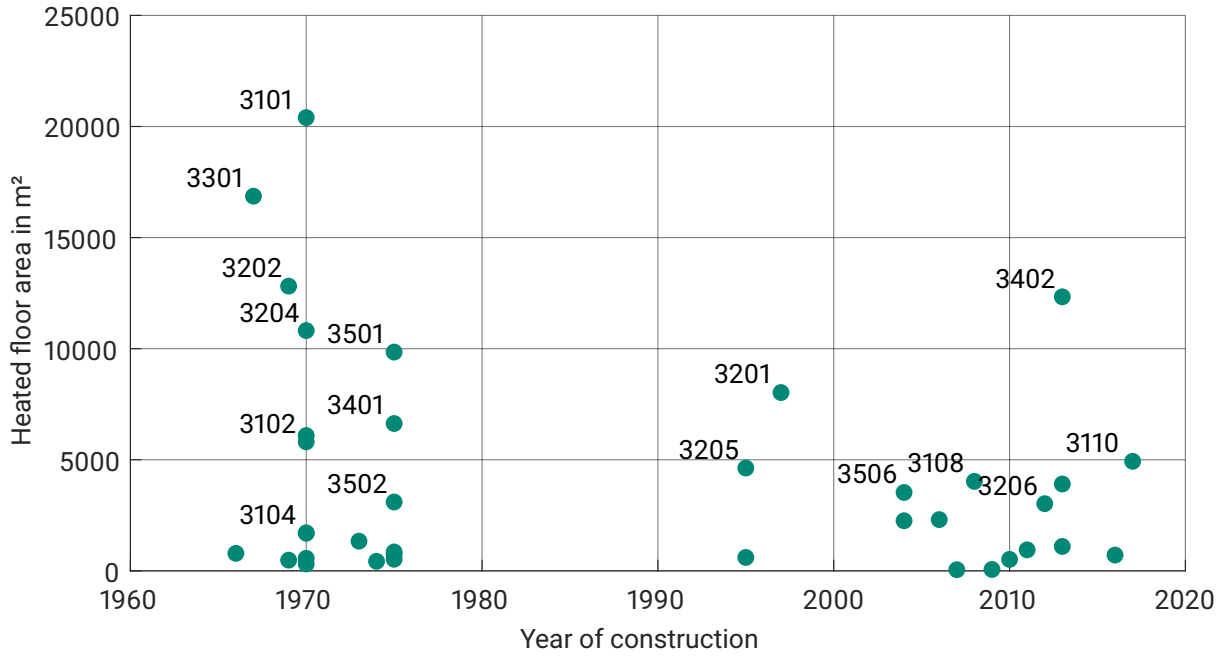

Fig. 3.3: Buildings total heated floor area over construction year.

Table 3.3: Buildings at campus Lichtwiese.

Building name	**Building number**	**Year**	**Heated space in** m^2	**Heat demand in** MWh/a	**Specific heat demand in** kWh/m^2a	**DH**	**DC**
Mechanical Engineering Institutes	3101	1970	20400	2060	100	x	x
Mechanical Engineering Laboratories 1	3102	1970	5805	995	170	x	x
Mechanical Engineering Laboratories 5	3103	1970	565	150	265	x	
Mechanical Engineering Laboratories 4	3104	1970	1700	445	260	x	
Mechanical Engineering Laboratories 3	3105	1970	1705	175	103	x	
Mechanical Engineering Laboratories 2	3106	1970	6090	1045	170	x	x
Mechanical Engineering Laboratories 6	3107	2006	2305	190	82	x	
Energy Center	3108	2008	4025	150	37	x	
CO_2 Laboratory	3109	2010	515	100	195	x	
Teaching Center Mechanical Engineering	3110	2017	4930	240	48	x	x
ETA-Factory (Energy Efficient Production)	3111	2016	710				
Automotive Laboratory	3112		190	20	104	x	
TU Darmstadt Heat and Power Station	3160	1966	790				
Material Science Institutes & Laboratories	3201	1997	8025	970	121	x	x
Organic Chemistry Institutes & Laboratories	3202	1969	12815	4075	320	x	x
Chemistry Lecture Halls	3203	1973	1335	660	495	x	x
Physical Chemistry Institutes & Laboratories	3204	1970	10815	1815	170	x	x
Inorganic Chemistry Institutes & Laboratories	3205	1995	4630	2560	555	x	
Center of Smart Interfaces	3206	2012	3025	280	95	x	x
M^3 Laboratory Building	3207	2013	3910	285	75	x	x
Heating and Cooling Substation Chemistry	3260	1970	670				
Disposal Center Chemistry	3266	1995	600	230	380	x	
Architecture Institutes	3301	1967	16865	2450	145	x	
Solar Decathlon Building 2007	3302	2007	50				
Solar Decathlon Building 2009	3303	2009	60				
Daycare center	3360	1969	480	115	240	x	
Kindergarten	3362	2011	945	60	65	x	
University dining hall	3401	1975	6630	840	125	x	
Lecture Hall & Media Center	3402	2013	12335	475	40	x	x
Civil Engineering Institutes Old	3501	1975	9850	1675	170	x	
Civil Engineering Laboratories 1	3502	1975	3100	560	180	x	
Civil Engineering Laboratories 4	3503	1975	750	135	180	x	
Civil Engineering Laboratories 3	3504	1975	520	95	180	x	
Civil Engineering Laboratories 2	3505	1975	850	155	180	x	
Civil Engineering Institutes New	3506	2004	3525	240	70	x	
Civil Engineering Laboratories 5	3507	2004	2255	155	70	x	
High-Performance Computer	3508	2013	1100				x
Recycling Center	3560	1974	430	75	175	x	

4 Thermal energy monitoring

To gain a comprehensive understanding of the behavior of a district energy system, monitoring data of the different energy types at different points in the system is essential. Reliable monitoring data is necessary for modeling purposes, as the model can only be as good as the assumptions made by the researcher. Detailed monitoring also makes it possible to detect operational errors both in the networks and in the buildings. Although energy monitoring does not directly improve the efficiency of a district energy system, it is a crucial prerequisite to identify where to apply which measures to reduce energy demand and temperatures most efficiently (see chapter 8). In the past, many district energy systems have been operated with little knowledge about key variables such as temperature and pressure distribution, due to high costs for manual meter readings [106]. Modern automatic meters make continuous monitoring easier and more common, setting the basis for a digitization of district heating and cooling, including continuous operation optimization [107].
TU Darmstadt disposes of a detailed continuous energy monitoring system for heating and cooling, including final energy supply at the HPS, the final energy demand at the building boundary, and in some cases also the distribution of heat inside the buildings.

In this chapter, an overview of the available data and measurement devices used in this thesis is given. Additionally, a discussion of measurement errors is carried out.

4.1 Monitoring of heat and cooling energy

Energy monitoring for heating and cooling is available at TU Darmstadt. It can be divided in primary and secondary side heat demand monitoring as well as cooling demand monitoring at the substation level, and monitoring of the heat supply at the exit of the HPS.

Heat is supplied from the district heating network (primary side) to the in-building distribution network (secondary side) at a substation. Substations at campus Lichtwiese are either designed with an indirect connection (heat transfer via heat exchanger, secondary side represents an independent hydraulic circuit) or a direct connection (no hydraulic separation between primary and secondary side), with or without an admixture of return flow on the secondary side to adapt the secondary supply temperature. Fig. 4.1 illustrates the two general substation concepts with a direct (Fig. 4.1a) or indirect (Fig. 4.1b) connection to the district heating network.

The secondary side distribution system consists of several different heating circuits, supplying heat to different parts of the building for space heating, ventilation and, in some cases, hot water preparation. Heat demand can not be measured directly, but is a function of the volume flow and the supply and return temperatures of

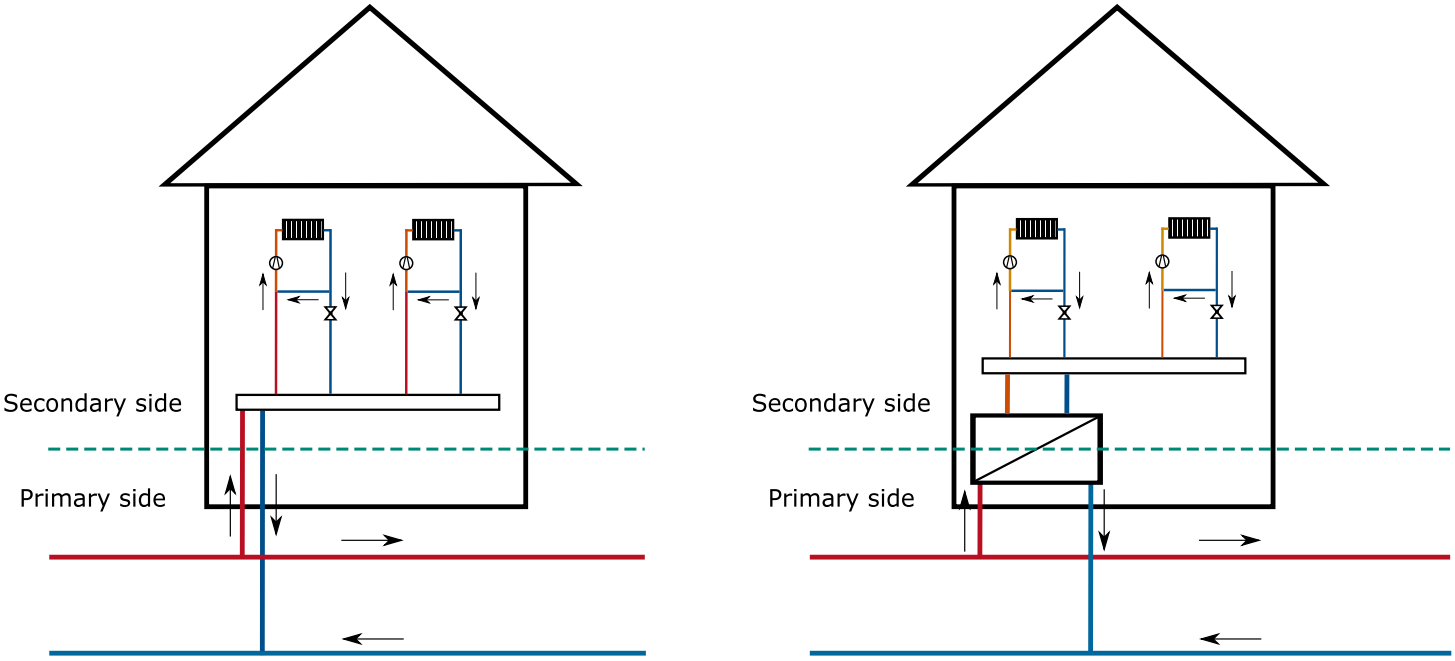

(a) Directly connected substation.

(b) Indirectly connected substation.

Fig. 4.1: Different district heating substation designs available at TU Darmstadt campus Lichtwiese.

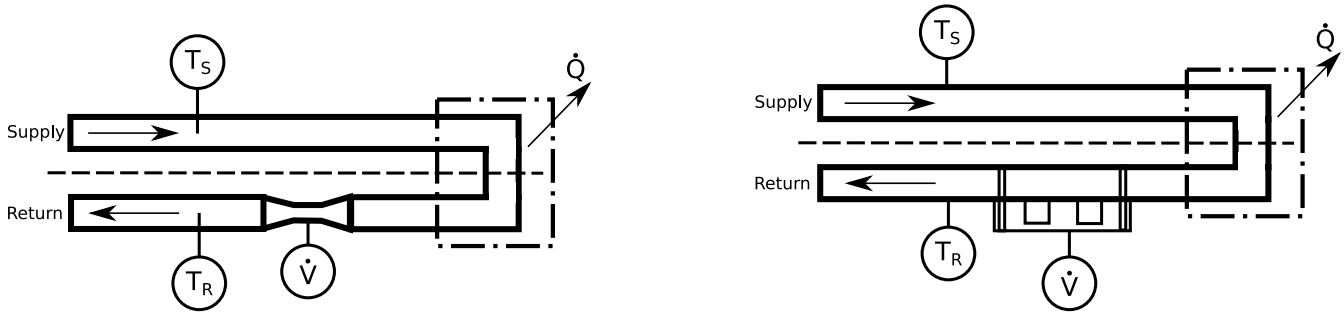

(a) In-line measurement principle.

(b) Clamp-on measurement principle.

Fig. 4.2: Different heat measurement principles used at TU Darmstadt campus Lichtwiese.

a heating circuit. The heat flow $\dot{Q}_{i,j}$ to the customer from the heating circuit j at time i is determined using a first law formulation for a stationary flow through the substation:

$$\dot{Q}_{i,j} = \dot{V}_{i,j} \cdot \rho_{\mathrm{W}} \cdot c_{\mathrm{W}} \cdot (T_{\mathrm{S},i,j} - T_{\mathrm{R},i,j}) \tag{4.1}$$

To calculate $\dot{Q}_{i,j}$, the volume flow $\dot{V}_{i,j}$ and the supply and return temperatures ($T_{\mathrm{S},i,j}$ and $T_{\mathrm{R},i,j}$) have to be measured. The density ρ_{W} and the specific heat capacity c_{W} of water can be found in the literature [108]. Volume flow and temperatures can be measured either within the pipes of the respective heating circuit (in-line) or using clamp-on sensors, which are installed on the pipe wall (see Fig.4.2). Clamp-on heat meters are a common solution for retrofitting purposes, because they do not require opening the pipe itself, facilitating the installation process in an existing heating circuit considerably.

For flow measurement, two different types of sensors are used at TU Darmstadt, Woltman flow sensors and ultrasonic flow sensors. Both technologies measure the flow velocity and calculate the volume flow multiplying the flow velocity with the inner pipe cross-sectional area. Woltman sensors are an in-line flow measurement technology. They measure the rotating speed of a turbine wheel that correlates with the flow velocity of the fluid. Ultrasonic flow sensors measure the flow velocity by comparing the transit-time difference of an ultrasonic pulse in and against the flow direction. For this purpose, two piezoelectric crystal elements exchange ultrasonic pulses, functioning as both emitter and receiver [4]. The difference in transit-time between a pulse in and against the flow direction corresponds with the flow velocity. Ultrasonic flow sensors can either be in-line sensors with emitters/receivers opposing each other, or clamp-on sensors, exchanging ultrasonic pulses reflected by the opposing side of the pipe wall (see Fig. 4.2b). Ultrasonic meters do not contain moving parts and require little or no maintenance.
The temperatures of the water in the supply and return pipes is measured using resistance temperature detectors (RTD), consisting of platinum wires with a resistance of 100 Ω or 1000 Ω (Pt100 or Pt1000) at 0 °C, using a four-wire setup to eliminate an influence of the cable resistance on the measurement. In-line heat meters come with temperature sensors located inside the pipes, while clamp-on meters use temperature sensors located on the pipe wall.

Primary side heat monitoring is based on in-line meters and has been available at TU Darmstadt for the last decades for heat billing purposes. In old buildings, Woltman sensors are used for volume flow measurement, while in newer buildings, in-line ultrasonic sensors were installed. Primary side heat meters measure the heat demand mostly building-wise, even though in a few cases, several buildings are monitored together. In some of the big old buildings, such as the Organic Chemistry building 3202, the Mechanical Engineering instute building 3101, or the Architecture institute building 3301, separate primary heat meters exist for space heating, ventilation, and hot water preparation. The primary heat meters measure with a temporal resolution of 15 minutes. Historical data had not been stored in the past, which is why continuous primary side heat demand data is only available since the end of 2016.

Secondary side heat monitoring is a product of the research project ”EnEff:Stadt Campus Lichtwiese” and was retrofitted at the beginning of 2020. All secondary side heat meters are of the same type (Dynasonics TFX 5000 [109]), using ultrasonic clamp-on volume flow sensors and on-pipe RTD. The resolution of the secondary side heat meters is 3 seconds. All monitoring data is stored centrally on a data base that can be accessed remotely. Fig. 4.3 shows an example of the secondary side heat monitoring sensors. Secondary side heat monitoring only measures the most important heating circuits in each building. In addition to the permanently installed meters, TU Darmstadt owns a mobile heat meter Dynasonics DXN [110], which is used to go into more detail once an issue is detected in a specific building. In the Organic Chemistry building 3202, secondary side heat monitoring was not installed, since this building is currently undergoing a comprehensive renovation. Fig. 4.4 shows an overview of the primary and secondary heat meters installed at campus Lichtwiese. The numbers indicate the names of the primary side heat meters for each building or group of buildings, the colors show the amount of heating circuits measured with secondary heat meters in each building. In the buildings 3104, 3108, 3502 and 3506, secondary side heat meters have been installed, but no data from these meters was available for the time period used in the study on temperature reduction carried out in chapter 8.5. The Mechanical Engineering laboratory buildings 3102 and 3106 are supplied from the same substation located in 3102, with heating circuits supplying both buildings at the same time. Accordingly, only one primary heat meter measures both buildings, and all of the installed secondary side heat meters in 3102 cover both buildings at the same time.

For cooling energy demand monitoring, the same meter types as for primary side heat monitoring are used. Heat supply monitoring at the exit of the HPS is being carried out with ultrasonic clamp-on heat meters of the same type used for secondary side heat demand monitoring. While the HPS is connected to five heating

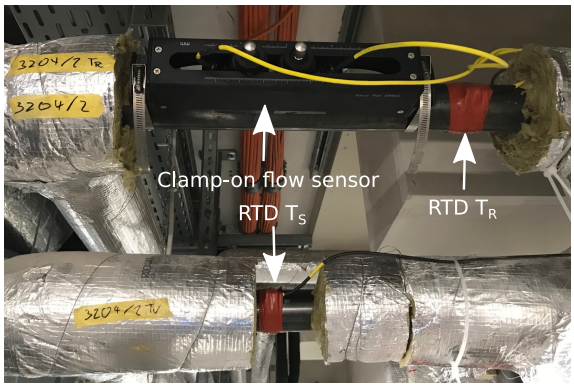

Fig. 4.3: Sensors of secondary side heat meters (here without insulation).

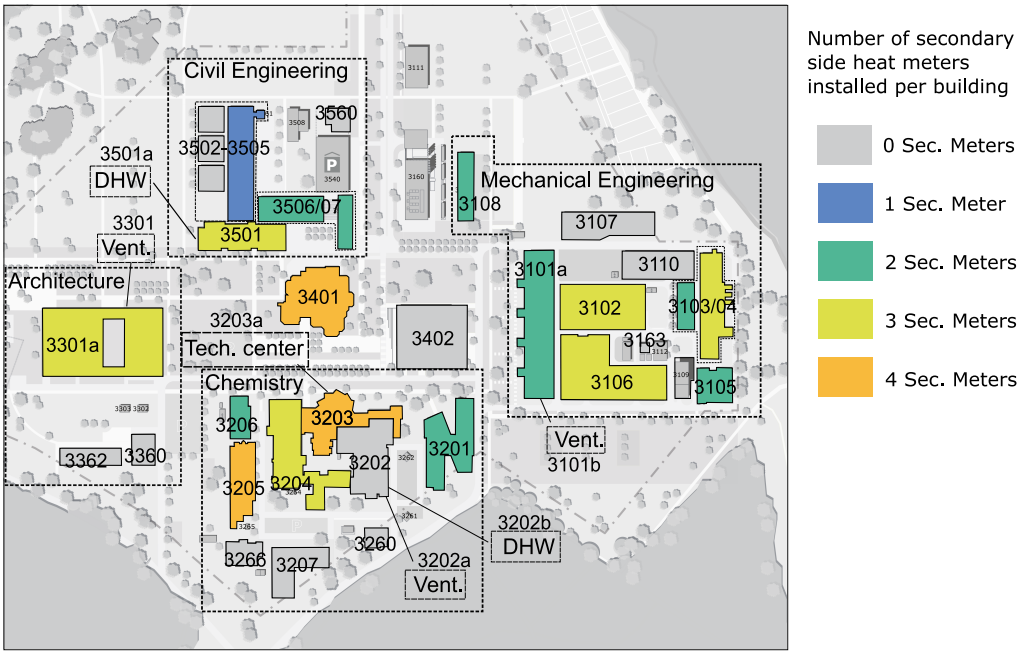

Fig. 4.4: Primary and secondary side heat meters at campus Lichtwiese.

circuits supplying different parts of TU Darmstadt, so far only one meter is available, measuring the heat supply for the western part of campus Lichtwiese. This meter is used to validate the model developed in the context of this thesis (see chapter 6.6).

4.2 Measurement uncertainty of thermal energy meters

Measurement uncertainty in heat monitoring occurs in any of the variables necessary to calculate the heat flow (see eq. 4.1). In this section, the different sources of measurement uncertainty in heat monitoring are discussed. Table 4.1 summarizes these uncertainties.

Woltman flow sensors reach a high accuracy for high volume flows ($\pm 0.25\,\%$) [111]. At low volume flow, the accuracy decreases, due to energy losses in the measurement device itself. Therefore, the range of Woltman

Table 4.1: List of measurement uncertainties.

Value	Uncertainty
Volume flow $\dot{V}$	$\pm$0.25 % - $\pm$1 %
Temperature T	max. $\pm$0.85 K (at 100 °C)
Specific heat capacity water c_W	$\pm$0.5 %
Water density ρ_W	$\pm$2 %

flow sensors is small, often no more than 1:10 [4]. The meter accuracy of the clamp-on ultrasonic flow meters used at TU Darmstadt is certified by the manufacturer to be below 1 % of the measured value (see Appendix). Additional measuring errors are related to the installation of the flow sensors. To calculate the volume flow, the inner pipe diameter has to be known. While the outer pipe diameter can be measured easily, it is more difficult to determine the pipe thickness and the respective inner pipe diameter accurately when the specifications of the manufacturer are not available. To reach accurate measurement results, the clamp-on sensors have to be positioned at the correct distance, which depends on the pipe diameter and thickness. Ultrasonic flow sensors are capable of measuring small and high flow rates accurately, reaching a range of 1:250 [4]. For all sensor types, swirl flows can influence the measurement result, thus sensors should not be installed too close to a bend or a valve. It is recommended to leave a straight pipe length of at least 10 times the pipe diameter upstream of the sensor and 5 times the pipe diameter downstream of the sensor [4].

The accuracy of the RTD depends on the measured temperature and increases with the latter, leading to a maximum error of 0.85 K at 110 °C, according to DIN EN 60751 [112] and DIN EN 1434-1 [113]. Additional measurement uncertainties result from the installation of the temperature sensor. In the case of on-pipe temperature measurement, an uninsulated RTD measures a temperature several Kelvin below the temperature inside the pipe, due to the influence of the surrounding air. The uncertainty resulting from the heat resistance of the pipe is small, because of the low thermal resistance of steel pipes used for heating applications and the low wall thicknesses of a few millimeters. In case of both in-pipe and on-pipe sensors, very low mass flows can lead to a measurement uncertainty, because temperatures are not constant over the pipe diameter anymore, once the flow regime changes from turbulent to laminar flow. In the case of cooling demand meters, accurate temperature measurement is even more important than for heat metering, since the temperature difference in a district cooling network is a lot smaller than in a district heating network.

Both the specific heat capacity c_W and the density ρ_W of water are not constant, but depend on the temperature. Since district heating is operated in a comparatively limited temperature range, this uncertainty is small and a simplified heat flow calculation with constant water heat capacity ($c_W = 4.19\,\mathrm{kJ/kgK}$) and density ($\rho_W = 980\,\mathrm{kg/m^3}$) can be justified.

A more important error arises from instationary effects. In large heating circuits with high inertia, a change in the supply temperature does not have an immediate effect on the return temperature. When the overall temperature level of a heating circuit is increased, an overestimation of the heat flow, thus a ”virtual peak” occurs. Equally, a negative ”virtual peak” can occur during a sudden decrease in temperature level. The issue does not apply to a change in the mass flow, because the latter has an almost immediate effect on the entire heating circuit.

Fig. 4.5 shows this phenomenon, using the example of the heating circuit 3103/2 in the Mechanical Engineering workshop building: After a sudden change in supply temperature at around 6:40 pm on March 23, 2020, the meter measures a peak in the heat flow, because the return temperature takes about 20 minutes longer than the supply temperature to adjust to the new temperature level. To cope with this circumstance, an adjustment

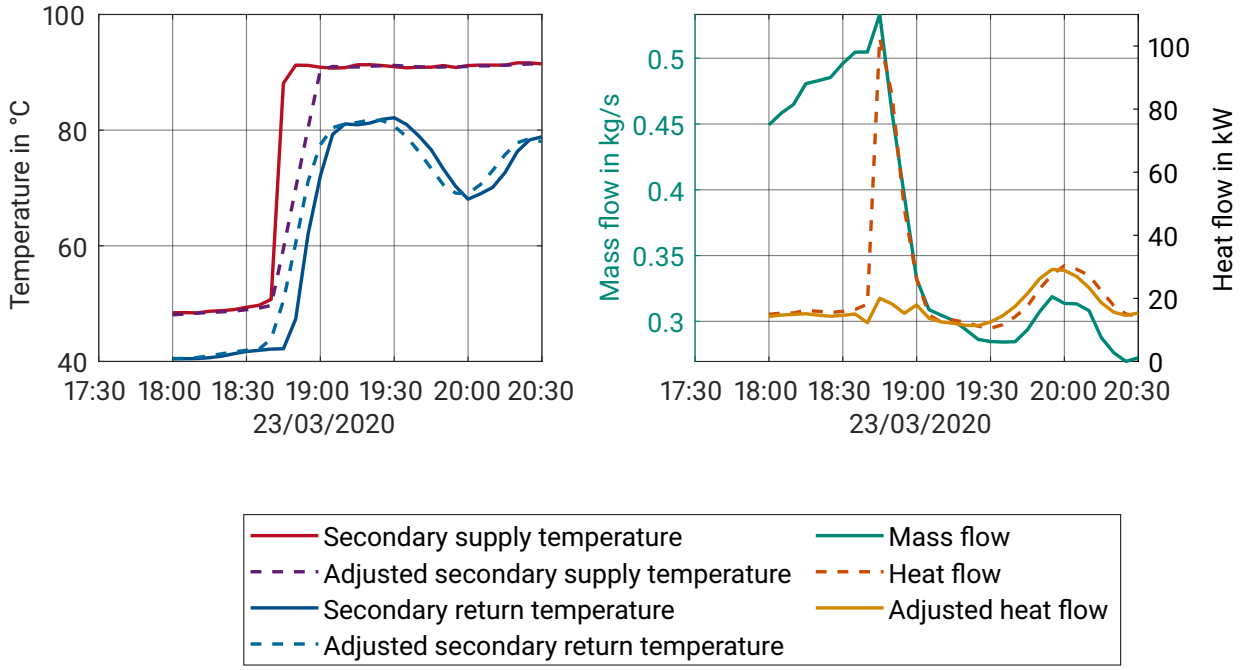

Fig. 4.5: Adjusting temperatures to eliminate inertia related heat flow peaks in heating circuit 3103/2.

of the data is necessary, virtually moving the measured temperature data closer to the radiator or ventilation heat exchanger (see Fig. 4.6).

There are several ways to do so: A simple approach would be to move the supply temperature data forward in time and the return temperature back. The problem with this approach is that it conserves the gradient of the temperature change for both the supply and the return temperature. Since the mass flow is reduced considerably while the change in temperatures occurs (see right side of Fig. 4.5), the gradient of the return temperature change is lower than the one of the supply temperature change, because it occurs at lower flow velocity. This approach thus can never completely eliminate the ”virtual peak”. An alternative option is the use of a moving average of both the supply and return temperatures, which is applied in Fig. 4.5. This results in similar gradients for both the adjusted supply and return temperature and thus eliminates the ”virtual peak” almost entirely. The downside of this approach is that an averaging of data points slightly underestimates real life peaks occurring not as a result of a change in the overall temperature level, but due to a peak in the mass flow. The error induced by this approach is nevertheless considerably smaller than the remaining ”virtual peak” in the case of the simple movement of the measured data over time. An exact solution would require a detailed simulation of the fluid dynamics inside the heating circuit and is not within the scope of this thesis.

The influence of inertia only plays a role in large heating circuits performing sudden changes in their overall temperature level. At campus Lichtwiese, such changes can be seen in secondary side heating circuits, especially in space heating circuits with control faults (see chapter 8.5.4).

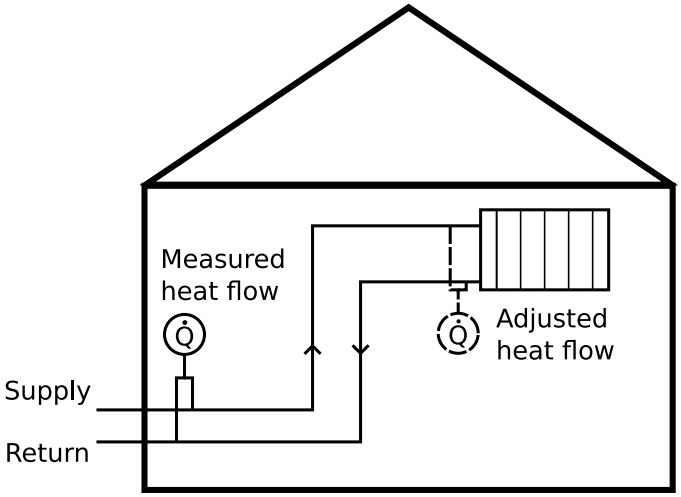

Fig. 4.6: Measured vs. adjusted heat flow: virtual movement of measurement location of temperature data.

5 Basic methods and objectives

This chapter explains basic methods to perform an energy and exergy analysis of a system using Sankey diagrams, and the attribution of CO_2 emissions and costs to heat and electric energy in CHP plants. It also introduces the objective variables used to evaluate the impact of the proposed measures to improve the efficiency of the energy system at TU Darmstadt campus Lichtwiese. In the context of this thesis, an improvement of the efficiency of an energy system is defined as a reduction of final energy supply and CO_2 emissions, without increasing energy-related costs. In the following, the assumptions made to calculate the final energy supply, CO_2 emissions and annuities of energy-related costs are presented.

In the context of an energy system analysis such as the one performed here, primary energy supply is often used as an additional objective variable, using primary energy factors, such as those defined by the German standard DIN V 18599-1 [114]. Those factors are politically driven and do not necessarily represent physical realities. Fossil fuels such as oil, natural gas, lignite, or hard coal all have the same primary energy factor, even though they represent very different resources. Primary energy supply is hence not considered as an objective variable in the context of this thesis.

5.1 Energy & exergy analysis

Sankey flow diagrams help to visualize conversion processes between the input of the system in form of gas and grid electric energy, and the energy provided to the users as useful energy. While an energy analysis gives a quantitative understanding of the system, exergy analysis shows the quality of the energy flows. Exergy describes the thermodynamic quality of a certain type of energy and is defined as the maximum amount of work to be extracted from a system when bringing it into equilibrium with a reference state [115].

The exergy of a system depends on the reference environment, which has to be defined before an exergy analysis can be carried out. Several different criteria have to be fulfilled by the reference environment: It has to be in a state of thermodynamic equilibrium, must not be changed by the system under consideration, and has to be readily available for exchange with the system [116]. As described by Falk [117], there are four different options to define the reference environment for a exergy analysis of a district energy system. Falk names the universe at near zero Kelvin, the air inside the buildings, the undisturbed ground and the ambient air. The most common choice in the context of a district energy system and the one used in this thesis is the ambient air, because it is readily available at the system boundary of the buildings at all times and can be regarded as unchanged by the processes occurring inside the buildings, though it varies with time and space and is not in a thermodynamic equilibrium [116].

The exergy analysis carried out in this thesis deals with chemical exergy of the gas entering the system, which can be calculated using an exergy coefficient of $\gamma_{ex,gas} \approx 1.04$ for its lower heating value [118], physical exergy in the form of exergy of the mass flows in the different thermal networks, and exergy of heat inside the buildings. For electric energy, the exergy content is the same as the energy content.

5.2 Attribution of CHP CO_2 emissions and costs to heat and electric energy

By design, CHP plants always generate heat and electric energy simultaneously. Hence, it is necessary to define how to divide the resulting CO_2 emissions and costs between heat and electric energy. To realize this task, several different measures have been discussed in the literature [119, 120], which can be divided into three different categories. The first category divides the CO_2 emissions occurring in the CHP plant according to a certain logic, e.g. according to the energetic efficiency of the conversion from gas to heat and electric energy or the exergy content of both products of the conversion process. The second category allocates the emissions taking into account the efficiencies of reference plants generating heat and electric energy separately. The third category extends the system boundary and includes a bonus for the heat or electric energy replaced by the CHP plant [121]. Nowadays, the most common methods are based on the third logic. In the context of the German energy savings directive (Energieeinsparverordnung – EnEV), the allocation is realized based on the replacement mix method [122], which is defined in the AGFW directive FW 309-1 [123]. The same is true for the power bonus method, which is part of the European norm EN 15316 [124].

The system boundary for this thesis is the district campus Lichtwiese and the objective is to create concepts to decrease CO_2 emissions at the local level. Therefore, the allocation is carried out using the exergy method [125]. In this method, which belongs to the first kind presented above, the allocation is realized based on the exergy content of heat and electric energy. The allocation of costs or CO_2 emissions to heat and electric energy is described in AGFW FW 309-6 [126]:

$$\begin{aligned} f_{\mathrm{CHP,th}} &= \frac{Ex_{\mathrm{th}}}{Ex_{\mathrm{th}} + Ex_{\mathrm{el}}} \\ f_{\mathrm{CHP,el}} &= 1 - f_{\mathrm{CHP,th}} \end{aligned} \tag{5.1}$$

In this context, $f_{\mathrm{CHP,th}}$ stands for the allocation factor of CO_2 emissions and costs to CHP heat. $f_{\mathrm{CHP,el}}$ represents the allocation factor to CHP electric energy. $f_{\mathrm{CHP,th}}$ is defined as the fraction of the exergy of the CHP heat Ex_{th} over the total exergy after the CHP conversion process (heat exergy Ex_{th} and electric exergy Ex_{el}). The exergy of the CHP heat is calculated via the Carnot efficiency of the CHP heat in the district heating network, using the logarithmic mean temperature of the district heating network and the ambient air temperature as reference temperature. All temperatures in eq. 5.2 are time-dependent.

$$Ex_{\mathrm{th}} = E_{\mathrm{th}} \cdot \left(1 - \frac{T_{\mathrm{amb}}}{\frac{T_{\mathrm{S,DHN}} - T_{\mathrm{R,DHN}}}{\ln\left(\frac{T_{\mathrm{S,DHN}}}{T_{\mathrm{R,DHN}}}\right)}} \right) \tag{5.2}$$

This method is also called power loss method, because it devides the CO_2 emissions and costs between the electric energy of the CHP plants and the theoretical amount of electric energy (i.e. exergy) extractable from the CHP heat.

5.3 Target variables

In the following section, the calculation methods for each of the objective variables used to evaluate the measures developed in this thesis will be presented.

5.3.1 Final energy supply

The final energy supply represents all energy streams leaving the heat and power station as heat, cooling and electric energy (see Fig. 3.1). The energy can either be transported directly to the users via the different networks, or first be stored in an energy storage to be used at a later point in time. Heat is supplied by HOB and CHP plants, cooling energy by absorption chillers and compression chillers, and the electric energy supply is divided in the supply from the CHP plants and from the electric grid. Electric energy needed to operate the energy system itself, such as energy for the district heating and cooling network pumps or the heat pump for the data center waste heat utilization, is declared as electric energy supplied to the contractor, not to the university. Energy for operational purposes is taken entirely from the electric grid and is not taken into account when calculating the share of CHP electric energy in the university's energy mix (see chapter 3.1).

5.3.2 CO_2 emissions

The CO_2 emissions of the different energy streams supplied are calculated using CO_2 emissions factors for natural gas and grid electric energy entering the system. Natural gas has a CO_2 emissions factor of $f_{\mathrm{CO2,gas}} = 0.202\,\mathrm{t_{CO2}}/\mathrm{MWh}$ [127]. The CO_2 emissions factor for grid electric energy depends on the mix of energy sources in the grid and theoretically changes constantly. The German Federal Environment Agency (Umweltbundesamt) publishes a yearly report on the development of the average CO_2 emissions factor of the German power mix [128]. To calculate the CO_2 emissions of campus Lichtwiese, the predicted factor for 2018 $f_{\mathrm{CO2,el,2018}} = 0.474\,\mathrm{t_{CO2}}/\mathrm{MWh}$, published in 2019, is used.

In order to further reduce its CO_2 emissions, the university itself purchases renewable electric energy. Renewable sources, such as photovoltaic or wind, are often considered to be emission free, omitting emissions for production, transport and disposal of the facilities [129]. Considering renewable electric energy instead of the German power mix in the context of this thesis would lead to the trivial solution to buy all electric energy from the grid and switch the heating and cooling supply to heat pumps and compression cooling with emission free electric energy. Since the goal of this work is to present measures to reduce emissions within a district and not by using external renewable energy, considering 100 % renewable grid electric energy is not within the scope of this thesis (see chapter 2.2).

5.3.3 Energy-related costs

To calculate the costs of the energy supply, the annuity method based on VDI 2067 [130] is used. This standard divides the total costs into capital-related costs (investment), operation-related costs, and demand-related costs (energy costs), and makes it possible to calculate the average total annual costs (annuity) over a defined period of time, taking into account an interest rate and a price change factor. In the context of this thesis, the capacity costs charged by the gas and electric grid operator for the maximum 15 minute average gas and electric power supply during a year, are taken into account as well. Additionally, CO_2 emissions cost are calculated, allocating a price to the climate impact of the energy system. The nominal interest rate is set to $q = 1.05$ and the price change factor to $r = 1.02$, which represents the desired inflation rate in the Euro zone [131]. The observation period is $t = 10\,\mathrm{a}$, which represents a short time compared to the average lifetime of the facilities in the district energy system. Decision-makers are often reluctant to base their investment decisions on very long observation periods, thus a short observation period is reasonable in this context. For longer observation periods, the profitability of the measures proposed in the following chapters would be even higher.

The annuity of the capital-related costs A_{inv} is determined multiplying the initial investment C_0 with the annuity factor f_{a}:

$$A_{\text{inv}} = C_0 \cdot f_{\text{a}} = C_0 \cdot \frac{q-1}{1-q^{-t}} \tag{5.3}$$

The annuity of the demand-related (energy) costs is calculated multiplying the demand-related costs of the current year $C_{\text{dem},1}$ with the annuity factor f_{a} and the price-dynamic cash value factor f_{b}:

$$A_{\text{dem}} = C_{\text{dem},1} f_{\text{a}} f_{\text{b}} = C_{\text{dem},1} \cdot \frac{q-1}{1-q^{-t}} \cdot \frac{1-\left(\frac{r}{q}\right)^t}{q-r} \tag{5.4}$$

The same approach is used to calculate the annuity of the capacity costs:

$$A_{\text{cap}} = C_{\text{cap},1} f_{\text{a}} f_{\text{b}} \tag{5.5}$$

The annuity of the operation-related costs A_{op} represents a share of the initial investment:

$$A_{\text{op}} = C_0 f_{\text{op}} f_{\text{a}} f_{\text{b}} \tag{5.6}$$

The factor f_{op} combines the cost factors for maintenance, servicing and inspection. In [130], detailed factors for each facility are listed. In the context of this thesis, simplified approach is used and an average factor for operation-related costs $f_{\text{op}} = 1.03$ is taken into account for all facilities.

The cost of CO_2 emissions depends on the assumed specific CO_2 emissions price c_{CO2} and the CO_2 emissions factor f_{CO2}. In this study, $c_{\text{CO2}} = 135\,\text{US\$}_{2010}/\text{t}$ ($c_{\text{CO2}} = 123\,€/\text{t}$) is used, which is the minimum specific CO_2 emissions price necessary in 2030 to reach a maximum global temperature increase of 1.5 °C according to the Intergovernmental Panel on Climate Change (IPCC) [132]. A study by the German "Umweltbundesamt" suggests that even this price might be too low to mitigate the consequences of climate change effectively, suggesting a price of $c_{\text{CO2}} = 180\,€_{2016}/\text{t}$ as the cost of damages created by the emission of CO_2. The annuities of the CO_2 prices for gas $c_{\text{CO2,gas}}$ and grid electric energy $c_{\text{CO2,el}}$ can be calculated as follows:

$$\begin{aligned} c_{\text{CO2,gas}} &= f_{\text{CO2,gas}} \cdot c_{\text{CO2}} f_{\text{a}} f_{\text{b}} \\ c_{\text{CO2,el}} &= f_{\text{CO2,el,2018}} \cdot c_{\text{CO2}} f_{\text{a}} f_{\text{b}} \end{aligned} \tag{5.7}$$

Table 5.1 shows the assumptions made for the calculation of the costs of the energy supply at TU Darmstadt campus Lichtwiese. All prices include taxes and other charges. The table also states for which year the prices were defined in the respective sources.

Table 5.1: Assumptions for the cost calculations.

Description	Variable	Value	Year	Source	Comment
Energy price gas	$c_{E,gas}$	32 €/MWh	2019	[133]	
Energy price grid electric energy	$c_{E,el}$	160 €/MWh	2019	[133]	
CO_2 emissions price	c_{CO2}	123 €/t_{CO2}	2019	[132]	
Capacity cost gas	$c_{cap,gas}$	6550 €/MW	2020	[134]	Calculated based on capacity demand reference scenario
Capacity cost grid electric energy	$c_{cap,el}$	44 400 €/MW	2020	[135]	Medium voltage 20 kV
Investment HOB	$c_{gen,HOB}$	27 000 €/MW_{th}	2013	HOB TU Darmstadt	
Investment CHP	$c_{gen,CHP}$	250 000 €/MW_{th}	2014	[136]	
Investment AC	$c_{gen,AC}$	380 000 €/$MW_{th,cool}$	2012	[16]	
Investment CC	$c_{gen,CC}$	215 000 €/$MW_{th,cool}$	2012	[16]	
Investment HP/HPC	$c_{gen,HP/HPC}$	250 000 €/$MW_{th,heat}$	2020	Heat pump TU Darmstadt	
Investment PV	$c_{gen,PV}$	1 140 000 €/MW_p	2019	[137]	
Investment BHS	$c_{TES,BHS}$	4310 €/MWh	2013	[15]	Costs converted from €/m^3 to €/MWh
Investment SHS	$c_{TES,SHS}$	1230 €/MWh	2013	[15]	Considering economies of scale
Investment CS	$c_{TES,CS}$	57 500 €/MWh	2006	[138]	

6 Model description

To carry out an analysis of the current performance of an energy system and to derive improvement measures, a model of the system has to be created. A model is a description of a real system and serves to better understand the effects of changes in the energy demand of buildings or in the generation infrastructure or the distribution network on the economic and ecologic performance of the energy system as a whole. With the help of a model, different scenarios for the future design and operation of an energy system can be compared, or optimization algorithms can be implemented to determine the optimal scenario for a given energy demand. Before setting up a model, the possible and necessary level of detail has to be decided upon. Depending on the available data and the goal of the analysis, input and output variables as well as system boundaries have to be defined.

In the context of this thesis, a model of the TU Darmstadt energy system was created. With the help of this model, annual simulations of the operation of the campus energy system are carried out. The model determines the losses in the district heating network and the efficiency of the generation units and storage, depending on the building energy demand and the network temperature at each time step. It derives an operation strategy and calculates the resulting demand of natural gas and grid electric energy as well as the resulting CO_2 emissions and costs. The model was developed using the MATLAB/Simulink software packages [139] as well as the Simulink toolbox CARNOT [140], which offers predefined components for the modeling of thermal energy systems. To gain a comprehensive understanding of the operation of an energy system, all relevant components have to be included in one model. Therefore, all available generation plants (CHP, HOB, absorption chiller, compression chillers) as well as available and possible future thermal storage (buffer heat storage, seasonal heat storage, cold storage) are mapped. The model also includes a detailed representation of the district heating network and the buildings at campus Lichtwiese, as well as the aggregated energy demand and temperatures of the other campus areas belonging to TU Darmstadt. The district cooling network is not modeled in detail, because temperature differences between the average network temperature and the ground are small, and network heat losses or gains in district cooling are negligible. Fig. 6.1 gives an overview of the components of the model. In this chapter, the model input and output data as well as the components included and the simulation parameters will be explained in detail. Chapter 6.6 presents a validation of the model.

In the following chapters, this model is referred to as ”energy system model”. The purpose of the model is to compare different measures to improve the design and operation of the energy system to the current setup (chapter 7), and to evaluate the impact of a reduction of temperatures and heat demand (chapter 8) as well as the use of the waste heat from the university data center (chapter 9). All measures will be compared based on the target variables final energy supply, CO_2 emissions and costs presented in chapter 5. Therefore, different improvement scenarios are compared to a reference scenario representing the current (2018) design of the system.

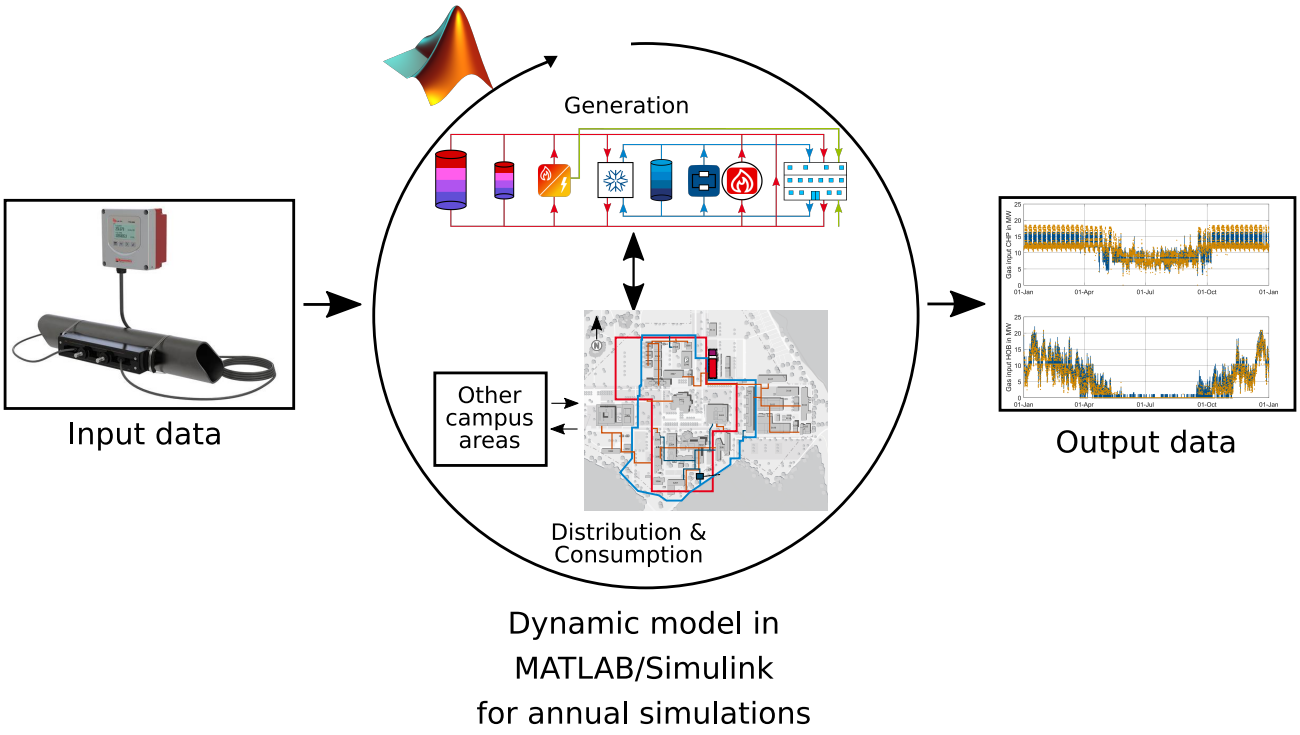

Fig. 6.1: Dynamic MATLAB/Simulink simulation model of the TU Darmstadt energy system.

6.1 System boundary

Although campus Lichtwiese represents a stand-alone area on the outskirts of Darmstadt, it is closely connected to other campus areas of TU Darmstadt. The HPS does not only supply the campus itself but also the rest of the university with electric energy and heat, thus the other areas must also be taken into account when optimizing its design and operation. The chosen modeling approach includes the supplied areas outside of campus Lichtwiese in an aggregated form. Final energy demand, CO_2 emissions and costs are attributed to campus Lichtwiese according to the fraction of final energy supplied to the campus in each time step. District cooling is only available at campus Lichtwiese and consequently attributed entirely to this area.

6.2 Model input data

Central input of the model are annual time series from the primary side heat monitoring of the final energy supply at the buildings' boundary. Additionally, aggregated annual time series for cooling as well as electric power demand are used, and climate data for network heat loss calculation is supplied by a nearby weather station of the German weather service (Deutscher Wetterdienst - DWD) [141]. While the weather station measures ambient air temperature, the heat losses depend on the ground temperature, which has a reduced amplitude by about 20 % compared to the air temperature, and a time lag of several weeks at a depth of 0.5-1 m [4].

6.2.1 Building heat demand and standardization of heat demand data

Substation heat monitoring consists of a measurement of the supply and return temperatures and the mass flow. The network supply temperature is not controlled at the substations, but centrally at the HPS. It depends on the building with the highest supply temperature demand. Even though heat monitoring at the HPS is available (see chapter 4.1), the respective meter only measures one out of five heating circuits of the TU Darmstadt district heating network (see chapter 3.2). The supply temperature is not necessarily the same in all heating circuit and the measured supply temperature may be below the temperature demand of the critical building. Therefore, the supply temperature in the model represents the maximum of the supply temperatures measured at the individual buildings. In the model, different supply temperatures are defined for campus Lichtwiese and the remaining campus areas, reflecting the operation of the real system.

Based on the network supply temperature, the model calculates the resulting supply temperature at each substation depending on the distribution heat losses. Together with the building heat demand and the substation return temperature, which are used as model input data, the mass flow at each substation can be calculated. The resulting mass flow once again has an impact on the substation supply temperature. The mass flow measurement data from the heat meters is not an input variable to the model, but serves for validation purposes (see chapter 6.6).

The heat demand curve of TU Darmstadt is typical for the climate region the university is located in, showing significant temperature differences between warm summers and cold winters. The heat demand is directly related to the ambient temperature and other environmental influences, such as humidity and wind speed. Thus, the demand of two consecutive years can differ significantly. To deduce general conclusions for the future design and operation of the district, it is necessary to standardize the heat demand, deriving a heat demand curve valid not for one specific year, but for a year with typical ambient conditions. The influence of different environmental factors on the heat flow is determined via polynomial regression. The regression is based on measurement data of the buildings' heat demand recorded between the end of 2016 and the middle of 2019 and carried out using the statistics software package R [142]. An evaluation of different possible regression models showed that independent variables with an influence on the building heat demand are ambient temperature T_{amb}, relative humidity ψ and wind speed w. The wind speed has an influence on the natural ventilation of the buildings, and increases the building heat demand depending on the difference between the ambient temperature of the infiltrated air and the room temperature [143].

Due to the heat storage capacity of the buildings, not only the ambient temperature at a certain point in time is relevant for the heat flow at that moment, but also the historical development of the ambient temperature. Directly after a sudden ambient temperature drop, heat flow is lower than after several days at the same low temperature, due to the heat stored in the building structure during warmer days, which supplies part of the building's heat demand for a certain time. Therefore, first differences of the ambient temperature with a delay of 24 ($T_{\text{amb,24}}$), 48 ($T_{\text{amb,48}}$) and 72 ($T_{\text{amb,72}}$) hours are taken into account in the regression model. The impact of this phenomenon depends on the heat storage capacity of each building. In addition, dummy variables are introduced, to distinguish between day and night f_{dn}, weekday and weekend f_{w}, and summer and winter f_{winter}. ϵ represents the residual of the regression.

After the comparison of different regression models, the following option turned out to yield the highest adjusted coefficients of determination R^2_{adj} for the heat flow of the buildings j. The coefficient of determination R^2 is defined as the proportion of the variance of the dependent variable described by the regression compared to the total variance. Since R^2 will always increase when more independent variables are considered, the

adjusted coefficient of performance R^2_{adj} takes into account the number of independent variables in the regression [144].

$$\begin{aligned}\dot{Q}_{\text{reg},j} = (&\beta_{0,j} + \beta_{1,j} T^3_{\text{amb}} + \beta_{2,j} T^2_{\text{amb}} + \beta_{3,j} T_{\text{amb}} + \beta_{4,j} w^2 + \beta_{5,j} w + \beta_{6,j} \psi + \\ &\beta_{7,j} T_{\text{amb,24}} + \beta_{8,j} T_{\text{amb,48}} + \beta_{9,j} T_{\text{amb,72}} + \beta_{10,j} f_{\text{dn}} + \beta_{11,j} f_{\text{w}}) \cdot f_{\text{winter}} + \epsilon\end{aligned} \tag{6.1}$$

Fig. 6.2 shows the comparison of the measured heat flow and the regression results as well as the residual $\epsilon = \dot{Q}_{\text{meas}} - \dot{Q}_{\text{reg}}$ of the regression for two example buildings. The old Civil Engineering institute building 3501 displayed in the upper part of the diagram represents the old building infrastructure built in the 1960s and 1970s. The energy center 3108 displayed in the lower part stands for the recent construction activity in the last decade. For all building types, the model yields a good correlation between the heat demand measured and the result of the regression analysis. The adjusted coefficient of determination for the models lies between $R^2_{\text{adj}} = 0.75$ and $R^2_{\text{adj}} = 0.95$, depending on the building. Based on the results of the regression analysis, standardized heat demand curves that do not depend on one year's weather characteristics can be created, using the test reference year weather data published by the DWD [141]. This data statistically summarizes the characteristic weather pattern of an average year. Fig. 6.3 shows the heat demand curve of the old civil engineering institute building 3501 for the test reference year.

Unlike heat demand, supply and return temperatures as well as substation mass flow for each building are not standardized. The heat demand is connected to the temperature difference, but the actual temperature level depends on additional factors such as the design of substation and heaters as well as the operation strategy applied. Those factors are difficult to model in a regression, hence the simulation relies on measured temperature data from 2018. The mass flow depends on both the heat demand and the difference between supply and return temperatures.

6.2.2 Building cooling demand

A central cooling network is only available at campus Lichtwiese, and cooling energy is mainly used for process cooling purposes in the data center and in laboratories in the Mechanical Engineering and Chemistry departments. Peak demand in the summer season is related to space cooling of critical areas such as lecture halls. Air conditioning for offices is not available and not foreseen by the university in the near future. Nevertheless, it is expected that cooling demand will be rising, because of an increased demand for constant ambient conditions for ever more sophisticated experiments.

Currently, twelve buildings are connected to the district cooling network, the most important user being the high performance computer with an annual average cooling load of $\overline{\dot{Q}}_{\text{cool}} = 550\,\text{kW}$. Additional decentral cooling supply via small compression chillers exists in several buildings. No documentation is available about decentral chillers, hence these facilities are not considered explicitly for the studies carried out here. The energy demand of those chillers is part of the electric energy demand. Fig. 6.4 shows the aggregated cooling energy demand of campus Lichtwiese, not including decentral compression chillers.

In theory, cooling monitoring data has been available since the end of 2016. However, most buildings supplied by the district cooling network were connected only over the course of 2017. The total cooling energy demand in 2018 was $Q_{\text{cool}} = 8000\,\text{MWh/a}$. Since process cooling is mostly independent from climate conditions, no standardization of cooling demands is carried out. The temperatures in the supply and return lines of the district cooling network are considered to be constant at the design temperatures of $T_{\text{s,DC}} = 6\,°\text{C}$ (supply

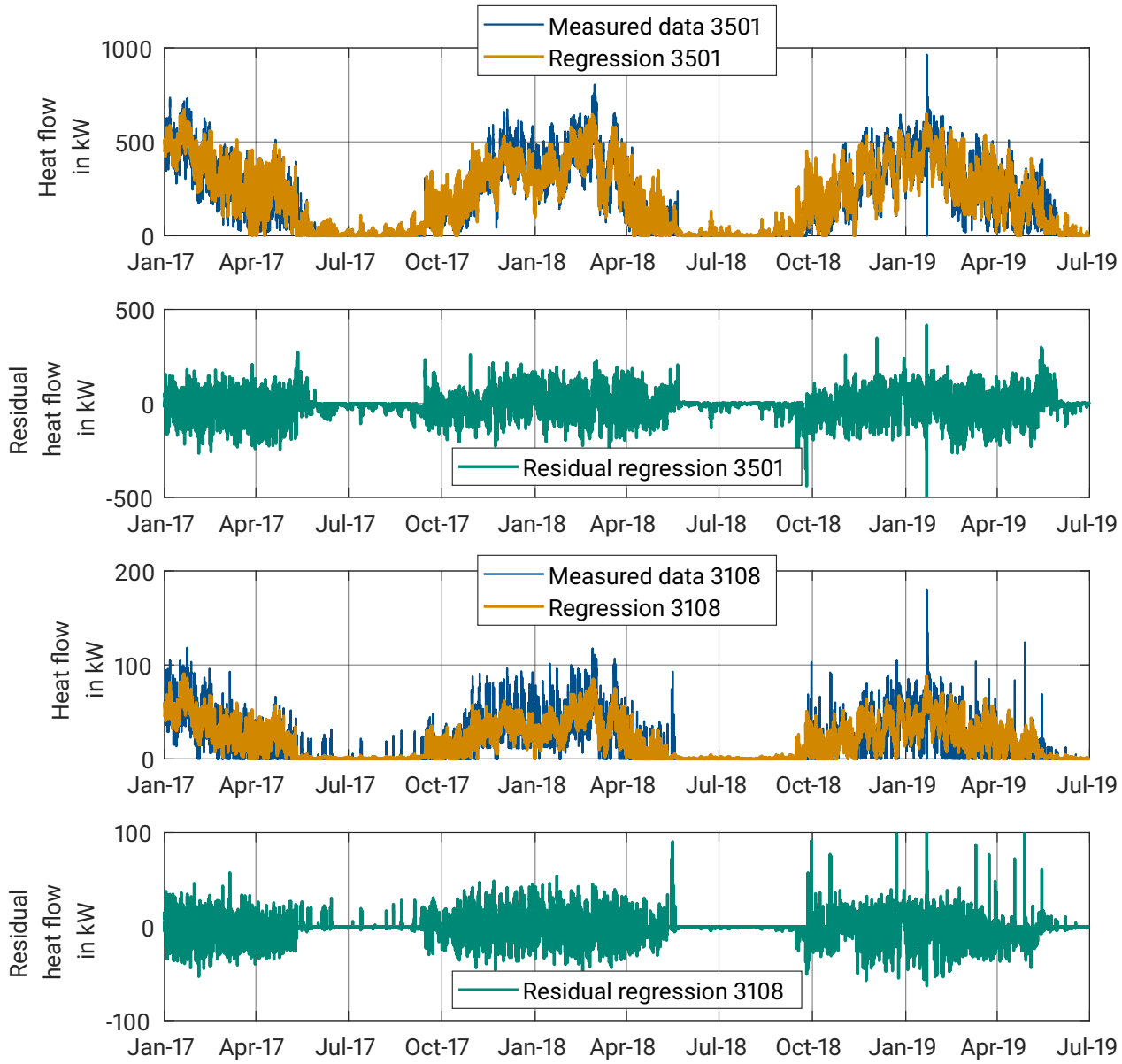

Fig. 6.2: Measured heat flow data vs. regression results in the old Civil Engineering institute building 3501 and the energy center 3108 (resolution: 1 h).

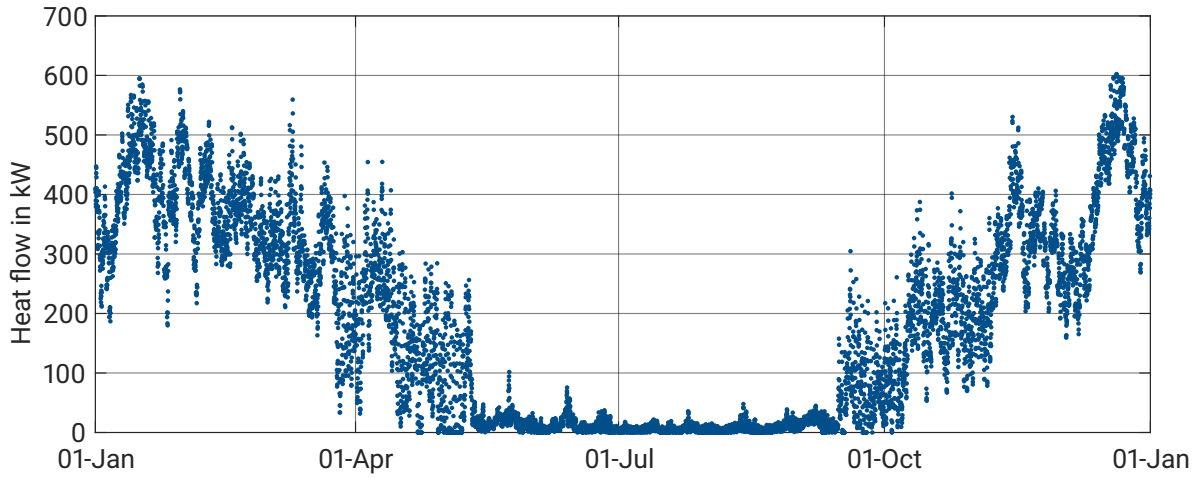

Fig. 6.3: Annual standardized heat flow old Civil Engineering institute building 3501 (resolution: 1 h).

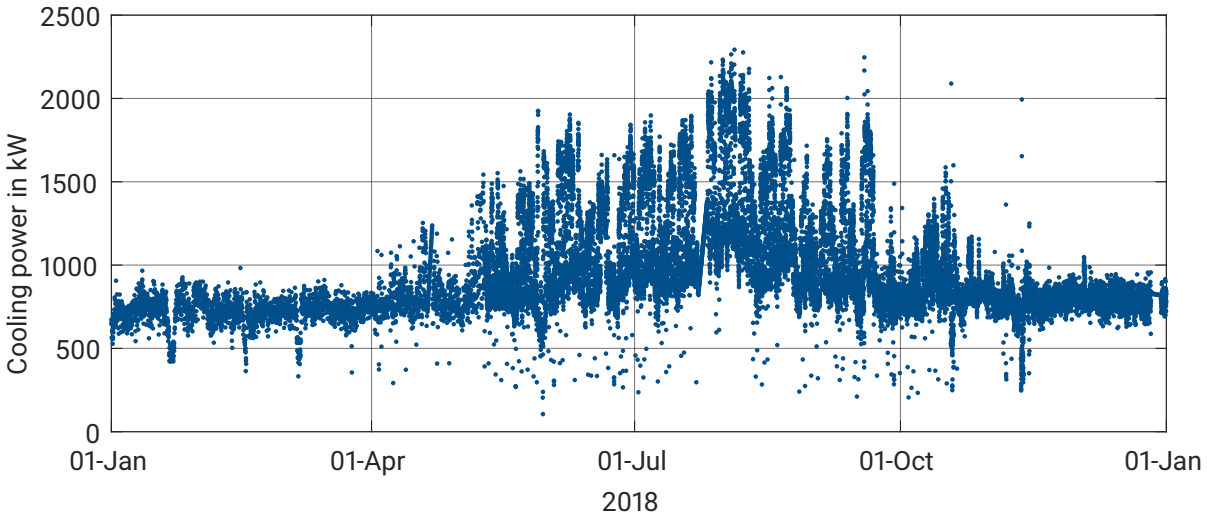

Fig. 6.4: Cooling power demand Lichtwiese 2018 (resolution: 1 h).

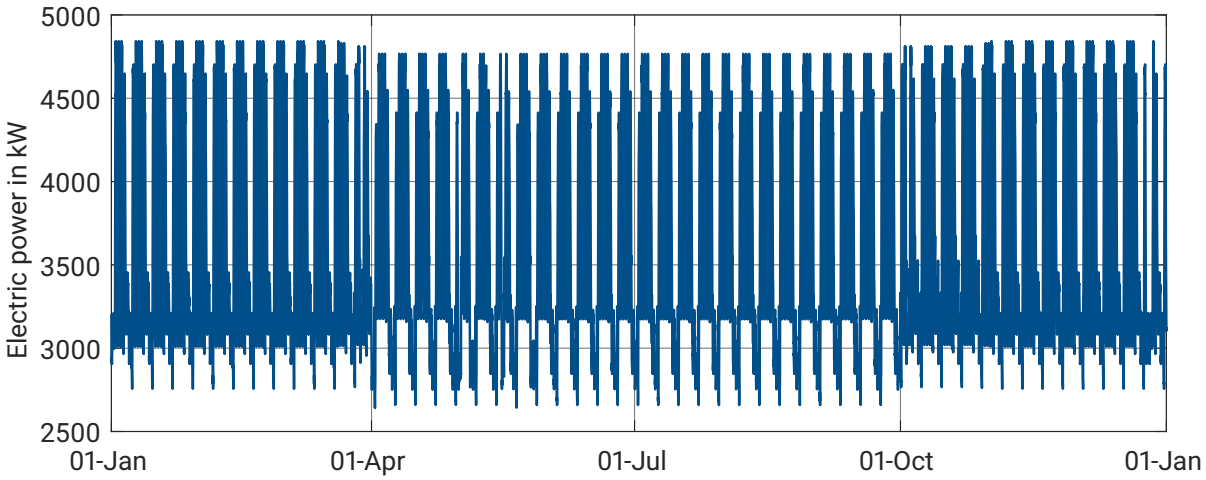

Fig. 6.5: Yearly demand load pattern for electric power at campus Lichtwiese (resolution: 15 min).

temperature) and $T_{\mathrm{R,DC}} = 12\,°\mathrm{C}$ (return temperature). In reality, both supply and return temperatures fluctuate slightly around the design value, but since network losses in the cooling network are negligible, a detailed modeling of the network temperature would not lead to a considerable improvement of the accuracy of the simulation results.

6.2.3 Electric energy demand

For the electric energy demand, in the past only monthly or quarterly manual meter readings in the different buildings were carried out for accounting purposes. The resolution of this data is too low for the analyses carried out in this thesis. Instead of using historic monitoring data, mobile measuring equipment was installed during three weeks in the summer of 2016 and the winter of 2017, during the semester and between semesters, to test for seasonal differences in demand. The result of this measurement campaign shows that the electric energy demand depends only marginally on seasonal effects and shows a low volatility over the course of the year. Since all buildings on campus are non-residential, most students and university employees are present only during daytime on weekdays, leading to characteristic daily and weekly cycles. It was concluded that the measured patterns can be extrapolated to generate a yearlong electric energy demand curve. Fig. 6.5 shows the resulting yearly electric energy demand curve for campus Lichtwiese. The resolution of the data is 15 minutes, as in the case of the heating and cooling data. Based on this curve, the total electric energy demand of campus Lichtwiese amounts to $E_{\mathrm{el}} = 31\,300\,\mathrm{MWh/a}$. To use this curve as a model input representing the electric energy demand of the entire university, it was multiplied by a factor of $f_{\mathrm{el,TUD}} = \frac{54\,600\,\mathrm{MWh/a}}{31\,300\,\mathrm{MWh/a}} = 1.74$ (2018), which is the ratio between the electric energy demand of campus Lichtwiese and the entire university.

Part of the electric energy demand is the demand for grid pumps and central compression chillers. Since TU Darmstadt does not pay the contractor for the energy required for generation, but for energy consumption for heating, cooling, and electric energy in the respective buildings, the electric energy for generation purposes, such as for network pumps, central compression chillers or the heat pump for data center waste heat utilization, is not part of the university's electric energy demand. This electric energy is attributed to the contractor. It is subtracted from the campus demand profile and it is assumed that this demand is met entirely by grid electric energy.

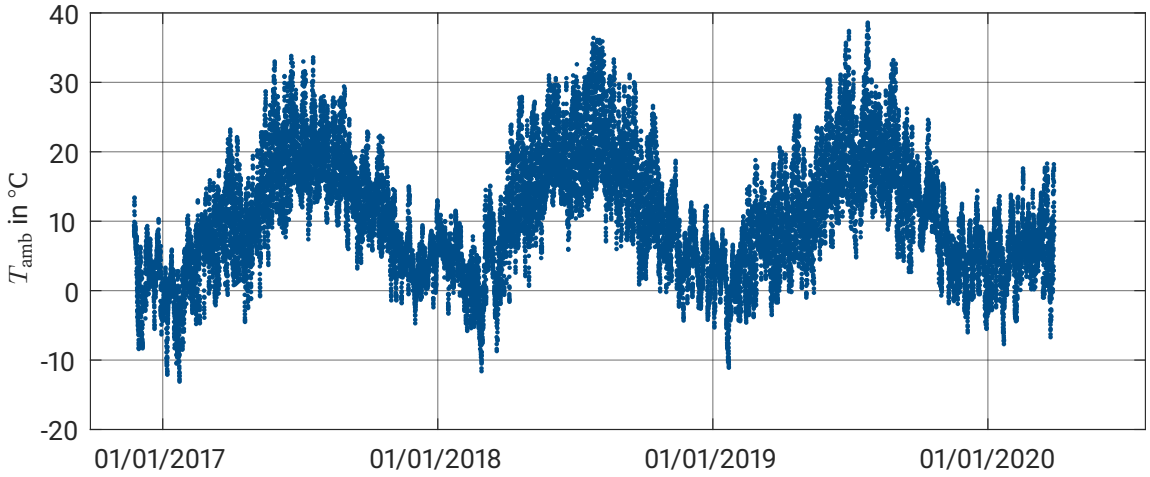

Fig. 6.6: Ambient temperature Darmstadt November 2016 - March 2020 (resolution: 1 h).

6.2.4 Climate data

In addition to the data regarding the buildings' energy demand, climate data is essential for modeling purposes. It is needed to predict future building heat demand and to calculate the losses in the district heating network as well as the resulting temperatures in the pipes. The closest weather station recording data for the national weather service (Deutscher Wetterdienst) is station 917 located about 2 km off campus Lichtwiese [145]. The weather station records not only ambient air temperatures, but also other relevant data such as relative humidity and wind speed. Fig. 6.6 shows the development of ambient air temperatures between November 2016 and March 2020. In the last three years, winters have been extraordinarily mild and temperatures below −10 °C have occurred only on very rare occasions. The annual average ambient air temperature for the years 2017-2019 is 11.1 °C, compared to the long term average of 10.2 °C. Nevertheless, the temperature profiles of these last years provide a good indication for the future climate situation in Darmstadt, where climate change will most probably make mild winters and hot and dry summers more common.

To calculate the heat losses from the district heating pipes in the energy system model, the ambient ground temperatures have to be considered. They depend on the ambient air temperature, but show lower amplitudes. In the model, an amplitude reduction by 20 % is considered [4].

6.3 Modeling of the generation units and thermal storage

A special focus in the modeling of the energy system is put on generation plants and thermal storage facilities (see Fig. 6.7). In this section, the different generation and storage options used at TU Darmstadt are described in detail.

6.3.1 CHP plants

The combined heat and power units installed at the TU Darmstadt consist of a gas engine to generate electrical energy and four different heat exchangers connected in series to cool the engine and recover its waste heat.

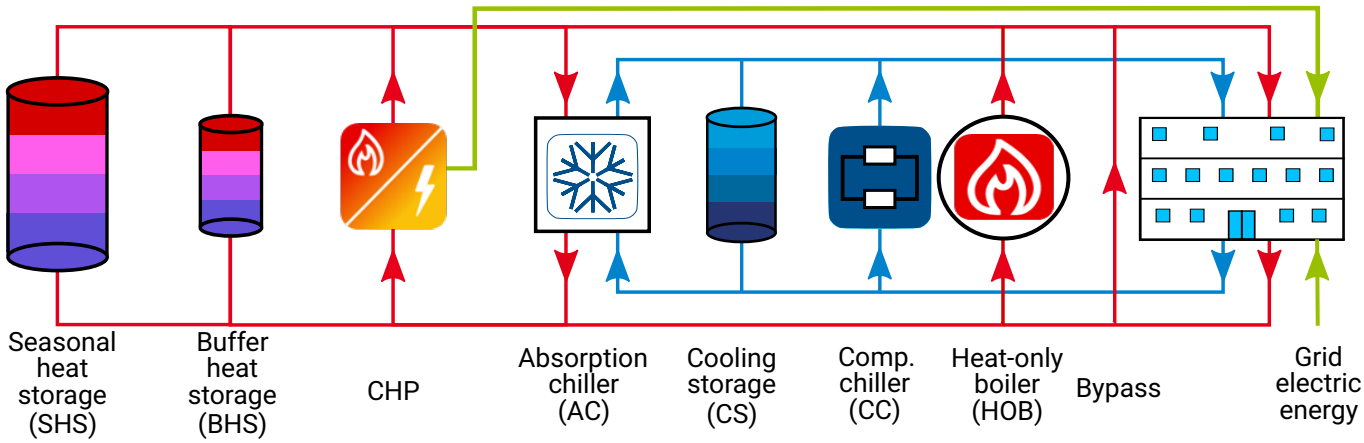

Fig. 6.7: Schematic representation of the energetic infrastructure at TU Darmstadt.

The heat exchangers serve to cool the fuel-air mixture after the compression in the engine's turbocharger, the lubricant oil supply as well as the engine itself. They also recover the heat from the exhaust gas leaving the combustion process. Fig. 6.8 illustrates the setup of the heat exchangers in the new CHP plant GE Jenbacher JMS 620, installed at the HPS in 2017.

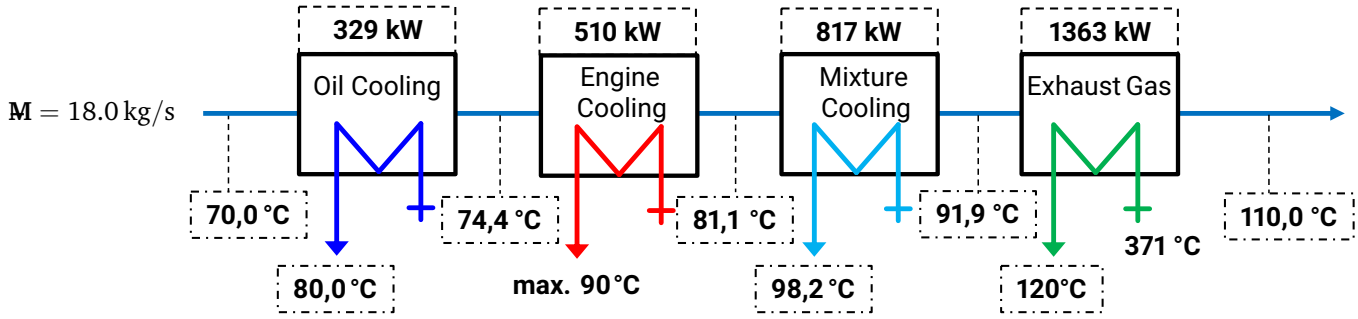

Fig. 6.8: Heat exchangers in GE Jenbacher JMS 620 CHP plant including temperatures, mass flow and heat flow at full load (adapted from datasheet of CHP plant installed at TU Darmstadt).

The thermal and electric efficiency of CHP plants varies, depending on the supply and return temperatures of the district heating system they are connected to, and the partial load they are operating at. The lower the temperatures of the district heating system, the higher the thermal efficiency of the plant, at approximately constant electric efficiency. Operation at partial load increases the exhaust gas temperature at the inlet of the exhaust gas heat exchanger, i.e. improves the thermal efficiency, but lowers the electric efficiency of the unit. The model of the CHP plants calculates the input gas power for each time step. The heat recovered in the exhaust gas heat exchanger is calculated considering the thermodynamics of the combustion process. The first law for the exhaust gas stream states:

$$\dot{Q}_{\mathrm{exh}} = \sum_{n} \Delta h_n \cdot \dot{M}_n \tag{6.2}$$

The heat flow rate $\dot{Q}_{\mathrm{exh}}$ from the exhaust gas flow depends on the specific enthalpy difference Δh_n of the components n of the exhaust gas that is calculated using the average heat capacity $[c_{p,n}]_0^T$ of each component:

$$\Delta h_n = [c_{p,n}]_0^{T_{\mathrm{in,exh}}} \cdot T_{\mathrm{in,exh}} - [c_{p,n}]_0^{T_{\mathrm{out,exh}}} \cdot T_{\mathrm{out,exh}} \tag{6.3}$$

In the CHP plants at TU Darmstadt, natural gas H with an average lower heating value (LHV) of $H_\mathrm{i} = 10.1\,\mathrm{kWh/m^3}$ is used. Its exhaust gas mainly comprises water vapor (H_2O), carbon dioxide (CO_2) and nitrogen (N_2). Since the cogeneration plants realize a lean combustion, the exhaust gas also contains unprocessed oxygen (O_2). The exhaust gas temperatures at the entry and exit of the exhaust gas heat exchanger $T_\mathrm{in,exh}$ and $T_\mathrm{out,exh}$ are defined as a model input. The reference incoming exhaust gas temperature is $T_\mathrm{in,exh} = 371\,°\mathrm{C}$. $T_\mathrm{out,exh}$ depends on the fluid temperature at the exit of the heat and power station, i.e. the network supply temperature T_S. The model makes it possible to quantify the increase of the thermal efficiency generated by decreasing the outgoing exhaust gas temperature $T_\mathrm{out,exh}$ [103]. If the network return temperature were decreased below the dew point temperature of water in the flue gas (usually between 40-60 °C, depending in the water vapor concentration in the flue gas [146]), flue gas condensation could be realized. Flue gas condensation makes use of the phase change enthalpy of the water in the exhaust gas, increasing the thermal efficiency of the plant by about 10 % [147]. For this purpose, the order of the heat exchangers in the CHP plants would have to be adapted, setting a condensation exhaust gas heat exchanger as the first one in the line. Due to a high space requirement for a condensation heat exchanger, such a device cannot be installed in all CHP plants, including the HPS at campus Lichtwiese. Therefore, flue gas condensation heat exchangers are not foreseen to be installed at the HPS and not included in the model either.

In the current setup, the CHP plants at TU Darmstadt are operated at constant temperatures of $T_\mathrm{in,CHP} = 70\,°\mathrm{C}$ input and $T_\mathrm{out,CHP} = 110\,°\mathrm{C}$ output temperature. When the return temperature from the network is lower than the required level, supply water can be added via a bypass, increasing the HPS input temperature. When the network return temperature is above 70 °C, hybrid coolers are used to dissipate heat to the environment, making sure that the maximum input temperature of the CHP plants is respected at all times. This operation mode allows the heat exchangers to operate at their design temperatures at all times, but it also becomes impossible to profit from increases in efficiency after lowering temperatures. In the model, temperature-dependent efficiencies were implemented, but will not be taken into consideration when calculating the potential savings in energy and CO_2 emissions generated by an optimization of the design and operation of the system (see chapter 7). To demonstrate the potential of a reduction the network temperatures, flexible input and output temperatures for the CHP plants will be considered in chapter 8.

The efficiency of CHP plants also depends on the partial load they are operating at. The lower the partial load operating point, the higher the thermal efficiency and the lower the electric efficiency of the engine. Above a partial load of 60 % of the electric capacity of the CHP plant, the change in electric efficiency is low, below 50 % efficiency decreases significantly [136]. Therefore, the operation strategy turns off a CHP plant when the electric power supply from that plant falls below 50 % of the nominal output. Between 50 % and 100 % nominal output, the plants are considered to be capable of a flexible operation. Nevertheless, load changes should be minimized to maximize the engines' life time.

6.3.2 Heat-only boilers

The efficiency of the heat-only boilers also depends on supply and return temperatures as well as partial load operation, but the influence of these factors is small compared to the case of the CHP plants. Therefore, a constant efficiency of $\eta_\mathrm{th,HOB} = \frac{\dot{Q}_\mathrm{HOB}}{\dot{E}_\mathrm{gas,LHV}} = 0.9$ according to [148] is considered in the context of this model. In contrast to CHP plants, HOB can operate at very low partial loads down to a minimum of 10 % of their design load, without significant losses in efficiency. This is especially important during summer months, when heat is almost exclusively used for hot water preparation and the demand falls below the minimum load of the CHP plants. The resulting gap needs to be closed by the HOB or by thermal storage if available.

6.3.3 Absorption and compression chillers

The absorption chiller installed in the campus Lichtwiese HPS in 2017 has a COP of $COP_{\mathrm{AC}} = \frac{\dot{Q}_{\mathrm{cool}}}{\dot{Q}_{\mathrm{CHP}}} = 0.74$ [149]. In reality, the COP of the AC depends on the temperatures on both the hot and the cold side. Since the temperatures of both the heat supply ($T_{\mathrm{in,CHP}} = 70\,°\mathrm{C}/T_{\mathrm{out,CHP}} = 110\,°\mathrm{C}$) and the cooling output ($T_{\mathrm{S,DC}} = 6\,°\mathrm{C}/T_{\mathrm{R,DC}} = 12\,°\mathrm{C}$) are constant, the COP_{AC} can be considered to be constant as well. Within the model, the AC is limited to using CHP heat. When the building heat demand is higher than the total thermal capacity of the CHP plants, heat for the AC would have to be supplied by the HOB at low total efficiency. This would lead to higher costs and CO_2 emissions than for cooling energy supplied via compression cooling. The energy efficiency ratio (EER) of the compression chillers depends on partial load operation and is determined based on [16]. At full load, the EER is $EER_{\mathrm{CC}} = \frac{\dot{Q}_{\mathrm{cool,CC}}}{\dot{E}_{\mathrm{el,CC}}} = 5.6$.

6.3.4 Thermal storage

Thermal storage systems represent a central component in energy systems based on combined heat and power. CHP plants always generate heat and power simultaneously and can only operate when there is sufficient demand for both types of energy in the system connected. Thermal energy for heating and cooling can be stored more easily and at much lower cost than electric energy, which is why thermal storage serves as a way to increase the flexibility of a CHP plant and shift the operation mode from a heat-guided to an electricity-guided regime. In chapter 7, it will be shown how larger storage capacities would make it possible to operate the TU Darmstadt energy system more closely depending on the electric power demand, decreasing the demand for grid electric power and ultimately the resulting CO_2 emissions.

Typical storage technologies for low temperature thermal energy are sensible stratified water storage tanks, providing a very inexpensive and efficient solution to store heat or cooling energy at temperatures between 0 °C and 95 °C to about 150 °C, depending on the pressure in the tank. For smaller volumes, tank storage is a very good solution, for larger volumes, pit storages can make sense because they reach very low specific costs. Another option are borehole thermal energy storages, using the heat capacity of the ground instead of water [150]. As long as temperatures remain below 100 °C, storages can be designed pressure-less, above this threshold temperature the storage has to be pressurized, to avoid boiling of the storage fluid, increasing the investment costs [15]. A stratified storage system has a higher exergy content than a storage with the same energy content and a homogeneous temperature, because exergy is destroyed during the destratification process [117].

The model makes it possible to evaluate the potential efficiency gains through an increase in storage capacities. In addition to heat and cooling buffer storage, which might be increased in size in the future, the model also takes into account a seasonal heat storage, a technology not yet available on site. The target temperature range of the storage tanks lies between the supply and the return temperatures of the respective networks. In the case of heat storage, this means a temperature range between 55 °C and 110 °C, depending on the season. For the seasonal storage, which is considered to be pressure-less, the maximum temperature is 95 °C. The lower temperature level is not limited, because an unused storage will always reach ambient temperatures in the long run, due to heat losses. The heat storage tanks in the model are considered to be in a discharged state at the beginning of the year, thus their initial temperature in the model is 55 °C.

The heat storage tanks are discharged directly into the supply line of the district heating system, hence the discharge temperature has to be in the range of the supply temperature of the network. To increase the temperature range in which the stored energy can be used, heat pumps are foreseen to boost the discharge

temperature when the temperature in the storage tank is approaching its lower limit. To ensure an efficient operation of the heat pumps, the minimum discharge temperature is defined to be at least $\Delta T_{\text{use}} = 10\,\text{K}$ above the return temperature. In the optimization of the system presented in chapter 7, the energy used for these heat pumps are taken into account. Alternatively, the increase of the temperature of the discharge mass flow from heat storage could also be realized via a supply flow admixture from the HPS, which would not lead to any additional investment costs. Therefore, investment costs for the heat pumps are not being taken into consideration

Since free space on campus is scarce, the maximum size of the seasonal heat storage is limited to 500 MWh (about 14 600 m^3, calculated using 65 °C as the minimum discharge temperature and 95 °C as the maximum storage temperature) in all scenarios. All three storage types (buffer heat storage, seasonal heat storage, cooling storage) are modeled as stratified tank storage. Although seasonal heat storage is often designed as a pit storage, it does make sense to consider a tank storage in this case, because the size of a possible seasonal storage in the case of TU Darmstadt is several times smaller than buffer storage tanks already constructed at other sites in Germany (e.g. in Mannheim with 43 000 m^3 [151]). The model divides the storage tanks into a predefined number of layers. Within one layer, the temperature is considered to be homogeneous. To quantify the thermal performance of the tanks, the German standard AGFW FW 313 [152] is used. The values for the thermal resistance originate from a reference project in Darmstadt, where the local utility company recently erected a stratified buffer heat storage with a size of 4000 m^3. This storage is insulated with mineral wool on the storage wall and the lid, while the bottom consists of an uninsulated concrete base plate. The maximum height for each storage type is predefined due to architectural constraints, the diameter depends on the result of the design optimization (see chapter 7). When charging the heat storage, the return flow is usually led back to the HPS. In the summer, when the network supply temperature is low and the storage temperature reaches its maximum, the return temperature while charging the storage can exceed the allowed return temperature of 70 °C for the CHP plants. When the return from the storage is above 75 °C, it is led directly to the network. This setup ensures that the heat loss in the HPS is low. Fig. 6.9 displays the different charging modes.

When describing the amount of energy available in a stratified heat storage, a distinction must be made between useful and stored energy content. The difference results from the respective reference temperature:

1. The useful energy content $E_{\text{TES,use},k}$ of a volume section k of a storage is the enthalpy difference between the mean temperature $\overline{T}_{\text{TES},k}$ of the section k and the return temperature of the district heating or district cooling network T_{R} at a given point in time. This represents the minimum or maximum temperature that the storage tank may reach in order to be useful. In the case of the heat storage, it makes sense to define the minimum temperature for discharge above the return temperature. This decreases the amount of useful heat for a certain storage volume, but also reduces the electric energy demand for a heat pump that is necessary to boost the temperature level of the storage discharge flow when operating at a low temperature level. In the context of the analysis carried out here, the minimum discharge temperature is $\Delta T_{\text{use}} = 10\,\text{K}$ above the return temperature.

$$E_{\text{TES,use},k} = V_{\text{TES},k} \cdot \rho_{\text{W}} \cdot c_{\text{W}} \cdot \left(\overline{T}_{\text{TES},k} - (T_{\text{R}} + \Delta T_{\text{use}})\right) \tag{6.4}$$

2. The stored energy content $E_{\text{TES,stor},k}$ represents the enthalpy difference between the mean temperature in a volume section k at a given point in time and the respective ambient temperature T_{amb}. The calculation of the stored energy is necessary to derive the thermal losses of the storage in the context of a linear optimization model:

$$E_{\text{TES,stor},k} = V_{\text{TES},k} \cdot \rho_{\text{W}} \cdot c_{\text{W}} \cdot \left(\overline{T}_{\text{TES},k} - T_{\text{amb}}\right) \tag{6.5}$$

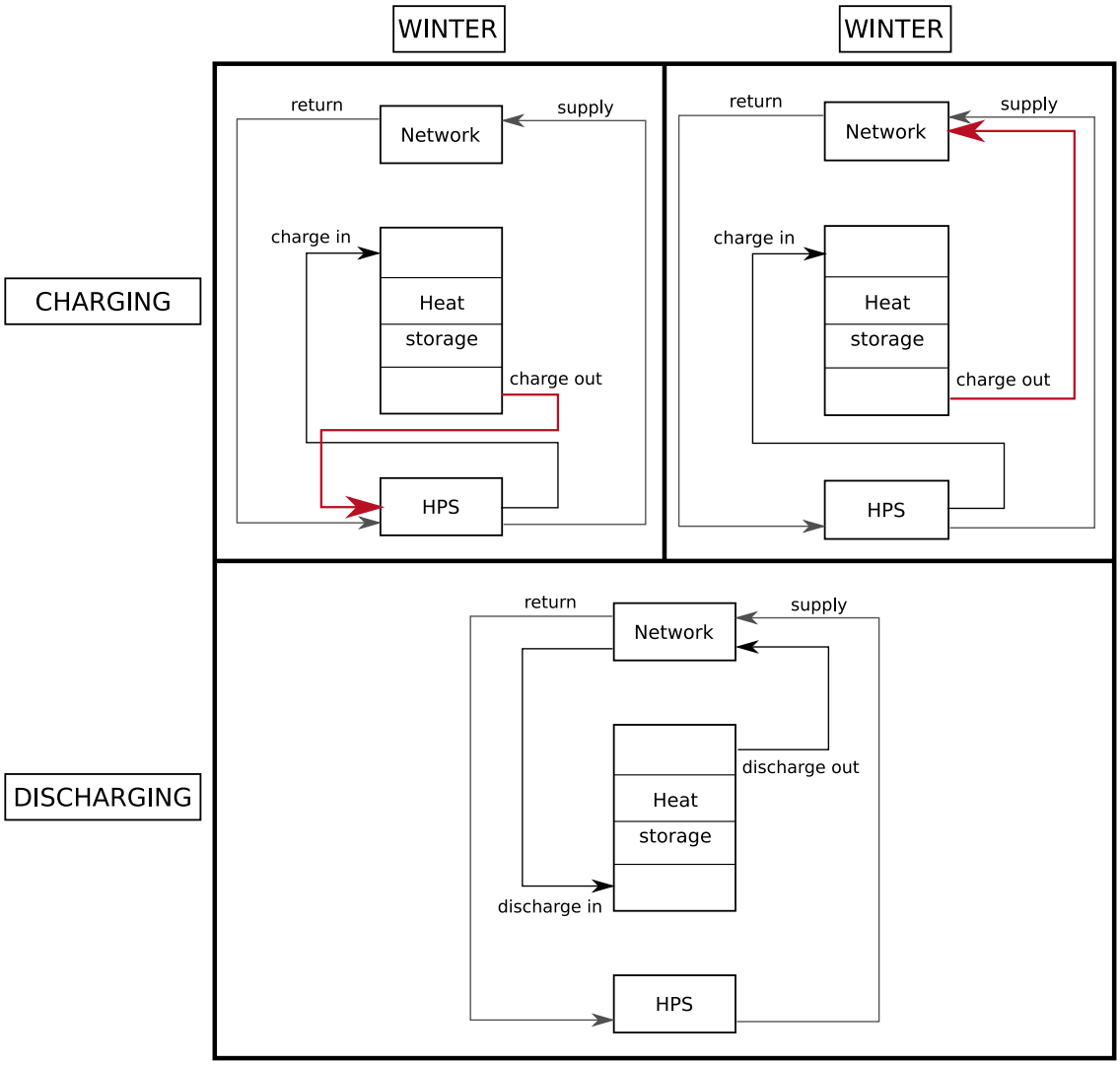

Fig. 6.9: Storage charging and discharging in summer and winter seasons.

3. In addition, it can be helpful to define the mean ambient temperature $\overline{T}_{\text{amb}}$ as a constant reference temperature. This makes it easier to determine in which periods the storage tanks are charged or discharged, because the changes of the energy content in the storage tank that otherwise occur due to fluctuations in the reference temperature are eliminated. The mean stored energy content $E_{\text{TES},\overline{\text{stor}},k}$ is defined as follows:

$$E_{\text{TES},\overline{\text{stor}},k} = V_{\text{TES},k} \cdot \rho_{\text{W}} \cdot c_{\text{W}} \cdot \left(\overline{T}_{\text{TES},k} - \overline{T}_{\text{amb}}\right) \tag{6.6}$$

The temperature range for the cooling storage is equal to the temperature level in the district cooling network between 6 °C and 12 °C. Equal to heat storage, the cooling storage is initially in a discharged state and its initial temperature in the model is 12 °C. In the cooling storage tank, depending on the ambient temperature, there is a heat flow from the tank to the environment (winter) or from the environment into the tank (summer). Since the average storage tank temperature corresponds approximately to the annual average ambient temperature, thermal losses play a subordinate role for cooling storage.

6.4 Modeling of the thermal networks

An important component of the model is a detailed representation of the district heating network at campus Lichtwiese. This is necessary to calculate the losses occurring in the heat distribution as realistically as possible. When calculating the heat losses of the pipes, it must be taken into account that the district heating pipes are not located in the undisturbed ground, but they influence each other. Therefore, the heat losses are calculated according to [4]:

$$\dot{Q}_{\text{DHN,loss}} = \frac{L\pi d \cdot \left[(T_{\text{S}} - T_{\text{amb,g}}) + (T_{\text{R}} - T_{\text{amb,g}})\right]}{R_{\text{ins}} + R_{\text{g}} + R_{\text{co}}} \tag{6.7}$$

The heat resistances of the insulation R_{ins}, the ground R_{g} and the coinciding temperature fields of the supply and return pipes R_{co} are defined as:

- Insulation resistance: $R_{\text{ins}} = (d/2\lambda_{\text{ins}}) \cdot \ln(D/d)$
- Ground resistance: $R_{\text{g}} = (d/2\lambda_{\text{g}}) \cdot \ln(4h/D)$
- Coinciding temperature resistance: $R_{\text{co}} = (d/2\lambda_{\text{g}}) \cdot \ln(((2h/s)^2 + 1)^{0.5})$

In this context, λ describes the thermal conductivity, L the route length of the pipes (i.e. the length of a single pipe in a 2-pipe network). d stands for the outer diameter of the pipe. The outer diameter can be used for heat loss calculation instead of the inner pipe diameter, because the temperature difference over the pipe wall is negligible compared to the temperature difference over the insulation material. D represents the outer diameter of the insulation material, s the distance between the centers of the two pipes and h the distance between the pipe centers and the ground surface. Fig. 6.10 shows the setup of the heat loss calculation for parallel heat distribution pipes.

In the model, the district heating pipes are divided in several discrete volume sections. The output temperature of each section represents the input temperature of its subsequent section. The greater the number of sections, the more precise the heat loss calculation becomes. At the same time, a more detailed resolution of the pipes also increases the computation time. With the help of the model and the primary side temperatures and mass flows at each building, the temperatures at the exit of the HPS can be simulated (Fig. 6.11).

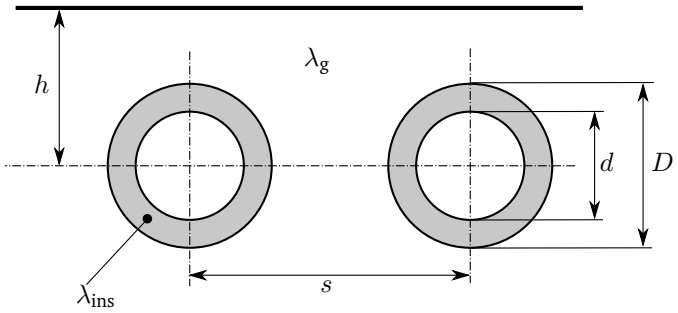

Fig. 6.10: Heat loss calculation for parallel distribution pipes (adapted from [4]).

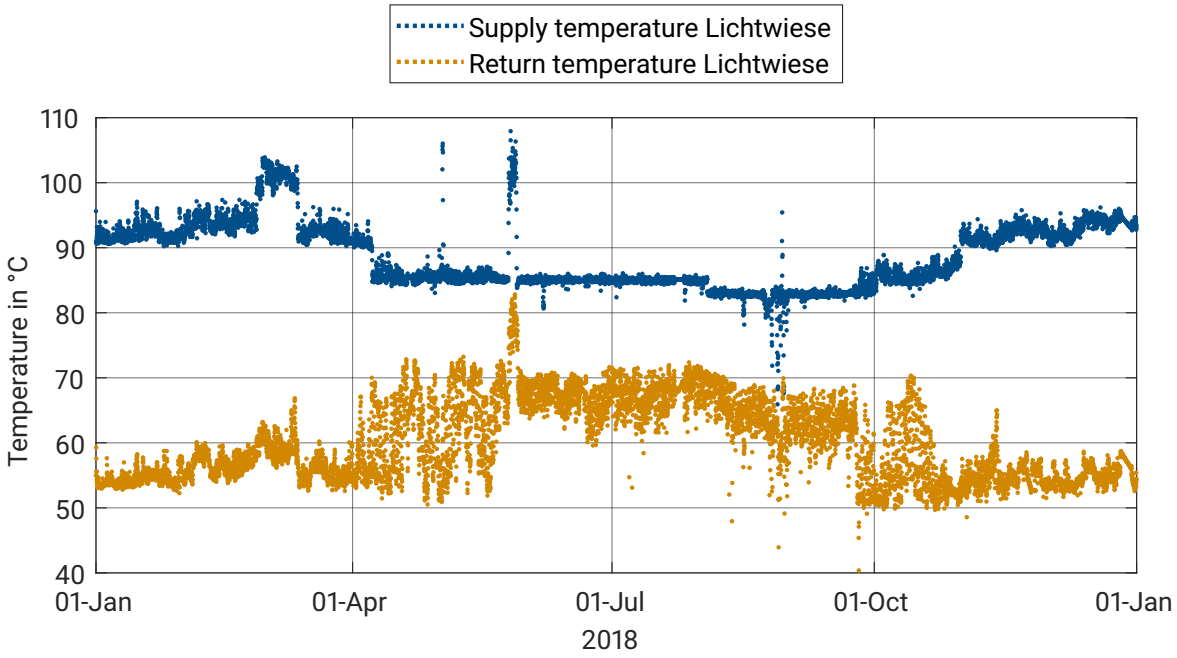

Fig. 6.11: HPS supply and return temperatures for TU Darmstadt Lichtwiese in 2018 (resolution: 1 h).

The network supply temperature is equal to the primary supply temperature of the building with the highest temperature requirement. The return temperature is the result of a mixing of the return flows from the different buildings, including network heat losses. Fig. 6.12 displays the supplied heat compared to the heat demand at campus Lichtwiese, with the difference being the network heat losses. Compared to the heat supplied, which undergoes significant seasonal changes, the network heat losses change only marginally throughout the year. This is because heat losses depend on the temperature difference between the fluid and the ground, which changes only to a small extend during the year. In summertime, the ground temperature rises and the supply temperature can be decreased, but return temperatures are higher than during winter months and the average temperature difference between the fluid and the ground remains roughly the same throughout the year. Accordingly, network heat losses reach up to 60 % of the total heat supplied in the summer, while in total 10 % of the heat supplied is lost in the network (resulting in total annual heat losses of $Q_{\text{loss,Liwi}} = 2600\,\text{MWh}$ for campus Lichtwiese). Network heat losses are even more significant for networks with lower heat demand densities or after an energetic renovation of the connected buildings. Therefore, it is crucial to focus on a reduction of network temperatures, otherwise the efficiency of district heating will

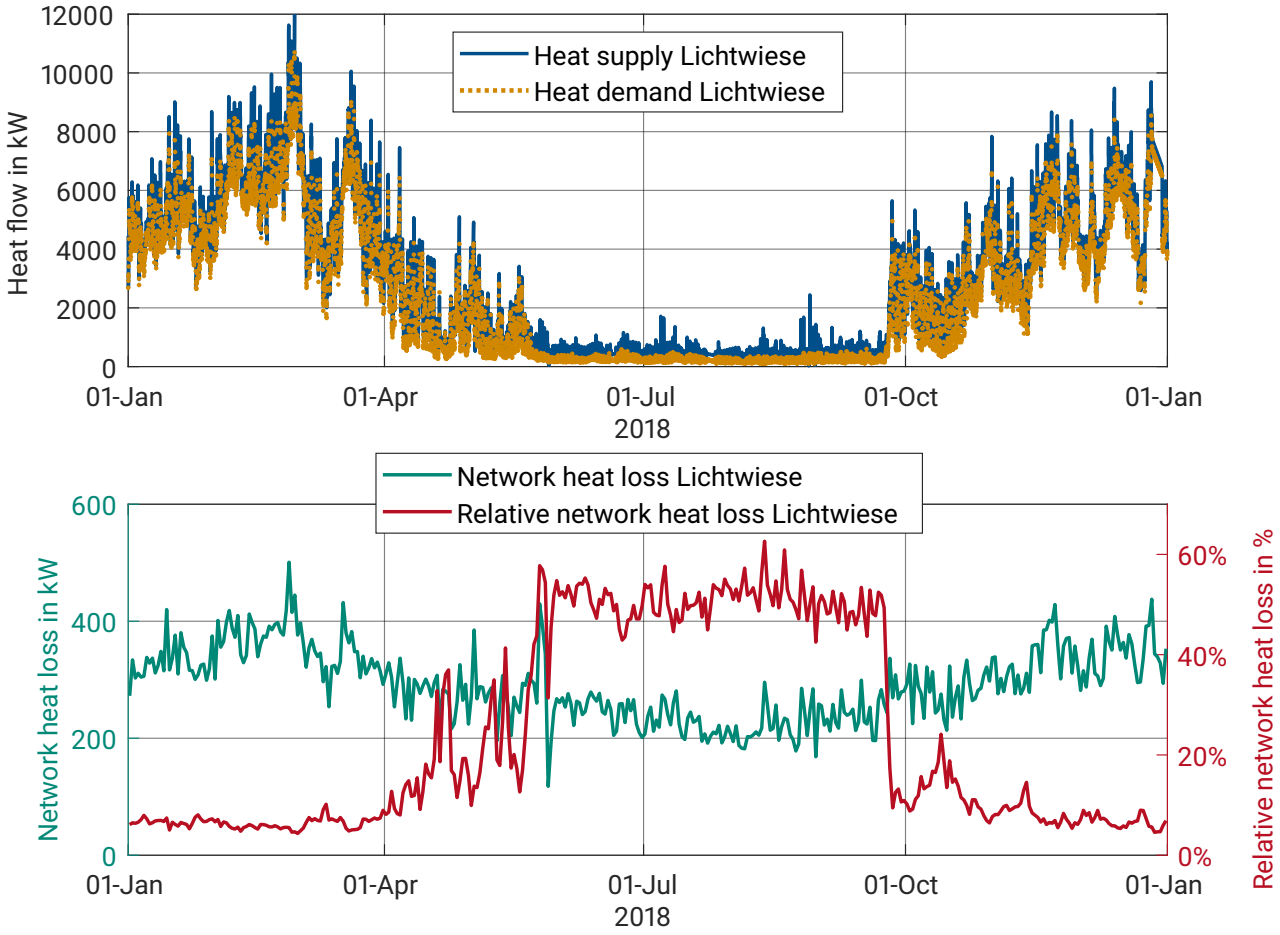

Fig. 6.12: Top: Comparison of heat supply and demand (resolution: 1 h) / Bottom: Absolute and relative network heat losses for campus Lichtwiese, based on measured data for 2018 (resolution: 24 h).

decline when the efficiency of the buildings increases. Chapter 8 will go into more detail on this topic.

Besides heat losses, pressure losses play an important role for the characterization of a district heating network. They increase with the velocity of the water mass flow and are thus dependent on the heat demand, the temperature difference between supply and return, and the pipe diameter. Large pipe diameters reduce pressure losses, but at the same time they lead to increasing heat losses. A compromise must be found to achieve the lowest possible total energy losses.

For the Lichtwiese campus, a detailed modeling of the network pressure losses cannot be realized. Many buildings are not hydraulically separated from the district heating network, hence a large part of the pressure losses occur within the buildings, where data on the pipe condition (length, diameter, number of bends) is not available. For this reason, an electric power demand for pumping of 0.5 % of the heat supply provided by the HPS is taken into account to compensate for pressure losses [4].

For the district cooling network, a simplified modeling approach is chosen. As the temperature level of the district cooling network is close to the annual average ambient temperature, it is assumed that the thermal

losses or inputs are negligible. Due to the much smaller temperature difference in the cooling supply compared to the district heating network, larger mass flows and thus larger pressure losses are present. Therefore, the electric power demand of the network pump is about 2 % of the cooling load [4].

6.5 Model simulation and output data

The model simulates the operation of the TU Darmstadt energy system over the course of one year. It a fixed time step size and a third-order explicit Runge-Kutta solver (ode3). The input data has a resolution of one hour per time step. Nevertheless, the step size for the solver is 8 s. This is necessary to avoid an error in the simulation, caused by a Courant number in the district heating pipes of $CFL = \frac{u \cdot \Delta\tau}{\Delta x} > 1$. In this equation, u stands for the flow velocity, $\Delta\tau$ describes the fixed time step size and Δx the length of each volume section in the pipe. When $CFL > 1$, the fluid in the pipes advances more than one volume section within a single time step and leads to an instability of the solver algorithm. Therefore, the step size has to be chosen depending on the volume flow in the pipes and the size of their volume sections.

The output data is recorded with a step size of one hour and includes the target variables final energy supply of heat, cooling and electric energy, CO_2 emissions and energy costs, exergy supply and demand as well as temperatures and mass flow at different points in the district heating system. The simulation results will be presented in detail in chapters 7-9.

6.6 Validation of the model

The model is validated using the results of a simulation with measured heat demand data at the substation level as input and comparing them to the data measured by the one meter installed at the HPS. Since the different parts of the university are connected via five different heating circuits, it is only possible to measure one circuit at a time. The meter available for validation purposes was installed at the beginning of 2018 on the western side of campus Lichtwiese heating ring.

The Lichtwiese west and Lichtwiese east heating circuits form the main ring of the campus district heating network, hence it is not clearly defined which buildings are supplied from which side. The best fit between the measured heat supply and the simulation is reached considering that the Lichtwiese west heating circuit supplies the civil engineering district (3501-3505 and 3560, excluding the new institute building 3506 as well as the new laboratory hall 3507), the university dining hall 3401, the center of smart interfaces (CSI) building 3206 as well as 60 % of the heat demand of the architecture district (3301, 3360, 3362). The exact distribution of the heat supply between Lichtwiese west and Lichtwiese east can only be determined once the Lichtwiese east heating circuit is also monitored via a heat meter. The area considered as supplied by the Lichtwiese west heating circuit is illustrated in Fig. 6.13.

In Fig. 6.14, the comparison between the measured and simulated heat supply for the Lichtwiese (Liwi) west heating circuit in 2018 is shown in the upper graph. The measurements were initiated by the end of January of 2018. As a consequence, no data is available for the first month of the year. In the lower graph, the absolute and relative deviation in heat supply between measurements and simulation is depicted. The absolute deviation is defined as $\Delta\dot{Q}_{\text{west}} = \dot{Q}_{\text{meas,west}} - \dot{Q}_{\text{sim,west}}$, the relative deviation as $\Delta\dot{Q}_{\text{rel,west}} = \frac{\Delta\dot{Q}_{\text{west}}}{\dot{Q}_{\text{meas,west}}}$. As can be observed, the model slightly underestimates the heat supply for the Lichtwiese west area in the

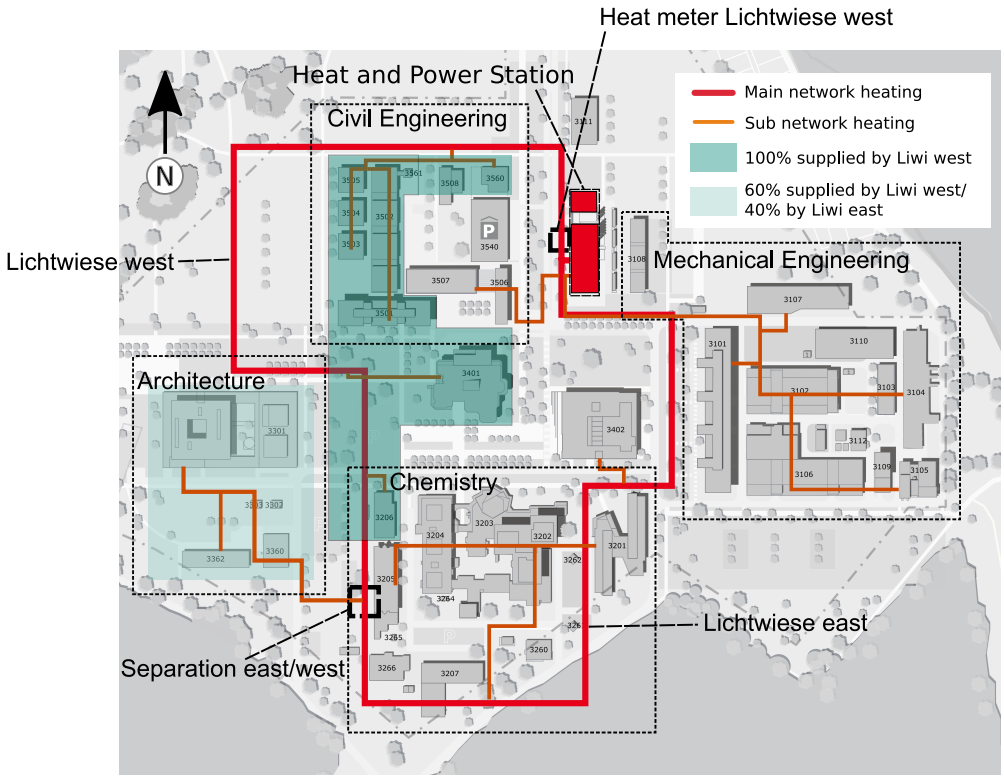

Fig. 6.13: Buildings supplied by the Lichtwiese west heating circuit.

spring and fall seasons, while during summer and winter, errors are evenly distributed. The annual mean deviation is $\overline{\Delta\dot{Q}}_{\text{west}} = -30\,\text{kW}$, while the standard deviation is $\sigma(\Delta\dot{Q}_{\text{west}}) = 60\,\text{kW}$.

While the absolute deviation is small in summertime, the relative deviation reaches its maximum during this season, due to the small overall heat supply. The mean of the relative deviation is $\overline{\Delta\dot{Q}}_{\text{rel,west}} = -5\,\%$ and its standard deviation is $\sigma(\Delta\dot{Q}_{\text{rel,west}}) = 11\,\%$.

Similarly to the heat supply, the measured return temperature $T_{\text{R,meas,west}}$ is compared to the simulated return temperature $T_{\text{R,sim,west}}$. The results can be seen in Fig 6.15.

The difference between the two values is on average $\Delta\overline{T}_{\text{R,meas-sim,west}} = 8.3\,\text{K}$ with a standard deviation of $\sigma(\Delta T_{\text{R,meas-sim,west}}) = 1.9\,\text{K}$, suggesting an error in the model or a malfunctioning reference heat meter. To find the source of the error, the weighted average return temperature from all substations $\overline{T}_{\text{R,sub,west}}$ is compared to measured data. This comparison reveals an interesting fact: During a significant time period in the fall, winter and spring seasons, the weighted average return temperature from all substations is lower than the measured return temperature at the HPS $T_{\text{R,meas,west}}$:

$$\overline{T}_{\text{R,sub,west}} = \frac{\dot{M}_j \cdot T_{\text{R},j}}{\sum_{j=1}^{n_{\text{sub}}} \dot{M}_j} < T_{\text{R,meas,west}} \tag{6.8}$$

Considering that the DH return temperature is always higher than the ambient temperature, this cannot be due to a heat flow from the ground to the pipes. Besides a malfunctioning of either the substation heat meters or the HPS heat meter, one possible reason is a shortcut mass flow within the DH network, allowing water to flow from the supply to the return line without cooling. To test this hypothesis, the mass flow measured

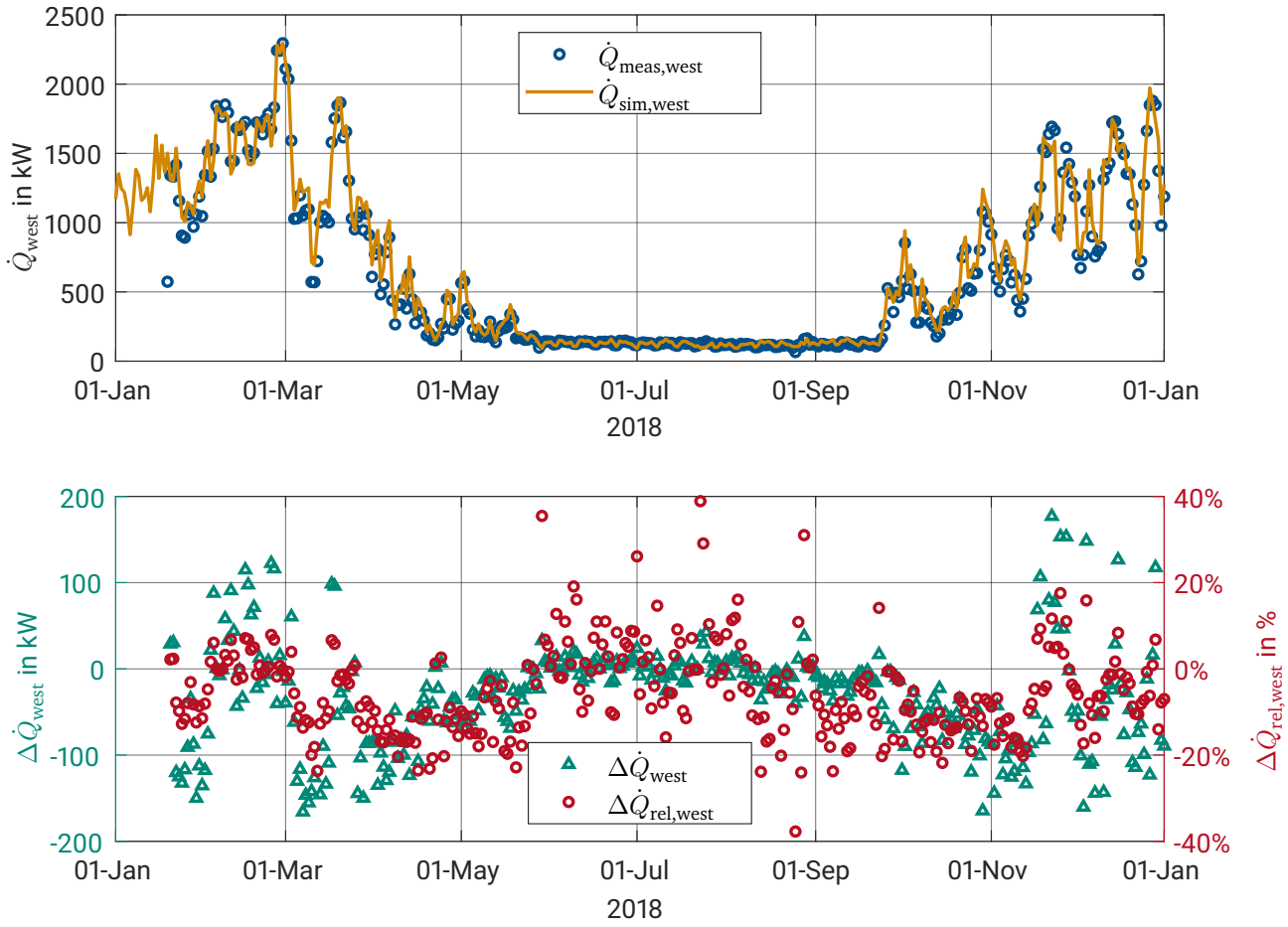

Fig. 6.14: Comparison of measured and simulated heat demand for Lichtwiese west in 2018 (resolution: 24 h).

at the HPS heat meter $\dot{M}_{\mathrm{meas,west}}$ is compared to the sum of the substation mass flows $\sum \dot{M}_{\mathrm{sub,west}}$ and the simulated mass flow $\dot{M}_{\mathrm{sim,west}}$ (see Fig. 6.16).

While $\sum \dot{M}_{\mathrm{sub,west}}$ and $M_{\mathrm{sim,west}}$ are almost the same, $\dot{M}_{\mathrm{meas,west}}$ is higher throughout the whole year, resulting in an average difference of $\overline{\Delta\dot{M}_{\mathrm{west}}} = \overline{\dot{M}_{\mathrm{meas,west}}} - \overline{\sum \dot{M}_{\mathrm{sub,west}}} = 1.2\,\mathrm{kg\,s^{-1}}$ and $\sigma(\overline{\Delta\dot{M}_{\mathrm{west}}}) = 0.8\,\mathrm{kg\,s^{-1}}$. If the difference between the measured and simulated return temperature were due to this shortcut flow, the resulting temperature (omitting network heat losses) could be calculated according to eq. 6.9:

$$T_{\mathrm{R,short,west}} = \frac{T_{\mathrm{R,sim,west}} \cdot \dot{M}_{\mathrm{sim,west}} + T_{\mathrm{S,meas,west}} \cdot \Delta\dot{M}_{\mathrm{west}}}{\dot{M}_{\mathrm{sim,west}} + \Delta\dot{M}_{\mathrm{west}}} \tag{6.9}$$

$T_{\mathrm{R,short,west}}$ is not exactly equal to $T_{\mathrm{R,meas,west}}$ (see Fig. 6.15), but significantly closer than $T_{\mathrm{R,sim,west}}$ or $\overline{T}_{\mathrm{R,sub,west}}$, at least during the heating season. This supports the hypothesis that the difference between the measured data and the results of the simulation is due to an undesired shortcut flow that is not taken into account in the model. This shortcut flow amounts to an annual average proportion of $f_{\mathrm{short}} = 25\,\%$ of the total measured

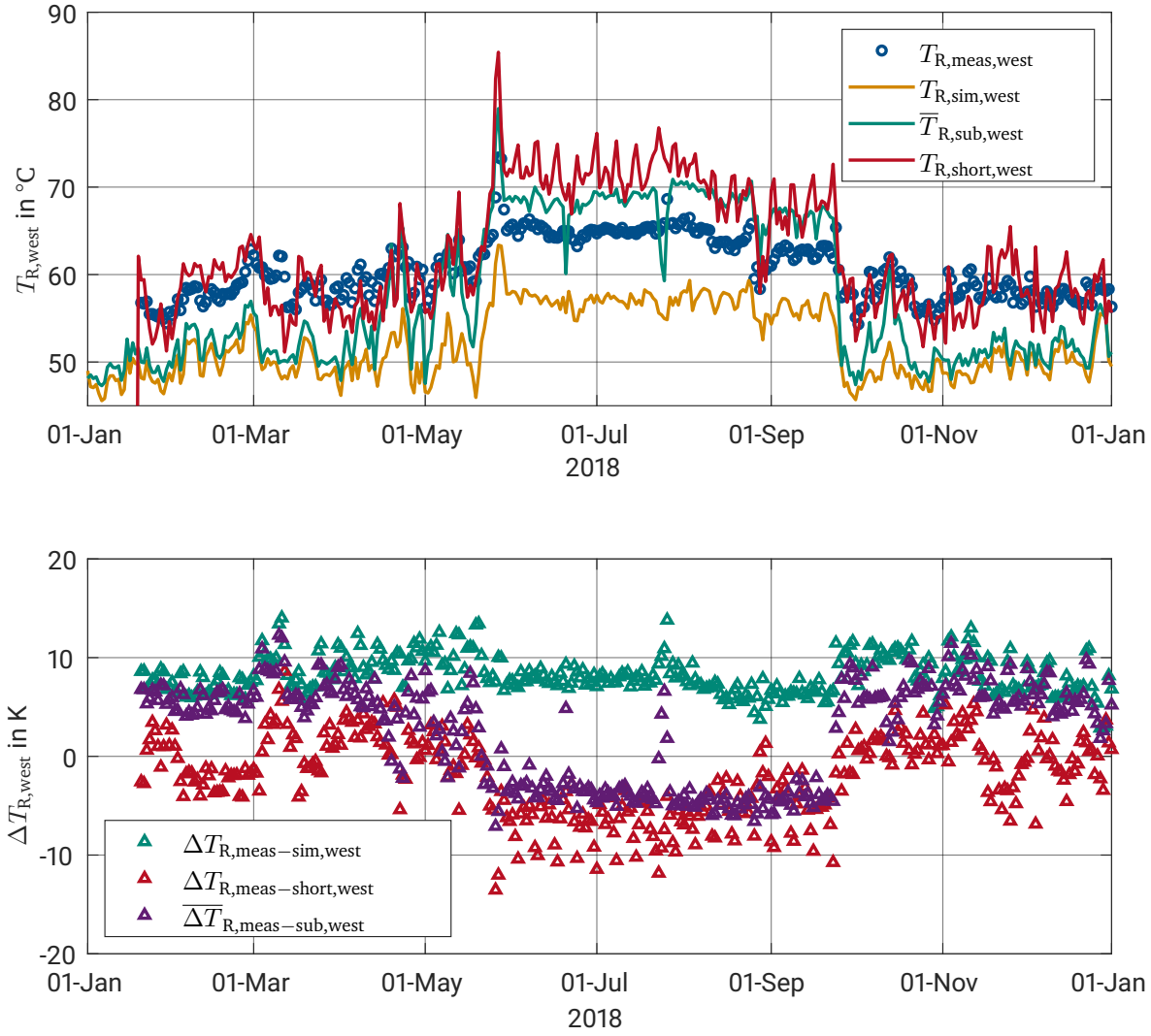

Fig. 6.15: Comparison of measured and simulated return temperature Lichtwiese west 2018 (resolution: 24 h).

mass flow, with peaks of up to $f_{\mathrm{short}} = 80\,\%$ during the summer months. To confirm the hypothesis, additional monitoring of temperatures and mass flow within the DH network would be necessary.

The supply temperature in the model is derived directly from the measured supply temperature at the HPS. Consequently, a validation of the supply temperature is not carried out.

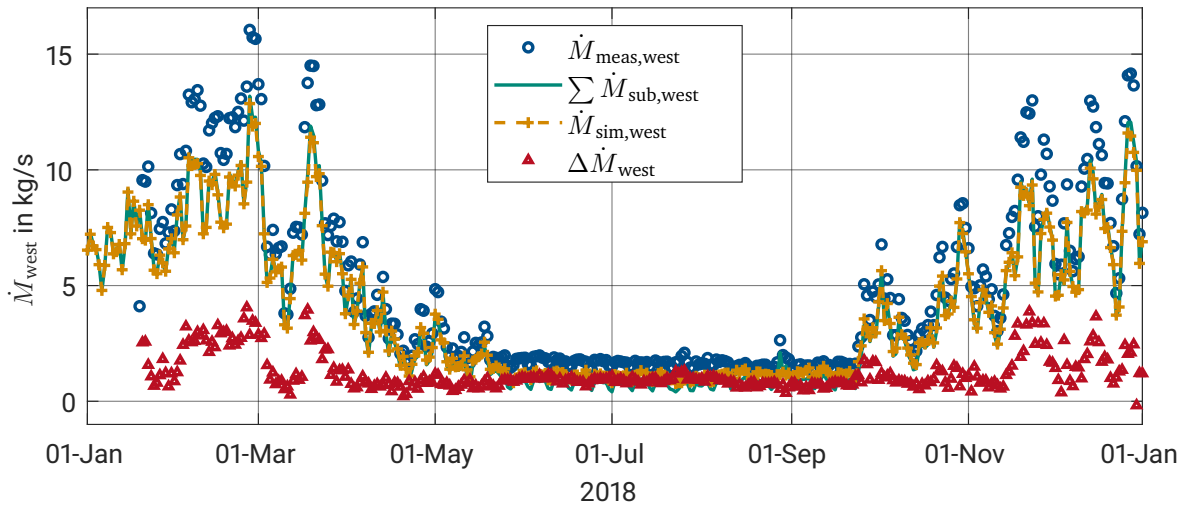

Fig. 6.16: Comparison of measured and simulated mass flow Lichtwiese west 2018 (resolution: 24 h).

7 Two-stage design and operation optimization of a district energy system

The control of a district heating system is based on the four variables supply temperature, return temperature, differential pressure between supply and return line and mass flow. Controlling a district heating system is a complex task, because both the return temperature and the mass flow do not depend on the district operator but on the individual buildings and the supply temperature propagates approximately with flow velocity, hence the time lag between an adjustment of the supply temperature at the HPS and the arrival of the change to the buildings can be very large, especially in big systems.

Due to the high inertia of the system and the high dependence of the network control on the individual customer, automation and optimization of the operation of district heating systems is still at the very beginning, even in the age of digitization. Bearing in mind the time lag in the propagation of the supply temperature, the operator must be able to predict the future heat demand to determine the correct supply temperature. If thermal storage is used to make the system more flexible, the forecast horizon must be increased with rising storage capacities. However, a lack of data frequently inhibits the development of prediction models, and most district heating systems are still controlled manually, based on the experience of the operators.

In this chapter, a two-stage method to improve the design and operation of the TU Darmstadt district energy system is developed, using mathematical optimization. First, a linear model is employed to optimize the design of the generation facilities and storage (see chapter 7.1). Subsequently, the results of the design optimization serve as input to the detailed model of the district energy system, where linear and mixed-integer optimization algorithms are employed to optimize the operation of the storage tanks and CHP plants (see chapter 7.2). The goal of the chapter is to illustrate how digitization in district heating can help not only to minimize CO_2 emissions in an energy system with predefined demand characteristics, but also to maintain low costs. The optimization problems are solved using the MATLAB Optimization Toolbox [139]. Fig. 7.1 presents the process of optimizing the design and operation of the TU Darmstadt campus Lichtwiese energy system, which will be explained in more detail in the following sections.

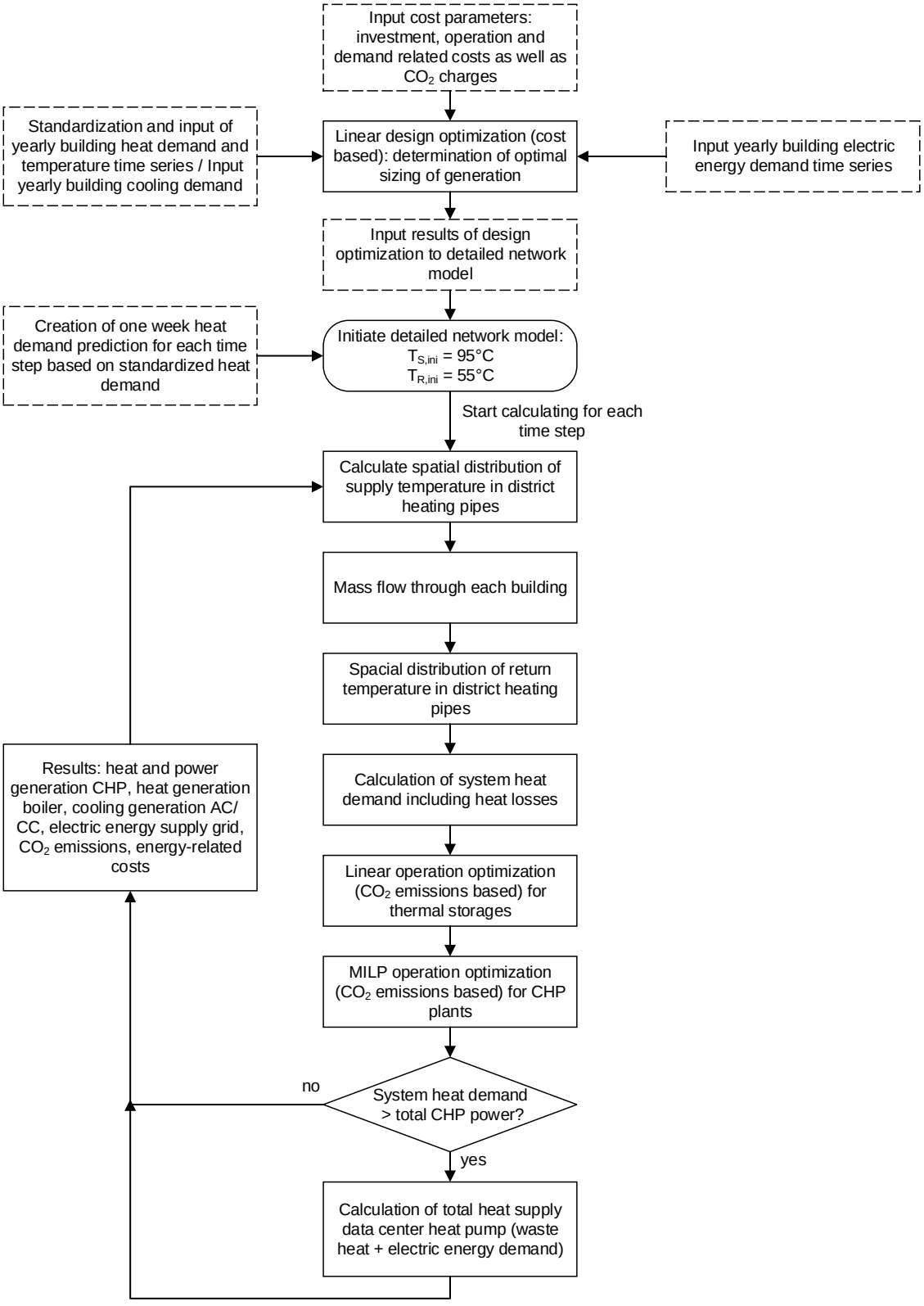

Fig. 7.1: Calculation flow chart for the design and operation optimization of the TU Darmstadt campus Lichtwiese energy system.

7.1 Linear design optimization

The first stage in the optimization process is the determination of the design of the energy generation facilities and storage tanks. The aim of the design optimization is to find out which technologies should be used for cost-optimized energy supply, regardless of the existing generation and storage units at TU Darmstadt. Therefore, a greenfield setup is considered, where everything has to be built from scratch. Possible technologies are heat and power generation via gas HOB and CHP plants, compression and absorption cooling and sensible stratified thermal storage for heat and cooling. Photovoltaic cells on the rooftops of the university buildings are an option to include renewables in the electric energy mix. Recycled heat is included in the form of data center waste heat. Renewable heat sources such as geothermal or solar thermal heat are not within the scope of this thesis. The algorithm does not include the optimization of the district heating network layout.

The following linear optimization problem is solved with an hourly resolution:

$$\begin{aligned}\min f(x) = &[3 \cdot P_{\text{gen,CHP}} \cdot c_{\text{gen,CHP}} + 3 \cdot P_{\text{gen,HOB}} \cdot c_{\text{gen,HOB}} + 3 \cdot P_{\text{gen,AC}} \cdot c_{\text{gen,AC}} + \\ &3 \cdot P_{\text{gen,CC}} \cdot c_{\text{gen,CC}} + 3 \cdot P_{\text{gen,HP/HPC}} \cdot c_{\text{gen,HP/HPC}} + 3 \cdot P_{\text{gen,PV}} \cdot c_{\text{gen,PV}} + \\ &3 \cdot E_{\text{TES,BHS}} \cdot c_{\text{TES,BHS}} + 3 \cdot E_{\text{TES,SHS}} \cdot c_{\text{TES,SHS}} + 3 \cdot E_{\text{TES,CS}} \cdot c_{\text{TES,CS}}] \cdot (f_{\text{a}} + f_{\text{op}} f_{\text{a}} f_{\text{b}}) + \\ &[E_{\text{gas}} \cdot (c_{\text{E,gas}} + c_{\text{CO2,gas}}) + (E_{\text{el,grid}} + E_{\text{el,contr}}) \cdot (c_{\text{E,el}} + c_{\text{CO2,el}}) + \\ &\left(\dot{E}_{\text{max,gas}}(1) + \dot{E}_{\text{max,gas}}(2) + \dot{E}_{\text{max,gas}}(3)\right) \cdot c_{\text{cap,gas}} + \\ &\left(\dot{E}_{\text{max,el}}(1) + \dot{E}_{\text{max,el}}(2) + \dot{E}_{\text{max,el}}(3)\right) \cdot c_{\text{cap,el}}] \cdot f_{\text{a}} f_{\text{b}}\end{aligned} \tag{7.1}$$

Table 7.1 gives an overview of the variables used in the linear design optimization function (eq. 7.1). The nomenclature in the optimization function is based on what was introduced in chapter 5.3.3 (Table 5.1). The annuities of the investment and operation-related costs are multiplied by three, given that the optimization period covers three years.

The university's standardized energy demand for heat as well as the measured demand of cooling and electric energy serve as input for the algorithm (see chapter 6.2.1). In the context of the linear design optimization, demands are considered as known beforehand for the entire period under consideration. In a real system, energy demand especially for heating strongly depends on weather conditions, which can be forecasted reliably for a week in advance at the most. The efficiencies of the generation technologies are considered to be constant. For the efficiency of the network, data resulting from a simulation of the non-optimized system taken into account.

When supply and storage units for a district heating system are designed, not only a typical demand should be considered, but also exceptional demand patterns, especially extreme winters, should be taken into account. All the same, it is not reasonable to optimize the whole system for the demand of an extremely cold winter, when such a scenario is likely to happen only every once in several years. For this purpose, the design optimization covers a time period of three years, two with normal and one with extreme winter conditions. The heat demand data for an extreme winter is created using the building heat demand regression models presented in chapter 6.2.1, based on Test Reference Year climate data for extreme winter conditions in Darmstadt [141].

Even though the main goal of the optimization is to minimize CO_2 emissions, the target value in the design optimization is cost. To minimize CO_2 emissions instead of costs in the design optimization, it would be necessary to dispose of data regarding the emissions generated in the production of a generation unit or a storage. For this purpose, life cycle analyses of all considered technologies would be necessary, which is not

Table 7.1: Variables of the design optimization.

Variable	Description	Unit
$P_{\text{gen,CHP}}$	design load CHP plants	MW
$P_{\text{gen,HOB}}$	design load HOB	MW
$P_{\text{gen,AC}}$	design load absorption chillers	MW
$P_{\text{gen,CC}}$	design load compression chillers	MW
$P_{\text{gen,HP/HPC}}$	design load heat pump data center waste heat utilization	MW
$P_{\text{gen,PV}}$	design load photovoltaic cells	MW
$E_{\text{TES,BHS}}$	maximum energy content buffer heat storage	MWh
$E_{\text{TES,SHS}}$	maximum energy content seasonal heat storage	MWh
$E_{\text{TES,CS}}$	maximum energy content cooling storage	MWh
E_{gas}	energy supply gas	MWh
$E_{\text{el,grid}}$	supply grid electric energy	MWh
$E_{\text{el,contr}}$	supply grid electric energy to contractor for operational purposes	MWh
$\dot{E}_{\text{max,gas}}$	annual maximum 15 minutes average gas power supply	MW
$\dot{E}_{\text{max,el}}$	annual maximum 15 minutes average electric power	MW
$c_{\text{gen,CHP}}$	specific investment costs CHP plants	€/MW
$c_{\text{gen,HOB}}$	specific investment costs HOB	€/MW
$c_{\text{gen,AC}}$	specific investment costs AC	€/MW
$c_{\text{gen,CC}}$	specific investment costs CC	€/MW
$c_{\text{gen,HP/HPC}}$	specific investment costs HP/HPC	€/MW
$c_{\text{gen,PV}}$	specific investment costs photovoltaic cells	€/MW
$c_{\text{TES,BHS}}$	specific investment costs buffer heat storage	€/MWh
$c_{\text{TES,SHS}}$	specific investment costs seasonal heat storage	€/MWh
$c_{\text{TES,CS}}$	specific investment costs cooling storage	€/MWh
$c_{\text{E,gas}}$	specific demand-related costs gas	€/MWh
$c_{\text{CO2,gas}}$	specific CO_2 emissions costs gas	€/MWh
$c_{\text{E,el}}$	specific demand-related costs grid electric energy	€/MWh
$c_{\text{CO2,el}}$	specific CO_2 emissions costs grid electric energy	€/MWh
$c_{\text{cap,gas}}$	capacity costs gas	€/MW
$c_{\text{cap,el}}$	capacity costs grid electric energy	€/MW
f_{a}	annuity factor	1/a
f_{b}	price-dynamic cash value factor	a
f_{op}	cost factor of operation-related costs	–

within the scope of this thesis. Nevertheless, CO_2 emissions can be considered in the design optimization, when a price per ton of CO_2 emitted during the operation of the system is assigned (see chapter 5.3.3).

7.2 Linear and mixed integer operation optimization

The second stage is the optimization of the operation of the storage tanks and CHP plants, which is carried out within the detailed energy system model presented in chapter 6. Future demand for heat, cooling, and electric energy with a prediction horizon of one week serve as input to the linear optimization algorithm. The time horizon of one week is chosen, because it represents a period for which reliable weather forecasts can be obtained, making it possible to predict future heat demand with sufficient accuracy. Based on this data, the optimal operation of the generation plants and storage facilities, minimizing the CO_2 emissions of the overall system, is determined. On one hand, the linear approach has two advantages: it uses short computing times and yields globally valid optima. On the other hand, its disadvantage is that all solutions must be possible within a solution space limited by constraints. Specifically, a constraint such as minimum power, which is common for generation units like CHP plants, cannot be considered. A constraint specifying a minimum power of 50 % of the maximum load for the CHP plants would imply that the optimization algorithm would not allow the CHP plants to be switched off, leading to an error in the summer, when the overall heat demand is low. Therefore, the results of the linear optimization are only used for the operation of the storage tanks, HOB and chillers. The optimization of the operation of the CHP plants is performed in a downstream mixed integer linear programming (MILP) model. This makes it possible to define binary variables that can be used to map a shutdown of the generation plants when demand falls below the minimum capacity. This procedure is computationally more intensive than linear optimization, hence the MILP algorithm does not include demand prediction, but optimizes the operation strategy for the CHP plants one step at a time. Since the specific costs and CO_2 emissions are defined as constant over time, no disadvantages arise from this approach.

7.3 Linearization of thermal storage

Temperatures and mass flow cannot be accounted for individually in a linear model, but only in an aggregated form as energy. This aspect creates certain challenges, especially in the case of thermal energy storage (TES), where different reference temperatures have to be considered for the calculation of useful and stored energy (see chapter 6.3.4).

For the linear optimization, the energy content of the storage has to be clearly defined and it is not possible to consider various reference temperatures. Consequently, no difference can be made between useful energy $Q_{\mathrm{TES,use}}$ and stored energy $Q_{\mathrm{TES,stor}}$. When selecting the network return temperature as the reference temperature, negative values for the storage useful heat content $Q_{\mathrm{TES,use}}$ would have to be possible. Consequently, the optimization algorithm would discharge the storage tanks to a specified negative minimum. This is not plausible if it is assumed that heat cannot be used at a temperature below the return temperature. Using a MILP model formulation, it would be possible to specify that negative amounts of heat may be reached, but the storage could only be discharged if a positive amount of heat was available. However, this would not be suitable for an optimization problem including a prediction of future energy demand over various time steps, due to high computation times. Within the framework of linear design optimization, the storage heat losses are specified as a proportion of the useful heat at each time step. The average hourly heat losses $\overline{Q}_{\mathrm{TES,loss}}$

depend on the storage temperature $\overline{T}_{\text{TES}}$, the ambient temperature $\overline{T}_{\text{amb}}$ as well as the thermal resistance of the storage envelope R:

$$\begin{aligned}\overline{Q}_{\text{TES,loss}} = \Bigg[& 2 \cdot r_{\text{TES}} \cdot \pi \cdot h_{\text{TES}} \cdot \frac{1}{R_{\text{wall}}} \cdot \left(\frac{\overline{T}_{\text{TES,top}} - \overline{T}_{\text{TES,bottom}}}{2} - \overline{T}_{\text{amb}} \right) + \\ & r_{\text{TES}}^2 \cdot \pi \cdot \frac{1}{R_{\text{top}}} \cdot \left(\overline{T}_{\text{TES,top}} - \overline{T}_{\text{amb}} \right) + \\ & r_{\text{TES}}^2 \cdot \pi \cdot \frac{1}{R_{\text{bottom}}} \cdot \left(\overline{T}_{\text{TES,bottom}} - \overline{T}_{\text{amb}} \right) \Bigg] \cdot 1\,\text{h}\end{aligned} \tag{7.2}$$

The average useful energy content of the storage tanks $\overline{Q}_{\text{TES,use}}$ is the product of the storage capacity $Q_{\text{TES,use}}$ and the average charging level of the storage $\overline{f}_{\text{TES}}$. In the case of the design optimization, the average charging level is $\overline{f}_{\text{TES}} = 34\,\%$:

$$\overline{Q}_{\text{TES,use}} = Q_{\text{TES,use}} \cdot \overline{f}_{\text{TES}} \tag{7.3}$$

Based on the average hourly heat losses $\overline{Q}_{\text{TES,loss}}$ and the average useful energy content of the storage tanks $\overline{Q}_{\text{TES,use}}$, the average storage efficiency can be calculated:

$$\overline{\eta}_{\text{TES}} = 1 - \frac{\overline{Q}_{\text{TES,loss}}}{\overline{Q}_{\text{TES,use}}} \tag{7.4}$$

The following parameters are used for the calculation of the average storage efficiency:

Table 7.2: Parameters for heat loss calculation in heat storage tanks.

Parameter	**Variable**	**Buffer heat storage**	**Seasonal heat storage**
Useful storage capacity	$Q_{\text{TES,use}}$	11 MWh	500 MWh
Volume	V_{TES}	215 m^3	14 600 m^3
Height	h_{TES}	10 m	30 m
Radius	r_{TES}	2.6 m	12.5 m
Yearly average temperature top	$\overline{T}_{\text{TES,top}}$	80 °C	75 °C
Maximum storage temperature	$T_{\text{TES,max}}$	110 °C	95 °C
Yearly average temperature bottom	$\overline{T}_{\text{TES,bottom}}$	60 °C	
Yearly average ambient temperature	$\overline{T}_{\text{amb}}$	10 °C	
Thermal resistance wall	R_{wall}	9.09 $\text{m}^2\text{K}\,\text{W}^{-1}$	
Thermal resistance top	R_{top}	8.89 $\text{m}^2\text{K}\,\text{W}^{-1}$	
Thermal resistance bottom	R_{bottom}	2.11 $\text{m}^2\text{K}\,\text{W}^{-1}$	
Average charging level	$\overline{f}_{\text{TES}}$	34 %	

The calculation of the storage heat losses is an iterative process and its result can be seen as a best guess solution. The resulting storage efficiency underestimates the storage losses when the storage load is low. To improve the accuracy of the calculation, storage temperatures would have to be known for each time step. A more accurate characterization of storage heat losses can only be carried out in the energy system model.

In the case of the linear operation optimization within the energy system model, the storage efficiency is $\eta_{\mathrm{TES}} = 1 - \frac{Q_{\mathrm{TES,loss}}}{Q_{\mathrm{TES,stor}}}$. In this context, a negative useful heat content $Q_{\mathrm{TES,use}} < 0\,\mathrm{MWh}$ can be accepted, because it can be defined within the model that stored heat can only be used if its temperature exceeds a certain threshold value.

7.4 Results of the linear design optimization

The results of the design optimization are a proposal for the dimensioning of the different generation technologies and thermal storage tanks for the TU Darmstadt energy system.

The left side of Fig. 7.2 illustrates the distribution of the average annual costs between investment, operation and energy demand, which is divided in energy costs and capacity costs. For the chosen observation period of $t = 10\,\mathrm{years}$, the annuity of the investment and operation costs represents 5 % of the overall annuity. In total, the annuity is 11.5 M€/a, with the energy costs for gas being the highest share (77 %). On the right side of Fig. 7.2, the shares of the different technologies in the total investment costs can be seen. For an optimum system design, the CHP plants represent 51 % of the total investment costs, followed by the seasonal heat storage and the HOB. The sum of the annuities of investment and operation-related costs are 630 000 €/a.

Alongside the dimensioning of the generation facilities and thermal storage, the linear design optimization also proposes an operation strategy. This strategy is optimal for an ideal system, where all input time series are known beforehand. For a real world system, in which a reliable weather forecast is available for a week in advance at the most, and future energy demands can be predicted only for the short term, such an operation strategy can be seen as a reference strategy. It does not replace a detailed nonlinear model. Nevertheless, some important conclusions can be derived from the operation strategy proposed by the design optimization algorithm.

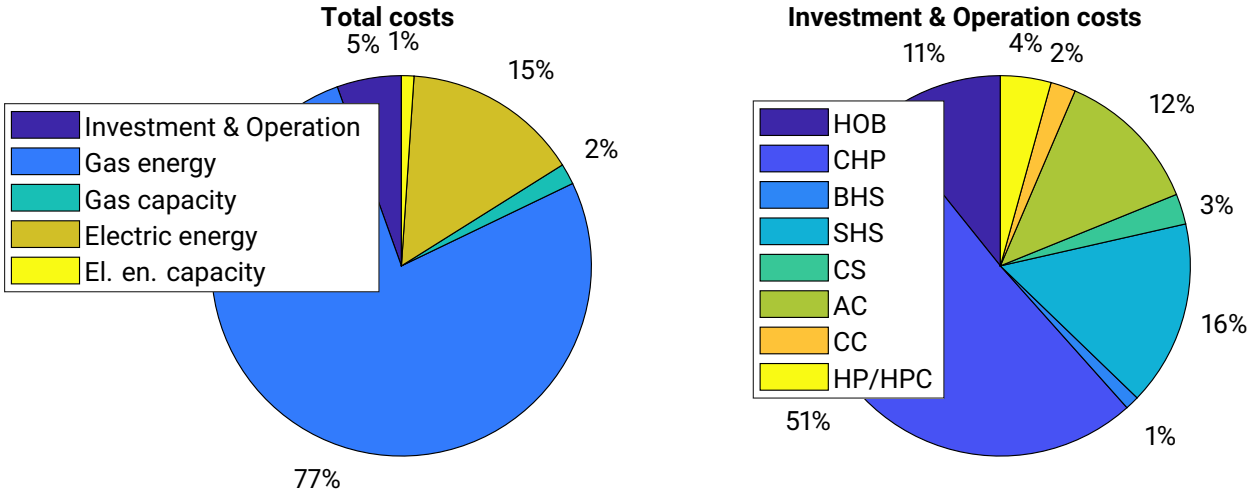

Fig. 7.2: Shares of investment, operation and demand in total costs (left) and the different facilities in the investment and operation costs (right) for the design optimization.

Table 7.3: Nomenclature for Investment & Operation costs in Fig.7.2.

Abbreviation	Facilities
HOB	Heat-only boilers
CHP	CHP plants
BHS	Buffer heat storage
SHS	Seasonal heat storage
CS	Cooling storage
AC	Absorption chiller
CC	Compression chiller
HP/HPC	Heat pump high performance computer

Fig. 7.3 shows the results of the linear design optimization for the heat flow supply and the total gas input in a standardized average year and a year with extreme winter conditions, based on test reference year (TRY) data. The additional heat flow necessary in the extreme winter is exclusively supplied by the HOB, since the maximum capacity of the CHP plants is defined by the electric power demand on the grounds that electric energy cannot be sold to the grid (see chapter 3.1). Although the heat flow supplied to the DH network includes several characteristic peaks in both an average year as well as during an extreme winter, the maximum gas demand never exceeds $\dot{E}_{\mathrm{max,gas}} = 28.6\,\mathrm{MW}$ in an average year and $\dot{E}_{\mathrm{max,gas}} = 31.6\,\mathrm{MW}$ in an extreme winter. Likewise, the grid electric power supply repeatedly touches a maximum of $\dot{E}_{\mathrm{max,el,grid+contr}} = 2.5\,\mathrm{MW}$ in case of an average year, and $\dot{E}_{\mathrm{max,el,grid+contr}} = 2.8\,\mathrm{MW}$ for a year with extreme winter conditions (see Fig. 7.4). This way, the linear design optimization algorithm minimizes the capacity charge both for gas input and grid electric power. The difference in maximum grid electric power supply is due to slightly lower summer heat flow demand in case of the extreme winter weather scenario compared to the average year.

Limiting the maxima of the gas input and the grid electric power demand is possible, because the model is based on time series for heat, cooling, and electric energy demand for the complete time period known beforehand. It can make optimal use of the flexibility provided by thermal energy storage. The time-depend useful energy content levels and charging/discharging trajectories for both the buffer heat storage and the seasonal heat storage are displayed in Fig. 7.5. The small pressurized buffer heat storage with a capacity of $Q_{\mathrm{BHS}} = 11\,\mathrm{MWh}$ ($V_{\mathrm{BHS}} = 215\,\mathrm{m}^3$) undergoes about 110 (average year) or 210 (extreme winter) short charging cycles of 12-24 h per cycle, helping to smoothen peak demand occurring due to changes between night and day or weekend and weekday operation strategies. The seasonal heat storage with a capacity of $Q_{\mathrm{SHS}} = 500\,\mathrm{MWh}$ ($V_{\mathrm{SHS}} = 14\,600\,\mathrm{m}^3$) is essentially loaded once during the summer when room heating is not operating and CHP plants cannot generate electric energy because their heat is not needed. The discharging of the seasonal heat storage starts between early October and mid-November, but the main discharging occurs during the cold winter months between mid-December and mid-February, when heat demand is highest in both an average year and in the extreme winter case. The linear design optimization includes the boundary condition that the useful energy content at the beginning and the end of each year have to be equal.

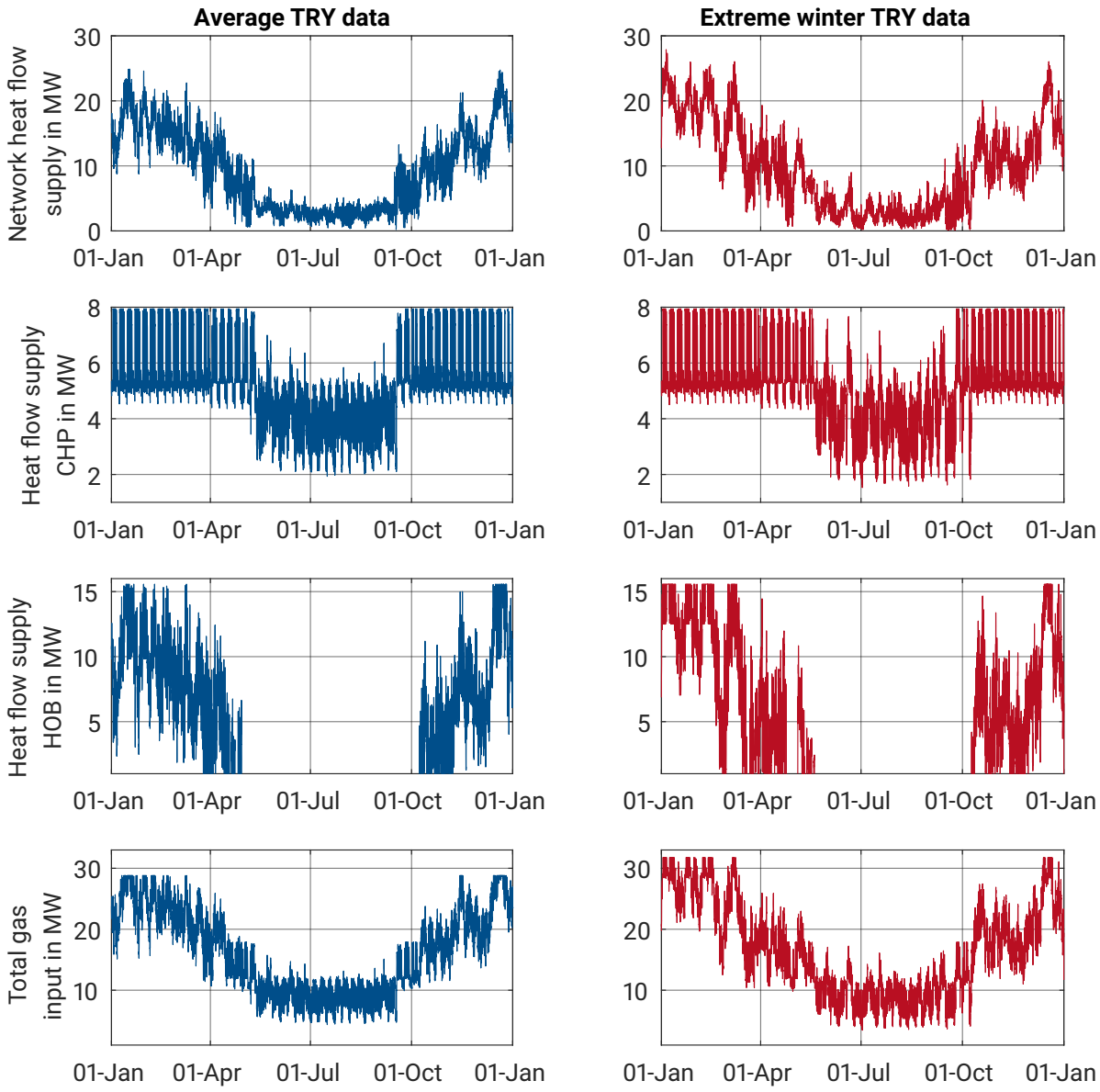

Fig. 7.3: Heat demand, heat supply CHP & HOB and total gas input TU Darmstadt in two test reference years (TRY), an average year (left column) and a year with extreme winter (right column).

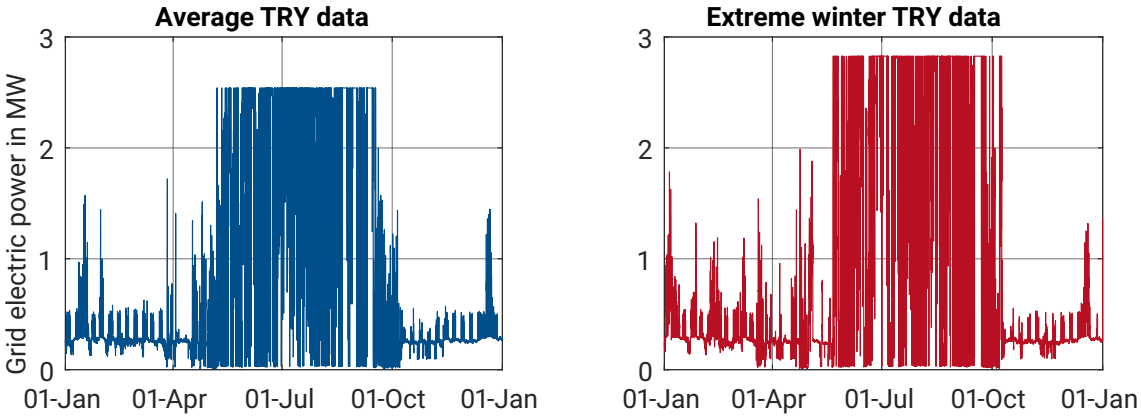

Fig. 7.4: Grid electric power demand TU Darmstadt in two test reference years (TRY), an average year (left column) and a year with extreme winter (right column).

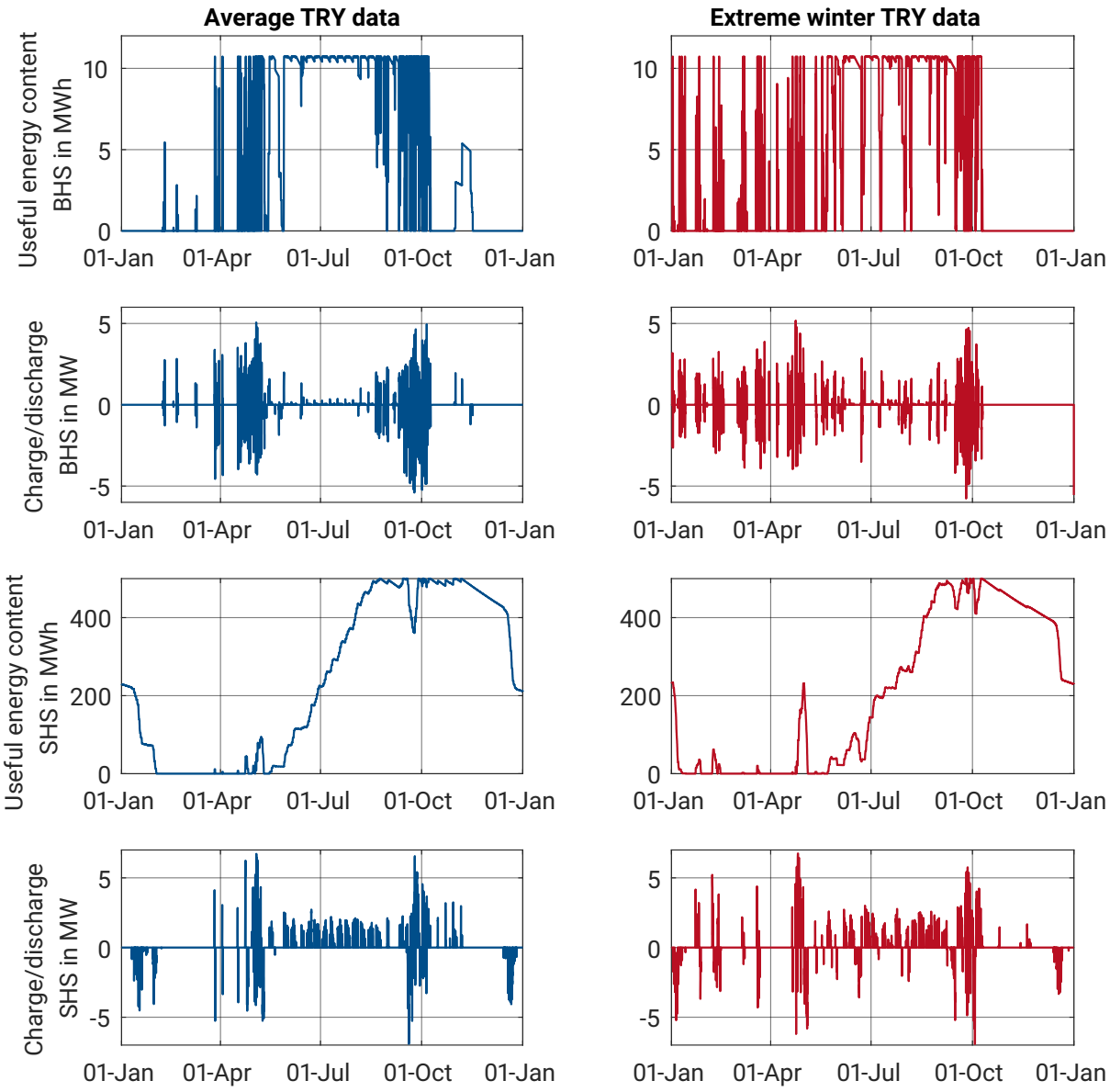

Fig. 7.5: Time-dependend useful energy content and charge/discharge of BHS & SHS in two test reference years (TRY), an average year (left column) and a year with extreme winter (right column).

7.5 Results of the integrated design and operation optimization

In this section, the benefits of an integrated design and operation optimization of the TU Darmstadt district heating system are shown, comparing different scenarios simulated within the detailed energy system model introduced in chapter 6:

1. Reference scenario (S_{ref}): Reference scenario using the available generation units in 2018, not including HPC hot-water cooling and waste heat utilization. To make a comparison to other scenarios possible, standardized heat demands for the buildings are used (see chapter 6.2.1). Although thermal storage was already available in the reference time period, they are not considered in this scenario, because storage tanks were not used in the context of an optimized operation strategy in the past.

2. Operation optimization scenario (S_{op}): Optimization of the operation regime of currently available generation units and storage, including data center hot-water cooling and waste heat utilization (see chapter 9), considering a standardized heat demand.

3. Design and operation optimization scenario ($S_{\text{des\&op}}$): Optimization of the design and operation of the generation units and storage, including data center hot-water cooling and waste heat utilization, considering a standardized heat demand.

Table 7.4 shows the generation units and storage tanks with their dimensions taken into consideration in each scenario. Since S_{op} is an optimization of the operation of the existing system, the system design is mostly identical to the reference case, except for an additional heat pump for data center waste heat utilization at TU Darmstadt's own high-performance computer "Lichtenberg-Hochleistungsrechner".

Table 7.4: Capacities of generation units and thermal energy storage in the three scenarios.

Facilities	S_{ref}	S_{op}	$S_{\text{des\&op}}$
CHP plants (CHP)	$2 \times 2\,\text{MW}_{\text{el}}/2\,\text{MW}_{\text{th}}$ $1 \times 3.25\,\text{MW}_{\text{el}}/3\,\text{MW}_{\text{th}}$	$2 \times 2\,\text{MW}_{\text{el}}/2\,\text{MW}_{\text{th}}$ $1 \times 3.25\,\text{MW}_{\text{el}}/3\,\text{MW}_{\text{th}}$	$2 \times 2.3\,\text{MW}_{\text{el}}/2.3\,\text{MW}_{\text{th}}$ $1 \times 3.7\,\text{MW}_{\text{el}}/3.4\,\text{MW}_{\text{th}}$
Heat-only boilers (HOB)	$3 \times 9.3\,\text{MW}_{\text{th}}$	$3 \times 9.3\,\text{MW}_{\text{th}}$	$3 \times 9.3\,\text{MW}_{\text{th}}$
Absorption chiller (AC)	$1\,\text{MW}_{\text{th}}$	$1\,\text{MW}_{\text{th}}$	$1.28\,\text{MW}_{\text{th}}$
Compression chillers (CC)	$3 \times 1\,\text{MW}_{\text{th}}$	$3 \times 1\,\text{MW}_{\text{th}}$	$2 \times 1\,\text{MW}_{\text{th}}$
Buffer heat storage (BHS)	$2 \times 125\,\text{m}^3$	$2 \times 125\,\text{m}^3$	$215\,\text{m}^3$
Seasonal heat storage (SHS)	—	—	$14\,600\,\text{m}^3$
Cooling storage (CS)	$2 \times 150\,\text{m}^3$	$2 \times 150\,\text{m}^3$	$260\,\text{m}^3$
Heat Pump (HP/HPC)	—	$420\,\text{kW}_{\text{th,heat}}$	$420\,\text{kW}_{\text{th,heat}}$

In the following section, the results of the optimization scenarios are compared to the reference case. First, the impact of the design and operation optimization on the operation regime of the CHP plants and HOB, the utilization of heat storage, electric power supplied from the grid and supply and demand of cooling energy is presented. Then, the results in terms of final energy supplied to the system as well as CO_2 emissions and annuities are compared for all three scenarios. Final energy, CO_2 emissions and annuities are attributed to the different generation technologies for heat, cooling, and electric energy, including grid electric energy and contractor electric energy for generation purposes. Last, an energy and exergy analysis and a sensitivity analysis of the electric energy demand in $S_{\text{des\&op}}$ is presented. To obtain comparable results and to cover seasonal differences comprehensively, a period of one year is simulated in each case.

The capacities of HOB and CC do not exactly reflect the results of the design optimization. The energy system model does not shave demand peaks as much as the linear design optimization, because of shorter prediction periods. To avoid a lack of generation capacities during peak demand, the capacities used for HOB and CC are slightly bigger than the design optimization suggests. The HOB capacity is the same in all three scenarios, while the capacity of CC is somewhat smaller in $S_{\text{des\&op}}$ than it is in S_{ref} and S_{op}. The main difference between the current system setup and the optimized design are expanded CHP capacities, a slightly bigger absorption chiller and the introduction of a seasonal heat storage. All of this helps to increase the share of CHP plants in the heat and power generation.

7.5.1 CHP and HOB operation

As a consequence of the increased CHP capacity in the $S_{\text{des\&op}}$ scenario, the gas input of the CHP plants grows by a total of 5.5 % (5300 MWh/a). The increase, which can be seen in Fig. 7.6 (upper graph), is mainly due to higher CHP loads during the winter months, but also comes from higher CHP utilization in the summer, made possible by the use of storage. Fig. 7.6 also depicts why increasing the CHP capacity beyond the size suggested by the design optimization is not advisable: Since the university is not allowed to sell electric energy to the grid and there is no electric energy storage available in the system, the CHP plants cannot supply more electric energy than what is consumed by the university (see Fig. 6.5). The increase in gas input for the CHP plants helps to reduce the amount of gas used for the HOB, by a total of 10 % (4100 MWh/a). CHP plants generate both heat and electric energy, thus the absolute decrease in HOB gas demand is lower than the increase CHP gas demand.

In both the operation of the CHP plants and the HOB, small gaps in the gas input of the design and operation optimization scenario $S_{\text{des\&op}}$ can be detected. This is due to the minimum load for both the CHP plants and the HOB. Although the CHP plants are a lot less flexible than the HOB, the MILP operation optimization (see chapter 7.2) minimizes the gap, operating several plants at partial load at the same time during summer months with low heat demand. Such an optimization algorithm was not implemented for the HOB. An additional HOB goes into operation only once the heat demand exceeds the capacity of the previous one. Since the minimum operation point of the HOB is 10 % of their design load (see chapter 6.3.2), the gaps in gas input to the HOB are more prominent than in the case of the CHP plants.

7.5.2 Heat storage utilization

In Fig. 7.7, the buffer and seasonal heat storage energy content for different reference temperatures (see chapter 6.3.4) as well as the temperatures at the top and the bottom of the storage tanks are shown for $S_{\text{des\&op}}$. The useful energy lies below the stored energy, because of the different reference temperatures used. The mean stored energy, calculated using the annual mean of the ambient temperature as reference, best explains the charging and discharging behavior of the storage, because it is not influenced by changes in the reference temperature.

Both the buffer and the seasonal heat storage essentially show the same characteristic behavior: during winter time, the storage tanks are not used, because all available heat goes directly to the buildings. The storage tanks are filled up starting in April, when building heat demand drops below the available CHP generation capacity, stay filled up during the summer season and are discharged in October, when heating is turned on and demand rises once again. While the seasonal heat storage undergoes only one annual charging cycle, the buffer storage is charged and discharged several times during the spring and the fall. The differences

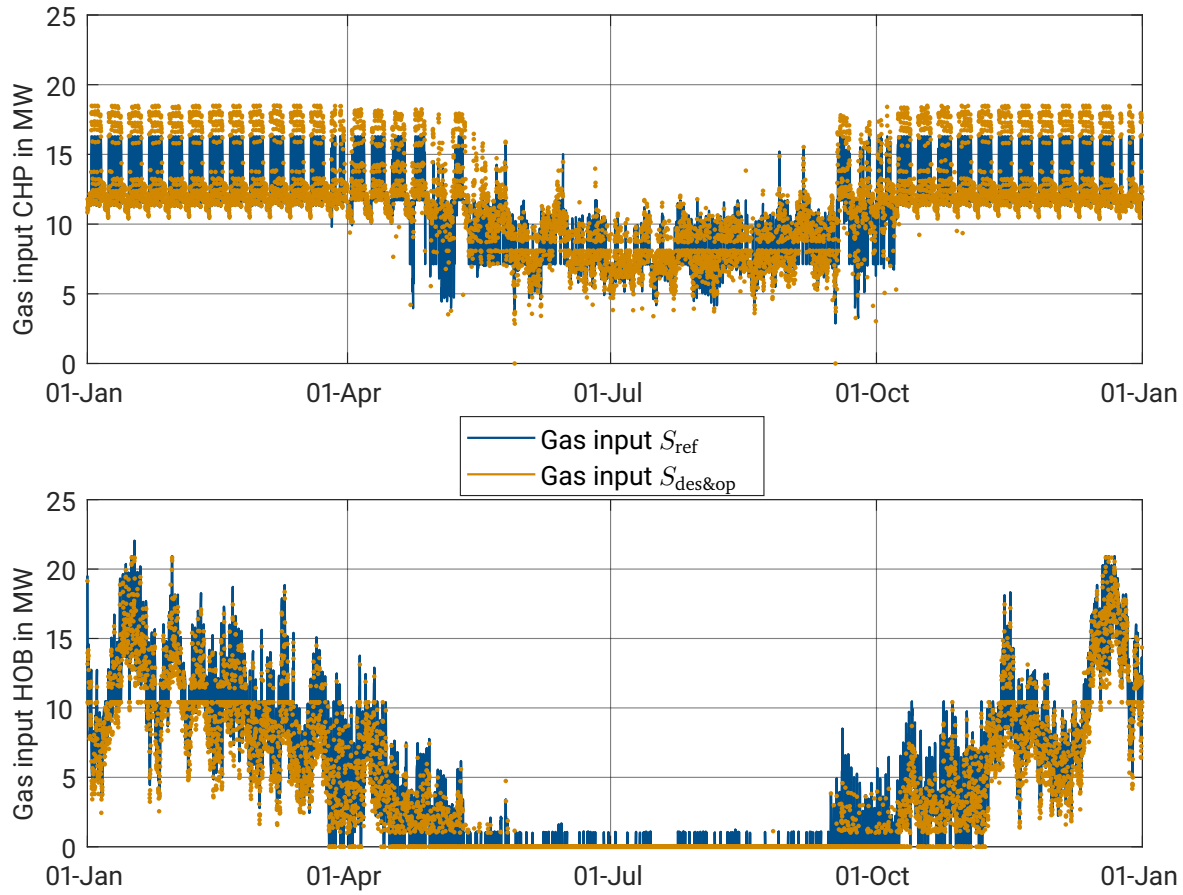

Fig. 7.6: CHP and HOB gas input in the reference scenario S_{ref} and the design and operation optimization scenario $S_{\text{des\&op}}$.

in storage use compared to the design optimization algorithm result from the differences in the underlying model setup: the design optimization minimizes total costs including capacity costs, while the operation strategy in the energy system model aims at minimizing CO_2 emissions and does not take into account capacity costs. Therefore, the storage tanks in the design optimization (see Fig. 7.5) undergo additional charging and discharging cycles during the winter season. Additionally, the energy demand of the entire observation period of one year is known beforehand in the case of the design optimization algorithm, while the energy system model considers a prediction period of one week. This leads to an earlier and faster charging process of the seasonal heat storage in the energy system model (early April to mid-May instead of mid-May to late August). The optimization algorithm within the energy system model optimizes the system for the prediction horizon at each time step and does not take into account that it might make more sense in the long run to fill the storage slowly throughout the entire summer period. The same is valid for the discharging process: In the energy system model discharging is carried out at the beginning of the heating season in October, while the design optimization discharges the storage during the entire winter season, using stored heat to shave peak demand occurring at that time of the year. Contrary to the linear design optimization, the storage energy content at the beginning and the end of the year differs slightly. It is not possible to require the final storage

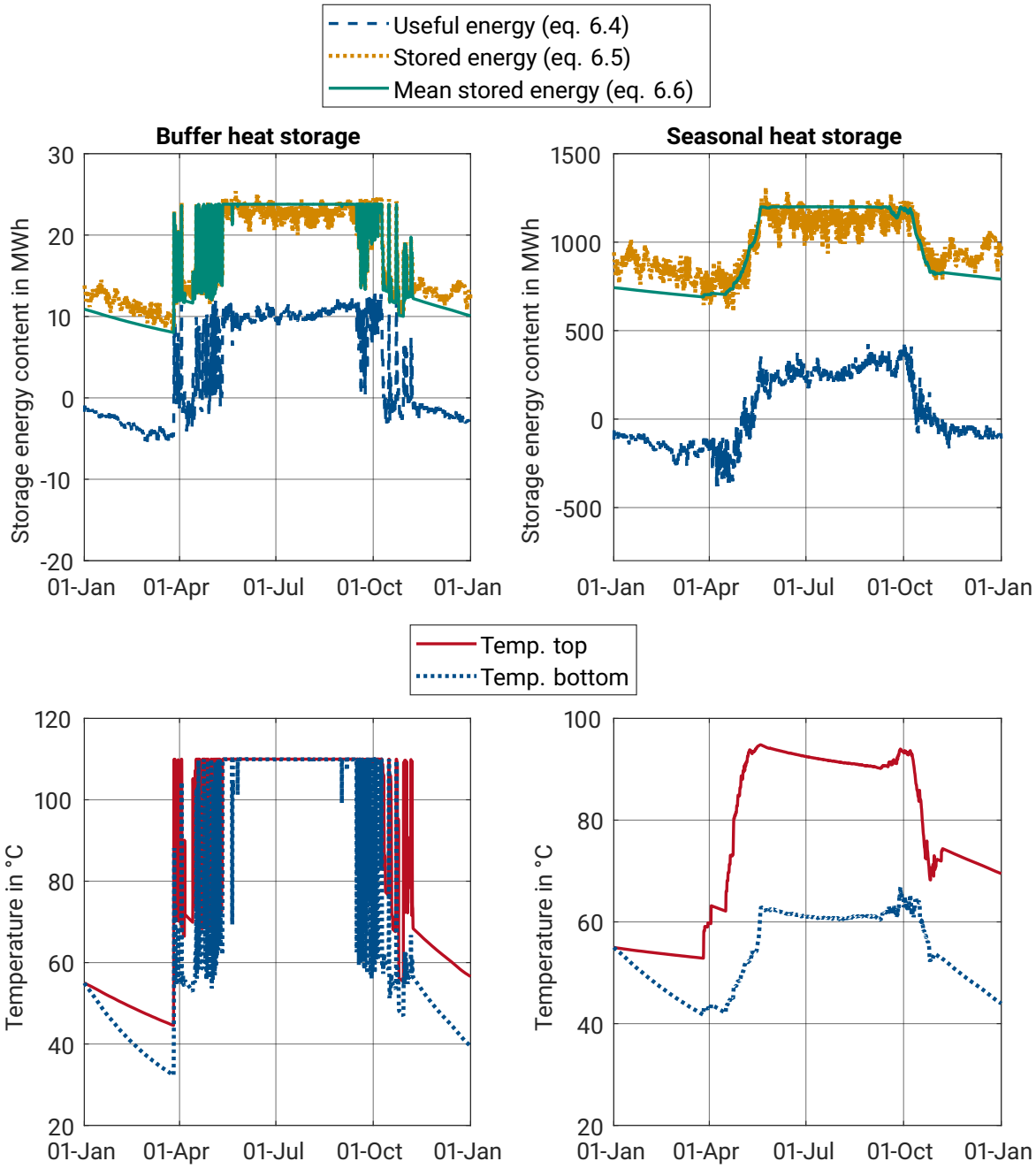

Fig. 7.7: Storage energy content and temperatures in the design and operation optimization scenario $S_{\text{des\&op}}$.

energy content to be equal to its initial level, due to the shorter prediction period. Nevertheless, the total change in stored energy in both the buffer and seasonal heat storage between the beginning and the end of the simulation period only represents 0.01 % of the final energy supply in $S_{\text{des\&op}}$ and can thus be neglected.

7.5.3 Grid electric power supply

Since a combined generation of heat and power is economically and ecologically more efficient than buying electric energy from the grid and supplying heat via HOB, the optimization algorithm intents to maximize the share of CHP generation in the total energy mix. The increase in CHP capacity in $S_{\text{des\&op}}$ compared to S_{ref} helps to lower the amount of grid electric power supply, especially due to lower demand in winter months (see Fig. 7.8). In total, electric energy from the grid can be reduced by 20 % (1100 MWh/a).

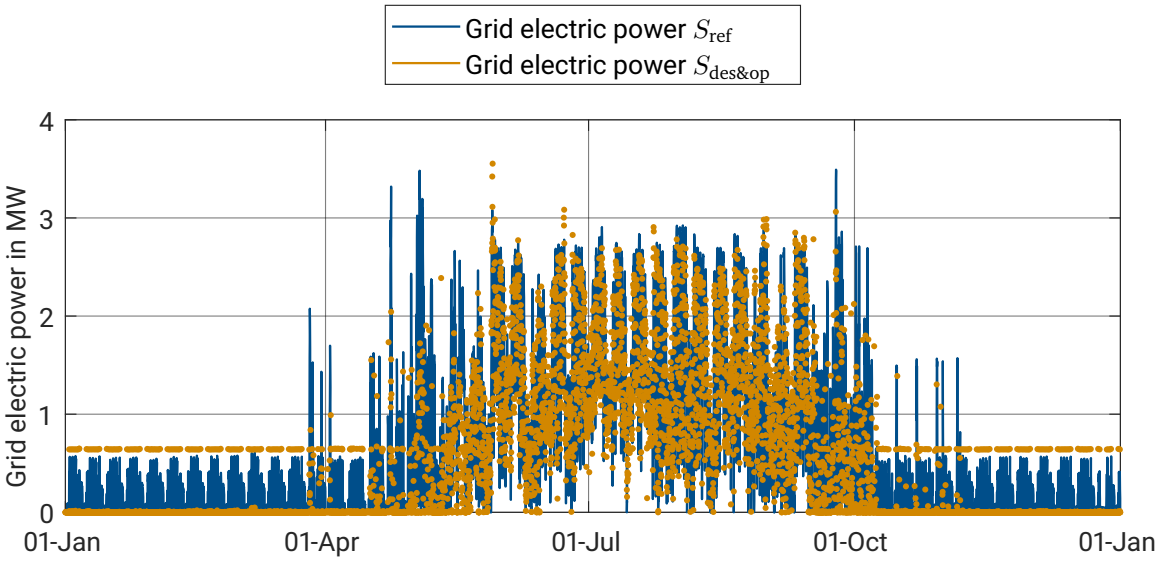

Fig. 7.8: Grid electric power supply in the reference scenario S_{ref} and the design and operation optimization scenario $S_{\text{des\&op}}$.

7.5.4 Cooling power supply and demand

As a result of the installation of hot-water server cooling at "Lichtenberg Hochleistungsrechner" (see chapter 9), the demand for cooling is reduced significantly between S_{ref} and $S_{\text{des\&op}}$. In Fig. 7.9, the total cooling power supply from absorption cooling and compression cooling in S_{ref} and $S_{\text{des\&op}}$ as well as the cooling power demand are displayed. The data center represents a base load in the cooling power demand of campus Lichtwiese. After the transition from cold-air cooling to hot-water cooling for the HPC section of the data center, the cooling power demand is reduced by $\Delta\dot{Q}_{\text{cool,HPC}} = 360\,\text{kW}$ [79]. Nevertheless, the design optimization algorithm proposes an increase of the capacity of the absorption chiller from $\dot{Q}_{\text{cool,AC}} = 1000\,\text{kW}$ to $\dot{Q}_{\text{cool,AC}} = 1280\,\text{kW}$. The greater AC capacity makes it possible to reduce the amount of cooling energy supplied by CC in the summer, and simultaneously increases the operating time of the CHP plants because of the additional heat demand by the absorption chiller. During the winter months, the building heat demand is higher than the thermal capacity of the CHP plants. If the absorption chillers were operated during this time of the year, heat from the HOB would have to be used to supply the necessary heat, leading to low efficiencies and higher CO_2 emissions. In $S_{\text{des\&op}}$ compared to S_{ref}, the total cooling energy demand decreases by 39 % (3150 MWh/a), the cooling energy supply from absorption cooling by 17 % (620 MWh/a) and the supply from compression cooling by 58 % (2540 MWh/a). As long as the CO_2 emissions factor for grid electric energy is high, the optimization algorithm intents to minimize the utilization of compression cooling during the

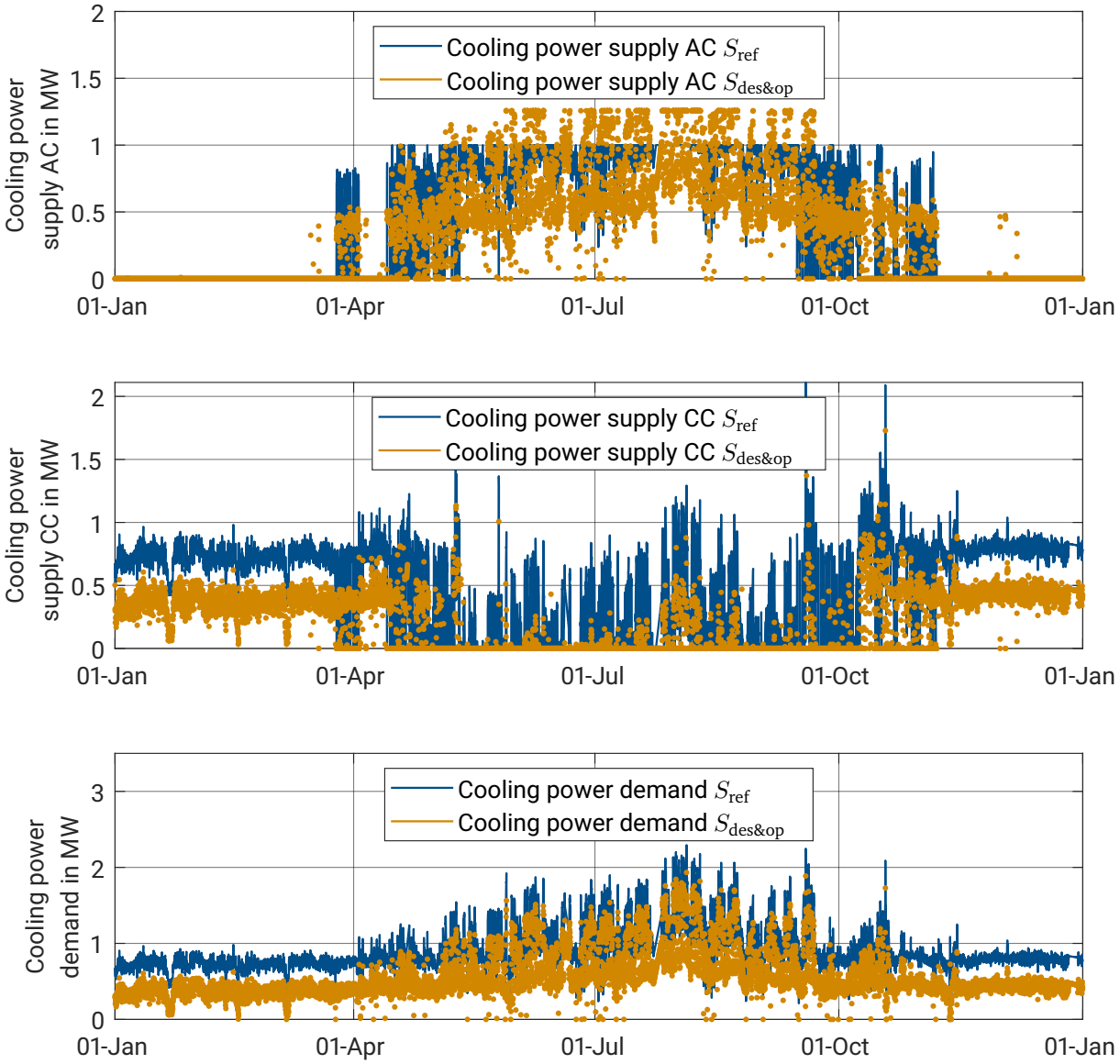

Fig. 7.9: Cooling power supply and demand in the reference scenario S_{ref} and the design and operation optimization scenario $S_{\text{des\&op}}$.

summer months, when excess heat from the CHP plants is available. However, when the share of renewables on the grid increases, it will most probably become ecologically more efficient to supply cooling energy via compression cooling instead of absorption cooling.

7.5.5 Final energy supply

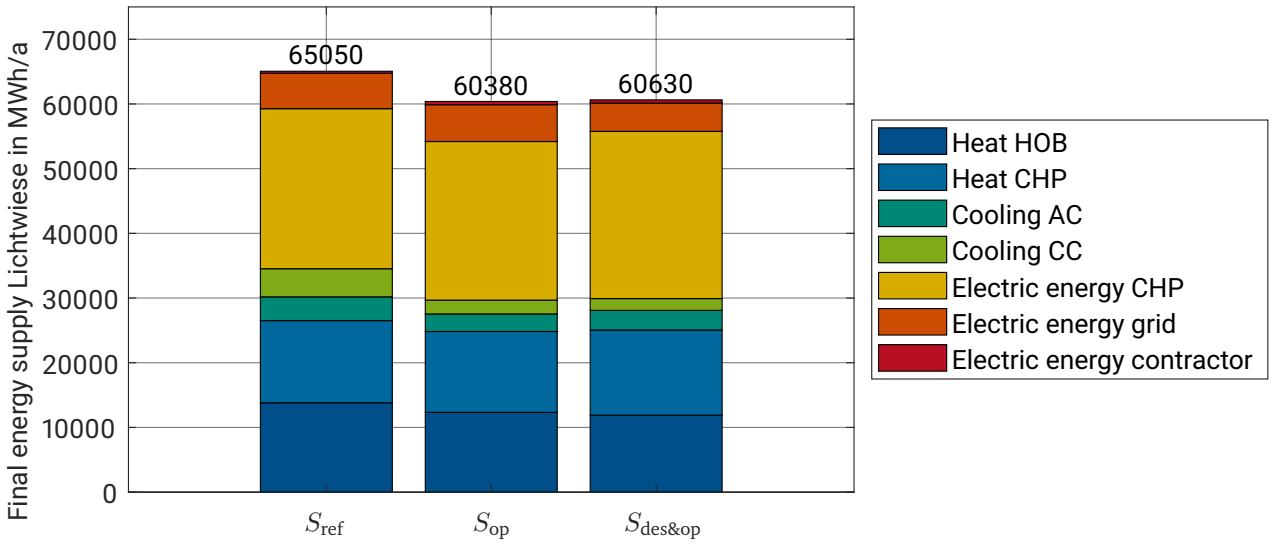

Fig. 7.10: Comparison of the annual final energy supply Lichtwiese in the three scenarios.

In Fig. 7.10, the final energy supplied at the HPS in the different scenarios is demonstrated. Between the reference scenario S_{ref} and the operation optimization scenario S_{op}, the total final energy supply can be decreased by more than 7 %, representing a reduction of almost 4700 MWh/a. The main part of this reduction is generated by a decrease in the cooling energy demand due to the decreased demand for cooling at the high performance computer after the introduction of hot-water-cooled CPU. About 48 % or 1500 MWh/a of the HPC waste heat can be reused (see chapter 9.5), making it possible to decrease the heat supplied by the HOB. Both in thermal and electric energy, the supply changes significantly between S_{op} and $S_{\text{des\&op}}$. Increased CHP capacities resulting from the design optimization help to increase the share of CHP heat, electric energy and absorption cooling energy in the total supply mix. The final energy supply in $S_{\text{des\&op}}$ is marginally higher than in S_{op}. This results from somewhat lower data center waste heat utilization due to increased CHP capacities. Waste heat can only replace HOB heat and must be dissipated to the environment as long as the thermal capacity of the CHP plants exceeds the demand, hence the amount of usable waste heat decreases when the installed CHP capacity is expanded.

Seen individually, an analysis of the final energy supply gives an incomplete picture of the performance of different scenarios, because it aggregates different types of energy supply streams, such as heat and electric energy, with different qualities. Nevertheless, the final energy supply becomes a valuable objective variable when used together with other objective variables such as CO_2 emissions (see chapter 7.5.6), taking into account the quality of the different energy streams. A comparison of both objective variables reveals that while electric energy only represents about half the total energy supply at campus Lichtwiese, more than three quarters of the CO_2 emissions can be attributed to the electric energy supply. This comparison also makes clear that a slightly higher total energy supply in $S_{\text{des\&op}}$ compared to S_{op} can be advantageous, as long as this helps to increase the share of CHP heat and power generation, decreasing the total CO_2 intensity of the energy supply compared to an individual supply of heat and electric energy.

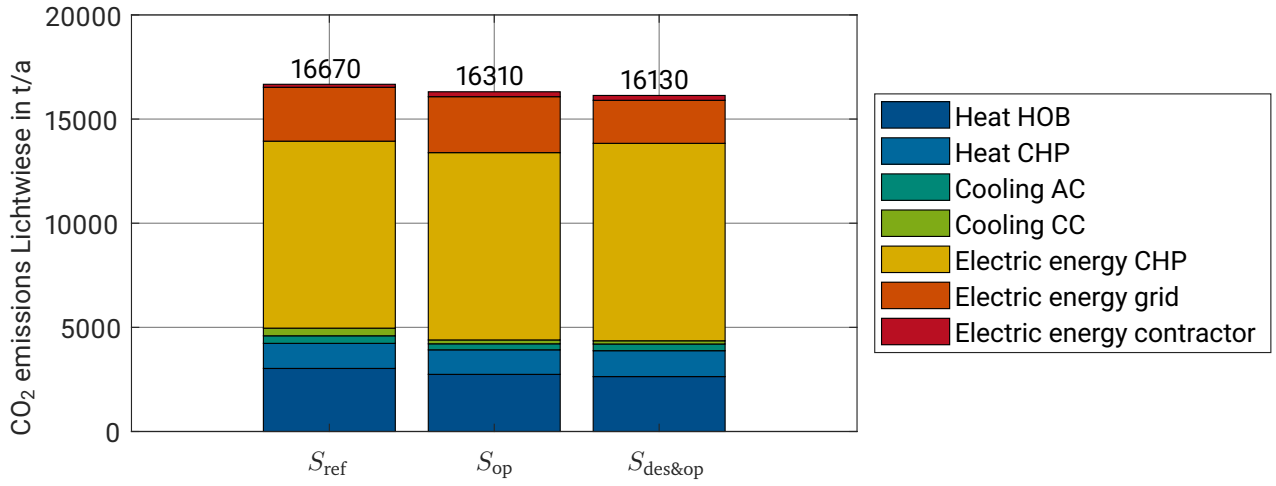

Fig. 7.11: Comparison of the annual CO_2 emissions Lichtwiese in the three scenarios.

7.5.6 CO_2 emissions

Optimizing the design and operation of the generation and storage facilities in the TU Darmstadt energy system and integrating data center waste heat, CO_2 emissions can be reduced by several hundred tons annually. Fig. 7.11 shows the annual CO_2 emissions generated for the energy supply of campus Lichtwiese in the three scenarios. Compared to S_{ref}, CO_2 emissions can be reduced by 2.2 % (360 t_{CO2}/a) in S_{op}, mainly because of reduced data center cooling demand and reduced HOB heat generation due to the integration of data center waste heat in the district heating network. In $S_{des\&op}$, CO_2 emissions reduction reaches 3.2 % (530 t_{CO2}/a) compared to S_{ref}. Compared to S_{op}, the CO_2 emissions from CHP electric energy increase by 5.4 % (480 t_{CO2}/a) in $S_{des\&op}$, while the CO_2 emissions from grid electric energy fall by 23 % (620 t_{CO2}/a).

These results clearly demonstrate that an improvement of the design and operation of the HPS including storage makes it possible to increase the share of CHP generation and to reduce CO_2 emissions. The main source of CO_2 emissions is the electric energy demand, which needs to be further reduced in the future, in order to reach the university's own climate protection goals.

7.5.7 Annuities of investment, operation-related, demand-related and CO_2-related costs

Fig. 7.12 and Fig. 7.13 compare the three different scenarios in terms of annuities for capital-related costs (investment costs), operation-related costs, demand-related costs and costs related to CO_2 emissions (CO_2 emissions costs), as defined in chapter 5.3.3. Demand-related costs are divided in energy demand costs and capacity charges for network usage (capacity costs). The energy demand, CO_2 emissions and capacity costs are calculated for campus Lichtwiese, the investment and operation-related costs represent the annuity of the respective facilities as a whole. A breakdown of investment and operation-related costs into shares for the different campus areas was not made, since those cost types cannot be explicitly attributed to one area.

The annuities of the investment and operation-related costs are almost the same in S_{ref} and S_{op}, except for the heat pump necessary to realize the HPC waste heat utilization. In $S_{des\&op}$, the annuity of the investment and operation-related costs is increased by 24 % (140 000 €/a) compared to S_{ref}, because new facilities are added to the system. Higher investment costs mainly result from the additional seasonal heat storage and increased

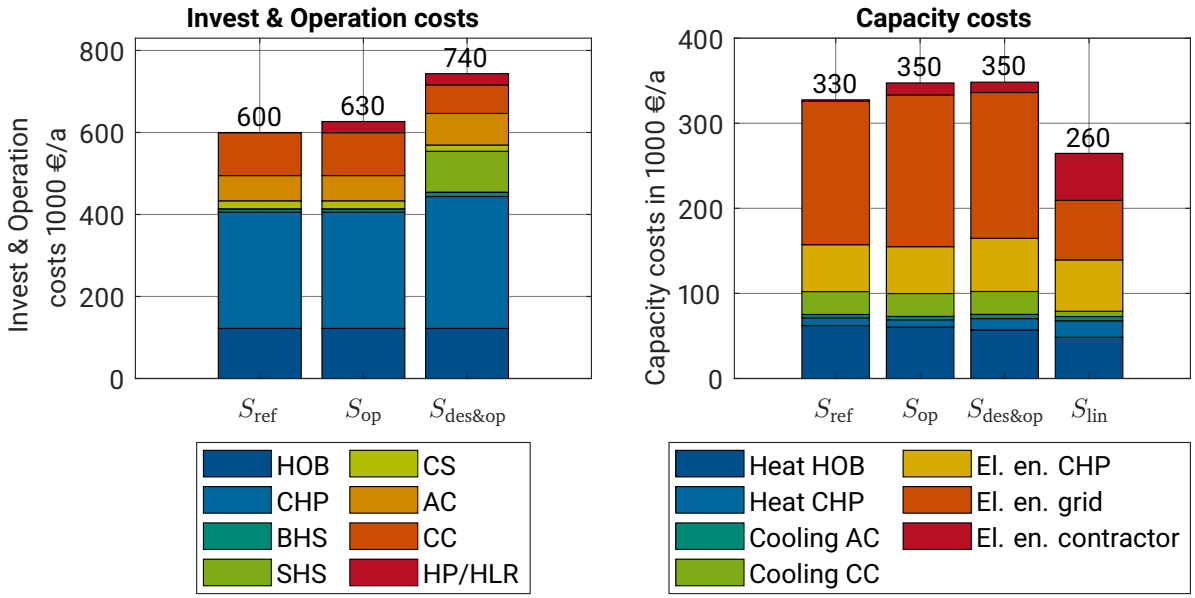

Fig. 7.12: Comparison of the annuities of the investment and capacity costs in the three scenarios, as well as capacity costs of linear design optimization S_{lin} (benchmark).

CHP capacities. Capacity costs are lowest in S_{ref} and rise by 6 % (20 000 €/a) in S_{op} and $S_{\text{des\&op}}$. The increase is due to higher CHP capacity costs resulting from increased capacities, and a higher maximum grid electric power demand. In the diagram, capacity costs resulting from the case of the linear design optimization S_{lin} were added as a benchmark. Due to the long prediction period, the design optimization minimizes peak supply and capacity costs. This affects the operation of the HOB and the amount of electric energy supplied from the grid. The benchmark shows that it would be possible to lower the capacity costs in $S_{\text{des\&op}}$ by 20 % (70 000 €/a) compared to S_{ref}. This would require reliable predictions of the energy demand for periods a lot longer than the weekly prediction horizon applied here.

The main cost driver for the demand-related costs is the electric energy demand of the campus, representing about 70 % of the total demand-related costs. A reduction of the university's electric energy demand is not only a priority to reduce CO_2 emissions (see chapter 7.5.6), but also to reduce energy costs. Demand-related costs can be decreased in S_{op} and even more in $S_{\text{des\&op}}$, compared to S_{ref}. In S_{op}, the demand-related costs are 2 % (70 000 €/a) below the costs in S_{ref}, mainly due to the decrease in HOB heat supply after the integration of data center waste heat. In $S_{\text{des\&op}}$, the demand-related costs are 6 % (230 000 €/a) below the costs in S_{ref}. In addition to the decrease in HOB heat supply, electric energy supply is moved from grid electric energy to CHP electric energy, which comes at lower costs. The comparison of CO_2 emissions costs shows the same characteristics as the comparison of the CO_2 emissions (see chapter 7.5.6).

Fig. 7.14 depicts the total costs of the energy supply in the three scenarios. More than half of the total costs in each scenario are demand-related. $S_{\text{des\&op}}$ shows the highest share of investment, operation-related and capacity costs, but the total costs are 2 % (130 000 €/a) lower than in S_{ref}.

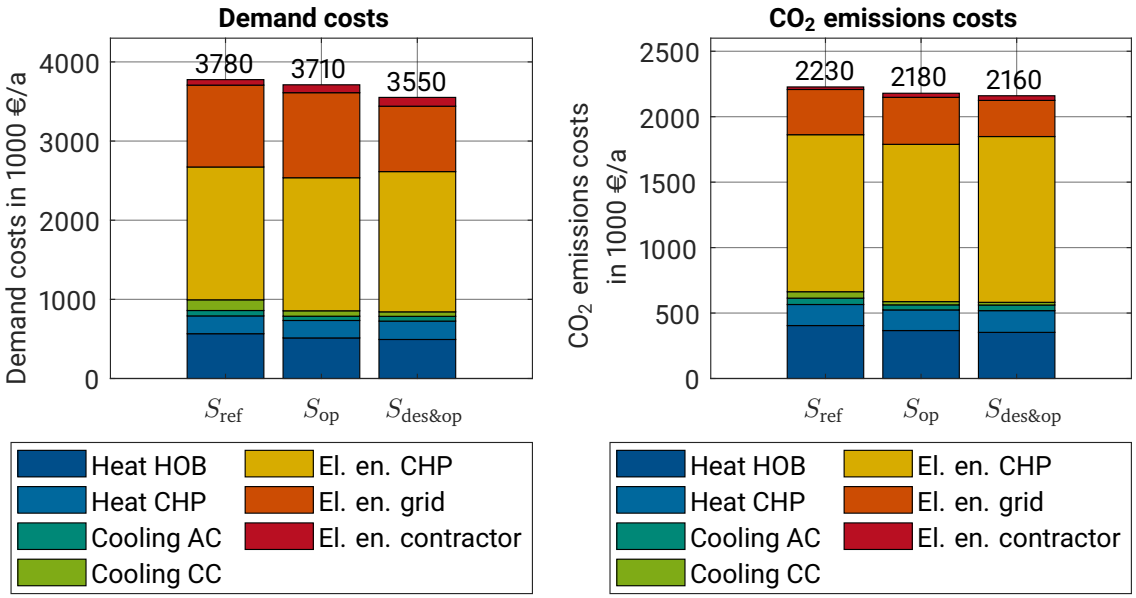

Fig. 7.13: Comparison of the annuities of energy demand costs and CO_2 emissions charges in the three scenarios.

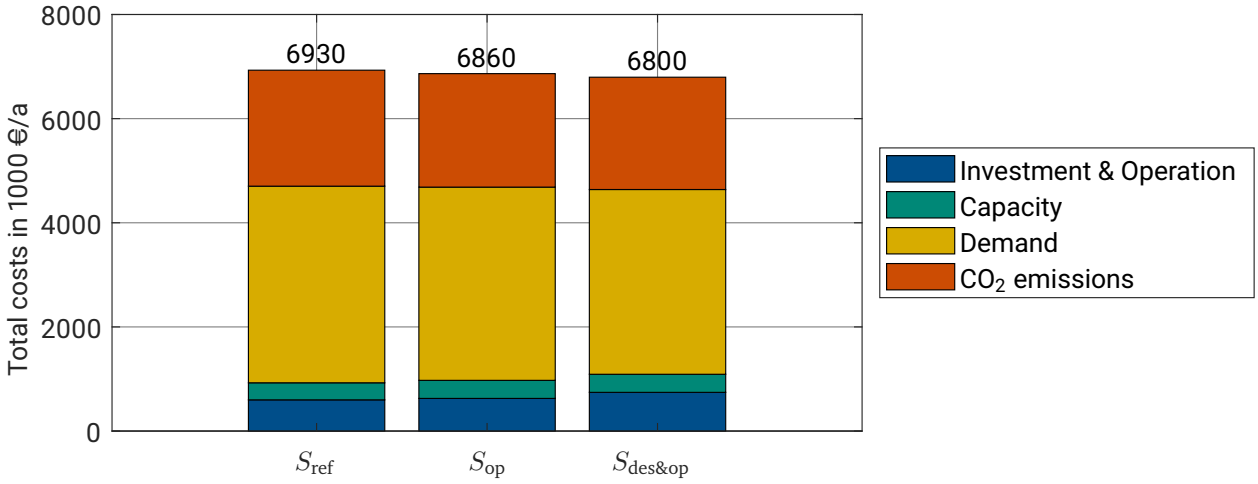

Fig. 7.14: Comparison of the total annual costs in the three scenarios.

7.5.8 Energy and exergy analysis

The following Sankey flow diagrams show the quantitative (energy) and qualitative (exergy) losses within the energy system of TU Darmstadt in the reference scenario S_{ref} and the design and operation optimization scenario $S_{des\&op}$. Energy and exergy enter the system as gas, HPC waste heat and grid electric energy, and are supplied to campus Lichtwiese as well as the other campus areas as heat, cooling, and electric energy. Due to the integration of an optimized storage operation strategy and hot-water cooling as well as waste heat utilization at TU Darmstadt's high-performance computer "Lichtenberg-Hochleistungsrechner", scenario

$S_{\text{des\&op}}$ is significantly more complex than S_{ref}.

The differences between S_{ref} and $S_{\text{des\&op}}$ are an increase in CHP based heat and power generation, resulting in a decrease in HOB heat generation and grid electric energy demand. Due to the data center hot-water cooling and waste heat utilization, the cooling demand decreases significantly. Even though the fraction of stored heat and cooling energy is small compared to the overall demand, the storage usage in $S_{\text{des\&op}}$ has an important impact on the generation mix compared to S_{ref}, where no optimized operation strategy for the storage tanks was implemented.

While energetic losses from the HOB are smaller than from the CHP plants, exergetic losses are significantly higher in the case of the HOB, making clear why combined generation of heat and power is preferable in a system with demand for both. A significant portion of the exergy content of the supplied heat is destroyed at the exit of the HPS, due to the return flow admixture reducing the supply temperature at that point in the system. Cooling exergy demand is almost negligible, because its temperature level is very close to the ambient temperature, which serves as reference for the exergy analysis (see chapter 5.1).

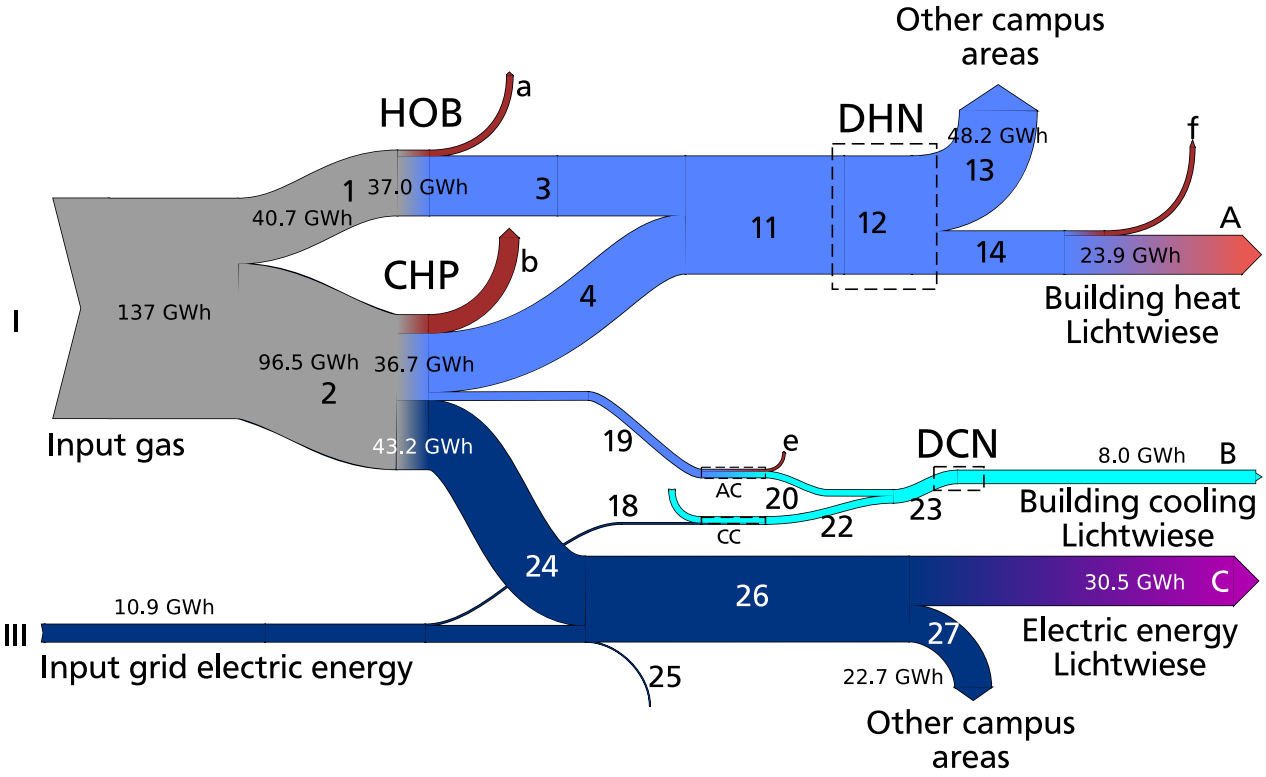

Fig. 7.15: Energy flow diagram for the reference scenario S_{ref}.

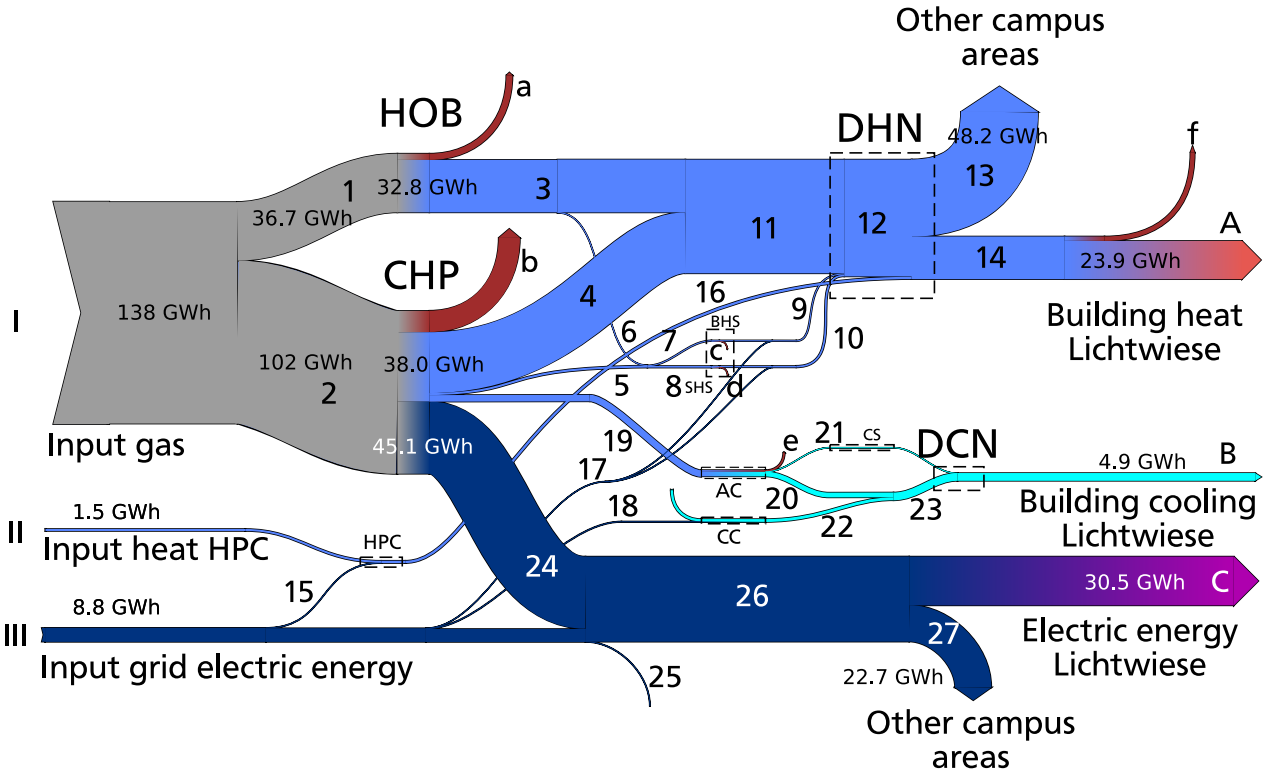

Fig. 7.16: Energy flow diagram for the design and operation optimization scenario $S_{\text{des\&op}}$.

Table 7.5: Labeling of the energy flow diagram for scenarios S_{ref} and $S_{\text{des\&op}}$ in Fig. 7.15 and Fig. 7.16.

Number	Description	Number	Description
I	Input natural gas	17	Electric energy HP storage
II	Input HPC waste heat	18	Electric energy CC
III	Input grid electric energy	19	CHP heat AC
1	Natural gas HOB	20	AC cooling energy to network
2	Natural gas CHP	21	Cooling energy to storage
3	District heat HOB	22	CC cooling energy to network
4	District heat CHP	23	District cooling energy
5	Charge storage CHP	24	Output electric energy CHP
6	Charge storage HOB	25	Electric energy network pumps
7	Charge buffer heat storage	26	Electric energy demand TU Darmstadt
8	Charge seasonal heat storage	27	Electric energy demand other campus areas
9	Discharge buffer heat storage	a	Energy loss HOB
10	Discharge seasonal heat storage	b	Energy loss CHP
11	Generation district heat	c	Heat loss buffer heat storage
12	Generation district heat and storage heat	d	Heat loss seasonal heat storage
13	District heat to other campus areas	e	Energy loss AC
14	District heat campus Lichtwiese	f	Heat loss district heating network Lichtwiese
15	Electric energy HP/HPC	A	Building heat demand Lichtwiese
16	Network heat HPC	B	Cooling energy demand Lichtwiese
		C	Electric energy demand Lichtwiese

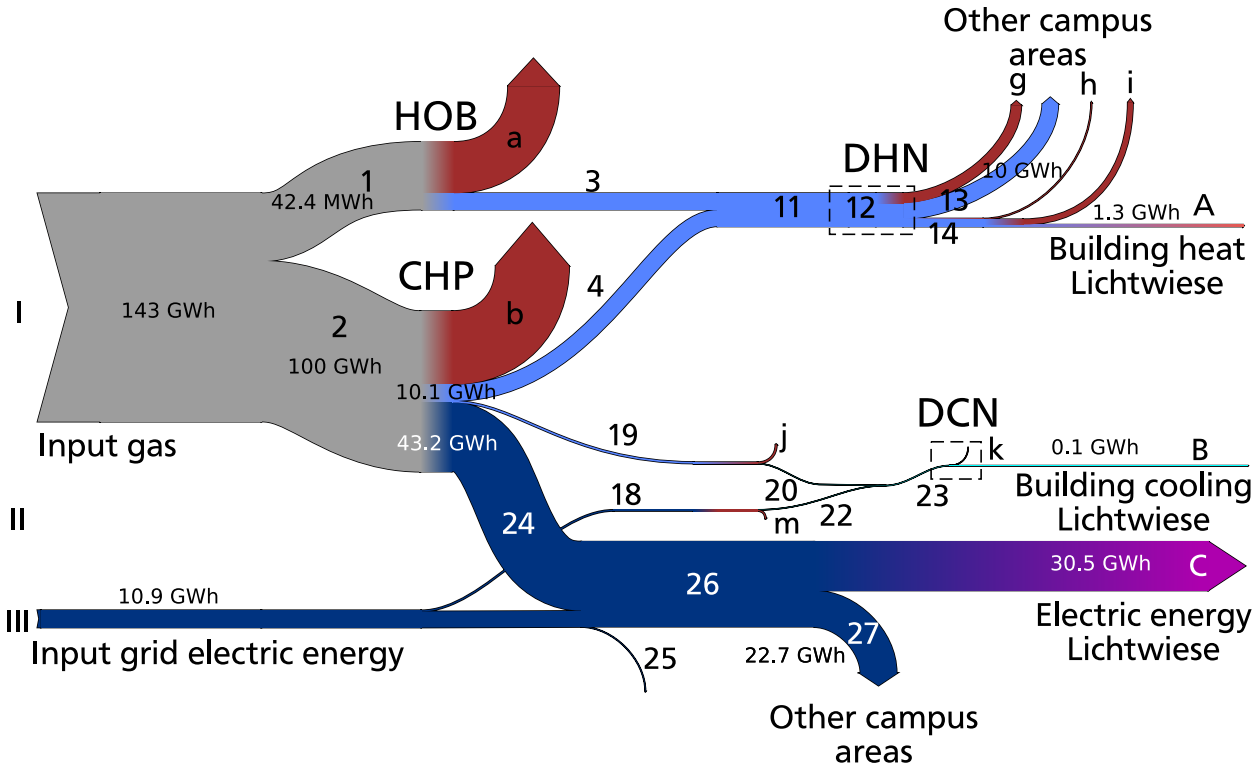

Fig. 7.17: Exergy flow diagram for the reference scenario S_{ref}.

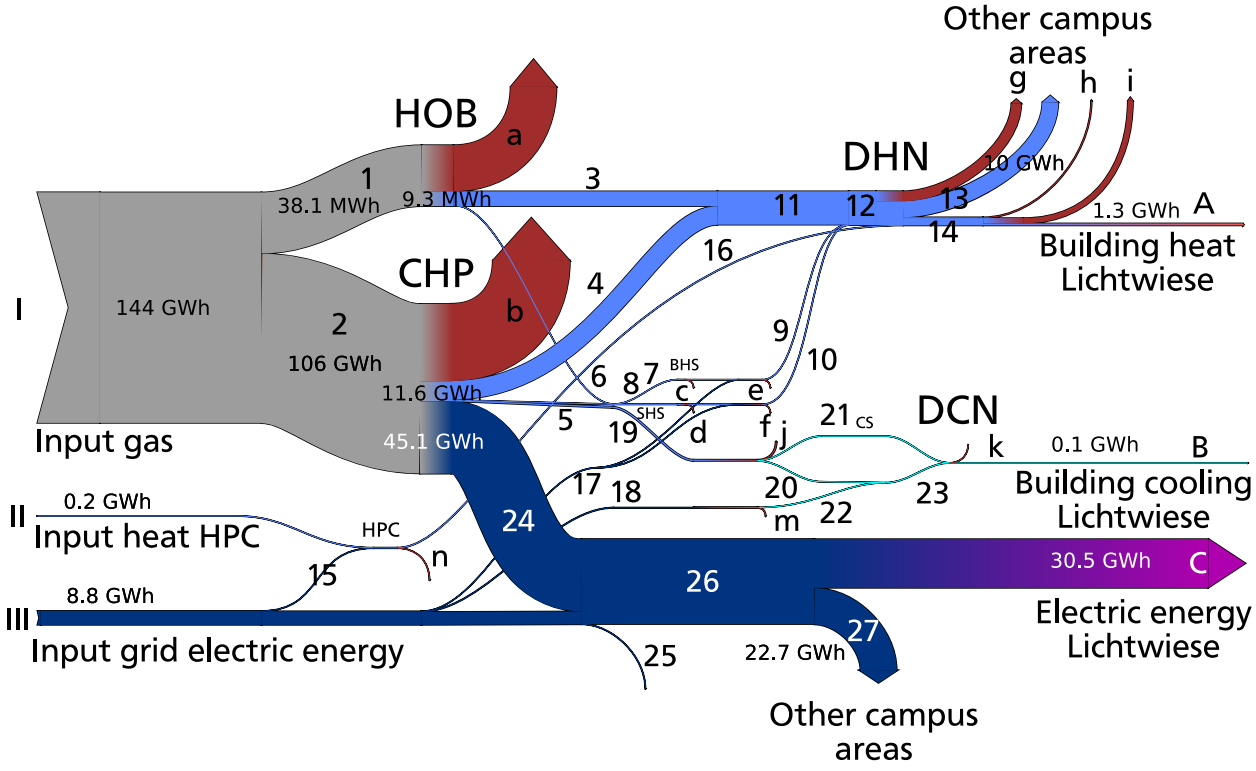

Fig. 7.18: Exergy flow diagram for the design and operation optimization scenario $S_{\text{des\&op}}$.

Table 7.6: Labeling of the exergy flow diagram for scenarios S_{ref} and $S_{\mathrm{des\&op}}$ in Fig. 7.17 and Fig. 7.18.

Number	Description	Number	Description
I	Input natural gas	21	Cooling exergy to storage
II	Input HPC waste heat	22	CC cooling exergy to network
III	Input grid electric energy	23	District cooling exergy
1	Natural gas HOB	24	Output electric exergy CHP
2	Natural gas CHP	25	Electric exergy network pumps
3	District heat HOB	26	Electric exergy demand TU Darmstadt
4	District heat CHP	27	Electric exergy demand other campus areas
5	Charge storage CHP	a	Exergy loss HOB
6	Charge storage HOB	b	Exergy loss CHP
7	Charge buffer heat storage	c	Exergy loss buffer heat storage
8	Charge seasonal heat storage	d	Exergy loss seasonal heat storage
9	Discharge buffer heat storage	e	Exergy loss heat pump buffer heat storage
10	Discharge seasonal heat storage	f	Exergy loss heat pump seasonal heat storage
11	Generation district heat	g	Exergy loss return flow admixture exit HPS
12	Generation district heat and storage heat	h	Exergy loss network Lichtwiese
13	District heat to other campus areas	i	Exergy loss substations
14	District heat campus Lichtwiese	j	Exergy loss heat AC
15	Electric energy HP/HPC	k	Exergy loss network cooling
16	Network heat HPC	m	Exergy loss CC
17	Electric exergy HP storage	m	Exergy loss HP/HPC
18	Electric exergy CC	A	Exergy heat demand Lichtwiese
19	CHP heat AC	B	Cooling exergy demand Lichtwiese
20	AC cooling exergy to network	C	Electric energy demand Lichtwiese

7.5.9 Sensitivity analysis electric energy demand

The results of the design and operation optimization depend on the underlying assumptions regarding the energy demand for heat, cooling, and electric energy. Especially the electric energy demand has a great influence on the target variables final energy supply, CO_2 emissions, and total costs, while the input data for electric energy demand depends on three week-long monitoring campaigns, because continuous electric monitoring is not yet available (see chapter 6.2). It can also be assumed that the electric energy demand will change in the future. Both an increase due to additional buildings or electrification of heating and cooling, as well as a reduction through improved energy efficiency on the consumer side are possible scenarios. Therefore, the effects of both an increase and a reduction of the electric energy demand of the TU Darmstadt (not including electric energy attributed to the contractor) by 10 % on the design and operation optimization scenario $S_{\text{des\&op}}$ are examined. First of all, it is determined how the change in electric energy demand affects the optimal design of the generation facilities and storage. Subsequently, a comparison of the grid electric energy supply in the different scenarios is presented, and the resulting CO_2 emissions are calculated. Table 7.7 shows the dimensioning of the generation plants and storage facilities according to the design optimization algorithm for the different scenarios. HOB and CC are not included in the table, because their capacity is defined to remain constant for all scenarios of the sensitivity analysis. Photovoltaic cells are too costly to be considered in any of the scenarios (see chapter 7.1).

Fig. 7.19 shows the grid electric power supply for the different cases of the sensitivity analysis. Even though the optimal CHP capacity grows with higher electric energy demand, the average share of CHP in the electric supply decreases from 88.5 % in $S_{\text{des\&op,90\%}}$ to 83.4 % in $S_{\text{des\&op,110\%}}$. It is not feasible to increase the CHP capacity even more when the electric energy demand goes up, because the yearly operating hours decrease for higher CHP capacities, as long as the total heat demand does not change.

The electric energy demand has a significant impact on overall CO_2 emissions. An increase or decline of electric energy demand by 10 % leads to a change in total CO_2 emissions by 7 % (see Fig. 7.20). With rising electric energy demand, the CO_2 emissions for heating and cooling show a slight decrease due to higher CHP capacities, but the savings do not compensate the additional emissions due to higher electric energy supply both from the CHP and the grid.

The sensitivity analysis shows the importance of the impact of electric energy demand on total CO_2 emissions. It becomes clear that an improvement of the energy generation system as proposed by the design optimization algorithm (see chapter 7.1) only has a limited impact on reducing the CO_2 emissions. In the future, it will be necessary to prioritize the improvement of the electric efficiency of the users as well as the integration of renewable electric energy to reach TU Darmstadt's climate protection goals.

Table 7.7: Capacities generation units and storage for different electric energy demands in $S_{\text{des\&op}}$.

	90% of electric energy demand 2018	**Electric energy demand 2018**	**110% of electric energy demand 2018**
Total thermal capacity CHP	7120 kW_{th}	7940 kW_{th}	8765 kW_{th}
Cooling capacity AC	1275 kW_{th}	1280 kW_{th}	1290 kW_{th}
Capacity BHS	8 MWh_{th}	11 MWh_{th}	13 MWh_{th}
Capacity SHS	500 MWh_{th}	500 MWh_{th}	500 MWh_{th}
Capacity CS	1.7 MWh_{th}	1.8 MWh_{th}	1.9 MWh_{th}

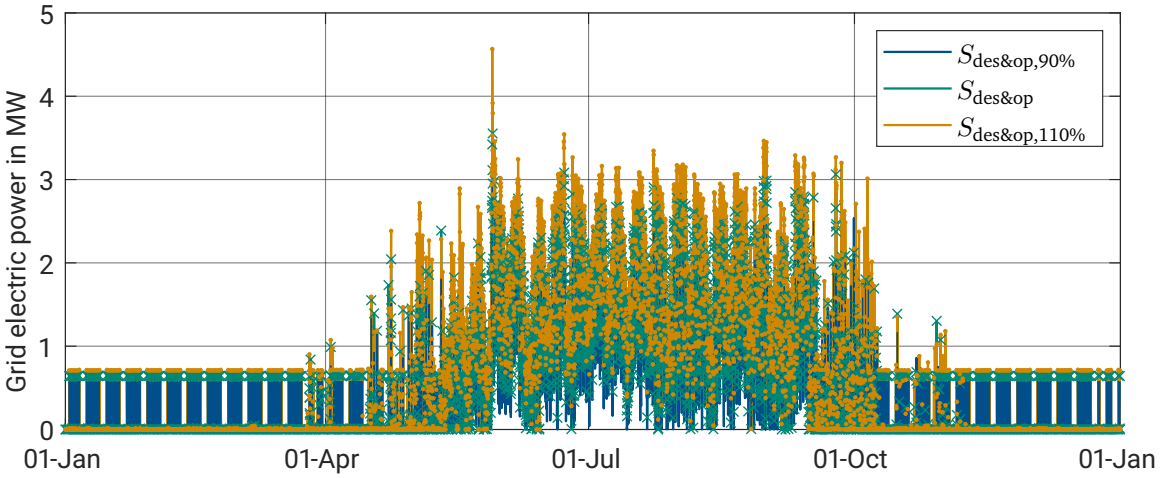

Fig. 7.19: Sensitivity analysis of grid electric power supply in the design and operation optimization scenario $S_{\text{des\&op}}$.

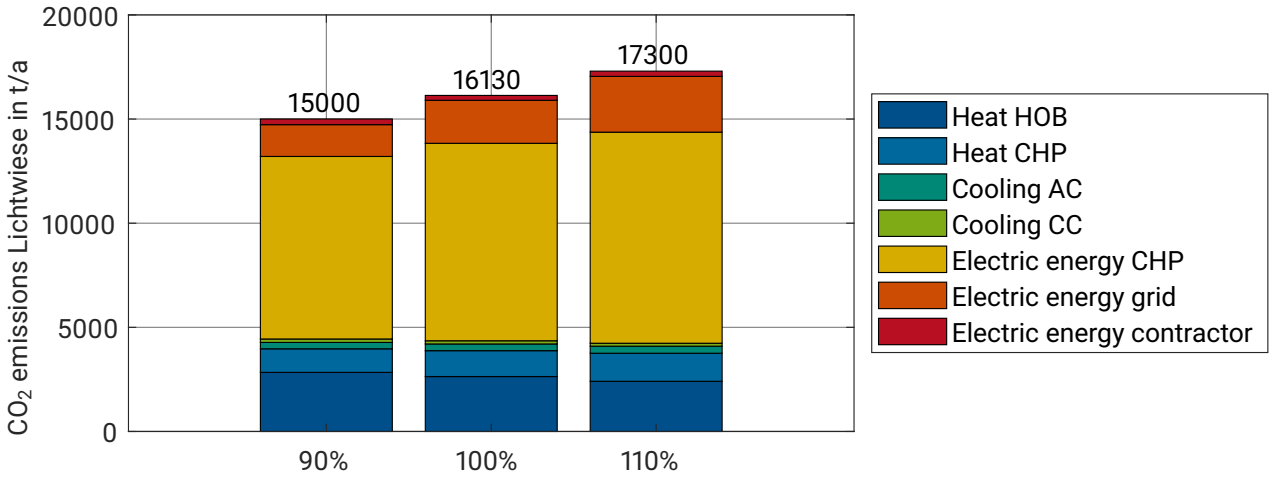

Fig. 7.20: Sensitivity analysis of CO_2 emissions in the design and operation optimization scenario $S_{\text{des\&op}}$.

7.6 General application of the two-stage optimization method

The two-stage optimization method presented in this chapter was developed for the design and operation optimization of the TU Darmstadt energy system. Nevertheless, this approach can be used to improve the design and operation of any district energy system including demand for heat, cooling, and electric energy. For the method to be applied successfully to other districts, the necessary data has to be available, especially data on energy demand, costs, and CO_2 emissions factors. The method can either be used to determine the optimal design and operation of an existing system as benchmark, or to plan the energy supply in a new district.

As long as renewable energy sources are not readily available, the most efficient way to generate heat and power in a district energy system is cogeneration. Consequently, an optimization of the design and operation of a classic district energy system will always maximize the operating hours of the CHP units available in the

system. In the future, district energy systems will face more complex circumstances when renewable sources of heat and electric energy with very low economic and ecologic marginal costs are integrated into the system. Sources of renewable heat are often available at decentralized locations, as in the case of data center waste heat, or fluctuate due to external factors, as in the case of solar-thermal heat. Additionally, renewable electric energy will make the CO_2 emissions factor for grid electric energy fall below the emissions factor of electric energy from cogeneration. In Germany, it will probably take another 10-15 years until this point is reached, thus cogeneration will continue to play a major role in district heat and power supply for the time being. Therefore, intelligent design and operation strategies for cogeneration-based district energy systems remain necessary.

At the same time, district heating operators have to keep in mind that the results of a design and operation optimization are always based on the specific demands, efficiencies, costs, and emissions factors provided as model inputs, and that the optimal system layout evolves with changes in the aforementioned parameters. To reach local and national climate protection goals, renewable energy sources will have to become the main component of district energy systems in the future. The optimal design of a district energy system will thus change in upcoming years, and decision-makers have to anticipate the transition to prepare their systems for decarbonization.

8 Fourth generation district heating: Reducing network temperatures

The reduction of both supply and return temperatures in district heating systems has been a priority for district heating operators since the development of the first networks in the late 19th century, and continues to be a major focus of academic research (see chapter 2). Reducing temperatures in district heating systems helps to improve the efficiencies of the generation units, leads to lower network heat losses and allows to integrate renewable and other heat sources more efficiently, such as waste heat from data centers as described in chapter 9. Lower return temperatures decrease the mass flow at constant heat demand and make it possible to reduce pumping costs, decrease pipe diameters and connect additional users to an existing network. Fig. 8.1 (adopted from [43]) outlines the historic development of district heating since the 1880s.

District heating networks are categorized into generations according to their temperature level and potential heat sources. The first generation encompasses networks constructed in the late 19th and early 20th century operated with steam, second generation networks include those constructed during the 20th century and operated with water at supply temperatures above 100 °C, and the third generation represents the current standard, i.e. networks with supply temperatures close to but below 100 °C. Current research focuses on the

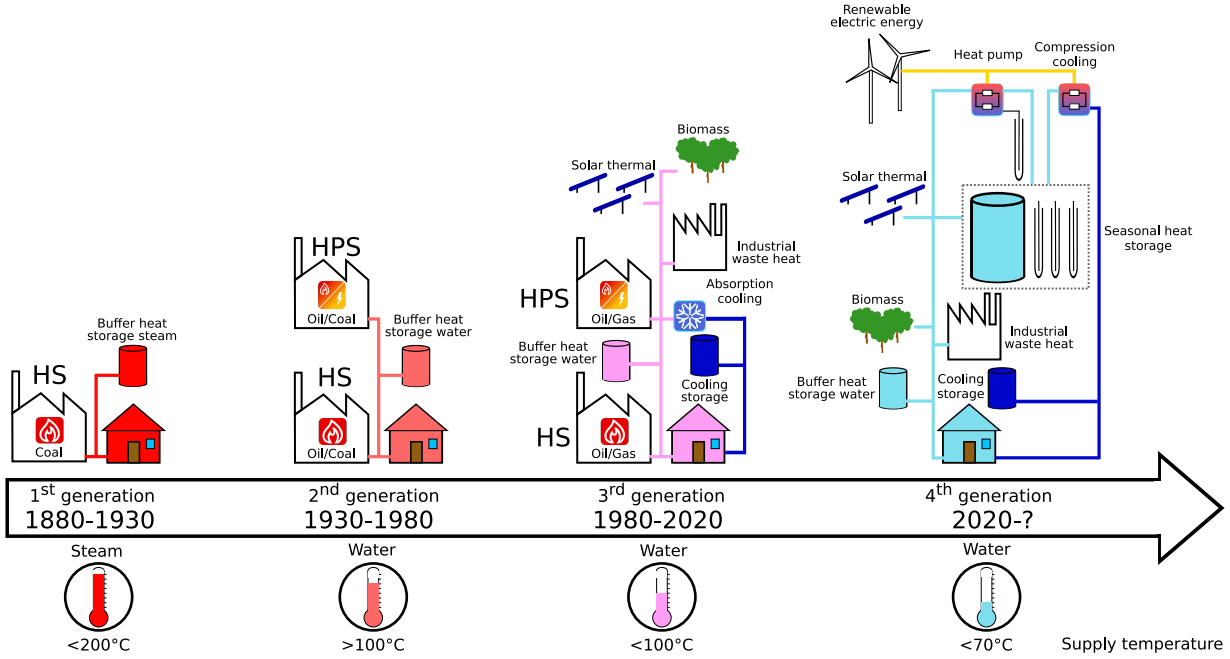

Fig. 8.1: Historic development of district heating temperatures and heat sources (adopted from [43]).

development and implementation of fourth generation district heating concepts at supply temperatures well below 100 °C [43, 46].

Temperatures in a district heating system depend on the specific characteristics of the buildings connected to the system, which is why the buildings play a key role when reducing the temperatures in an existing district heating system. Guaranteeing the comfort temperature for users serves as a boundary condition for reducing the supply temperature, and the return temperature of the network results from the mix of return temperatures at the individual substations. Each substation has a unique impact on the district heating system. The system supply temperatures may be high due to the requirement of one substation for a high temperature, while all other substations might be able to ensure their users' comfort temperatures at a lower level. On the return side, a substation with a high return temperature usually operates at a small temperature difference between supply and return and demands a high mass flow, resulting in an above-average influence on the system return temperature. On one hand, this means that a high return temperature in one substation can be decisive for the return temperature of the whole network. On the other hand, improvement measures taken in a few buildings with bad performance can have a great impact on the entire system. To benefit from this situation, it is necessary to identify which substations are critical and what measures should be applied in order to have the highest impact at minimal effort.

At TU Darmstadt campus Lichtwiese, heat is supplied to the substations for space heating, ventilation heating and, in a few cases, hot water preparation. Due to a high demand for ventilation especially in laboratory buildings, ventilation heat demand plays a major role in this particular energy system. Ventilation heating does not serve to supply heat to the buildings, but only to ensure that the air supply enters the room at room temperature instead of ambient temperature. The building heat demand is provided by the water-based space heating system. In the context of this thesis, ventilation heating refers to conditioning the incoming ambient air to room temperature, not to an air-based room heating system.

Centralized hot water preparation via district heating plays a subordinate role at TU Darmstadt campus Lichtwiese, because most buildings have a very low hot water demand and are supplied by decentralized direct electric heaters. Nevertheless, the hot water heating circuits connected to district heating do have a significant impact on the network temperatures. In the following, the three types of heat distribution inside the buildings are evaluated in detail.

Reducing district heating network temperatures represents a crucial step to prepare the TU Darmstadt campus Lichtwiese energy system for decarbonization. Only after a reduction of network temperatures it will be possible to replace the current mostly fossil-based heat supply with renewable sources, such as geothermal and solar-thermal heat. The purpose of this chapter is to offer practitioners at TU Darmstadt and beyond an easy way to identify where in their system which kind of inefficiencies occur and which issues should be prioritized to generate the highest possible impact on the overall system temperature.

8.1 Defining average district heating network temperatures

In a district heating system with a central heating plant, the network return temperature for each time step $T_{\mathrm{R,DHN},i}$ can be measured directly. If the necessary data is not available, as is the case at TU Darmstadt campus Lichtwiese, it can be simulated with the help of an energy system model, such as the one presented in chapter 6. The goal of this chapter is to offer simple approaches to identify inefficiencies in the operation of the heat supply systems inside the buildings connected to the network, and to propose improvement measures. Therefore, the first step is to define how to calculate network return temperatures without setting up a detailed model.

When monitoring data is available at the substation level but not at the HPS, the network return temperature $T_{\mathrm{R,DHN},i}$ can be approximated as the weighted average of the return temperatures of each substation j at time step i $T_{\mathrm{R},i,j}$, with n_{sub} being the number of substations in the system and $\dot{M}_{i,j}$ the mass flow through substation j:

$$T_{\mathrm{R,DHN},i} = \frac{\sum_{j=1}^{n_{\mathrm{sub}}} \dot{M}_{i,j} \cdot T_{\mathrm{R},i,j}}{\sum_{j=1}^{n_{\mathrm{sub}}} \dot{M}_{i,j}} \tag{8.1}$$

There are two different ways to define the annual average return temperature of a network over a certain number of time steps n_{ts}, either a time-averaged or a mass-averaged approach. The time-averaged approach simply calculates the average of the network return temperature over the time period under consideration. Eq. 8.2 and eq. 8.3 assume a constant time step length.

$$\overline{T}_{\mathrm{R,DHN},\tau} = \frac{1}{n_{\mathrm{ts}}} \sum_{i=1}^{n_{\mathrm{ts}}} \frac{\sum_{j=1}^{n_{\mathrm{sub}}} \dot{M}_{i,j} \cdot T_{\mathrm{R},i,j}}{\sum_{j=1}^{n_{\mathrm{sub}}} \dot{M}_{i,j}} \tag{8.2}$$

The mass-averaged approach weights the network return temperature $T_{\mathrm{R,DHN},i}$ with the network mass flow $\sum_{j=1}^{n_{\mathrm{sub}}} \dot{M}_{i,j}$, resulting in the temperature of a theoretical tank containing the entire aggregated mass that has passed through the system during the time period under consideration:

$$\overline{T}_{\mathrm{R,DHN,M}} = \frac{\sum_{i=1}^{n_{\mathrm{ts}}} \left(\sum_{j=1}^{n_{\mathrm{sub}}} \dot{M}_{i,j} \cdot T_{\mathrm{R},i,j} \right)}{\sum_{i=1}^{n_{\mathrm{ts}}} \left(\sum_{j=1}^{n_{\mathrm{sub}}} \dot{M}_{i,j} \right)} \tag{8.3}$$

The two approaches serve different purposes. The time-averaged approach gives an understanding of the average temperature in the return pipe and hence serves as a reference when calculating the return pipe heat losses. The heat losses from the pipe to the environment depend on the temperature difference between the flow temperature and the surrounding ground temperature, not on the mass flow transported in the pipe. This is why the time-averaged approach is also used when defining the return temperature reduction potential (see chapter 8.4.1).

The mass-averaged approach is used to calculate the average return temperature of the heat flow transported in the system. In the summer, when the district heat demand is very low, the return temperature at campus Lichtwiese is significantly higher than during winter months (see Fig. 6.11). This is a result of excessive return temperatures from ventilation heating circuits at low demand, as described in chapter 8.5.3. Using the mass-averaged approach, time periods with high return temperatures at very low heat flow are weighted less than periods with high heat flow, eliminating the influence of the operational errors in the ventilation heating circuits. This approach is used when calculating the annual average return temperature of the campus Lichtwiese district heating system (see Table 3.1).

The same approaches can be applied when heat is fed into the system at various points and no individual measurement point represents the overall district return temperature, or when the return temperature of a sub-district is of interest. Both approaches neglect the temperature decrease over the length of the return pipe due to network heat losses between the buildings and the heating plant.

The network supply temperature is not controlled by the buildings, but set centrally at the heating plant itself. It is the same for all substations except for the heat losses within the supply pipe. The supply temperature provided by the plant has to meet the highest temperature demand of all buildings connected to the network. The annual average of the supply temperature $\overline{T}_{\mathrm{S,DHN}}$ can be calculated using either a time-averaged or a mass-averaged approach using the mass flow at the HPS. In a non-residential network where hot water demands are small, temperatures in some parts of a network can be very low (close to ambient temperature)

in summertime, when the heat demand at certain substations falls to zero. A time-averaged approach would lead to a biased annual average supply temperature, which is why the mass-averaged approach is used to calculate $\overline{T}_{\mathrm{S,DHN}}$ (see Table 3.1).

8.2 Measures to decrease network temperatures in an existing district heating system

The following list names seven different measures typically applied to improve the energy efficiency of a building that also have an impact on the supply and return temperatures of the building's heat distribution system. More complex and cost-intensive measures such as the installation of surface heating, or a comprehensive building renovation should not be implemented without eliminating control issues and assuring correct hydraulic balancing.

In the context of this thesis, the term surface heating is used as a general term for different kinds of panel heating systems, such as underfloor heating, wall heating or ceiling heating.

1. Maintenance in heat distribution: Heat distribution installations inside buildings need regular maintenance, to avoid errors such as broken temperature sensors or valves that are stuck, leading to under- or overflow. Typical errors in ventilation heating are excessive bypass flows due to broken valves or malfunctioning control. Due to excessive bypass flows, ventilation heating can turn into an undesired second room-heating system. This should be avoided, because air-heating is a lot less efficient than the water-based space heating system intended to supply the building heat demand.
   Bypasses are necessary for recirculation in ventilation heating circuits to protect them from freezing, but should be equipped with a thermostatic valve to minimize flow and return temperature. If a ventilation heating system includes heat recovery, recirculation becomes unnecessary at most times during the year, as incoming air will usually be heated up to a temperature above freezing in the heat recovery heat exchanger. In some cases, high return temperatures occur due to a lack of communication, e.g. when parts of the ventilation system are removed but the heat supply for these areas is still in place, resulting in a shortcut. A frequent problem in space heating is air trapped inside radiators or surface heating systems, reducing the useful heat transfer area and consequently increasing the necessary temperature level. Air should be removed from the system once a year at the beginning of the heating season.
2. Improvement of substation flow control: The desired secondary side supply temperature depends on the ambient temperature and is set by a valve controlling the district return flow. When the secondary side supply temperature falls below the desired level, the valve opens up to increase the primary side flow in the respective substation. A differential pressure control should be included in this setup, to avoid overflow and to ensure a constant pressure drop over the building heating system. Otherwise, changes in the network differential pressure have an impact on the flow inside the building, counteracting its hydraulic balance.
3. Improvement of in-building flow control: In a hydraulically unbalanced heating system, radiators or ventilation heat exchangers close to the district heating substation receive high mass flows, while those located further away will not be supplied sufficiently or only once the rooms near the substation reach their design room temperature and their thermostatic valves close. To deal with complaints of users in cold rooms, the operator will often increase the supply temperature and the differential pressure in the respective heating circuit, which results in a higher return temperature and electric energy demand for pumping. To avoid this issue, it is necessary to balance the mass flow between the different heat

exchangers (radiators, ventilation). This can be realized using either fixed or dynamic differential pressure control. Fixed differential pressure control is based on the design load of the system, which only occurs on very cold winter days. It is preferable to use dynamic differential pressure control, providing a constant pressure drop over all heating circuits inside a building for varying demand conditions. This makes it possible to achieve an equally distributed flow over all heat exchangers, independent of the demanded load, assuring low return temperatures at all times.

4. User behavior: Users can create inefficiencies in district heating through incorrect use of their installations. In many households, people will not use all available radiators, hoping to reduce energy demand, while instead increasing the demand and consequently the temperature at the remaining radiators. The same is true for a night setback operation mode, which mostly shifts night time heat demand to the early morning hours. This results in a peak demand that should better be avoided. Therefore, a control pattern without night setback is the preferable way to operate a heating circuit [106]. Another user-made inefficiency are installations covering the radiators. This can be due to a lack of space when furniture needs to be placed in front of a radiator, or due to aesthetic considerations (concealers).

5. Installation of decentralized hot water (HW) preparation: Hot water preparation via district heating can be a source of high return temperatures. To avoid legionella growth, the hot water inside a building has to be maintained above a minimum temperature of 55 °C and heated up to at least 60 °C once a day, according to German regulation [63]. The two technologies used to realize hot water supply via district heating are instantaneous hot water preparation via heat exchangers and hot water tanks. Instantaneous hot water heat exchangers require a constant circulation of supply water to avoid long waiting times for customers. The circulation works as a shortcut, allowing supply water to reach the return line without any cooling [51]. Hot water tanks avoid constant circulation, but come with additional heat losses via the storage wall and the requirement of at least 60 °C water temperature inside the tank [63].
   In a commercial or industrial district heating system with a low demand for hot water preparation, one solution for this problem is to replace instantaneous hot water preparation based on district heating or hot water tanks with decentralized heat pumps or direct electric heaters for those customers who require hot water. Another option is a three-pipe district heating system as proposed by Averfalk and Werner [51]. The authors suggest a second return pipe of small size for circulation at supply temperature, avoiding what they call ”return temperature contamination”.

6. Correct sizing and maintenance of heat exchangers: The amount of heat transmitted via a heat exchanger is a function of its surface area. The greater the surface, the lower the logarithmic mean temperature difference (LMTD) between the surface and the room or air temperature necessary to transmit the same amount of heat. To reduce temperatures in heating circuits with well-functioning control systems, ventilation heat exchangers have to be replaced with heat exchangers of a larger surface area, or additional surface heating has to be installed to increase the heat transfer area of a space heating circuit. The same is true for substation heat exchangers in hydraulically disconnected substations: they are designed for a certain LMTD and can become too small once the network temperatures are decreased. If excessive temperature differences occur even though the control of the heating circuit works correctly and the heat exchanger size is sufficient, the malfunctioning can be due to fouling, which can be solved by cleaning the heat exchanger.

7. Comprehensive renovation of the thermal envelope and installation of ventilation heat recovery systems: An energetic renovation of the building envelope or the installation of a heat recovery for the ventilation system are among the costliest options to decrease temperatures and primarily serve to lower building heat demands. All the same, buildings with a poor energetic standard are those that have the highest impact on the network temperatures. It often makes more sense to invest in a full energetic renovation

instead of just installing surface heating or renewing the control of the ventilation system and thereby designing the retrofitting measures for the high heat demand of the building before renovation. Even when the return temperature from a critical substation lies only slightly above the target temperature, high heat demand comes with a high mass flow, leading to a significant negative impact on the network temperature as a whole. If a comprehensive renovation is carried out in a building, the aforementioned measures should always be taken into consideration as well. After renovating the thermal envelope of a building, other components such as surface heating panels can be designed smaller, while still reaching the same low temperatures, due to decreased heat demands. This results in lower costs.

Before investing in any improvement measure, it makes sense to compare the secondary side supply temperatures within the buildings with the primary side supply temperature in the network. Space heating circuits usually include a bypass for return flow admixture to control the secondary side supply temperature, because the primary supply temperature is above what is needed for space heating. This is not necessarily the case in ventilation or hot water heating circuits, which are supplied directly with the primary supply temperature in most buildings. Nevertheless, the supply temperature needed in the critical building and the one provided by the heating plant do not always match. This happens because the district heating operator does not know the exact supply temperature necessary for each building and wants to make sure the supply temperature never becomes too low to provide the guaranteed comfort temperature for each customer.

8.3 Data bases for the identification of temperature reduction opportunities

To identify where to apply which measure to decrease the network temperatures, both primary and secondary side heat monitoring data is used (see chapter 4.1). Primary side data serves to determine which substations have the highest impact on the network return temperature and where specific heat demand is highest. Secondary side monitoring makes it possible to go into more detail on the operation modes of different heating circuits. Thereby, it helps to determine what kind of issue leads to high temperatures in a certain building and how complex it will be to solve the problem. It is usually easier to fix an error in the control of a heating circuit than to replace the ventilation heat exchangers or install additional radiators or surface heating.

Historic primary side monitoring data is available at TU Darmstadt going back several years, which makes it possible to derive average values of the metrics presented below. The averaged metrics are based on time periods of complete years, because supply and return temperatures depend on ambient conditions. Therefore, averaged metrics based on shorter time periods might be biased by an overestimation of the impact of a specific season. The secondary side monitoring system was implemented only recently and yearlong time series are not yet available. Nevertheless, the characteristic operation modes of different substations can also be identified using the shorter time series available.

8.4 Definition of metrics

In this section, different metrics to evaluate the performance of a district heating substation and individual heating circuits inside buildings will be introduced. The metrics serve to identify the critical substations for temperature reduction and help to determine where to apply the measures presented above, in order to achieve a high temperature reduction with minimum effort.

The first two metrics help to allocate critical substations based on primary side meter data. The remaining two metrics go into detail inside the buildings with the help of secondary side heat demand data, to find specific sources of inefficiencies in the operation of the heat supply systems inside the buildings.

8.4.1 Return temperature reduction potential

From the perspective of the network operator, the most critical buildings in terms of return temperatures are not necessarily those with the highest temperatures, but those that have the biggest impact on the overall network return temperature. This impact will be called return temperature reduction potential $\overline{\Delta T}_{\mathrm{R},j}$ in the following. $\overline{\Delta T}_{\mathrm{R},j}$ describes the potential reduction of the annual time-averaged network return temperature $\overline{T}_{\mathrm{R,DHN},\tau}$ through a reduction of the annual average return temperature $\overline{T}_{\mathrm{R},j}$ from the substation j to the target temperature T_{target}. To calculate it, the measured return temperature $T_{\mathrm{R},i,j}$ for each time step i is compared to T_{target} and weighted with the share of the mass flow $\dot{M}_{i,j}$ from substation j in the mass flow of the district heating network $\sum_{j=1}^{n_{\mathrm{sub}}} \dot{M}_{i,j}$:

$$\overline{\Delta T}_{\mathrm{R},j} = \frac{1}{n_{\mathrm{ts}}} \sum_{i=1}^{n_{\mathrm{ts}}} \frac{\left(T_{\mathrm{R},i,j} - T_{\mathrm{target}}\right) \cdot \dot{M}_{i,j}}{\sum_{j=1}^{n_{\mathrm{sub}}} \dot{M}_{i,j}} \tag{8.4}$$

The resulting $\overline{\Delta T}_{\mathrm{R},j}$ is valid under the condition that the return temperature from all substations can be lowered to the target temperature at the same time. If the return temperatures from the substations are lowered one after the other, the network return temperature reduction achievable by decreasing the temperature in one substation is smaller, because the return temperature reduction leads to a decrease in the mass flow, reducing the share of the individual substation in the total mass flow of the network. If measures are implemented in several but not all substations, the resulting reduction per substation lies between the two cases.

8.4.2 Share of building in district heat demand compared to area-specific heat demand

In order to find out where to apply a comprehensive building renovation most efficiently, the share of the heat demand at the substation j in the heat demand of the district $f_j = \frac{Q_j}{Q_{\mathrm{DHN}}}$ is compared to the area-specific heat demand of each building $q_j = \frac{Q_j}{A_{\mathrm{ref},j}}$. From the point of view of the system, the most important buildings for an energetic renovation are those with high absolute as well as specific heat demands. These buildings represent the highest potential for both a reduction in heat demand as well as temperature level. A high area-specific heat demand can be due to a low quality of the thermal envelope (walls, roof, windows), but also a result of problems with the ventilation system, especially malfunctioning or missing ventilation heat recovery.

8.4.3 Regression of heat demand flow over the return temperature for ventilation heating circuits

Inside the buildings, an analysis of the performance of the ventilation heating circuits can help to identify sources of high return temperatures. Two general control principles are used for ventilation heating circuits:

1. Operation at constant secondary side supply temperature, typically very close to the primary side supply temperature, and adaptation of the mass flow according to the heat demand. This is a typical setup for old buildings and can result in very low return temperatures, when executed properly. For such a control system, a reduction of the primary side supply temperatures directly leads to an increase in the return temperature. Therefore, it can be necessary to replace existing heat exchangers or increase the supply temperature locally when the network supply temperature is lowered.

2. Constant mass flow and adaptation of the supply temperature to the heat demand. Such a control comes with the advantage of both low supply and return temperatures necessary for low-temperature district heating, but also with the disadvantage of increased electric energy demands for the circulation pump.

Many ventilation heat exchangers are located on building roofs outdoors or in unheated spaces. Because of this, they are equipped with a bypass between the supply and return lines, allowing for a recirculation mass flow to avoid freezing of the water in the pipes during cold winter days, when the ventilation is not operating. A typical error in ventilation heating circuits are excessive mass flows through the ventilation heat exchanger or the bypass, resulting in high return temperatures. This error can either be present at all times or only during hours of low demand.

The performance of a ventilation control system can be determined comparing the heat demand $\dot{Q}_{\text{vent},j}$ to the return temperature $T_{\text{R,vent},j}$ of the ventilation heating circuit j using a simple linear regression function:

$$\dot{Q}_{\text{vent},j} = \xi_{0,j} + \xi_{1,j} \cdot T_{\text{R,vent},j} + \epsilon_j \tag{8.5}$$

In this function, ξ_0 and ξ_1 represent the regression parameters, while ϵ stands for the residual of the regression. The higher the gradient of the regression function ξ_1, the lower the ventilation return temperature at a specific heat demand. If operating correctly, both control principles introduced above will lead to a positive ξ_1. If the gradient of the regression function is $\xi_1 < 0$, the reason can be an excess mass flow through the heat exchanger or the bypass. In a system with an excess mass flow through a well-designed heat exchanger, the temperature of the air entering the room exceeds the room temperature and the ventilation becomes a second room heating system, which is an undesired operation mode. Another reason for a negative ξ_1 is an excessive recirculation mass flow at times with low heat demand leading to high return temperatures, while return temperatures decrease drastically as soon as the heat demand increases. Such a behavior indicates that the recirculation mass flow is too high, due to an error at the control valve. Excessive mass flows through ventilation heating circuits not only lead to high return temperatures, but also unnecessarily increase the electric energy demand for the circulation pumps. An excessive recirculation mass flow can be detected comparing the factor between the maximum and minimum heat flow $f_{\dot{Q}_{\text{vent}},j} = \frac{\max(\dot{Q}_{\text{vent},j})}{\min(\dot{Q}_{\text{vent},j})}$ with the factor between the maximum and minimum mass flow $f_{\dot{M}_{\text{vent,j}}} = \frac{\max(\dot{M}_{\text{vent},j})}{\min(\dot{M}_{\text{vent},j})}$. If $f_{\dot{Q}_{\text{vent}},j}$ is a lot bigger than $f_{\dot{M}_{\text{vent}},j}$, an excessive recirculation mass flow is a probable cause.

Even when the control system is functioning correctly, the return temperature can still be high, due to an undersized ventilation heat exchanger. A small heat exchanger leads to a small ξ_1 and high supply and return temperatures to transmit the necessary heat. Heat exchangers can be undersized because they were designed for 3GDH network temperatures, or because the ventilation itself was retrofitted with a bigger fan and higher heat demands after the heat exchanger was already in place.

8.4.4 Time-averaged secondary side supply and return temperature

The time-averaged secondary side supply and return temperatures $\overline{T}_{\mathrm{S,II},\tau,j}$ and $\overline{T}_{\mathrm{R,II},\tau,j}$ are used to calculate the average performance of the ventilation and space heating circuits j:

$$\overline{T}_{\mathrm{S/R,II},\tau,j} = \frac{1}{n_{\mathrm{ts}}} \sum_{i=1}^{n_{\mathrm{ts}}} T_{\mathrm{S/R,II},i,j} \tag{8.6}$$

Both temperatures have to be low to decrease the network heat losses, improve the efficiency of the heat and power generation and to facilitate the integration of renewable heat. High average temperatures can either be due to an error in the control of the respective heating circuit, or indicate the necessity to increase the size of radiators and surface heating systems as well as ventilation heat exchangers.

8.5 Temperature reduction in the TU Darmstadt campus Lichtwiese district heating network

In the following section, the metrics developed above are applied to TU Darmstadt campus Lichtwiese. Hereby, the critical building in terms of network temperatures and specific issues inside each building are identified. The data used for this analysis covers the time period between April 1, 2017, and March 31, 2019, in case of the primary heat meters. Since the secondary heat metering did not go into operation until March 2020, a time series of a whole year is not yet available from these meters. Thus, the time period between March 18 and March 26, 2020, is used for the respective analyses. In the secondary side analysis, well-functioning and faulty heating circuits will be compared to each other. Chapters 8.5.1 and 8.5.2 are based on primary side measurement data and give an overview of the performance of the different substations on campus. Chapters 8.5.3-8.5.6 use secondary side measurement data and go into detail on the reasons for inefficiencies inside individual buildings.

8.5.1 Impact of a renovation of ventilation heating and space heating as well as hot water preparation on the campus return temperature

Fig. 8.2 shows the return temperature reduction potential for each substation, considering that temperatures at all substations are reduced simultaneously to an average target return temperature of $T_{\mathrm{target}} = 35\,°\mathrm{C}$. Table 8.1 gives an overview of the substations connected to the network, and identifies what kind of heating circuits (ventilation, space heating, hot water preparation) each substation includes.

The return temperature reduction potential of the substations 3102/3106 and 3202a is significantly higher than the one of all other substations. Faultily controlled substations are highlighted, making it obvious that control errors, such as shortcut mass flows in ventilation heating circuits or hydraulically unbalanced space heating, are a major cause for high return temperatures in this district. Another cause are water tanks for hot water preparation. The specific sources of control errors at TU Darmstadt campus Lichtwiese will be discussed in chapters 8.5.3-8.5.5. In Fig. 8.3, a comparison of the return temperature reduction potential $\overline{\Delta T}_{\mathrm{R},j}$ and

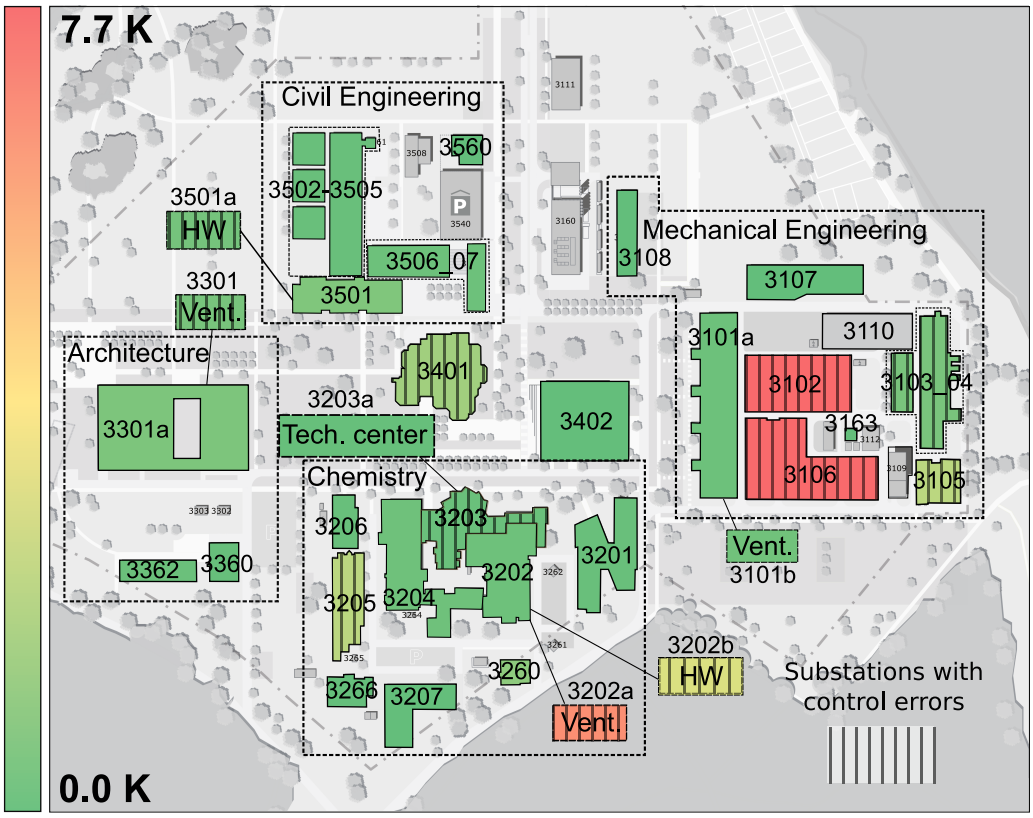

Fig. 8.2: Return temperature reduction potential campus Lichtwiese.

the mass-averaged return temperature $\overline{T}_{\mathrm{R},\dot{M},j}$ from each substation j is shown. The size of the dots represents the average annual heat demand for each building Q_j (see Table 3.3).

$$\overline{T}_{\mathrm{R},\dot{M},j} = \frac{\sum_{i=1}^{n_{\mathrm{ts}}} \left(\dot{M}_{i,j} \cdot T_{\mathrm{R},i,j} \right)}{\sum_{i=1}^{n_{\mathrm{ts}}} \left(\dot{M}_{i,j} \right)} \tag{8.7}$$

The analysis shows that the substations with the highest return temperature reduction potential are those with both high return temperatures and high heat demand. The five most critical substations in the Mechanical Engineering laboratories 3102/3106, the Organic as well as the Inorganic Chemistry buildings 3202 & 3205 and the university dining hall 3401 each have a return temperature reduction potential of more than 1.5 K, while the reduction potential of all other substations is below 1 K. The hot water preparation in the Organic Chemistry building 3202 has a comparatively high potential, due to its very high average return temperature, even though its heat demand is low. The Inorganic Chemistry building 3205 reaches a high return temperature reduction potential due to its high heat demand, while its average return temperature is lower than in many other buildings. The five critical substations represent a return temperature reduction potential of almost 21 K.

If only the return temperature from the most critical substations is lowered, the resulting district heating temperature reduction is somewhat smaller, due to the decrease in mass flow at the critical substations. In

Table 8.1: List of primary side substations campus Lichtwiese.

Substation name	Substation number	Venti-lation	Space heating	Hot water preparation
Mechanical Engineering Institutes	3101a		x	
Mechanical Engineering Institutes	3101b	x		
Mechanical Engineering Laboratories 1&2	3102/3106	x	x	
Mechanical Engineering Laboratories 5&4	3103/04	x	x	
Mechanical Engineering Laboratories 3	3105	x	x	
Mechanical Engineering Laboratories 6	3107	x	x	
Energy Center	3108	x	x	
Material Science Institutes & Laboratories	3201	x	x	
Organic Chemistry Institutes & Laboratories	3202		x	
Organic Chemistry Institutes & Laboratories	3202a	x		
Organic Chemistry Institutes & Laboratories	3202b			x
Chemistry Lecture Halls & Library	3203		x	
Chemistry Lecture Halls & Library	3203	x		
Physical Chemistry	3204	x	x	
Inorganic Chemistry	3205	x	x	
Center of Smart Interfaces	3206	x	x	
M^3 Laboratory Building	3207	x	x	
Disposal Center Chemistry	3266		x	
Architecture Institutes	3301	x		
Architecture Institutes	3301a		x	
Daycare Center	3360		x	
Kindergarten	3362		x	
University Dining Hall	3401	x	x	x
Lecture Hall & Media Center	3402	x	x	
Civil Engineering Institutes Old	3501	x	x	
Civil Engineering Institutes Old	3501a			x
Civil Engineering Laboratories 1-4	3502-3505		x	
Civil Engineering:Institutes New & Laboratories 5	3506/07	x	x	
Recycling Center	3560		x	

this case, the return temperature reduction potential $\overline{\Delta T}_{\mathrm{R},j}$ can be calculated using the following equation:

$$\begin{aligned} \overline{\Delta T}_{\mathrm{R},j} &= \frac{1}{n_{\mathrm{ts}}} \sum_{i=1}^{n_{\mathrm{ts}}} \frac{\left(T_{\mathrm{R},i,j} - T_{\mathrm{target}}\right) \cdot \dot{M}_{\mathrm{rmf},i,j}}{\sum_{j=1}^{n_{\mathrm{sub}}} \dot{M}_{m,i,j}} \\ \dot{M}_{\mathrm{rmf},i,j} &= \frac{\dot{Q}_{i,j}}{\left(T_{\mathrm{S},i,j} - T_{\mathrm{target}}\right) \cdot c_{\mathrm{W}}} \\ \sum_{j=1}^{n_{\mathrm{sub}}} \dot{M}_{m,i,j} &= \sum_{j=1}^{n_{\mathrm{sub}}} \dot{M}_{i,j} - \sum_{j=1}^{m} \dot{M}_{i,j} + \sum_{j=1}^{m} \dot{M}_{\mathrm{rmf},i,j} \end{aligned} \tag{8.8}$$

$\dot{M}_{\mathrm{rmf},i,j}$ represents the reduced mass flow from substation j after the reduction of its return temperature to

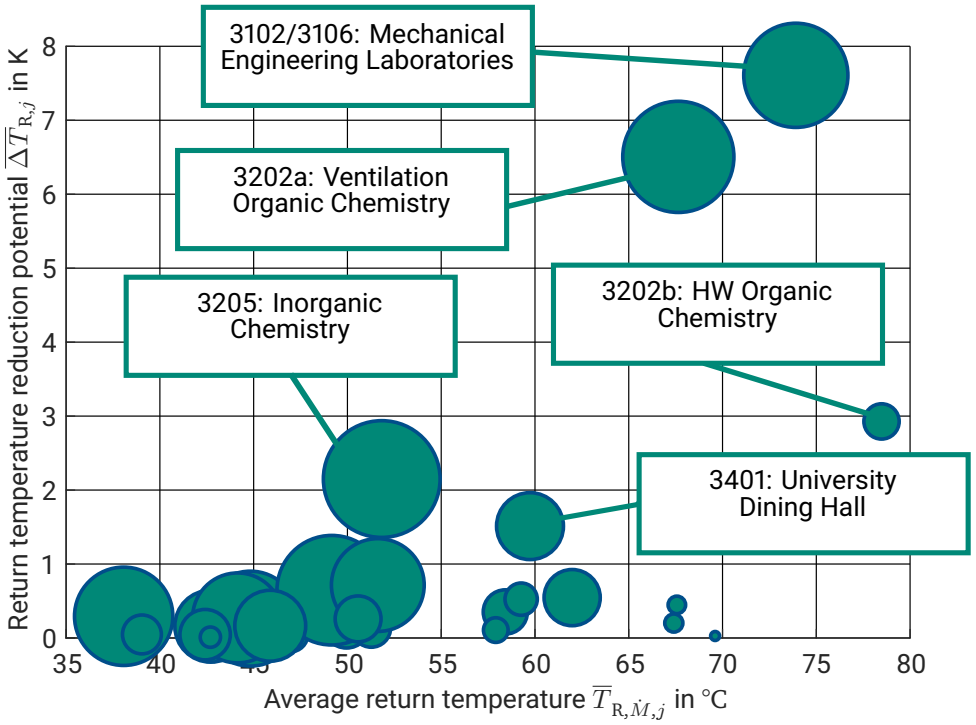

Fig. 8.3: Return temperature reduction potential over average return temperature per substation (size of symbol proportional to heat demand).

T_{target} and $\sum_{j=1}^{n_{\text{sub}}} \dot{M}_{\text{m},i,j}$ is the sum of the mass flow in the district heating network after the reduction of the return temperature from m substations. If the temperature from the five most critical substations presented above and visualized in Fig.8.3 can be lowered at the same time, the average return temperature reduction potential amounts to $\overline{\Delta T}_{R,j} = 14.5\,\text{K}$. The additional reduction potential from these substations calculated for a temperature reduction at all substations can be exploited once the temperature at the remaining substations is also reduced.

Fig. 8.4 shows the impact of the Mechanical Engineering laboratory buildings 3102/3106 on the return temperature of the network. Due to the high return temperature and the resulting small temperature difference between supply and return line, the mass flow at the substation for these buildings is high, leading to a substantial return temperature reduction potential. During the time period under consideration, it has already been possible to lower this impact. Unlike during the summer of 2017, the ventilation heat supply was shut down in the summer of 2018, avoiding an excessive shortcut mass flow. In order to continue the improvement of the temperature performance, shortcut mass flows have to be avoided also during the heating season. While the ventilation heating was shut off in the summer of 2018, it was possible to lower the return temperature at the substation to 20-30 °C and the mass flow to almost zero.

8.5.2 Comprehensive building renovation: Ventilation heat recovery and thermal envelope

In Fig. 8.5, the results of an analysis on the energetic performance of the buildings can be seen. For those buildings containing several primary side heat meters, the analysis was based on the aggregated heat demand of all meters inside the respective building. A few meters measure the combined heat demand of several

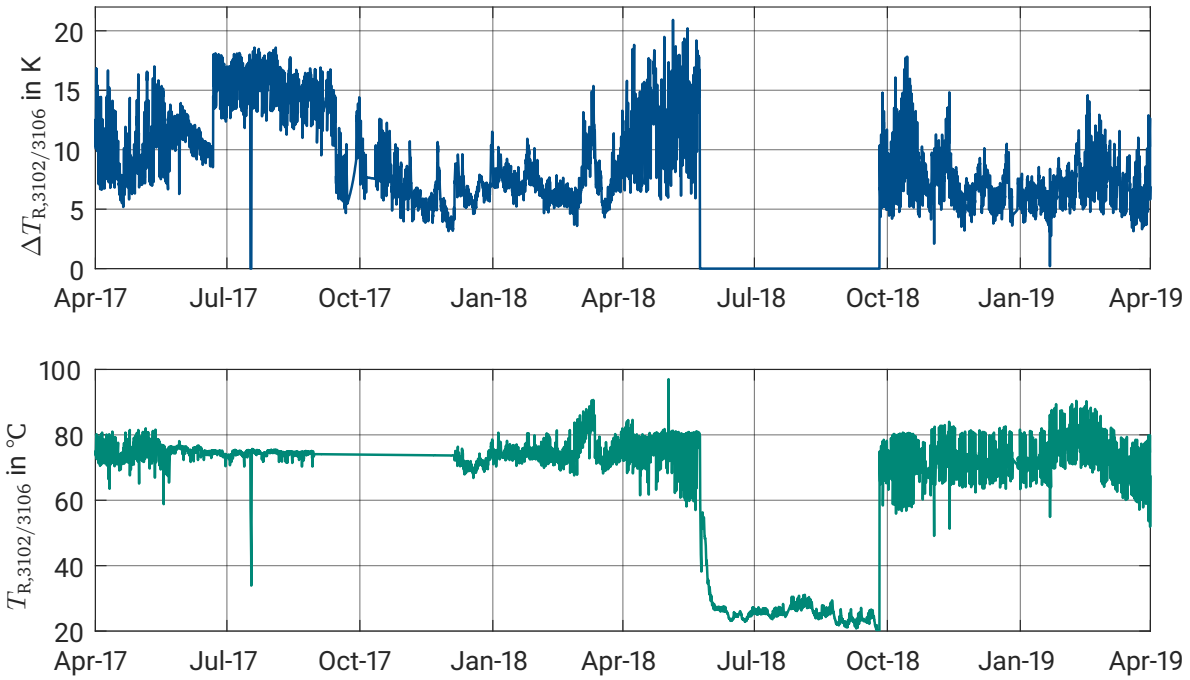

Fig. 8.4: Time series of the return temperature reduction potential $\Delta T_{R,3102/3106}$ and substation return temperature $T_{R,3102/3106}$ in the Mechanical Engineering laboratory buildings.

buildings, which is indicated in Fig. 8.5 correspondingly. For a list of the building names please consult Table 3.3 in chapter 3.3.

Only a few buildings are within the range or below the reference values for specific heat demand in non-residential buildings in Germany (between 90 kWh/m^{2}a and 140 kWh/m^{2}a, depending on the building type) [153]. While this demonstrates that most buildings should be renovated in the future, the first priority are the Organic Chemistry (3202) and Inorganic Chemistry (3205) buildings, where both specific heat demand and share in total district heat demand are significantly higher than in all other buildings. In both cases, the ventilation system represents a major part of the heat demand. Another study carried out by David Sauerwein at TU Darmstadt (personal communication, October 30, 2019) concluded that the installation of a ventilation heat recovery system could save about 55 % of the annual heat demand in the Organic Chemistry building 3202, and almost 70 % in the Inorganic Chemistry building 3205. A few other buildings, such as the chemistry lecture hall and library building (3203) and the waste disposal building (3266), also represent very high specific heat demands, but a comparatively low share in the overall heat demand of the district, which is why they are not first priority for renovation measures. The Mechanical Engineering laboratory buildings 3102/3106 perform comparatively well in terms of absolute and specific heat demand, suggesting that in those cases, a reduction of the return temperature through an improvement of the ventilation system control is sufficient, and a comprehensive renovation of these buildings is not amongst the first steps to take. Nevertheless, these and other large buildings with a specific heat demand between 100 kWh/m^{2}a and 200 kWh/m^{2}a will have to be renovated in the upcoming decades as well, in order to reach the university's climate protection goal until 2050.

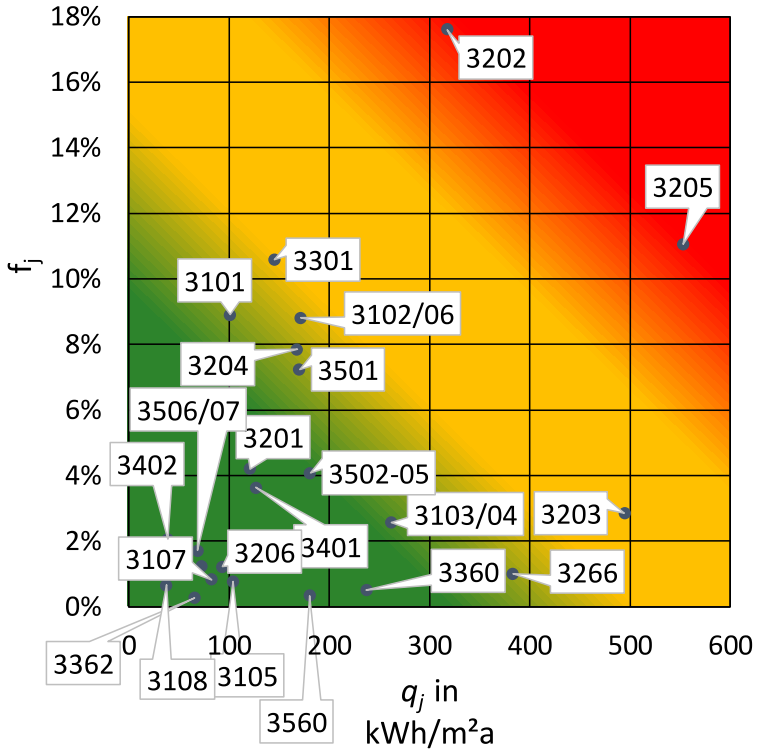

Fig. 8.5: Share of building in district heat demand over area specific heat demand.

8.5.3 Performance of ventilation heating circuits

The ventilation heating circuits at TU Darmstadt campus Lichtwiese can be divided into five categories V1-V5. The first three categories V1-V3 represent correctly controlled heating circuits, while V4 and V5 are a result of errors in the ventilation control system. Fig. 8.6 shows the time series of the primary and secondary side supply temperature as well as the secondary side return temperature (left), the time series of the heat flow and the mass flow (center), and the regression of the heat flow over the return temperature (right) of the three categories of well-functioning ventilation heating circuits.

V1. High supply temperature and fluctuating mass flow: The first category V1 can be shown using the example of the ventilation heating circuit of the Material Science building 3201/2. The supply temperature in this heating circuit is close to the primary supply temperature, while the mass flow as well as the return temperature fluctuate with the heat demand. The regression of the heat demand over the return temperature yields a high positive gradient of $\xi_{1,3201/2} = 9.5\,\mathrm{kW/K}$ (coefficient of determination $R^2_{3201/2} = 0.79$). A reduction of the primary supply temperature would lead to an increase in the return temperature from this type of heating circuit. To decrease the return temperature, increasing the size of the ventilation heat exchanger would be necessary.

V2. Low supply temperature and fluctuating mass flow: The ventilation heating circuit 3206/1 of the modern ”Center of Smart Interfaces” (CSI) constructed in 2011 serves as an example for the second category V2. In this category, the secondary side is hydraulically disconnected from the primary side via a substation heat exchanger, and the ventilation heating supply temperature is significantly lower than the primary side supply temperature. As for the Material Science building ventilation system, the mass flow is closely related to the heat demand. Also in this category, the regression of the heat demand over

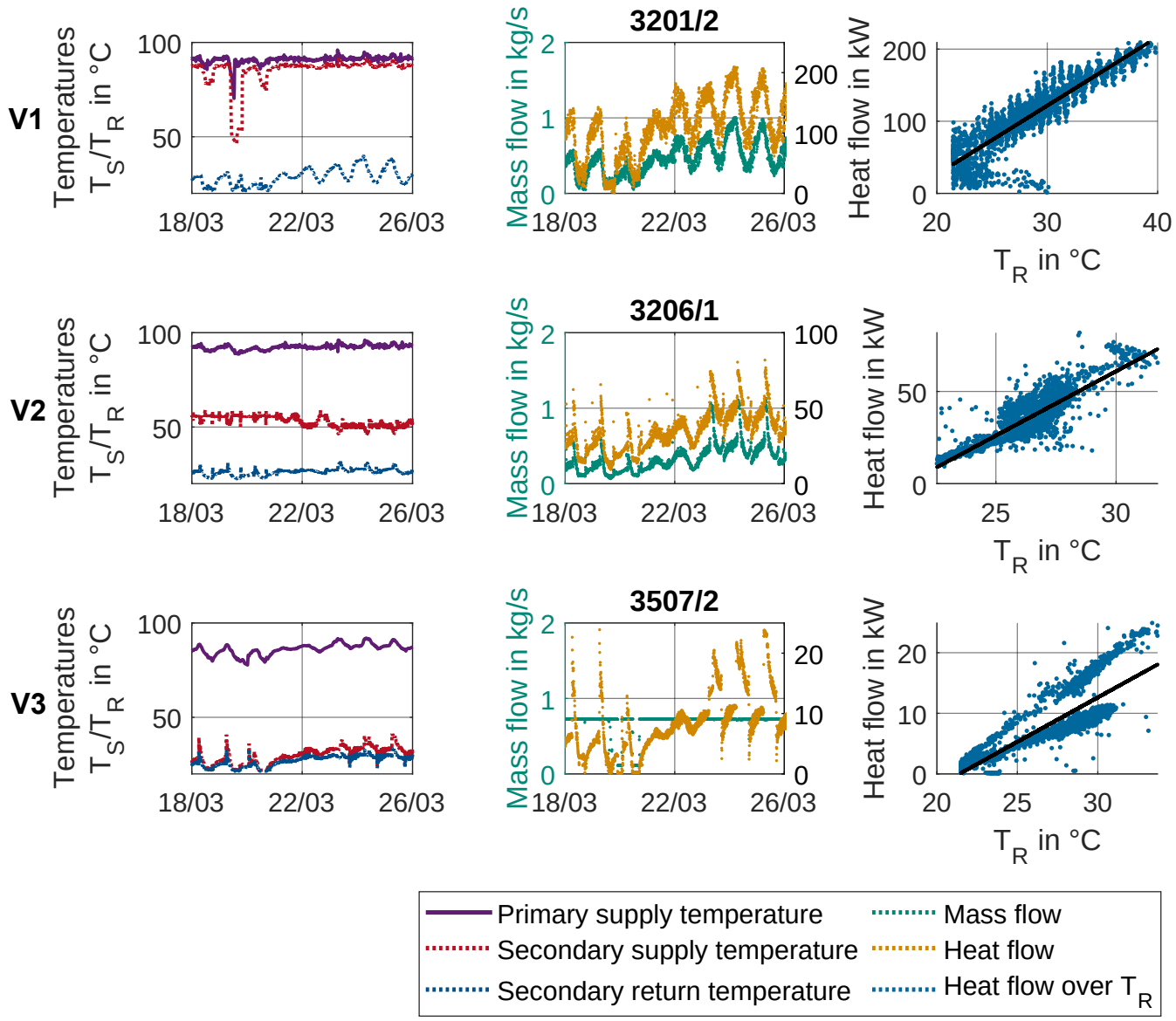

Fig. 8.6: Temperatures, mass flow, heat flow, and heat flow over T_R for the three categories V1-V3 of well-functioning ventilation heating circuits.

the return temperature yields a positive gradient of $\xi_{1,3206/1} = 7.0\,\mathrm{kW/K}$ ($R^2_{1,3206/1} = 0.75$).
Both the first and the second category are examples of the first control principle presented in chapter 8.4.3, with the difference being that the Material Science building 3201 is directly connected to the district heating system, while the CSI building 3206 includes a substation heat exchanger, reducing the supply temperature before it enters the ventilation heating circuit.

V3. Low supply temperature and constant mass flow: The third category V3 is an example of the second control principle and can be found in the ventilation heating circuit of the new Civil Engineering laboratory building 3507/2. Both supply and return temperature are adapted to the heat demand, while

the mass flow is constant, except when the heat demand falls to $\dot{Q}_{\text{vent},j} = 0\,\text{kW}$ and the circulation pump is turned off. The regression of the heat demand over the return temperature results in a positive gradient of $\xi_{1,3507/2} = 1.5\,\text{kW/K}$ ($R^2_{3507/2} = 0.67$). This operation mode yields both low supply and return temperatures and is a good option for 4GDH applications. When no heat demand and consequently no mass flow exists, the supply and return temperatures are determined by the ambient temperature inside the substation and are almost equal, except for measurement uncertainties.

Fig. 8.7 shows the results for the two categories V4 and V5 of faulty ventilation control systems occurring at TU Darmstadt Lichtwiese.

V4. High supply and high return temperature: Several ventilation heating circuits show a behavior comparable to the one in the old Mechanical Engineering laboratories buildings 3102/3106 (displayed here using the example of ventilation heating circuit 3102/4). In this example of category V4, the secondary side supply temperature is close to the primary side supply temperature as in the ventilation heating circuit of the Material Science building 3201/2, but the return temperature is only about 10 K lower and fluctuates between 80 °C and 85 °C, resulting in a very high mass flow. While the heat demand in the well-functioning ventilation heating circuit 3201/2 and the faulty circuit 3102/4 are in the same range, the mass flow is about five times higher in the latter. The gradient of the regression of the heat flow over the return temperature is negative ($\xi_{1,3102/4} = -3.8\,\text{kW/K}$), but the correlation between the two variables is low for this heating circuit ($R^2_{3102/4} = 0.13$). The most probable reason for the excessive return temperature from this heating circuit is an undesired bypass mass flow, but it could also be a result of an undersized ventilation heat exchanger.

V5a. High return temperature at low heat demand: A typical error in ventilation heating circuits at TU Darmstadt Lichtwiese are high return temperatures due to recirculation mass flows, here shown using the example of the ventilation heating circuit in the university dining hall 3401/1. In this example of category V5, an excessive recirculation mass flow at low heat demand leads to a negative gradient of the regression of the heat demand over the return temperature $\xi_{1,3401/1} = -2.2\,\text{kW/K}$ ($R^2_{3401/1} = 0.89$). The factor between the maximum and minimum heat flow $f_{\dot{Q}_{\text{vent}}} = 19$ is almost five times higher than the factor between the maximum and minimum mass flow $f_{\dot{M}_{\text{vent}}} = 4$.

V5b. High return temperature at low heat demand: Another example representing category V5 is the ventilation heating circuit 3205/4 in the Inorganic Chemistry building. At first glance, it seems comparable to the one of heating circuit 3201/2 ($\xi_{1,3205/4} = 4.7\,\text{kW/K}$), but the coefficient of determination is very low ($R^2_{3205/4} = 0.08$). Fig. 8.7 shows that the behavior of this heating circuit is essentially a mix of categories V1 and V5a. As long as the heat demand is sufficiently high, the heating circuit behaves like a V1 heating circuit, but during nights with low heat demand, the mass flow is not reduced sufficiently, leading to high return temperatures as in the case of 3401/1. Since the heat demand in this building is generally high, critical low heat demands are seldom reached, leading to an overall positive regression gradient $\xi_{1,3205/4}$. The regression makes this aspect visible showing two different characteristic areas, one with a high positive gradient as in category V1, and one with a negative gradient typical for category V5. Even though this heating circuit yields comparatively low return temperatures during the time period considered here, it will contribute to high return temperatures during the summer season.

Table 8.2 compares the performance of the different ventilation heating circuits in terms of the time-averaged secondary side return temperature $\overline{T}_{\text{R,II},\tau,j}$, time-averaged secondary side supply temperature $\overline{T}_{\text{S,II},\tau,j}$ and the gradient ξ_1 of the regression of the heat demand $\dot{Q}_{\text{vent},j}$ over the secondary side return temperature $\overline{T}_{\text{R,II},\tau,j}$. Well-functioning ventilation heating circuits in categories V1-V3 reach low average secondary side return

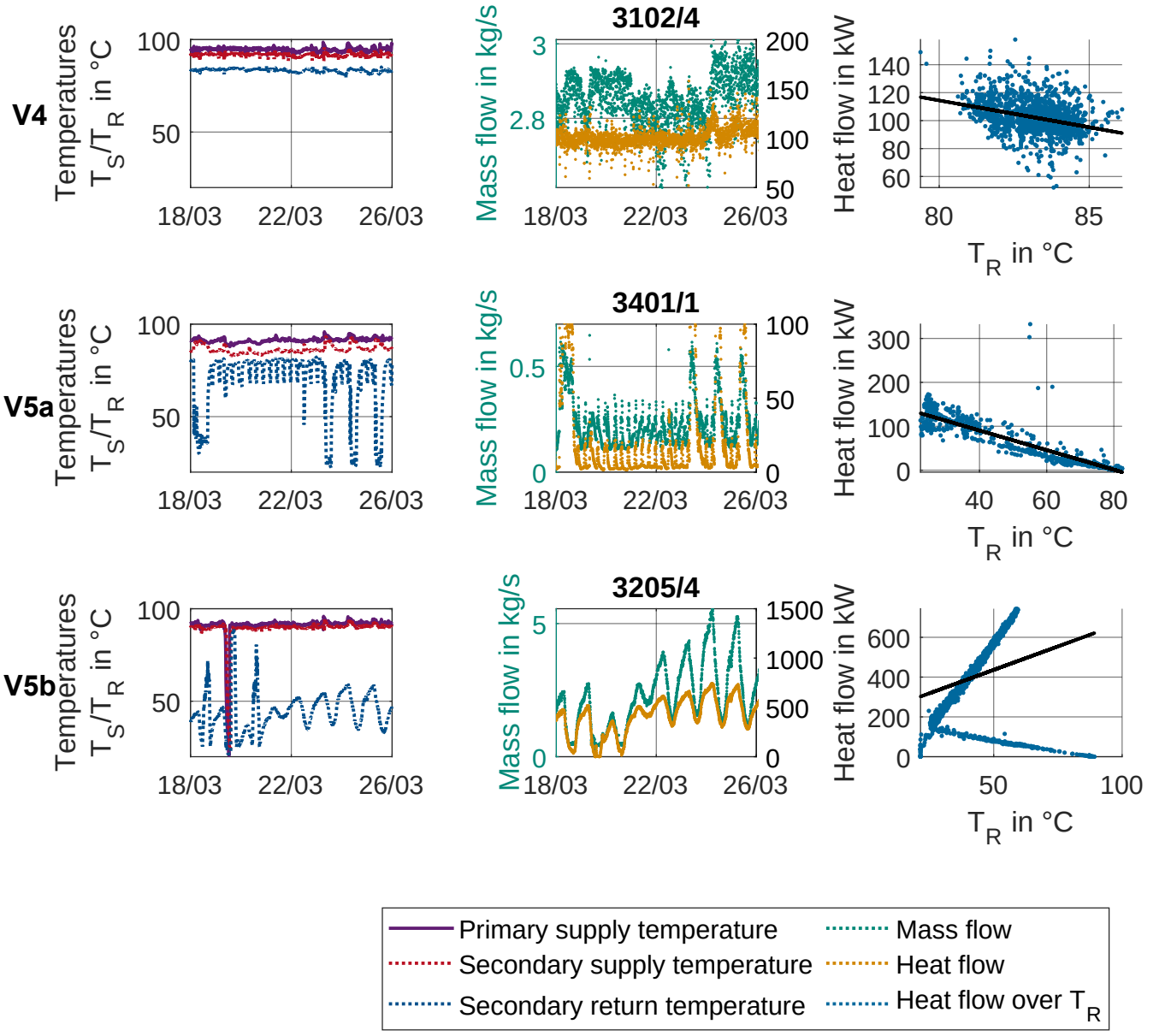

Fig. 8.7: Temperatures, mass flow, heat flow, and heat flow over T_R for the two categories V4 & V5 of faulty ventilation heating circuits, including a distinction between category V5a and V5b.

temperatures $\overline{T}_{\mathrm{R,II},\tau,j} < 30\,°\mathrm{C}$, except for the heating circuit 3501/3 ($\overline{T}_{\mathrm{R,II},\tau,3501/3} = 38.5\,°\mathrm{C}$), even though it is also considered as operating correctly. Ventilation heating circuits with control errors show characteristic high return temperatures ($\overline{T}_{\mathrm{R,II},\tau,j} > 54\,°\mathrm{C}$, except for the two heating circuits 3205/3 and 3205/4 in category V5b). The average secondary supply temperature $\overline{T}_{\mathrm{S,II},\tau,j}$ is in the range of the primary supply temperature, except for the heating circuits in categories V2 and V3.

Table 8.2: Comparison of the performance of the ventilation heating circuits.

Heating Circuit	Operation Mode	$\overline{T}_{\mathrm{R,II},\tau,j}$ in °C	$\overline{T}_{\mathrm{S,II},\tau,j}$ in °C	ξ_1 in kW/K	R^2
3201/2	V1	28.7	85.2	9.5	0.79
3501/3	V1	38.5	90.0	2.7	0.43
3206/1	V2	26.2	53.1	7.0	0.75
3203/2	V3	24.8	31.7	0.1	0.03
3507/2	V3	27.0	29.8	1.5	0.67
3102/3	V4	74.5	91.9	-4.4	0.58
3102/4	V4	83.4	91.9	-3.8	0.13
3105/1	V4	81.6	89.8	-3.9	0.43
3203/1	V5a	56.0	85.7	-0.6	0.17
3301/3	V5a	54.5	86.8	-2.7	0.75
3401/1	V5a	69.4	86.4	-2.2	0.89
3205/3	V5b	27.9	88.7	0.5	0.08
3205/4	V5b	44.3	89.3	4.7	0.08

8.5.4 Performance of space heating circuits

The operation of the space heating circuits can be divided into four different categories S1-S4, three of which result from well-controlled systems, while S4 contains faults.

S1. No night setback and low temperatures: The most typical operation mode for space heating is shown using the example of the heating circuit 3101/1 (see Fig. 8.8). In this category S1, supply and return temperatures depend on the ambient temperature. During night hours, heat demand and temperatures increase, while they are lower during the day, when ambient temperatures are higher.

S2. Night setback and low temperatures: The second category S2 can be found in the space heating circuits of the university dining hall 3401 as well as the Mechanical Engineering workshop building 3103. It comes with two different characteristic supply and return temperature levels, one during daytime and one during night hours and on weekends, due to night setback. Nevertheless, this operation mode is considered as correctly controlled.

S3. High supply temperature: The third category S3, which can be found in the Inorganic Chemistry building 3205, is characterized by a constant supply temperature close to the primary supply temperature. The heat demand and the return temperature increase during cold night hours, and go down during warm days. During a short period on March 19, 2020, the substation heat flow demand as well as the mass flow in the heating circuit drop to zero, resulting in a sharp drop in primary and secondary supply temperature as well as secondary return temperature. This behavior indicates that this heating circuit will not contribute to high network return temperatures during summer months. Since the heating circuits with these characteristics must be considered as correctly operated, supply and return temperatures can only be decreased installing additional radiators or surface heating.

Fig. 8.9 displays category S4, characterized by fast fluctuations in temperatures during night time. To gain a better understanding of these fluctuations, a close up view is shown in the second row of the diagram.

S4. Night time fluctuations: Category S4 is demonstrated using the example of the heating circuit 3102/6 in one of the old Mechanical Engineering laboratory buildings. During nights and early mornings, supply and return temperatures as well as mass flow oscillate significantly, leading to a fluctuation

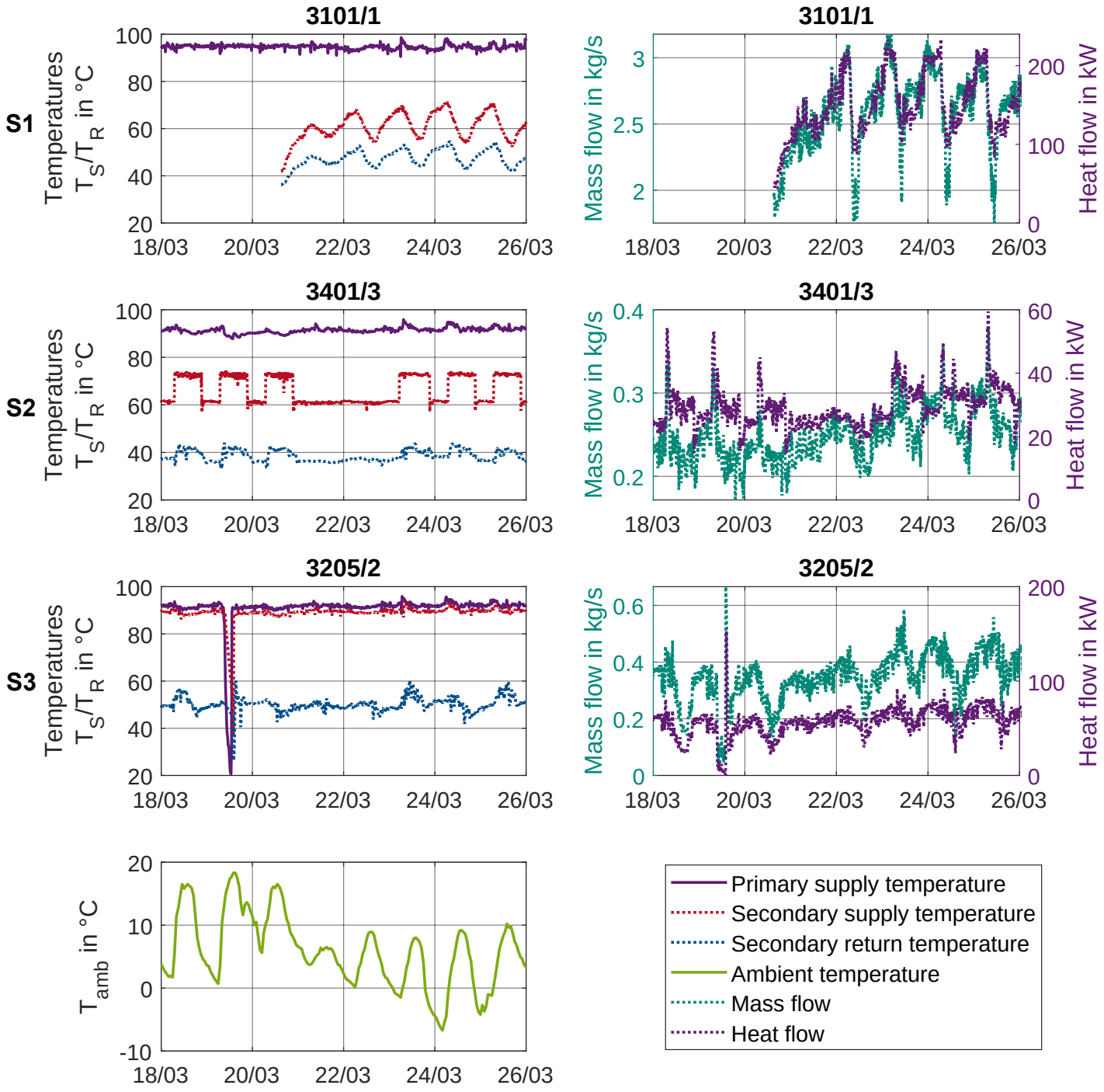

Fig. 8.8: Temperatures, mass flow, and heat flow for the three categories S1-S3 of well-functioning space heating circuits.

of the adjusted heat flow between $\dot{Q}_{\mathrm{SH},3102/6} = 70\,\mathrm{kW}$ and $\dot{Q}_{\mathrm{SH},3102/6} = 200\,\mathrm{kW}$. The second row of Fig. 8.9 shows a close-up view of the night time fluctuations on March 23, 2020. During this time, the temperatures show a sinusoidal behavior with a cycle duration of 1 hour and an amplitude of 10 K

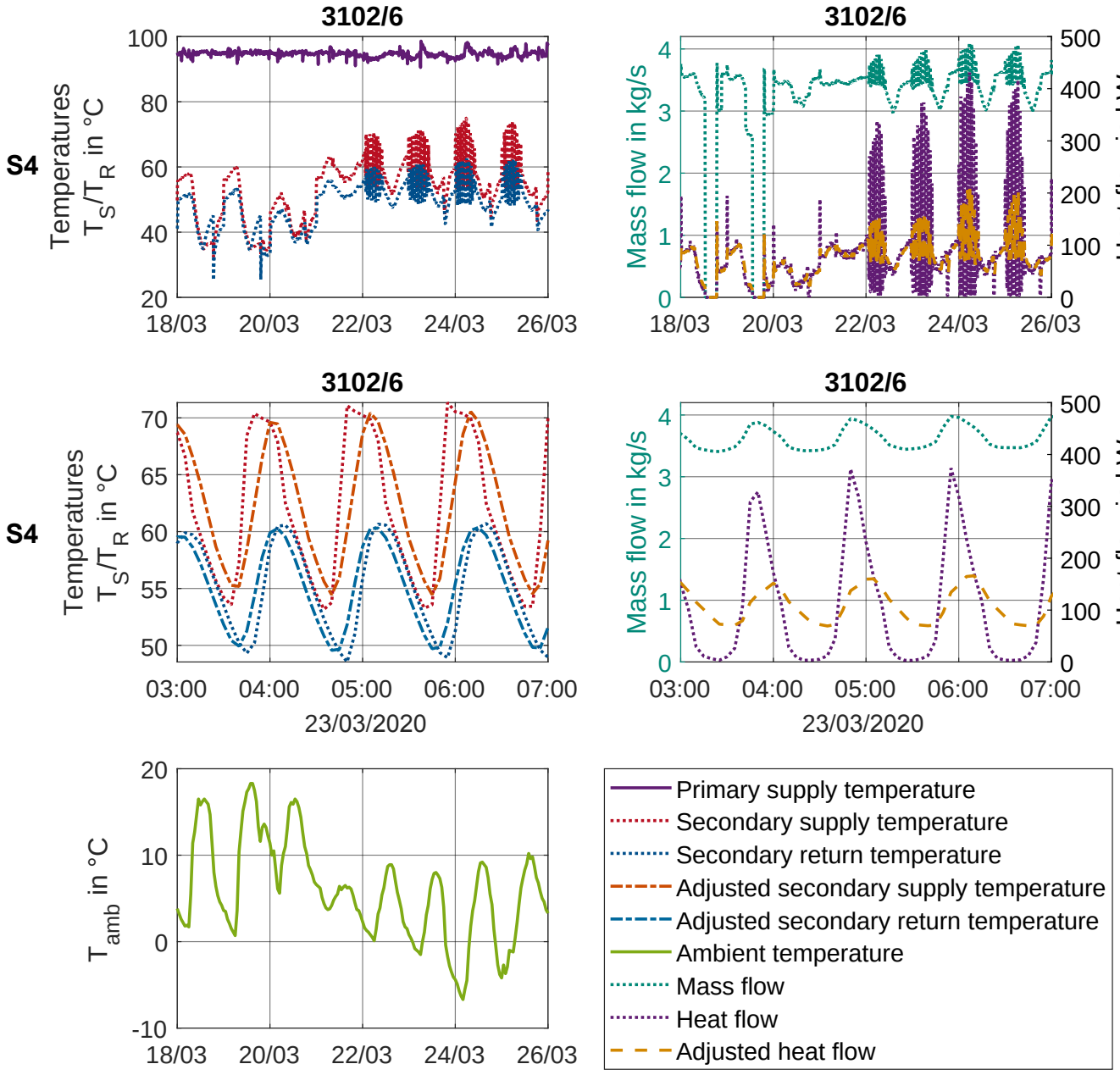

Fig. 8.9: Temperatures, mass flow, and heat flow for faulty space heating circuits category S4, including a close up view of night-time fluctuations.

(return temperature) and 15 K (supply temperature). In this close-up view, the influence of the system inertia discussed in chapter 4.2 can be seen, which is why adjusted temperatures and heat flow are calculated. This behavior can be the result of a badly functioning return flow admixture thermostatic valve, constantly opening and closing. The mass flow is high at all times, leading to a small temperature difference between the supply and the return line.

Table 8.3 compares the performance of the different space heating circuits. In comparison to the ventilation heating circuits, the difference in the average secondary return temperature $\overline{T}_{\mathrm{R,II},\tau,j}$ between a well-controlled and a faulty space heating circuit is not as evident. The highest $\overline{T}_{\mathrm{R,II},\tau,j}$ can be seen in the correctly controlled heating circuits of the Mechanical Engineering workshop building 3103 and the Inorganic Chemistry building 3205, indicating undersized radiators. The average secondary side supply temperatures differ significantly. In the Inorganic Chemistry building, space heating is operated at almost primary side supply temperature, while in the Mechanical Engineering laboratory building 3105 the average secondary side supply temperature is only $\overline{T}_{\mathrm{S,II},\tau,3105/2} = 37.8\,°\mathrm{C}$.

Solving control errors in faulty heating circuits should be the first priority to improve the performance of space heating at campus Lichtwiese. Nevertheless, it can be necessary to also increase the heat transfer area in well-functioning heating circuits, in order to decrease temperatures more significantly.

Table 8.3: Comparison of the performance of the space heating circuits.

Heating Circuit	**Operation Mode**	$\overline{T}_{\mathrm{R,II},\tau,j}$ **in** °C	$\overline{T}_{\mathrm{S,II},\tau,j}$ **in** °C
3101/1	S1	47.5	61.1
3101/2	S1	45.7	55.4
3105/2	S1	32.6	37.8
3201/1	S1	47.1	54.1
3203/3	S1	40.0	49.0
3203/4	S1	41.3	48.8
3204/3	S1	36.4	45.7
3206/2	S1	33.6	42.2
3301/1	S1	46.4	55.4
3301/2	S1	42.4	53.3
3501/1	S1	41.5	50.6
3501/2	S1	51.4	63.4
3507/1	S1	29.7	38.4
3103/1	S2	54.9	72.4
3103/2	S2	58.1	72.0
3401/3	S2	38.5	66.3
3401/4	S2	44.0	66.4
3205/1	S3	55.6	90.0
3205/2	S3	50.2	89.0
3102/1	S4	48.8	53.8
3102/2	S4	48.3	55.1
3102/5	S4	48.0	53.9
3102/6	S4	48.3	53.1

8.5.5 Performance of hot water preparation

All buildings at campus Lichtwiese are non-residential, which is why hot water (HW) preparation plays a minor role in the total heat demand. Nevertheless, some HW heating circuits have a significant impact on the network return temperatures. HW is needed mainly for coffee kitchens. In some cases, HW is also used for laboratory purposes, and a few buildings are equipped with showers. Different technologies are used to supply HW. In most buildings, hot water is supplied decentrally, using in-line electric heaters. In a few cases,

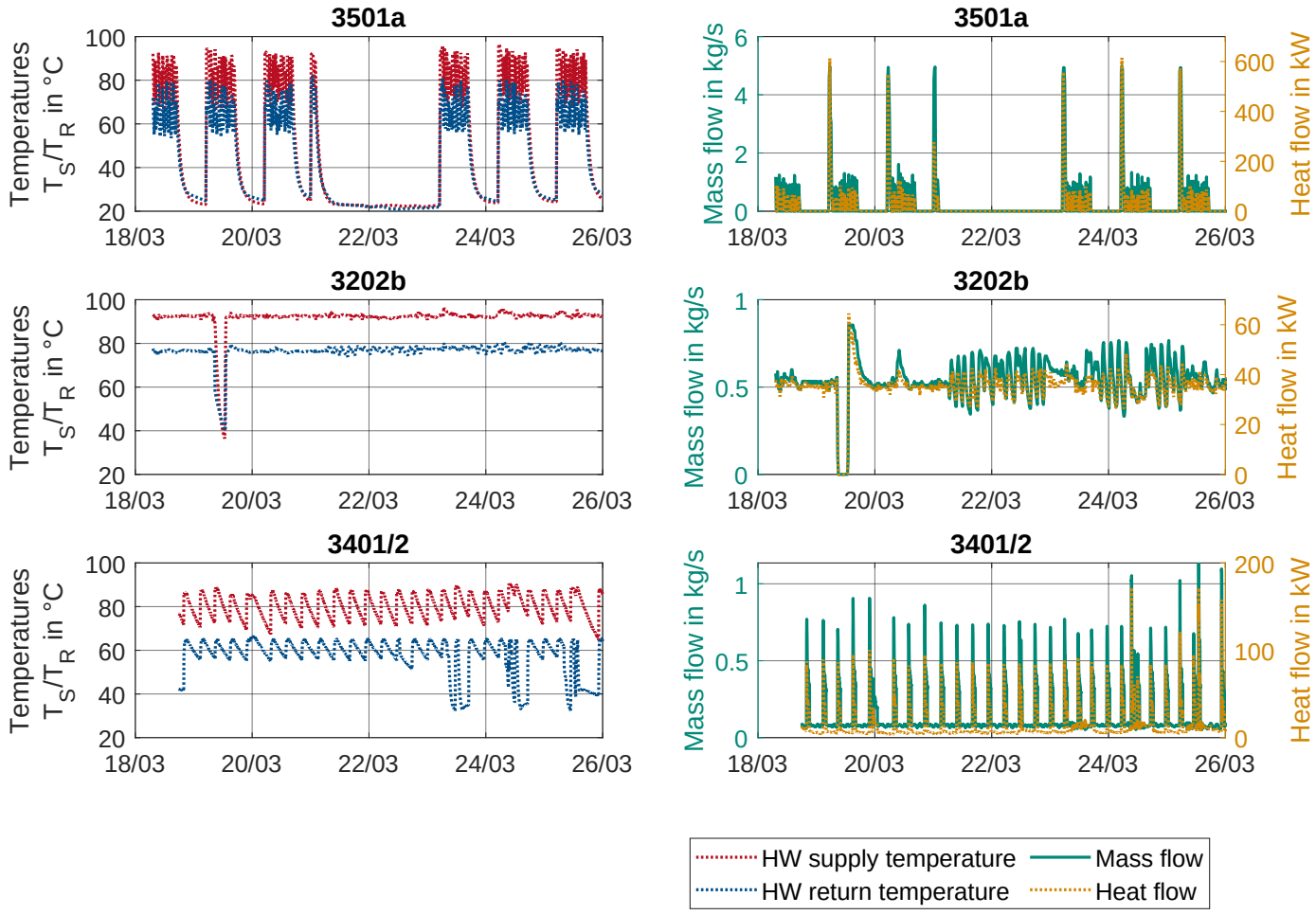

Fig. 8.10: Temperatures, mass flow, and heat flow of the hot water heating circuits.

tanks equipped with district heating heat exchanger are used for hot water preparation. Three hot water preparation heating circuits on campus are equipped with meters, all three of which show different operation modes. These are presented in Fig. 8.10.

The first one, located in the old Civil Engineering institute building 3501 (3501a), undergoes hourly heating cycles during workdays between 6:00 am and 6:00 pm, and is turned off during nights and weekends. Mass flow and heat demand see high peaks in early mornings and modulate at a low level over the rest of the day. The second heating circuit, supplying the Organic Chemistry building 3202 (3202b), operates at roughly constant and very high supply and return temperatures. Heat demand and mass flow are low and see little fluctuation. The third example, representing the HW preparation in the university dining hall 3401, shows a saw tooth profile for both supply and return temperatures, indicating regular heating cycles of the hot water tank every 6 h. While the tank is heated up, both its supply and return temperatures rise steeply. After a heating period of 1 h, the temperature once again starts to decrease slowly. Due to a minimum mass flow of about $\dot{M}_{3401/2} = 0.1\,\mathrm{kg/s}$, the return temperature remains high even when no heat is used.

All three setups have a negative effect on the campus thermal energy system as a whole, because they result in high return temperatures. While the first setup (3501a) has the lowest average impact on the return

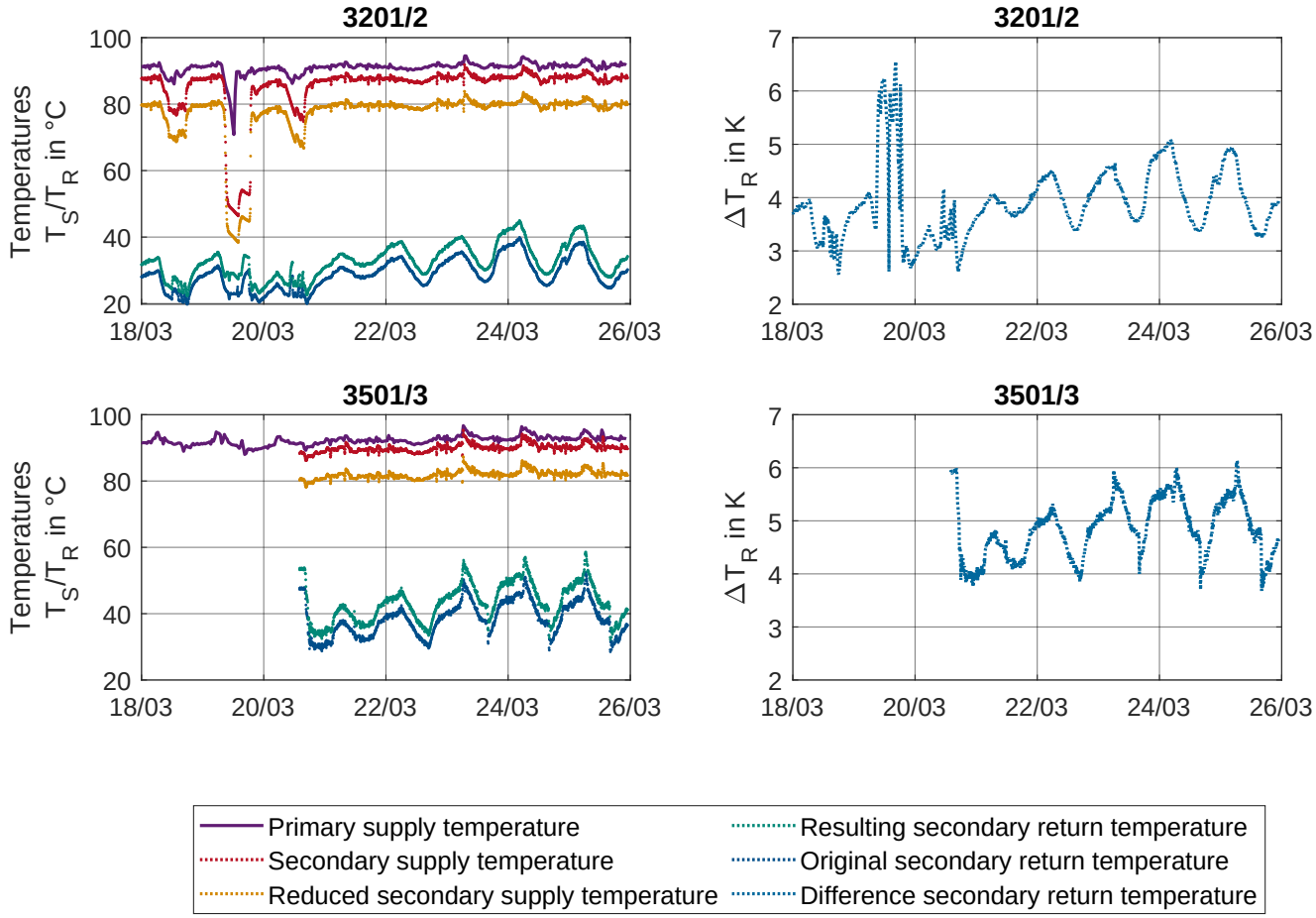

Fig. 8.11: Temperatures before and after supply temperature reduction for the heating circuits 3201/2 and 3501/3.

temperature, it comes with the disadvantage of high peaks in heat demand in early mornings. Only a minor part of the total campus heat demand is used for hot water preparation, thus switching to in-line electric heaters or heat pumps in buildings currently equipped with storage tanks would be the recommended solution.

8.5.6 Reduction of the district supply temperature

As can be seen in the examples shown above, many heating circuits, especially for space heating, do not make use of the high primary side supply temperature. For ventilation, supplying the heat exchanger at primary supply temperature is a lot more common, but a well-functioning ventilation heating circuit operates at very high temperature differences and would still be able to reach reasonable return temperatures if the supply temperature were slightly lower. Fig. 8.11 shows the impact of a reduction of the supply temperature on the two well-functioning ventilation heating circuits operating at about primary supply temperatures. A reduction of the primary supply temperature by $\Delta T_S = 8\,\mathrm{K}$ would lead to an increase in the return temperature by about 5 K on average in these heating circuits.

In well-functioning heating circuits with high temperatures, a local increase of the supply temperature via a heat pump instead of a retrofitting of radiators or ventilation heat exchangers might be a solution. If there

exists an error in the control of a heating circuit, this error should be solved first, rather than investing in an additional heat pump. A booster heat pump only makes sense for space heating in the Inorganic Chemistry building 3205. These heating circuits come with constantly high supply and return temperatures, but their control is considered to be functioning correctly.

8.5.7 Recommendations for action

Based on the analysis carried out in this chapter, the following measures were identified as the most pressing issues to lower district heating temperatures and heat demand at TU Darmstadt campus Lichtwiese:

1. Correction of ventilation control errors: The first priority is to reduce recirculation mass flows in the ventilation heating circuits 3102/3, 3102/4 and 3105/1 of the Mechanical Engineering laboratory buildings as well as in the Organic Chemistry ventilation system 3202a. Additionally, it makes sense to take care of the high return temperatures at low heat demand in the ventilation heating circuits 3203/1, 3205/3, 3205/4, 3301/3 and 3401/1.

2. Hot water preparation: The hot water preparation tank in the Organic Chemistry building (heating circuit 3202b) should be replaced with an in-line electric heater, and the operation mode of the hot water tank in the university dining hall 3401 should be adapted as follows. If the rules for water hygiene allow it, the tank could be heated only during operating hours of the dining hall, as realized in the case of the hot water tank in the Civil Engineering institute building 3501 (heating circuit 3501a). This is not a perfect solution, but it is an easy way to reduce the average return temperature from this heating circuit with no additional costs.

3. Building renovation: Comprehensive building renovation should be carried out in the Inorganic Chemistry building 3205. In this case, the specific heat demand and the temperatures are high, although the control of the space heating circuits is functioning correctly, suggesting that the heat demand increased after the initial installation of the heating system. To lower the high specific heat demand as well as the temperatures, the installation of a heat recovery system for the ventilation is a high priority. Additionally, surface heating would be an option to reduce space heating temperature demands. Even though this building is one of the more recently constructed buildings on campus (erected in 1995), it shows constructive issues, such as a leaking roof. Therefore, user comfort and conservation of the building structure are further arguments for a comprehensive renovation of this building. The Organic Chemistry building 3202, which also shows a very high specific heat demand, is already being renovated. Preparing the building for low-temperature heating is a crucial aspect of this process.

4. Supply temperature reduction: Many heating circuits do not require the current high supply temperature level, but operate at significantly lower secondary supply temperatures. Those which do make use of the primary supply temperature often show control errors. After resolving control errors in the buildings 3102/3106, 3105, 3202, 3203, 3205, 3301 and 3401, the supply temperature can be reduced step by step. In the ventilation heating circuits 3201/2 and 3501/3, such a reduction will lead to a slight increase in return temperatures. Instead of installing surface heating in the Inorganic Chemistry building, increasing the supply temperature locally using a booster heat pump would also be an option to avoid exceptionally high return temperatures from those substations.

For TU Darmstadt campus Lichtwiese, significant construction activities are projected for the upcoming decades, thus the low temperature heat supply should also be considered when new buildings are being planned. This includes high standards for the thermal envelope of the buildings, surface heating with differential pressure

control, appropriate sizes for ventilation heat exchangers and decentralized hot water preparation. In new buildings, thermal energy monitoring on the primary and secondary side of the substation should become standard equipment.

8.5.8 Comparison of the different measures in terms of final energy supply, CO_2 emissions, and annuities

In the following section, results on the impact of an implementation of the measures proposed in chapter 8.5.7 will be presented. Two different scenarios will be compared to the reference scenario S_{ref}, which was introduced in chapter 7.5. The first scenario S_{HR} (heat recovery) considers a reduction of the return temperature in the five most critical substations (3102/3106, 3202a, 3202b, 3205 and 3401) to an average return temperature of 35 °C and an installation of ventilation heat recovery in the Organic and Inorganic Chemistry buildings (3202 and 3205). The second scenario $S_{\mathrm{HR\&T_S}}$ additionally takes into account a reduction of the network supply temperature by 8 K. For this to be possible, control errors in ventilation heating circuits with high supply and return temperatures have to be resolved first. It is considered that the return temperatures in the Material Science building 3201 and the old Civil Engineering institute building 3501 increase slightly due to the reduction of the supply temperature. Additionally, the installation of a heat pump in the Inorganic Chemistry building 3205 is foreseen, in order to increase the supply temperature for this building locally. First, annual time series of the resulting return temperatures, network heat losses, and changes in total heat supply will be presented. Subsequently, results regarding final energy supply, CO_2 emissions, and annuities will be discussed.

In Fig. 8.12, the impact of different measures on the campus return temperature, network heat losses and the change in total heat supply is shown. The median return temperature reduction in S_{HR} is $\widetilde{\Delta T}_{\mathrm{HR}} = 11\,\mathrm{K}$, while the reduction in $S_{\mathrm{HR\&T_S}}$ is slightly lower ($\widetilde{\Delta T}_{\mathrm{HR\&T_S}} = 8\,\mathrm{K}$). The reduction of the supply temperature leads to increased mass flows in substations where return temperatures have not been decreased yet, making their influence on the overall return temperature grow. The temperature reduction is slightly higher in summer months than it is during wintertime, because excessive return temperatures, especially in ventilation heating circuits, are more frequent in the summer than they are during the winter season (see category V5 in chapter 8.5.3). The second graph shows the total heat loss from the district heating pipes in all three scenarios. Network heat losses can be reduced by 5 % in S_{HR} and 10 % in $S_{\mathrm{HR\&T_S}}$. The reduction of the supply temperature is a main driver for savings in network heat losses, because the main fraction of the heat losses occurs in the supply pipes. The third graph makes it possible to understand the influence of the proposed measures on the total heat supply of the campus. In S_{HR}, the yearly heat supply $Q_{\mathrm{th,Liwi,HR}}$ is reduced by 15.5 %, mainly due to savings created by the installation of ventilation heat recovery in the critical buildings. In $S_{\mathrm{HR\&T_S}}$, the reduction is similar to the one in S_{HR} during the winter season and becomes more significant in summer months, reaching up to 25 % due the aforementioned savings in network heat losses. Nevertheless, the total annual reduction in heat supply is about the same ($-16\,\%$), since heat supply in summertime is only a fraction of what is supplied during the winter.

The final energy supply for both S_{HR} and $S_{\mathrm{HR\&T_S}}$ is compared to S_{ref} in Fig. 8.13. In both scenarios, final energy demand can be reduced by about 6 % in total. The main reduction comes from a decrease in HOB heat supply, which is reduced by 22 % (3000 MWh) in both cases. CHP heat supply is also reduced by 9-10 %, leading to increases in grid electric energy supply by 9 %. The difference between the two scenarios is very small. S_{HR} and $S_{\mathrm{HR\&T_S}}$ do not include data center waste heat utilization, thus the final energy supply in these scenarios is somewhat higher than in S_{op} and $S_{\mathrm{des\&op}}$ in chapter 7.5.5.

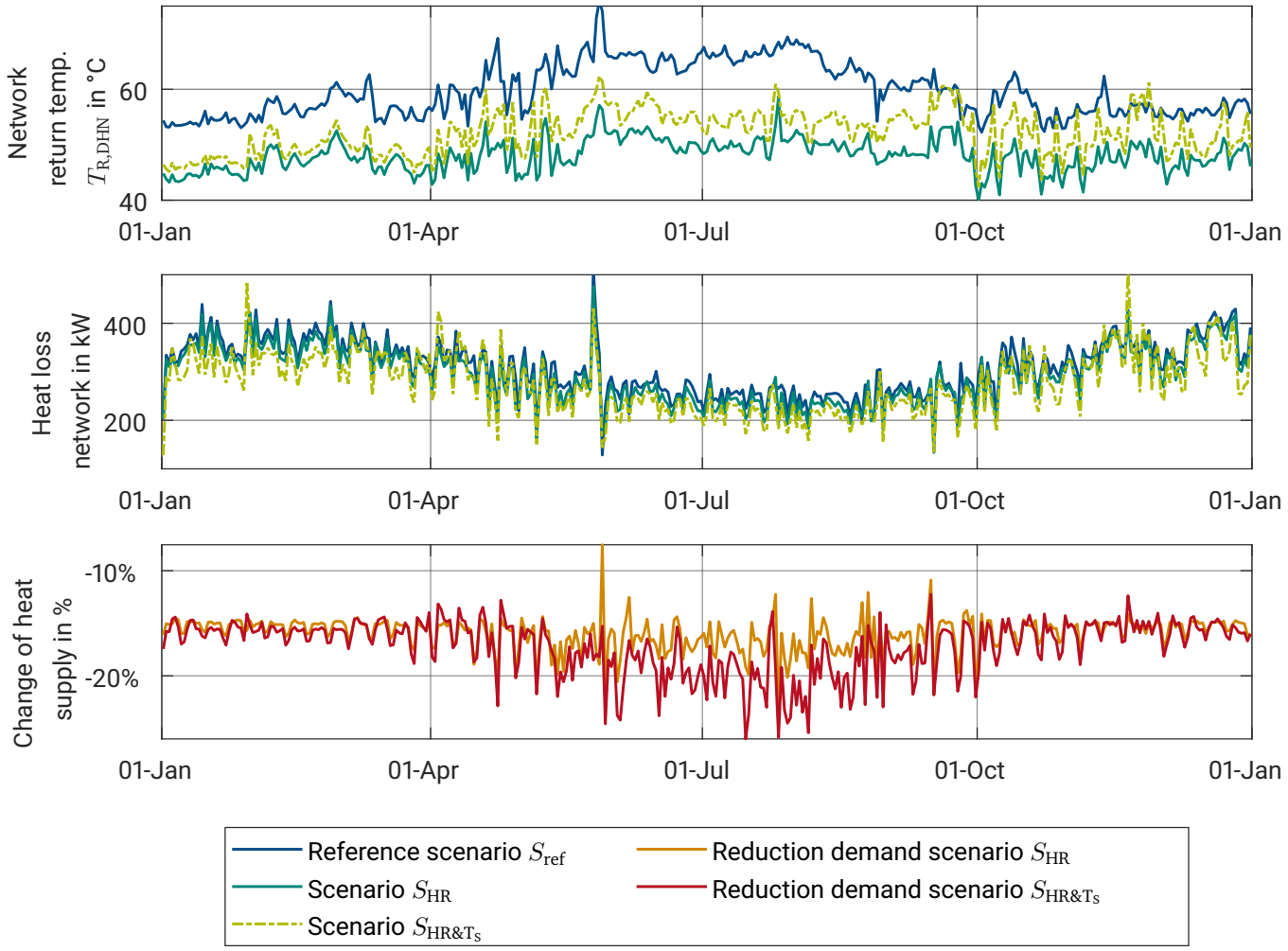

Fig. 8.12: Impact of the proposed temperature reduction measures on network return temperatures, heat losses, and heat supply.

CO_2 emissions are also reduced significantly in both future scenarios compared to S_{ref} (see Fig.8.14). The total CO_2 emissions are reduced by 4.5 % in both cases, while the heat supply related emissions (Heat HOB and Heat CHP) see a reduction of 19 %. Heat supply related CO_2 emissions drop from 25 % to 21 % of the total emissions generated in the campus energy system. The emissions in $S_{HR\&T_S}$ are slightly higher than the ones in S_{HR}, mainly because of the additional electric energy demand for the booster heat pump in the Inorganic Chemistry building 3205. Nevertheless, a reduction in supply temperatures is a crucial step towards a decarbonization of the heat supply. Many renewable heat sources such as solar-thermal or geothermal heat need low supply temperatures to be used efficiently.

Fig. 8.15 illustrates a comparison of the capacity, demand, and CO_2 emissions costs in the different scenarios. While demand-related and CO_2 emissions costs can be decreased in S_{HR} and $S_{HR\&T_S}$ compared to S_{ref}, capacity costs remain constant. Since a reduction in heat demand leads to a reduction in CHP electric energy generation, grid electric energy demand increases, leading to higher fractions of costs for electric energy supply. Between S_{HR} and $S_{HR\&T_S}$, differences are small.

Fig. 8.16 compares the total annuities in the three scenarios presented here. Compared to S_{ref}, the total annuity can be lowered by 200 000 €/a in both S_{HR} and $S_{HR\&T_S}$. Investment and operation costs of the

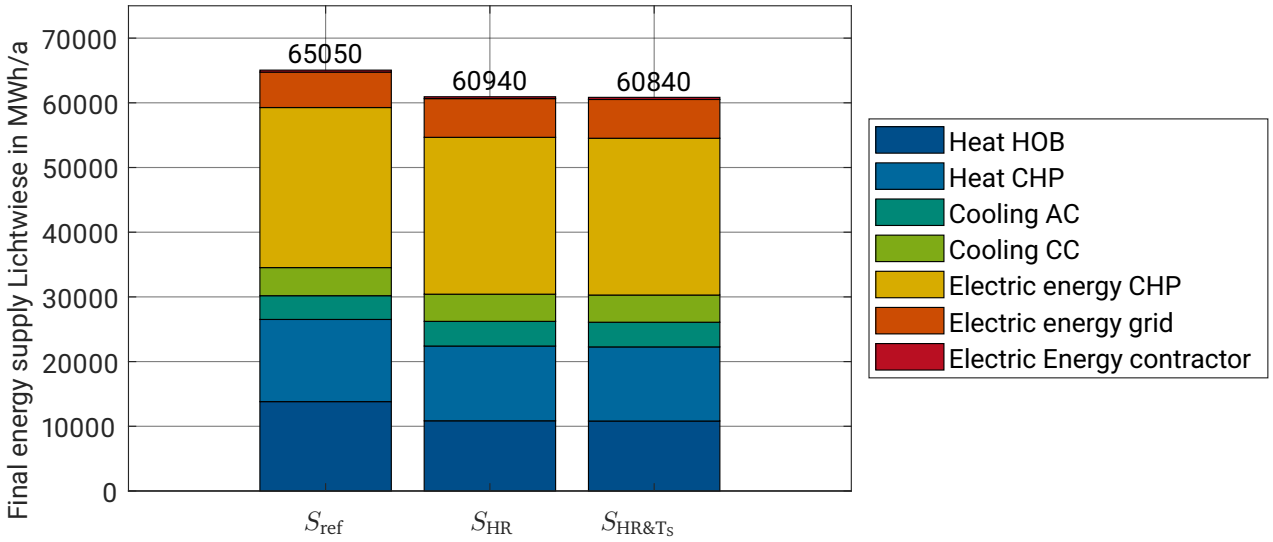

Fig. 8.13: Impact of the proposed temperature reduction measures on final energy supply.

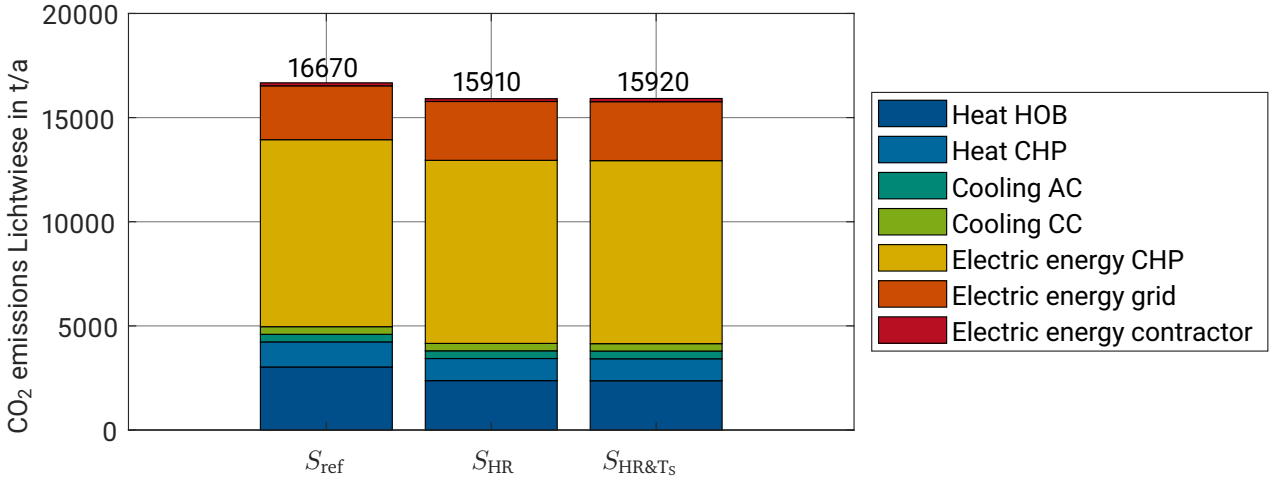

Fig. 8.14: Impact of the proposed temperature reduction measures on CO_2 emissions.

measures proposed were not included in this comparison. Instead, the maximum initial investment C_0 can be calculated, taking into account an annuity of the investment and operation-related costs equal to the decrease in capacity, demand-related and CO_2 emissions costs ($A_{inv} + A_{op} = 200\,000\,€/a$):

$$C_0 = \frac{A_{inv} + A_{op}}{f_a \cdot (1 + f_{op} f_b)} = 1.2\,M€ \tag{8.9}$$

Therefore, based on the assumptions presented in chapter 5.3.3, the proposed measures are economically feasible, as long as the total investment does not exceed 1.2 M€.

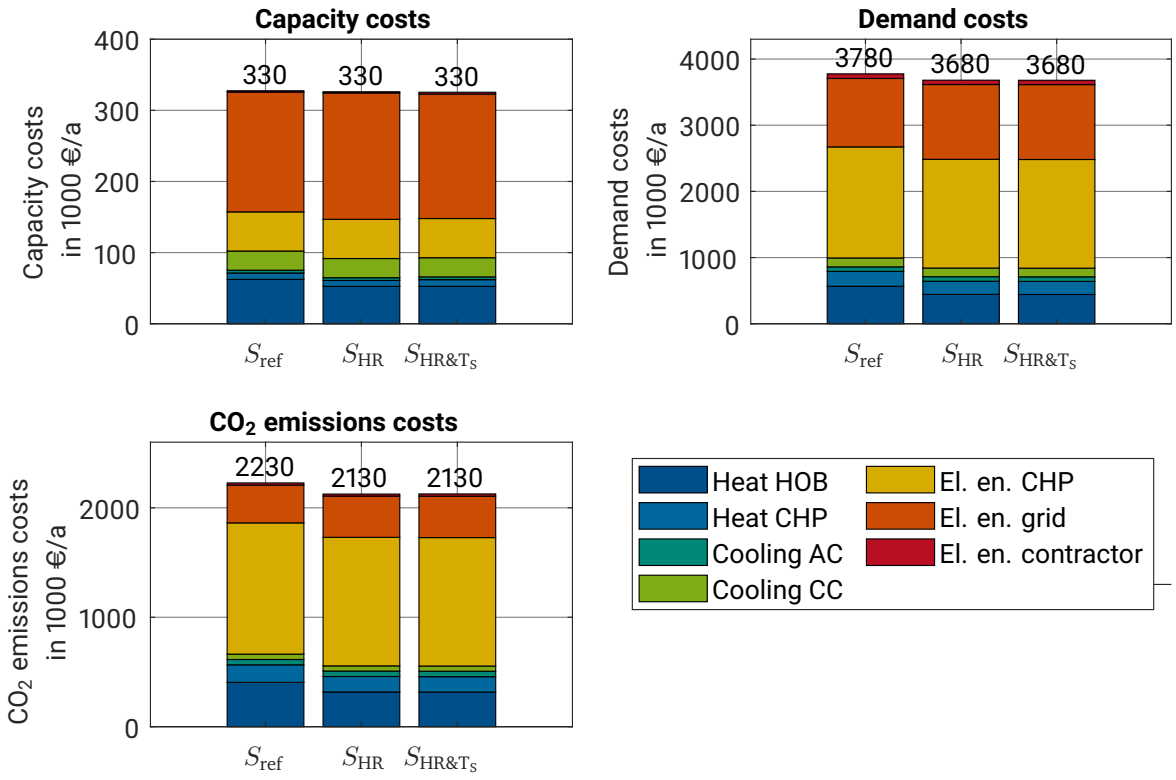

Fig. 8.15: Impact of the proposed temperature reduction measures on the capacity, demand, and CO_2 related costs.

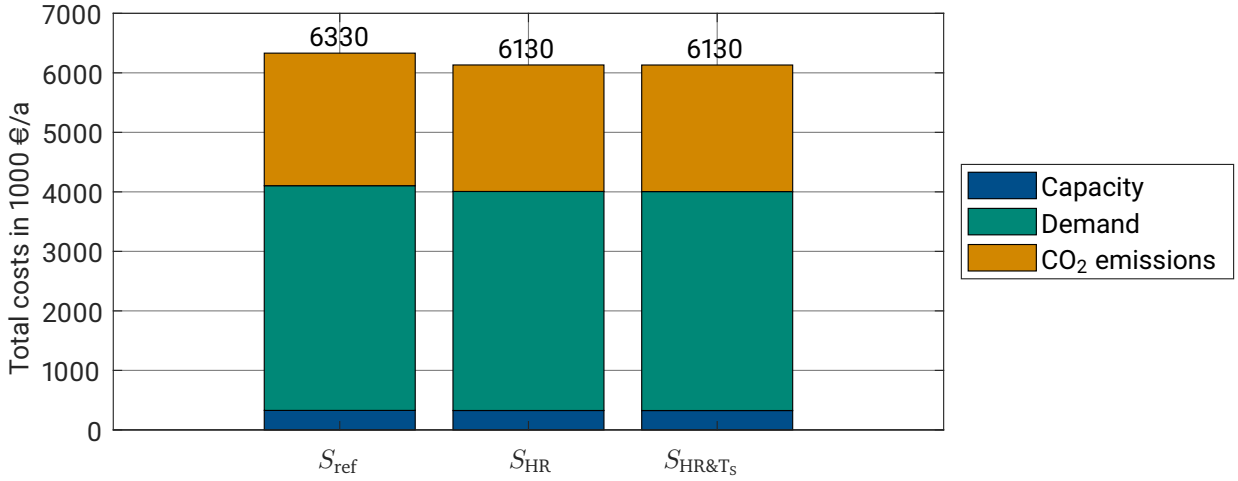

Fig. 8.16: Impact of the proposed temperature reduction measures on total energy-related costs.

8.5.9 Transferability of the case study

The analysis presented above can be applied to any district heating system, as long as the data necessary to calculate the metrics is available. The example of TU Darmstadt campus Lichtwiese illustrates the value of

detailed heat monitoring not only on the primary, but also on the secondary side of the substations. While the installation of heat meters itself does not directly reduce temperatures or decrease heat demand, it gives the operator a better understanding of the system, and makes it possible to identify operational errors and prioritize measures. This way, comprehensive heat monitoring is a crucial step to decrease temperatures and heat demand cost efficiently.

9 Data center waste heat integration in district heating

Although IT infrastructure is becoming increasingly more efficient, the energy demand of data centers has been growing rapidly in recent years, due to a high demand for new data center capacity. In Germany, the electric energy demand for data centers has increased from 10.5 TWh/a in 2010 to 13.2 TWh/a in 2017 [77]. On a global scale, the data center electric energy demand has risen from about 1.3 % of the world electric energy use in 2010 [154] to 2 % in 2018 [155] and is expected to keep growing to reach up to 13 % in 2030 [156]. Due to its high energy consumption, the data center industry emits about as much CO_2 as the airline industry [155]. Data centers operate at high and growing energy densities up to 100 times higher than for office accommodations [157], and the server electric energy demand is almost entirely transformed into heat.

In the context of this thesis, the term high-performance computer (HPC) is used to describe the heat emitting server racks themselves, and the term data center describes the facility as a whole, including all auxiliary installations such as cooling and the building. The concept for a waste heat utilization (WHU) from "Lichtenberg-Hochleistungsrechner" has previously been published in [79], which sets the basis for this chapter.

9.1 Data center cooling technologies and waste heat utilization

Cooling represents about 40 % of the total energy demand of a data center [158]. Reducing the energy demand for cooling is a high priority for data center operators. Higher overall data center energy demands have led to significantly increased energy densities in data center facilities, reaching up to 35 kW per rack [159], compared to about 1 kW per rack in the 1980s [160]. This development makes efficient cooling for data centers an ever more important and challenging task [161]. While the American Society of Heating, Refrigerating and Air-Conditioning Engineers recommends a cooling temperature range between 18 °C and 27 °C for air-cooled data centers [162], most publications consider temperatures at the processor level of up to 85 °C as reasonable [163–165]. This makes it clear that higher cooling temperatures for data centers would be possible if the heat transfer between the processors and the cooling unit were improved.

9.1.1 Air cooling and free cooling

Currently, most data centers use air-based cooling solutions to remove the heat from its IT equipment via computer room air conditioners [166, 167]. Various studies have been conducted on improving the air flow within the data center, eliminating hot-air recirculation or cold-air bypasses [168–171]. Other factors impacting the performance of data center cooling are ceiling height, where heat traps may occur, raised floor height and air flow direction [172]. A recent review article additionally identifies leakages, over- or under-provisioned air supply as well as a non-uniformity of airflow and air temperature as major inefficiencies in airflow management [173]. Many data centers are supplied with a constant air volume flow based on the design heat flow, resulting in high electric energy demands of circulation fans [174]. Variable air volume flow

can decrease this demand.
An important measure to improve the data center's cooling performance is an optimized design of the room layout [173, 175, 176]. Traditionally, equipment is split among different racks according to the maximum allowed power and heat capacity of each rack [177]. To achieve minimal thermal impact of increased power densities, Siriwardana et al. [178] couple CFD simulation with particle swarm optimization in order to determine an optimal data center layout. One widely-accepted and applied measure is the containment of the hot or the cold aisle in order to achieve a better separation of the air flow in different areas of the data center [179, 180]. Another approach to increase the energy efficiency of air-cooled racks is rear door water cooling, where the hot air passing through the rack is cooled down using cold water running through the rack's back door [181].

In cold climate areas, free cooling using cold ambient air is becoming more common, although many data center operators fear contamination possibly introduced by allowing ambient air inside their facility [182]. An overview of free cooling strategies can be found in Oró et al. [157].

9.1.2 Water cooling

To cope with the ever increasing data center energy density, new cooling technologies such as two-phase or water cooling will have to become more important in the future [183]. Direct hot-water cooling (HWC) profits from higher heat capacity and less thermal resistance than air cooling [161]. Based on these advantages, water-cooled data centers are able to deal with heat densities at least 10 times higher than air-cooled ones [161], making important savings in cooling energy demand possible [184]. At the same time, water cooling allows for high cooling inlet temperatures of up to 60 °C [82] and opens new opportunities for waste heat utilization, since the temperature of the available heat is the key factor for such an application [167]. Ellsworth et al. [185] note that water cooling not only increases the energy efficiency, but also the processor performance. Zimmermann et al. [78] demonstrate the feasibility of water cooling in a prototype hot-water-cooled data center. Chi et al. [186] present the case of a fully-immersed liquid cooled data center, reaching a cooling system temperature of about 50 °C. Due to the temperature increase possible with water cooling, operating times of free cooling can be increased in a water-cooled data center [187].

9.1.3 Waste heat utilization

Utilizing waste heat means to recycle the heat emitted by the computing process as a valuable resource, instead of simply discarding it into the environment in the most efficient way. Possible waste heat recovery technologies applicable to data centers depend on the temperature available and include the use for local space or hot-water heating at low temperatures (30-40 °C), district heating supply (50-60 °C) or the supply of cooling energy via absorption chillers (70-90 °C) [161, 167, 188]. Liu et al. [189] propose placing small cloud servers in individual homes to be used as a heating alternative. If the waste heat temperature of the data center is not high enough for direct use, its temperature can be upgraded using a heat pump [167]. For an efficient operation of the heat pump, the temperature difference between the waste heat temperature and the desired output temperature must be as low as possible. Barriers preventing the utilization of data center waste heat are listed in [80] and include unfitting temperature levels, lack of heat demand, high investment costs, differing interests of data center operators and district heating companies as well as inadequate business models.

9.2 Methodology

In the context of the replacement of TU Darmstadt's HPC with a new generation, the university decided to implement an innovative and energy efficient cooling technology, combining hot-water-cooled racks allowing for waste heat temperatures of 40-45 °C with waste heat integration into the district heating return line using a heat pump. The installation process of the new HPC servers will be carried out in two stages. The electric power demand of the first stage will be about $P_{\mathrm{HPC}} = 400\,\mathrm{kW_{el}}$, which is considered to be constant throughout the entire year. The electric input power is almost entirely converted into heat, of which 90 %, i.e. $\dot{Q}_{\mathrm{HPC}} = 360\,\mathrm{kW_{th}}$, can be recovered by means of an on-server water cooling unit. The rest of the heat goes into the server room and continues to be removed by the current air-cooling system. The hot-water alternative for server cooling generates two advantages. On one hand, the hot-water waste heat can be utilized for heating purposes, either in the context of the campus' district heating network or locally in the adjacent buildings. On the other hand, the compression-cooling demand is decreased significantly, and the servers are cooled either via the district heating network or free cooling. Free cooling is possible all year round, because waste heat temperatures always lie below ambient temperatures, including hot summer days. When calculating the ecologic and economic savings generated by HWC and WHU, a reduction of compression cooling demand by $\Delta\dot{Q}_{\mathrm{CC}} = 360\,\mathrm{kW_{th}}$ is considered as one of the advantages of this setup. To calculate the resulting energy savings, an all-year-round operation of the data center (8760 h/a) is considered. To utilize the waste heat most efficiently, several different concepts were taken under consideration, including the use of waste heat to generate cooling energy for the servers via adsorption or absorption cooling, the construction of a local low-temperature heating network connecting the data center to the nearby buildings and an integration of the heat into the return flow of the district heating network using a heat pump. Due to the following reasons, an integration of the heat into the district heating system was identified as the most suitable solution [190]:

- The waste heat temperatures are too low to be used directly to supply cooling energy via adsorption or absorption cooling. This means that a heat pump would have to be used to first increase the temperature of the heat before cooling energy could be supplied. Such a concept would not be efficient.
- In any district energy system, supply and demand must be balanced at all times. This is more difficult to control in a local low-temperature heating network than in a centrally operated network for the whole university.
- Waste heat supply from the HPC can fluctuate over time, due to changes in demand for computing capacities, or the servers can even be turned off completely for maintenance reasons at certain times. Therefore, data center waste heat cannot be the only source of heating and a local low-temperature heating network will always have to remain connected to the central district heating network as a backup heat source, making a local solution more complex and expensive than the centralized option of integrating the waste heat in the district heating system.

This case study quantifies the energetic, ecologic and economic value of a waste heat integration into the district heating system at TU Darmstadt Lichtwiese and compares it to the former cold water cooling solution.

9.2.1 Calculation of usable waste heat and reductions in CO_2 emissions

The amount of usable waste heat and consequently the CO_2 emissions savings from WHU depend on the system the data center is connected to. In the context of this case study, the purpose of the WHU is to substitute heat from HOB, not heat from CHP plants. If CHP heat were substituted by waste heat, this would also lead

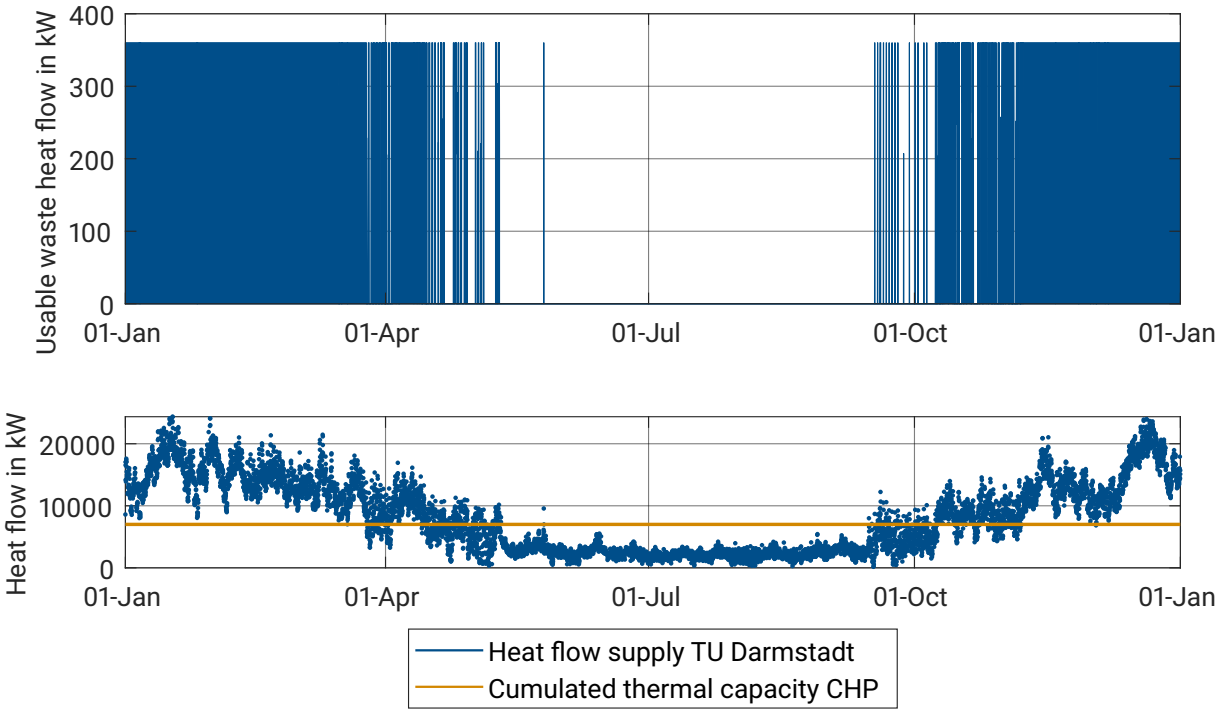

Fig. 9.1: Usable waste heat and total heat supply TU Darmstadt.

to a decrease in CHP electric energy generation. The electric energy no longer generated locally would have to be bought from the grid. Since the current energy mix of grid electric energy still relies on a significant portion of fossil fuels, this would lead to an increase in CO_2 emissions. Therefore, waste heat is only integrated into the district heating network when it does not replace CHP heat. In the summer months, when the heat demand of the university falls below the accumulated capacity of the installed CHP plants, the data center waste heat cannot be integrated in the district heating network and has to be dissipated via free cooling. Fig. 9.1 shows the usable waste heat based on the standardized heat demand of TU Darmstadt in scenario S_{ref} (see chapter 7.4). The usable waste heat modulates between $\dot{Q}_{\text{WHU}} = 360\,\text{kW}_{\text{th}}$ and $\dot{Q}_{\text{WHU}} = 0\,\text{kW}_{\text{th}}$, depending on whether the heat supplied to the buildings at TU Darmstadt is above or below the cumulated thermal power of the CHP plants (see lower part of Fig. 9.1).

The CO_2 emissions savings from WHU $\Delta CO_{2,\text{WHU}}$ are simulated using the detailed model of the TU Darmstadt Lichtwiese district energy system (see chapter 6), considering the utilized waste heat Q_{WHU}, the CO_2 emissions factor for gas $f_{\text{CO2,gas}} = 0.202\,\text{t}_{\text{CO2}}/\text{MWh}$ and the efficiency of the HOB $\eta_{\text{HOB}} = 0.9$. The thermal efficiency of the network is not taken into account in this case, because the savings are calculated at the feed-in point of the heat into the district heating system. The annual CO_2 emissions savings due to WHU can be calculated using eq. 9.1:

$$\Delta CO_{2,\text{WHU}} = \frac{\dot{Q}_{\text{WHU}}}{\eta_{\text{HOB}}} \cdot 8760\frac{h}{a} \cdot 0.202\frac{t_{\text{CO2}}}{MWh} \tag{9.1}$$

Considering that the temperatures in the HWC system are above ambient temperatures all year round, compression cooling can be eliminated and heat can be transferred to the environment via free cooling, in case the WHU is not in operation. In the reference scenario, cold water is supplied by a compression chiller with a seasonal energy efficiency ratio of $SEER = 3.61$, including free cooling. For the calculation of the CO_2 emissions savings due to reduced compression cooling demand, the CO_2 emissions factor for grid electric energy $f_{\mathrm{CO2,el,2018}} = 0.474\,\mathrm{t_{CO2}/MWh}$ is taken into account, because the electric energy for compression chillers counts as contractor energy demand, which cannot be supplied by the CHP plants (see chapter 5.3.1). The annual savings in CO_2 emissions due to reduced compression cooling demand $\Delta CO_{2,\mathrm{CC}}$ can be calculated using the following equation:

$$\Delta CO_{2,\mathrm{CC}} = \frac{\Delta \dot{Q}_{\mathrm{CC}}}{SEER} \cdot 8760 \frac{h}{a} \cdot 0.474 \frac{t_{\mathrm{CO2}}}{MWh} \tag{9.2}$$

Additional CO_2 emissions due to the electric energy demand of the heat pump $\Delta CO_{2,\mathrm{HP}}$ have to be considered. The COP of the heat pump COP_{HP} is calculated within the simulation according to the temperatures at both the evaporator and condenser of the heat pump. For the operation of the heat pump, the CO_2 emissions factor for grid electric energy is taken into account, as in the case of compression cooling. The additional CO_2 emissions can be calculated according to eq. 9.3:

$$\Delta CO_{2,\mathrm{HP}} = \frac{\dot{Q}_{\mathrm{WHU}}}{COP_{\mathrm{HP}} - 1} \cdot 8760 \frac{h}{a} \cdot 0.474 \frac{t_{\mathrm{CO2}}}{MWh} \tag{9.3}$$

The total CO_2 emissions savings due to HWC and WHU can be calculated combining the emissions saving from WHU and reduced compression cooling, and adding the additional emission due to the heat pump operation:

$$\Delta CO_{2,\mathrm{total}} = \Delta CO_{2,\mathrm{WHU}} + \Delta CO_{2,\mathrm{CC}} - \Delta CO_{2,\mathrm{HP}} \tag{9.4}$$

9.3 Energy efficiency metrics

To evaluate and compare the energetic performance of different data centers, energy efficiency metrics can be a very helpful tool. A multitude of metrics to characterize the energy efficiency of data centers have been used in the past [82]. They address different aspects of data centers from different perspectives, including the server itself [191], the heating, ventilation and air conditioning (HVAC) system [192] or the data center as a whole [193]. This study concentrates on the overall efficiency of the data center. The most common generic data center energy efficiency metric is the Power Usage Effectiveness (PUE), which compares the total annual energy demand of the data center to the annual energy demand of servers and necessarily needs to be equal to or greater than one [194]. This metric is not appropriate in a data center with WHU, since the value of the reused energy is not being taken into account. A better metric for data centers including WHU is the energy reuse effectiveness (ERE) as proposed in [80]:

$$ERE = \frac{Total\,Energy - Reuse\,Energy}{IT\,Energy} = \frac{E_{\mathrm{el,HPC}} + E_{\mathrm{HP}} - Q_{\mathrm{WHU}}}{E_{\mathrm{el,HPC}}} \,\mathrm{with}\, ERE \geq 0 \tag{9.5}$$

In this equation, $E_{\mathrm{el,HPC}}$ stands for the server electric energy demand, and E_{HP} for the electric energy demand of the heat pump. The disadvantage of this approach is that no difference is made between the different

energy forms in terms of their quality. While the energy input of the data center is electric energy, the reuse energy leaves the system as heat, creating a system with energy flows of different qualities. To account for these differences, an exergetic metric specifying the quality of the energy is more suitable. Based on a methodology developed for an analysis of the exergy destruction of an air-cooled data center [78], the exergy reuse effectiveness (ExRE) is calculated, taking into account the differences in quality of the different energy flows in the system:

$$ExRE = \frac{Total\,Exergy - Reuse\,Exergy}{IT\,Exergy} = \frac{Ex_{\text{el,HPC}} + Ex_{\text{el,HP}} - Q_{\text{WHU}} \cdot \left(1 - \frac{T_{\text{amb}}}{T_{\text{HPC,out}}}\right)}{Ex_{\text{el,HPC}}} \text{ with } ExRE \geq 0 \qquad (9.6)$$

In this equation, $Ex_{\text{el,HPC}}$ stands for the server electric exergy demand, and Ex_{HP} for the electric exergy demand of the heat pump. While for electricity energy and exergy content are the same, the exergy content of heat is significantly lower than its energy content. The exergy content of the usable waste heat Q_{WHU} is calculated for an HPC output temperature temperature $T_{\text{HPC,out}} = 45\,°\text{C}$, using the ambient temperature T_{amb} as reference temperature.

Both metrics are useful when both the amount of used energy and energy quality related factors such as CO_2 emissions play a role for the assessment the feasibility of WHU. In this study, both the ERE and ExRE for HWC and WHU are presented and compared to the ERE and ExRE of the traditional low-temperature air cooling formerly installed in the data center. The lower the value of the ERE and ExRE becomes, the better the performance of the data center cooling and the WHU.

9.4 Concept for HPC hot-water cooling and waste heat utilization at campus Lichtwiese

When waste heat is integrated in a district heating network, the conditions of the waste heat need to fulfill the requirements of the district heating network. The minimum temperature of the waste heat is determined by the district heating return temperature and must always be higher than the latter. Since the temperature of the district heating return flow at campus Lichtwiese varies between 50 °C and 70 °C throughout the year and the temperature of the waste heat is only 45 °C, a heat pump is necessary at all times to upgrade the waste heat temperature. On the other hand, the district heating return temperature is limited to a maximum of 70 °C, in order to guarantee the proper functioning of the CHP plants.

Fig. 9.2 shows the setup for the integration of the HPC waste heat into the district heating return flow. The HPC is water-cooled at the server level. The water used for the server cooling circuit has special quality requirements. Consequently, this circuit must be disconnected hydraulically from the rest of the cooling system using a heat exchanger (HX). The manufacturer of the HPC guarantees that the waste heat is released at a temperature not lower than 45 °C after the heat exchanger. To ensure the removal of the heat from the system even when it cannot be used in the district heating network, a hybrid cooler (HC) already in place at the data center is connected between the servers and a buffer storage (BS). Since the temperature at which the heat is emitted from the HPC in this scenario is a lot higher than it was in the low-temperature air cooling case, heat can be dissipated through the hybrid cooler all year round and no mechanical cooling is necessary, not even in the summer. The stratified buffer storage (BS) situated between the HPC and the heat pump serves to smooth out the cooling power demand of the HPC that potentially fluctuates over time, thereby decreasing

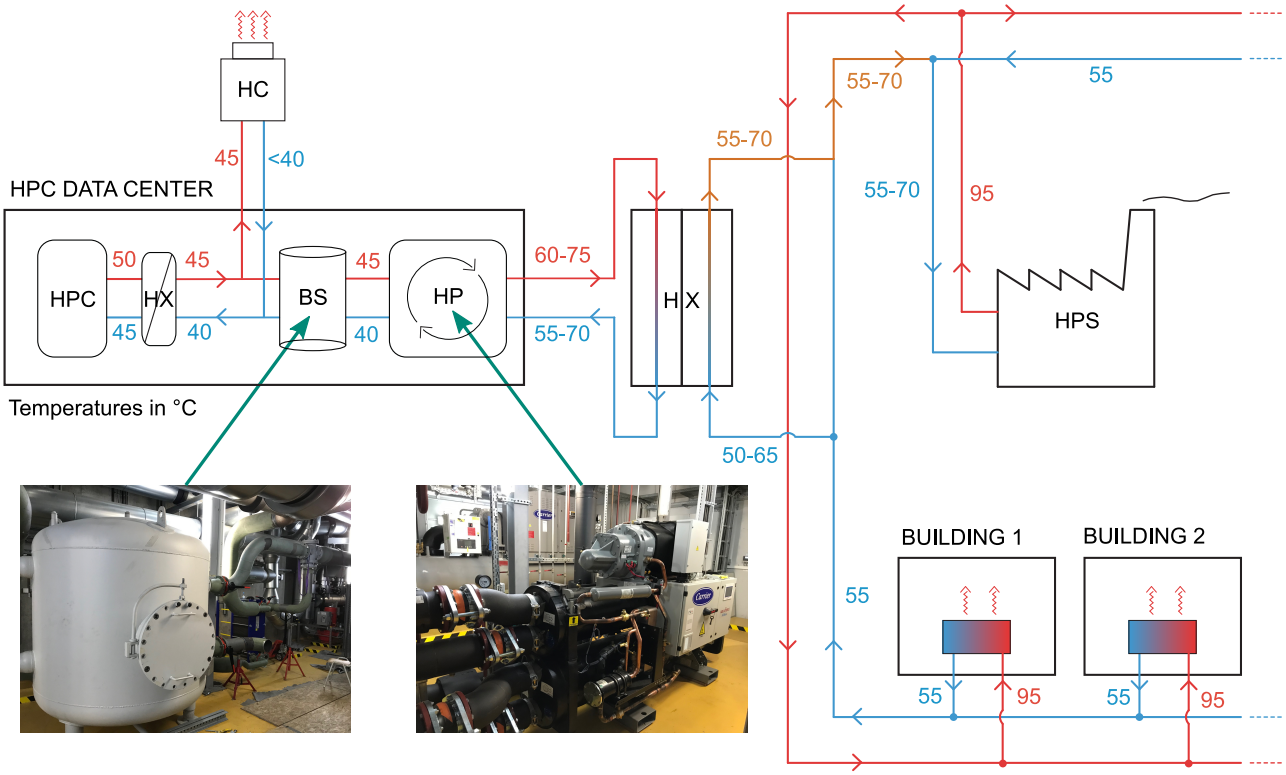

Fig. 9.2: Functional diagram of the HWC and district heating waste heat integration.

the amount of load shifts for the heat pump. The heat pump is the main component of this setup. It receives waste heat at the evaporator (cold side) at 45 °C. The output temperature at the condenser (hot side) depends on the district heating return temperature. Due to the high waste heat temperature entering the heat pump evaporator, this setup is very efficient, yielding an average COP of $COP_{\mathrm{HP}} = 6.8$. The hot circuit of the heat pump cannot be connected directly to the district heating return flow but must be separated hydraulically using another heat exchanger. For the purpose of this study, the logarithmic mean temperature difference over all heat exchangers is considered to be $LMTD = 5\,\mathrm{K}$. A model of the data center cooling system including the heat pump is integrated in the detailed model of the campus energy system (see chapter 6).

With the help of this model, the amount of useful waste heat can be computed, respecting the limitations in terms of the priority for CHP heat and maximum network return temperature. The data center is located at the end of the return line on the western side of the campus, with no other building connected in between the data center and the heat and power station. Therefore, the return flow at the data center can be heated up to the maximum CHP inlet temperature of 70 °C without risking overshooting the maximum return temperature by other buildings. Additionally, the model computes the amount of heat from HOB replaced by waste heat, the grid electric energy saved due to reduced demand in compression cooling and the additional electric energy demand for the heat pump. The electric energy demand for the circulation pumps necessary in each circuit of the data center cooling system is very low compared to the electric energy demand of the HPC and the heat pump. Therefore, the electric energy demand for pumping is neglected in the context of this study.

To be able to quantify the Exergy Reuse Effectiveness (ExRE), the exergy of the utilized waste heat must be calculated. This is done calculating the difference between the exergy of the mass flow leaving the district heating network and the one returning to the district heating network. The Test Reference Year ambient

temperature [141] serves as reference for this calculation. The future scenario, including hot-water server cooling and waste heat utilization, is compared to a business-as-usual scenario, in which the new generation of TU Darmstadt's high-performance computer would be cooled using low temperature air cooling as well as rear door water heat exchangers at 17-24 °C and free cooling as in the case of the former generation of the HPC.

9.5 Results

The goal of this analysis is to quantify how much waste heat from TU Darmstadt's "Lichtenberg-Hochleistungsrechner" can be used and what amount of CO_2 emissions reductions can be achieved. Additionally, the annuity of savings or additional expenses are presented. Fig. 9.3 shows available and useful waste heat on a monthly basis. The number above each bar indicates the total monthly useful waste heat. In general, waste heat use is high in the winter and no heat can be integrated in the district heating network in the summer, due to the constraint that waste heat is not allowed to replace CHP heat. In the winter, almost all available waste heat is integrated in the district heating system, while during the three hottest summer months June, July and August, no heat can be used. In total, about 48 % (1500 MWh) of the total available waste heat can be used on a yearly basis.

CO_2 emissions savings are generated on one hand by integrating waste heat in the district heating return line, and on the other hand by reducing the electric energy demand for compression cooling. While the savings from the waste heat itself depend on the amount of waste heat utilized, which changes throughout the year, the savings from reduced cooling demand are the same all year round, as long as the HPC operates at a constant capacity. Fig. 9.4 shows the monthly change in CO_2 emissions due to HWC and WHU compared to the reference scenario. The total CO_2 emissions savings amount to 685 t_{CO2}/a, with the savings due to a reduced demand for compression cooling accounting for 60 % of the total savings (410 t_{CO2}/a). The total savings represent 4.1 % of the campus Lichtwiese CO_2 emissions in S_{ref} (see chapter 7.5.6). Data center HWC and WHU can attribute a significant proportion to lower the university's CO_2 emissions and reach its climate protection goals.

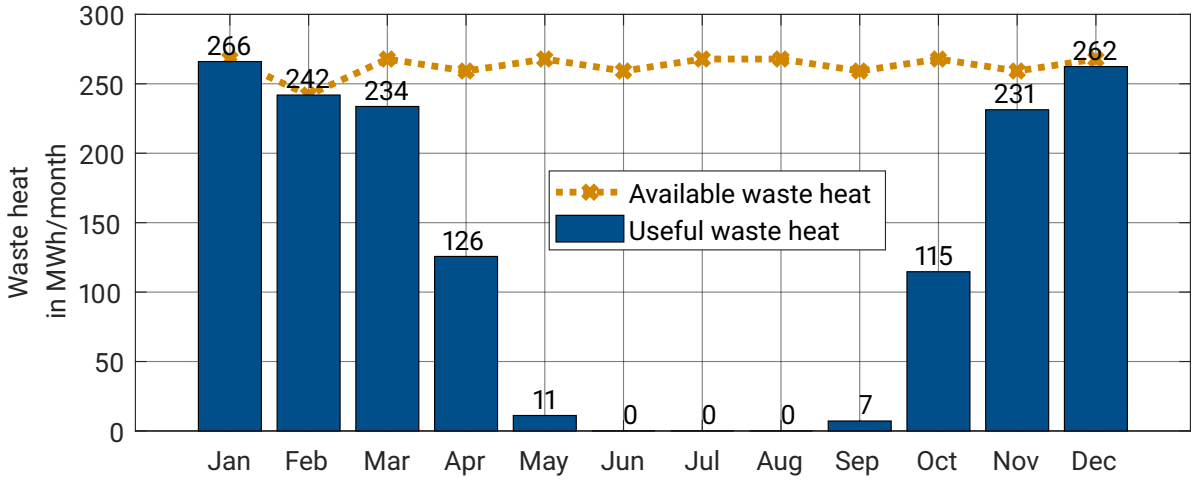

Fig. 9.3: Available and useful waste heat.

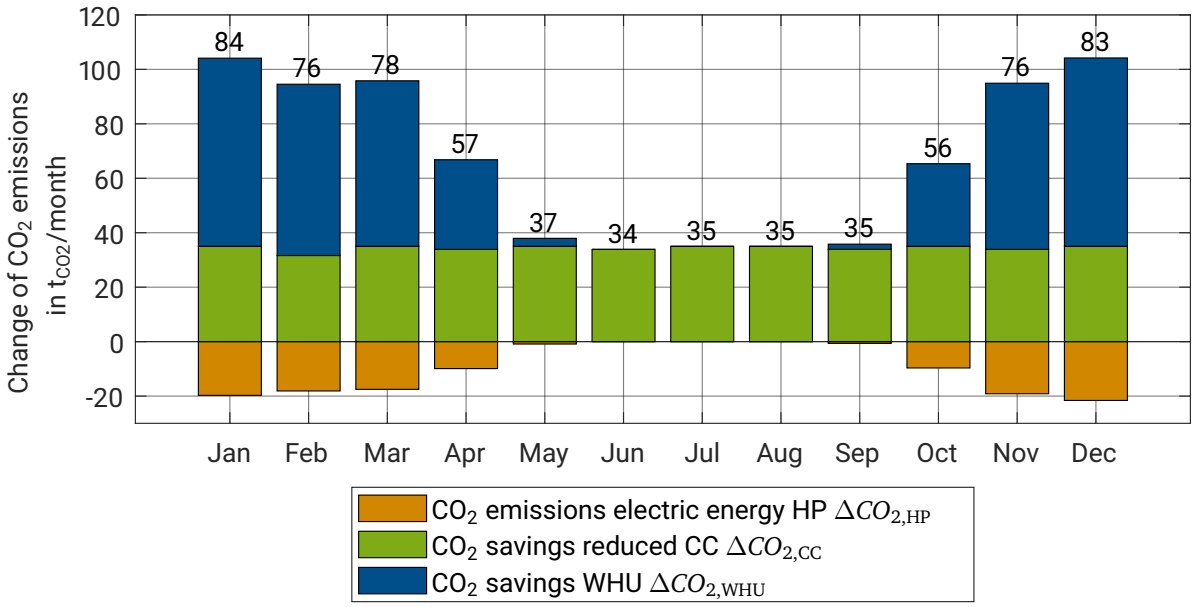

Fig. 9.4: Monthly changes in CO_2 emissions compared to the reference scenario.

Compared to the results presented for scenario 1 in [79], the useful waste heat and the savings in CO_2 emissions are slightly lower. This is due to the increased level of detail of the model used in this thesis. While in [79] equal supply temperatures for all parts of the university district heating system were used, the model used here reflects the differences in supply temperature between the Lichtwiese and the Stadtmitte campuses. Since the Lichtwiese district heating network is operated at lower temperatures than the Stadtmitte campus,this leads to lower total heat losses in the Lichtwiese district network and consequently to shorter periods with heat demand above the maximum thermal load of the CHP plants. Since data center waste heat is not supposed to replace CHP heat, it results in shorter utilization periods for data center waste heat.

To determine the economic impact of HWC and WHU, savings due to lower electric energy costs for compression cooling and decreased gas costs for heat generation are taken into account. On the other hand, costs are increased by the additional electric energy demand to supply the heat pump and by the annuity of the investment in the heat pump, additional piping for HWC and the connection to the district heating network. Costs for the hot-water on-server cooling technology itself are not taken into account in this study. It is considered that future HPC units will have to use water cooling in any case, since air cooling will not be able to handle the ever rising heat densities in HPC racks. Investment differences between on-server cooling elements for cold and hot-water cooling are small and can be neglected.

Fig 9.5 shows the monthly change in energy-related and CO_2-related costs due to HWC and WHU, as defined in chapter 5. In total, the annuity is decreased by about 110 000 €/a. If CO_2-related costs are not taken into account, still a reduction by 27 000 €/a results from the analysis. Compared to the total investment costs, these savings are small, and a small change in energy costs can affect them significantly. Conservatively speaking, it can be stated that the HWC and WHU will most probably not increase energy-related costs in the context of the HPC.

Table 9.1 lists the ERE and ExRE of the reference as well as the HWC & WHU scenarios. The HWC & WHU scenario makes it possible to lower both the ERE and ExRE and increase the HPC energy efficiency significantly.

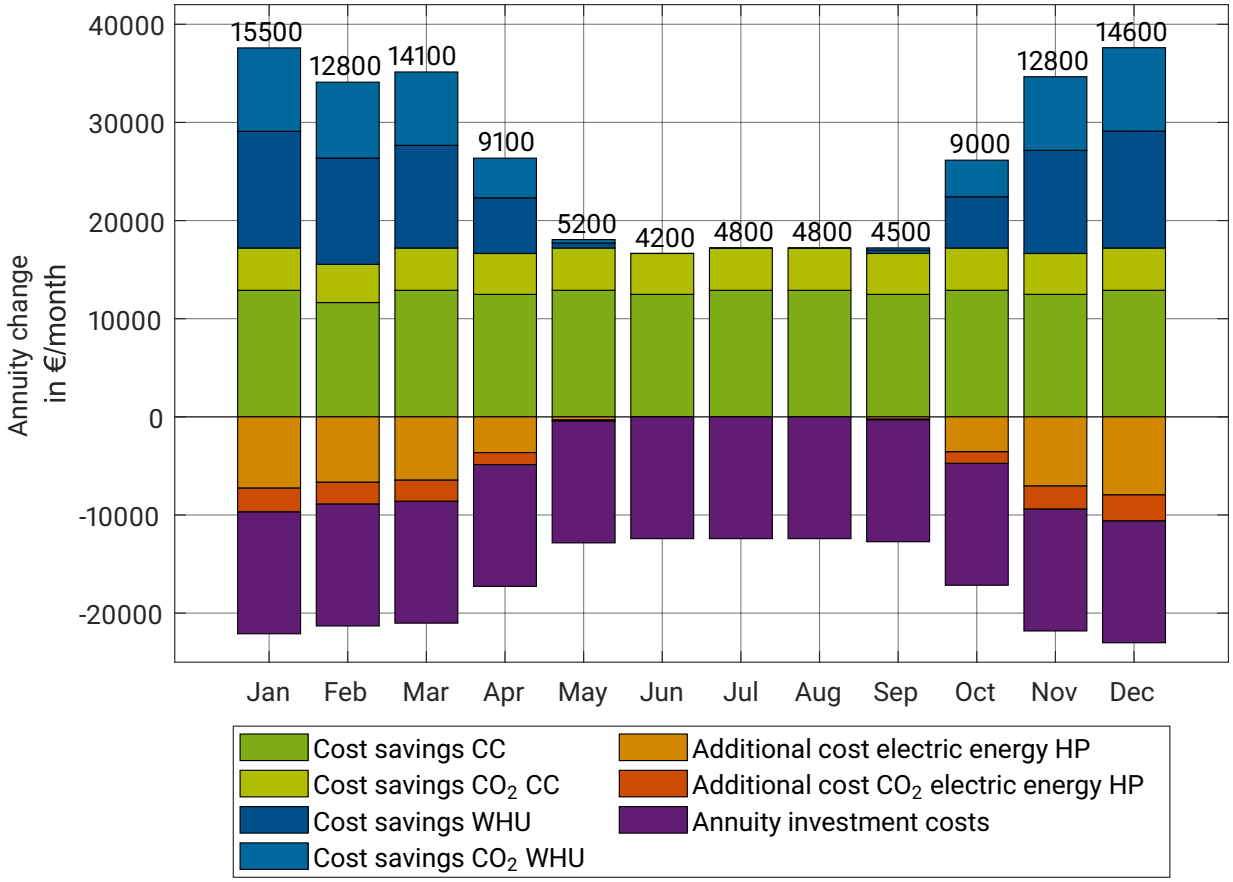

Fig. 9.5: Monthly changes in annuities compared to the reference scenario.

In the HWC & WHU scenario, the ExRE is higher than the ERE, because the exergy content of the waste heat is well below the exergy of the electric energy entering the HPC. In the reference scenario, all relevant energy flows are electric, hence in this case both ERE and ExRE are the same.

Table 9.1: Comparison of the ERE and ExRE in the reference and HWC & WHU scenarios.

	Reference	**HWC & WHU**
ERE	1.27	0.645
ExRE	1.27	1.015

10 The future of the TU Darmstadt campus Lichtwiese energy system

TU Darmstadt is committed to contributing to the German national climate protection goal, reducing its area-specific CO_2 emissions by 80 % until 2050, compared to the 1990 level [6]. Fig. 10.1 shows the development of the CO_2 emissions for campus Lichtwiese since 1990, the potential reductions based on the measures proposed in this thesis (S_{thesis}: design & operation optimization, temperature reduction, waste heat utilization), and the target values for 2050. In 1990, the heated floor area of the campus was 102 000 m^2, in the reference year 2018 it amounted to 155 000 m^2 and is expected to continue growing to 183 000 m^2 until 2022, serving as the reference year for S_{thesis}. Projections suggest substantial construction activities in upcoming decades and a total heated floor area of up to 300 000 m^2 until 2050.

Between 1990 and 2018, absolute CO_2 emissions have been reduced by 11 % and area-specific emissions by 41 %. The measures proposed in this thesis mainly serve to prepare the district energy system of TU Darmstadt campus Lichtwiese for the necessary energy transition, by showing ways to optimize the design and operation of the system, to reduce network temperatures and to include locally available waste heat into the district heating system. All the same, they allow an additional reduction of absolute emissions by 6 % and another reduction of area-specific emissions by 13 % compared to 1990. Compared to the goal of a reduction by 80 % with respect to the 1990 level, a gap of the area-specific emissions of 26 % still remains to be closed after the implementation of the measures presented in this thesis. The absolute CO_2 emissions consequently have to be reduced by another 24 % compared to 1990, taking into account a steep increase in total heated floor area at

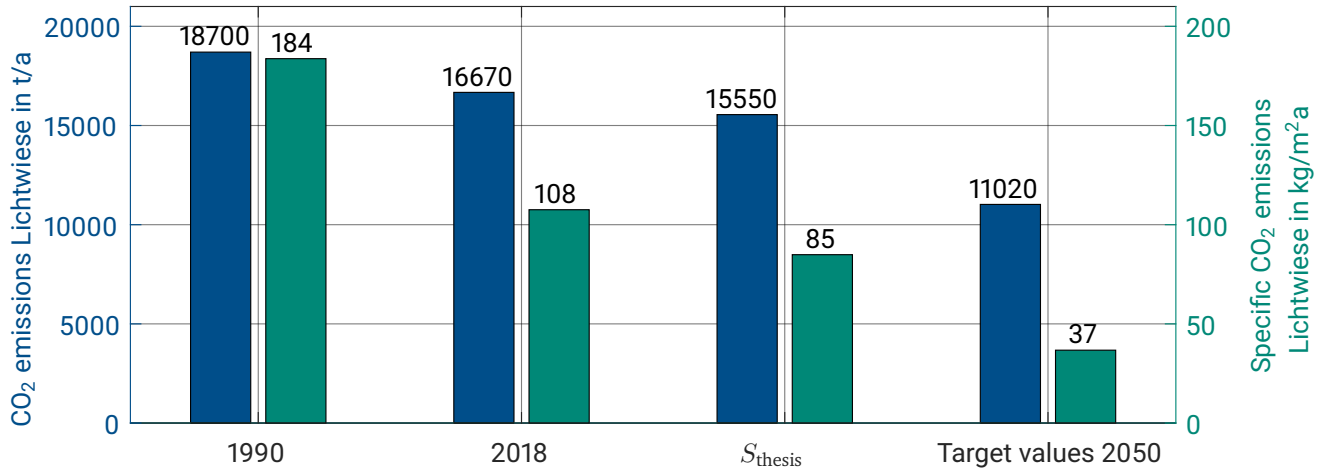

Fig. 10.1: Development of the absolute and specific CO_2 emissions since 1990 and projections after the implementation of the measures proposed in this thesis, as well as target values for 2050.

the same time. Experience shows that it is always easier to reduce emissions in early stages when low-hanging fruits can easily be collected at low costs. In later stages, measures necessary to achieve the last percentages of reduction become increasingly more complex and costly. Therefore, continued efforts will be necessary to bridge the remaining gap.

As was shown repeatedly in this thesis, the university's electric energy demand plays a key role in its total CO_2 emissions (see chapters 7.5.6 and 8.5.8). In the future, it will be crucial to reduce the carbon intensity of the electric energy demand. This can be done purchasing exclusively renewable electric energy from the grid. While this might be a suitable option in the long term, it is not feasible as a medium term solution if TU Darmstadt wants to serve as an example for the energy transition on the local level. As long as the national electric energy mix is not 100 % renewable, purchasing exclusively renewable energy at TU Darmstadt would simply reduce the share of renewables for other customers. Accordingly, a real impact on the electric energy related CO_2 emissions can only be achieved if electric energy consumption is reduced or additional renewable electric energy is generated locally, e.g. via photovoltaics. Measures to decrease the demand include the installation of variable speed circulation pumps for heating and cooling, variable speed ventilators in ventilation systems, renovation of lighting systems, installation of LEDs and purchase of efficient office appliances such as computers or refrigerators. Such efforts will only be successful if users become conscious about their consumption of energy and take an active role in reducing the demand. Comprehensive energy monitoring can be helpful to sensitize users for energy efficiency, making their demand transparent.

At the same time, reductions of the CO_2 emissions factor of grid electric energy due to an increase of the share of renewables in the national mix will make alternative options for local energy supply more interesting in the long run. For TU Darmstadt, it will be necessary to evaluate how much longer it makes sense ecologically to supply heat and power via fossil based CHP plants. An alternative might be to switch to a grid electric energy based local energy system, including heat pumps and compression chillers, as soon as the national CO_2 emissions factor drops below a certain value. Nevertheless, cogeneration will most probably remain a central part of the TU Darmstadt energy system at least for the next 10-15 years.

11 Conclusion and Outlook

The aim of this thesis was to develop measures to prepare the TU Darmstadt campus Lichtwiese energy system for decarbonization. Based on the literature review, three main research tasks were identified:

- Optimization of the design and operation of the generation facilities for heating, cooling and electric energy, including demand prediction, to make optimal use of thermal storage.
- Reduction of temperatures in district heating: Identification of errors in the design and control of district heating substations and in-building heat distribution, as well as development of metrics to determine where to apply which improvement measure to reduce network temperatures most efficiently.
- Integration of locally available waste heat into district heating, namely waste heat from data centers.

To realize these tasks, a dynamic simulation model of the TU Darmstadt energy system was developed in MATLAB/Simulink, including, the generation, distribution, and consumption of heat, cooling, and electric energy. Within this model, annual simulations of the operation of the system for different scenarios were realized. In these scenarios, the proposed improvement measures were applied to campus Lichtwiese, and analyzed energetically, ecologically and economically in comparison to the current system. The results of the design and operation optimization in chapter 7 show that, although small improvements are possible, the capacities of the generation units are already close to the optimum for the current energy demand structure. The system is being operated well, even without employing mathematical optimization algorithms and a simple improvement of current system will not be enough to fulfill the university's climate protection goals.

The more important leverage to decarbonize the campus energy system exists within the buildings, where design and operational errors in the heat distribution result in high temperature demands, and where poor energetic performance leads to high heat demands. In this thesis, metrics based on monitoring data from the primary and secondary sides of the district heating substations were developed. These metrics highlight critical buildings for network temperature reduction. Additionally, they help to identify what kind of problems lead to a high temperature or heat demand in a specific building (see chapter 8). The analysis shows that it is possible to reduce the temperature demand of the buildings, which is a necessary prerequisite for the transformation of the system from its current fossil-based to a future renewable-based energy supply.

Waste heat will play an ever more important role in future district heating networks. Nevertheless, integrating waste heat from a local source such as a data center is a complex task, as much from a technical as from an organizational point of view. From a technical point of view, the most difficult part is to synchronize the temperature levels of the heat source and the district heating system. From an organizational point of view, the challenge is to bring together data center and district heating operators, who have very different expertise and differing priorities. Such a joint venture of completely different industries makes a lot of communication and patience necessary. The case study on data center waste heat integration in district heating realized for this thesis serves as an example to be copied, showing the feasibility and benefits of such a setup (see chapter 9). It shows that an integration of data center waste heat into district heating is already ecologically reasonable today, even without a prior reduction of network temperatures.

The measures presented make it possible to prepare the campus to be decarbonized and supplied by an increased share of renewable heat in the context of the future energy concept for the time after 2030, which is developed in the context of the ”EnEff:Stadt Campus Lichtwiese” research project.

Outlook

This thesis proposes a path to prepare the decarbonization of the TU Darmstadt campus Lichtwiese district energy system. Based on the measures presented here, additional research will be necessary to determine how to realize the university's climate protection goals most efficiently, considering building renovation, integration of renewable heat and electric energy as well as increased efforts to reduce the electric energy demand.

A model of a district energy system serves to simulate different scenarios for the future development. The better the understanding of the real system, the better the results of the simulation represent possible future realities. Consequently, a further improvement of the energy monitoring system of the university is a high priority, adding detailed electric monitoring at the building level as well as monitoring of all relevant energy flows at the heat and power station to its energy management system. Based on these new data sources, it will be possible to improve the models used in this thesis, and to validate them at a more detailed level. It will also be possible to include new aspects, such as decentral renewable heat from geothermal or solar-thermal sources. Likewise, a repetition of the study on district heating network temperature reductions carried out here will give more in-depth insights into the functioning and errors of the district heating substations and in-building heating circuits once at least a year of continuous monitoring data is available. For the data center waste heat integration, it will be necessary to realize a proof of concept when the new high performance computer ”Lichtenberg II” goes online and operational data can be collected. Since an expansion of the university data center is already being planned, further studies will be necessary on how to integrate a rising waste heat potential in the district heating network. Additionally, it will be interesting to investigate how a future reduction of the network temperatures affects the waste heat utilization concept.

To transfer the strategies and measures presented in this thesis to other districts, details of the model and constraints need to be altered. Nevertheless, the developed concepts for design and operation optimization, network temperature reduction and data center waste heat utilization can help to provide substantial energy savings in any district energy system, as long as the necessary data is available.

Acknowledgment

Technische Universität Darmstadt was funded for this research by the German Federal Ministry of Economic Affairs and Energy (BMWi) in the projects “EnEff:Stadt Campus Lichtwiese” (03ET1356A) and ”EnEff:Stadt Campus Lichtwiese II” (03ET1638). Further financial support came from Deutsche Forschungsgemeinschaft (DFG) in the framework of the Graduate School of Excellence Energy Science and Engineering (GSC 1070). The copyright of the cover image belongs to Nikolaus Heiss, while the illustration of the smart energy system was realized by David Sauerwein.

Bibliography

[1] Behrang Talebi, Parham A. Mirzaei, Arash Bastani, and Fariborz Haghighat. “A Review of District Heating Systems: Modeling and Optimization”. In: *Frontiers in Built Environment* 2.16 (2016), p. 7839. ISSN: 2297-3362. DOI: 10.3389/fbuil.2016.00022.

[2] John F. Collins. *The history of District Heating*. 1959. URL: http://www.verenum.ch/Dokumente/1959_Collins_History.pdf (visited on Mar. 18, 2020).

[3] Sven Werner. “International review of district heating and cooling”. In: *Energy* 137 (2017), pp. 617–631. ISSN: 03605442. DOI: 10.1016/j.energy.2017.04.045.

[4] Svend Frederiksen and Sven Werner. *District heating and cooling*. 1st ed. Lund: Studentlitteratur, 2013. ISBN: 9789144085302.

[5] Bernard Aebischer, Martin Jakob, and Giacomo Catenazzi. *Impact of climate change on thermal comfort, heating and cooling energy demand in Europe*. Zürich, 2007. URL: http://www.verozo.be/sites/verozo/files/files/Impact%20ClimateChange_ETH%20Switzerland.pdf (visited on Apr. 27, 2020).

[6] Johannes Oltmanns. “Auf dem Weg zu einem energieeffizienten Campus: Projekt EnEff:Stadt Campus Lichtwiese - Weiterentwicklung eines Energiesystems auf Quartiersebene”. In: *Hoch3* 3 (2019), pp. 4–6. URL: https://www.tu-darmstadt.de/universitaet/aktuelles_meldungen/publikationen/publikationen_archiv/einzelansicht_10624.de.jsp (visited on July 7, 2020).

[7] Dave Olsthoorn, Fariborz Haghighat, and Parham A. Mirzaei. “Integration of storage and renewable energy into district heating systems: A review of modelling and optimization”. In: *Solar Energy* 136 (2016), pp. 49–64. DOI: 10.1016/j.solener.2016.06.054.

[8] Johannes Oltmanns, Martin Freystein, Frank Dammel, and Peter Stephan. “Improving the operation of a district heating and a district cooling network”. In: *Energy Procedia* 149 (2018), pp. 539–548. ISSN: 18766102. DOI: 10.1016/j.egypro.2018.08.218.

[9] Vittorio Verda and Francesco Colella. “Primary energy savings through thermal storage in district heating networks”. In: *Energy* 36.7 (2011), pp. 4278–4286. ISSN: 03605442. DOI: 10.1016/j.energy.2011.04.015.

[10] Thomas Schmidt, Thomas Pauschinger, Per Alex Sørensen, Aart Snijders, Reda Djebbar, Raymond Boulter, and Jeff Thornton. “Design Aspects for Large-scale Pit and Aquifer Thermal Energy Storage for District Heating and Cooling”. In: *Energy Procedia* 149 (2018), pp. 585–594. ISSN: 18766102. DOI: 10.1016/j.egypro.2018.08.223.

[11] Michał Leśko, Wojciech Bujalski, and Kamil Futyma. “Operational optimization in district heating systems with the use of thermal energy storage”. In: *Energy* 165 (2018), pp. 902–915. ISSN: 03605442. DOI: 10.1016/j.energy.2018.09.141.

[12] Kody M. Powell, Jong Suk Kim, Wesley J. Cole, Kriti Kapoor, Jose L. Mojica, John D. Hedengren, and Thomas F. Edgar. “Thermal energy storage to minimize cost and improve efficiency of a polygeneration district energy system in a real-time electricity market”. In: *Energy* 113 (2016), pp. 52–63. ISSN: 03605442. DOI: 10.1016/j.energy.2016.07.009.

[13] Sebastian Stinner, Kristian Huchtemann, and Dirk Müller. “Quantifying the operational flexibility of building energy systems with thermal energy storages”. In: *Applied Energy* 181 (2016), pp. 140–154. ISSN: 03062619. DOI: 10.1016/j.apenergy.2016.08.055.

[14] H. Gadd and S. Werner. “Thermal energy storage systems for district heating and cooling”. In: *Advances in thermal energy storage systems*. Ed. by Luisa F. Cabeza. Woodhead Publishing Series in Energy. Amsterdam: Elsevier Science, 2015, pp. 467–478. ISBN: 9781782420880. DOI: 10.1533/9781782420965.4.467.

[15] Andreas Hauer, Stefan Hiebler, and Manfred Reuß. *Wärmespeicher*. 5., vollständig überarbeitete Auflage. BINE-Fachbuch / BINE Informationsdienst, FIZ Karlsruhe. Stuttgart: Fraunhofer IRB Verlag, 2013. ISBN: 978-3816783664.

[16] Thorsten Urbaneck. *Kältespeicher: Grundlagen, Technik, Anwendung*. Munich, Germany: Oldenbourg Verlag, 2012. ISBN: 9783486707762.

[17] Elisa Guelpa and Vittorio Verda. “Thermal energy storage in district heating and cooling systems: A review”. In: *Applied Energy* 252 (2019), p. 113474. ISSN: 03062619. DOI: 10.1016/j.apenergy.2019.113474.

[18] D. F. Dominković, P. Gianniou, M. Münster, A. Heller, and C. Rode. “Utilizing thermal building mass for storage in district heating systems: Combined building level simulations and system level optimization”. In: *Energy* 153 (2018), pp. 949–966. ISSN: 03605442. DOI: 10.1016/j.energy.2018.04.093.

[19] Johan Kensby, Anders Trüschel, and Jan-Olof Dalenbäck. “Potential of residential buildings as thermal energy storage in district heating systems – Results from a pilot test”. In: *Applied Energy* 137 (2015), pp. 773–781. ISSN: 03062619. DOI: 10.1016/j.apenergy.2014.07.026.

[20] J. Le Dréau and P. Heiselberg. “Energy flexibility of residential buildings using short term heat storage in the thermal mass”. In: *Energy* 111 (2016), pp. 991–1002. ISSN: 03605442. DOI: 10.1016/j.energy.2016.05.076.

[21] Michał Turski and Robert Sekret. “Buildings and a district heating network as thermal energy storages in the district heating system”. In: *Energy and Buildings* 179 (2018), pp. 49–56. ISSN: 03787788. DOI: 10.1016/j.enbuild.2018.09.015.

[22] Daniel Basciotti, Florian Judex, Olivier Pol, and Ralf-Roman Schmidt. “Sensible heat storage in district heating networks: a novel control strategy using the network as storage”. In: *Conference proceedings of the 6th international renewable energy storage conference IRES*.

[23] Dmytro Romanchenko, Johan Kensby, Mikael Odenberger, and Filip Johnsson. “Thermal energy storage in district heating: Centralised storage vs. storage in thermal inertia of buildings”. In: *Energy Conversion and Management* 162 (2018), pp. 26–38. ISSN: 01968904. DOI: 10.1016/j.enconman.2018.01.068.

[24] Annelies Vandermeulen, Bram van der Heijde, and Lieve Helsen. “Controlling district heating and cooling networks to unlock flexibility: A review”. In: *Energy* 151 (2018), pp. 103–115. ISSN: 03605442. DOI: 10.1016/j.energy.2018.03.034.

[25] Alessandro Franco and Michele Versace. “Optimum sizing and operational strategy of CHP plant for district heating based on the use of composite indicators”. In: *Energy* 124 (2017), pp. 258–271. ISSN: 03605442. DOI: 10.1016/j.energy.2017.02.062.

[26] Amru Rizal Razani and Ingo Weidlich. “A Genetic Algorithm Technique to Optimize the Configuration of Heat Storage in District Heating Networks”. In: *International Journal of Sustainable Energy Planning and Management* 10 (2016).

[27] Akomeno Omun, Ruchi Choudhary, Adam Boies. “Distributed energy resource system optimisation using mixed integer linear programming”. In: *Energy Policy* 61 (2013), pp. 249–266. ISSN: 0301-4215. DOI: 10.1016/j.enpol.2013.05.009.

[28] Helge Averfalk, Fredric Ottermo, and Sven Werner. “Pipe Sizing for Novel Heat Distribution Technology”. In: *Energies* 12.7 (2019), p. 1276. ISSN: 1996-1073. DOI: 10.3390/en12071276.

[29] T. Mertz, S. Serra, A. Henon, and J. M. Reneaume. “A MINLP optimization of the configuration and the design of a district heating network: Study case on an existing site”. In: *Energy Procedia* 116 (2017), pp. 236–248. ISSN: 18766102. DOI: 10.1016/j.egypro.2017.05.071.

[30] Yaser Kialashaki. “A linear programming optimization model for optimal operation strategy design and sizing of the CCHP systems”. In: *Energy Efficiency* 11.1 (2018), pp. 225–238. DOI: 10.1007/s12053-017-9560-1.

[31] Na Deng, Rongchang Cai, Yuan Gao, Zhihua Zhou, Guansong He, Dongyi Liu, and Awen Zhang. “A MINLP model of optimal scheduling for a district heating and cooling system: A case study of an energy station in Tianjin”. In: *Energy* 141 (2017), pp. 1750–1763. ISSN: 03605442. DOI: 10.1016/j.energy.2017.10.130.

[32] Carl Haikarainen, Frank Pettersson, and Henrik Saxén. “A model for structural and operational optimization of distributed energy systems”. In: *Applied Thermal Engineering* 70.1 (2014), pp. 211–218. ISSN: 13594311. DOI: 10.1016/j.applthermaleng.2014.04.049.

[33] Marc Hohmann, Joseph Warrington, and John Lygeros. “A two-stage polynomial approach to stochastic optimization of district heating networks”. In: *Sustainable Energy, Grids and Networks* 17 (2019), p. 100177. ISSN: 23524677. DOI: 10.1016/j.segan.2018.11.003.

[34] Romain S.C. Lambert, Sebastian Maier, Nilay Shah, and John W. Polak. “Optimal phasing of district heating network investments using multi-stage stochastic programming”. In: *International Journal of Sustainable Energy Planning and Management* 9 (2016).

[35] Wenjie Gang, Godfried Augenbroe, Shengwei Wang, Cheng Fan, and Fu Xiao. “An uncertainty-based design optimization method for district cooling systems”. In: *Energy* 102 (2016), pp. 516–527. ISSN: 03605442. DOI: 10.1016/j.energy.2016.02.107.

[36] Dario Buoro, Piero Pinamonti, and Mauro Reini. “Optimization of a Distributed Cogeneration System with solar district heating”. In: *Applied Energy* 124 (2014), pp. 298–308. ISSN: 03062619. DOI: 10.1016/j.apenergy.2014.02.062.

[37] Samira Fazlollahi, Gwenaelle Becker, and François Maréchal. “Multi-objectives, multi-period optimization of district energy systems: III. Distribution networks”. In: *Computers & Chemical Engineering* 66 (2014), pp. 82–97. ISSN: 00981354. DOI: 10.1016/j.compchemeng.2014.02.018.

[38] Samira Fazlollahi, Gwenaelle Becker, Araz Ashouri, and François Maréchal. “Multi-objective, multi-period optimization of district energy systems: IV – A case study”. In: *Energy* 84 (2015), pp. 365–381. ISSN: 03605442. DOI: 10.1016/j.energy.2015.03.003.

[39] R. Bavière and M. Vallée. “Optimal Temperature Control of Large Scale District Heating Networks”. In: *Energy Procedia* 149 (2018), pp. 69–78. ISSN: 18766102. DOI: 10.1016/j.egypro.2018.08.170.

[40] Magnus Dahl, Adam Brun, and Gorm B. Andresen. “Using ensemble weather predictions in district heating operation and load forecasting”. In: *Applied Energy* 193 (2017), pp. 455–465. ISSN: 03062619. DOI: 10.1016/j.apenergy.2017.02.066.

[41] Tingting Fang and Risto Lahdelma. “Evaluation of a multiple linear regression model and SARIMA model in forecasting heat demand for district heating system”. In: *Applied Energy* 179 (2016), pp. 544–552. ISSN: 03062619. DOI: 10.1016/j.apenergy.2016.06.133.

[42] Christian Johansson, Markus Bergkvist, Davy Geysen, Oscar De Somer, Niklas Lavesson, and Dirk Vanhoudt. “Operational Demand Forecasting In District Heating Systems Using Ensembles Of Online Machine Learning Algorithms”. In: *Energy Procedia* 116 (2017), pp. 208–216. ISSN: 18766102. DOI: 10.1016/j.egypro.2017.05.068.

[43] Henrik Lund, Sven Werner, Robin Wiltshire, Svend Svendsen, Jan Eric Thorsen, Frede Hvelplund, and Brian Vad Mathiesen. “4th Generation District Heating (4GDH)”. In: *Energy* 68 (2014), pp. 1–11. ISSN: 03605442. DOI: 10.1016/j.energy.2014.02.089.

[44] T. Fruergaard, T. H. Christensen, and T. Astrup. “Energy recovery from waste incineration: Assessing the importance of district heating networks”. In: *Waste Management* 30.7 (2010), pp. 1264–1272. DOI: 10.1016/j.wasman.2010.03.026.

[45] Sven Werner. “District heating and cooling in Sweden”. In: *Energy* 126 (2017), pp. 419–429. ISSN: 03605442. DOI: 10.1016/j.energy.2017.03.052.

[46] Henrik Lund et al. “The status of 4th generation district heating: Research and results”. In: *Energy* 164 (2018), pp. 147–159. ISSN: 03605442. DOI: 10.1016/j.energy.2018.08.206.

[47] Dietrich Schmidt, Anna Kallert, Markus Blesl, Svend Svendsen, Hongwei Li, Natasa Nord, and Kari Sipilä. “Low Temperature District Heating for Future Energy Systems”. In: *Energy Procedia* 116 (2017), pp. 26–38. ISSN: 18766102. DOI: 10.1016/j.egypro.2017.05.052.

[48] Helge Averfalk and Sven Werner. “Economic benefits of fourth generation district heating”. In: *Energy* 193 (2020), p. 116727. ISSN: 03605442. DOI: 10.1016/j.energy.2019.116727.

[49] Dietrich Schmidt, Anna Kallert, Markus Blesl, Svend Svendsen, Haoran Li, and Natasa Nord. *Future Low Temperature District Heating Design Guidebook: Final Report of IEA DHC Annex TS1: Low Temperature District Heating for Future Energy Systems*. Ed. by AGFW-Project Company. Frankfurt am Main, Germany, 2017.

[50] Helge Averfalk and Sven Werner. “Essential improvements in future district heating systems”. In: *Energy Procedia* 116 (2017), pp. 217–225. ISSN: 18766102. DOI: 10.1016/j.egypro.2017.05.069.

[51] Helge Averfalk and Sven Werner. “Novel low temperature heat distribution technology”. In: *Energy* 145 (2018), pp. 526–539. ISSN: 03605442. DOI: 10.1016/j.energy.2017.12.157.

[52] A. Dalla Rosa, H. Li, and S. Svendsen. “Method for optimal design of pipes for low-energy district heating, with focus on heat losses”. In: *Energy* 36.5 (2011), pp. 2407–2418. ISSN: 03605442. DOI: 10.1016/j.energy.2011.01.024.

[53] Dietrich Schmidt. “Low Temperature District Heating for Future Energy Systems”. In: *Energy Procedia* 149 (2018), pp. 595–604. ISSN: 18766102. DOI: 10.1016/j.egypro.2018.08.224.

[54] Lisa Brange, Jessica Englund, Kerstin Sernhed, Marcus Thern, and Patrick Lauenburg. “Bottlenecks in district heating systems and how to address them”. In: *Energy Procedia* 116 (2017), pp. 249–259. ISSN: 18766102. DOI: 10.1016/j.egypro.2017.05.072.

[55] Lisa Brange, Patrick Lauenburg, Kerstin Sernhed, and Marcus Thern. “Bottlenecks in district heating networks and how to eliminate them – A simulation and cost study”. In: *Energy* 137 (2017), pp. 607–616. ISSN: 03605442. DOI: 10.1016/j.energy.2017.04.097.

[56] Lisa Brange, Kerstin Sernhed, and Marcus Thern. “Decision-making process for addressing bottleneck problems in district heating networks”. In: *International Journal of Sustainable Energy Planning and Management* (2019), pp. 37–50.

[57] Isabelle Best, Janybek Orozaliev, and Klaus Vajen. “Impact of Different Design Guidelines on the Total Distribution Costs of 4th Generation District Heating Networks”. In: *Energy Procedia* 149 (2018), pp. 151–160. ISSN: 18766102. DOI: 10.1016/j.egypro.2018.08.179.

[58] Linn Laurberg Jensen, Daniel Trier, Marcus Brennenstuhl, Marco Cozzini, and Belen Gomez-Uribarri Serrano. *Flexynets D3.1 - Analysis of Network Layouts in Selected Urban Contexts*. Ed. by PlanEnergi. 2016. URL: https://ec.europa.eu/research/participants/documents/downloadPublic?documentIds=080166e5b33cb050&appId=PPGMS (visited on Mar. 21, 2020).

[59] M. Jangsten, J. Kensby, J.-O. Dalenbäck, and A. Trüschel. “Survey of radiator temperatures in buildings supplied by district heating”. In: *Energy* 137 (2017), pp. 292–301. ISSN: 03605442. DOI: 10.1016/j.energy.2017.07.017.

[60] Anna Volkova, Igor Krupenski, Henrik Pieper, Aleksandr Ledvanov, Eduard Latõšov, and Andres Siirde. “Small low-temperature district heating network development prospects”. In: *Energy* 178 (2019), pp. 714–722. ISSN: 03605442. DOI: 10.1016/j.energy.2019.04.083.

[61] Dorte Skaarup Østergaard and Svend Svendsen. “Replacing critical radiators to increase the potential to use low-temperature district heating – A case study of 4 Danish single-family houses from the 1930s”. In: *Energy* 110 (2016), pp. 75–84. ISSN: 03605442. DOI: 10.1016/j.energy.2016.03.140.

[62] Xiaochen Yang, Hongwei Li, and Svend Svendsen. “Evaluations of different domestic hot water preparing methods with ultra-low-temperature district heating”. In: *Energy* 109 (2016), pp. 248–259. ISSN: 03605442. DOI: 10.1016/j.energy.2016.04.109.

[63] DVGW Deutsche Vereinigung des Gas- und Wasserfaches e.V. *Trinkwassererwärmungs- und Trinkwasserleitungsanlagen; Technische Maßnahmen zur Verminderung des Legionellenwachstums; Planung, Errichtung, Betrieb und Sanierung von Trinkwasser-Installation*. Bonn, 2004.

[64] Xiaochen Yang, Hongwei Li, and Svend Svendsen. “Alternative solutions for inhibiting Legionella in domestic hot water systems based on low-temperature district heating”. In: *Building Services Engineering Research and Technology* 37.4 (2016), pp. 468–478. ISSN: 0143-6244. DOI: 10.1177/0143624415613945.

[65] Xiaochen Yang, Hongwei Li, and Svend Svendsen. “Energy, economy and exergy evaluations of the solutions for supplying domestic hot water from low-temperature district heating in Denmark”. In: *Energy Conversion and Management* 122 (2016), pp. 142–152. ISSN: 01968904. DOI: 10.1016/j.enconman.2016.05.057.

[66] Nicolas Perez-Mora, Federico Bava, Martin Andersen, Chris Bales, Gunnar Lennermo, Christian Nielsen, Simon Furbo, and Víctor Martínez-Moll. “Solar district heating and cooling: A review”. In: *International Journal of Energy Research* 42.4 (2018), pp. 1419–1441. DOI: 10.1002/er.3888.

[67] Thorsten Urbaneck, Thomas Oppelt, Bernd Platzer, Holger Frey, Ulf Uhlig, Thomas Göschel, Dieter Zimmermann, and Dirk Rabe. “Solar District Heating in East Germany – Transformation in a Cogeneration Dominated City”. In: *Energy Procedia* 70 (2015), pp. 587–594. ISSN: 18766102. DOI: 10.1016/j.egypro.2015.02.164.

[68] Ciarán Flynn and Kai Sirén. “Influence of location and design on the performance of a solar district heating system equipped with borehole seasonal storage”. In: *Renewable Energy* 81 (2015), pp. 377–388. ISSN: 09601481. DOI: 10.1016/j.renene.2015.03.036.

[69] E. Carpaneto, P. Lazzeroni, and M. Repetto. “Optimal integration of solar energy in a district heating network”. In: *Renewable Energy* 75 (2015), pp. 714–721. ISSN: 09601481. DOI: 10.1016/j.renene.2014.10.055.

[70] Humberto Jose Quintana and Michael Kummert. “Optimized control strategies for solar district heating systems”. In: *Journal of Building Performance Simulation* 8.2 (2015), pp. 79–96. ISSN: 1940-1493. DOI: 10.1080/19401493.2013.876448.

[71] Leyla Ozgener, Arif Hepbasli, and Ibrahim Dincer. “Effect of reference state on the performance of energy and exergy evaluation of geothermal district heating systems: Balcova example”. In: *Building and Environment* 41.6 (2006), pp. 699–709. ISSN: 03601323. DOI: 10.1016/j.buildenv.2005.03.007.

[72] Philippe Dumas, Luca Angelino, Alexandra Latham, and Valentina Pinzuti. *Developing geothermal district heating in Europe*. Brüssel, 2014. URL: http://geodh.eu/wp-content/uploads/2012/07/GeoDH-Report-2014_web.pdf (visited on Apr. 24, 2020).

[73] Poul Alberg Østergaard and Henrik Lund. “A renewable energy system in Frederikshavn using low-temperature geothermal energy for district heating”. In: *Applied Energy* 88.2 (2011), pp. 479–487. ISSN: 03062619. DOI: 10.1016/j.apenergy.2010.03.018.

[74] Helge Averfalk, Paul Ingvarsson, Urban Persson, Mei Gong, and Sven Werner. “Large heat pumps in Swedish district heating systems”. In: *Renewable and Sustainable Energy Reviews* 79 (2017), pp. 1275–1284. ISSN: 13640321. DOI: 10.1016/j.rser.2017.05.135.

[75] Bjarne Bach, Jesper Werling, Torben Ommen, Marie Münster, Juan M. Morales, and Brian Elmegaard. “Integration of large-scale heat pumps in the district heating systems of Greater Copenhagen”. In: *Energy* 107 (2016), pp. 321–334. ISSN: 03605442. DOI: 10.1016/j.energy.2016.04.029.

[76] Brian Vad Mathiesen, Henrik Lund, and David Connolly. “Limiting biomass consumption for heating in 100% renewable energy systems”. In: *Energy* 48.1 (2012), pp. 160–168. ISSN: 03605442. DOI: 10.1016/j.energy.2012.07.063.

[77] Ralph Hintemann. *Boom führt zu deutlich steigendem Energiebedarf der Rechenzentren in Deutschland im Jahr 2017*. Ed. by Borderstep Institut für Innovation und Nachhaltigkeit gGmbH. Berlin, 2018. URL: https://www.borderstep.de/wp-content/uploads/2019/01/Borderstep-Rechenzentren-2017-final-Stand-Dez_2018.pdf (visited on June 4, 2020).

[78] Severin Zimmermann, Ingmar Meijer, Manish K. Tiwari, Stephan Paredes, Bruno Michel, and Dimos Poulikakos. “Aquasar: A hot water cooled data center with direct energy reuse”. In: *Energy* 43.1 (2012), pp. 237–245. ISSN: 03605442. DOI: 10.1016/j.energy.2012.04.037.

[79] Johannes Oltmanns, David Sauerwein, Frank Dammel, Peter Stephan, and Christoph Kuhn. “Potential for waste heat utilization of hot-water-cooled data centers: A case study”. In: *Energy Science & Engineering* 8.5 (2020), pp. 1793–1810. ISSN: 20500505. DOI: 10.1002/ese3.633.

[80] Mikko Wahlroos, Matti Pärssinen, Samuli Rinne, Sanna Syri, and Jukka Manner. “Future views on waste heat utilization – Case of data centers in Northern Europe”. In: *Renewable and Sustainable Energy Reviews* 82 (2018), pp. 1749–1764. ISSN: 13640321. DOI: 10.1016/j.rser.2017.10.058.

[81] Peter Sivengard. *Profitable Heat Recovery with Open District Heating*. Ed. by Stockholm Exergy. Stockholm, 2018. URL: https://heatpumpingtechnologies.org/annex47/wp-content/uploads/sites/54/2018/12/annex-47oppen-fjarrvarme.pdf (visited on June 4, 2020).

[82] Mikko Wahlroos, Matti Pärssinen, Jukka Manner, and Sanna Syri. “Utilizing data center waste heat in district heating – Impacts on energy efficiency and prospects for low-temperature district heating networks”. In: *Energy* 140 (2017), pp. 1228–1238. ISSN: 03605442. DOI: 10.1016/j.energy.2017.08.078.

[83] Max Smolaks. *Telia opens Finland’s largest shared data center*. Ed. by Data Center DynamicsS. 2018. URL: https://www.datacenterdynamics.com/news/telia-opens-finlands-largest-shared-data-center/ (visited on June 4, 2020).

[84] Metropolitan.fi. *Data center heats homes: Yandex sells server waste energy to district heating*. 2018. URL: http://metropolitan.fi/entry/data-center-heating-homes-yandex-sells-waste-energy-to-district-heating (visited on June 4, 2020).

[85] Data Center Dynamics. *Yandex data center heats Finnish city*. 2016. URL: https://www.datacenter%20dynamics.com/news/yandex-data-center-heats-finnish-city/ (visited on June 4, 2020).

[86] Veolia Industrie Deutschland GmbH. *Waste Energy from Data Centers in Braunschweig Germany*. Braunschweig, 2018. URL: https://www.veolutions.veolia.de/en/waste-energy-data-centers-braunschweig-germany (visited on June 4, 2020).

[87] Franziska Leitermann. *Cloud&Heat Data Center in the Eurotheum: Our Cloud is live!* Ed. by Cloud&Heat. 2018. URL: https://www.cloudandheat.com/blog/cloudheat-data-center-the-eurotheum-cloud-live/ (visited on Feb. 4, 2019).

[88] Robert Pawlik. *Abwärmenutzung in Rechenzentren*. Ed. by Cloud&Heat. 2018. URL: https://www.germandatacenters.com/fileadmin/images/events/kickstart/vortraege/05-Robert-Pawlik-Cloud-and-Heat.pdf (visited on June 4, 2020).

[89] Jens Struckmeier. *Serverheizung in kommunalen Einrichtungen*. 2014. URL: https://crm.saena.de/sites/default/files/civicrm/persist/contribute/files/7JKS_Dr.Struckmeier_Serverheizung_kommunal.pdf (visited on June 4, 2020).

[90] Marco Pellegrini, Augusto Bianchini, Alessandro Guzzini, and Cesare Saccani. “Classification through analytic hierarchy process of the barriers in the revamping of traditional district heating networks into low temperature district heating: an Italian case study”. In: *International Journal of Sustainable Energy Planning and Management* 20 (2019). DOI: 10.5278/ijsepm.2019.20.5.

[91] Anna Volkova, Vladislav Mašatin, and Andres Siirde. “Methodology for evaluating the transition process dynamics towards 4th generation district heating networks”. In: *Energy* 150 (2018), pp. 253–261. ISSN: 03605442. DOI: 10.1016/j.energy.2018.02.123.

[92] Henrik Gadd and Sven Werner. “Achieving low return temperatures from district heating substations”. In: *Applied Energy* 136 (2014), pp. 59–67. ISSN: 03062619. DOI: 10.1016/j.apenergy.2014.09.022.

[93] Henrik Gadd and Sven Werner. “Fault detection in district heating substations”. In: *Applied Energy* 157 (2015), pp. 51–59. ISSN: 03062619. DOI: 10.1016/j.apenergy.2015.07.061.

[94] Sara Månsson, Per-Olof Johansson Kallioniemi, Marcus Thern, Tijs van Oevelen, and Kerstin Sernhed. “Faults in district heating customer installations and ways to approach them: Experiences from Swedish utilities”. In: *Energy* (2019). ISSN: 03605442. DOI: 10.1016/j.energy.2019.04.220.

[95] Puning Xue, Zhigang Zhou, Xiumu Fang, Xin Chen, Lin Liu, Yaowen Liu, and Jing Liu. “Fault detection and operation optimization in district heating substations based on data mining techniques”. In: *Applied Energy* 205 (2017), pp. 926–940. ISSN: 03062619. DOI: 10.1016/j.apenergy.2017.08.035.

[96] Sara Månsson, Per-Olof Johansson Kallioniemi, Kerstin Sernhed, and Marcus Thern. “A machine learning approach to fault detection in district heating substations”. In: *Energy Procedia* 149 (2018), pp. 226–235. ISSN: 18766102. DOI: 10.1016/j.egypro.2018.08.187.

[97] Kristina Lygnerud. “Challenges for business change in district heating”. In: *Energy, Sustainability and Society* 8.1 (2018), p. 10. ISSN: 2192-0567. DOI: 10.1186/s13705-018-0161-4.

[98] Kristina Lygnerud. “Business Model Changes in District Heating: The Impact of the Technology Shift from the Third to the Fourth Generation”. In: *Energies* 12.9 (2019), p. 1778. ISSN: 1996-1073. DOI: 10.3390/en12091778.

[99] Kristina Lygnerud, Edward Wheatcroft, and Henry Wynn. “Contracts, Business Models and Barriers to Investing in Low Temperature District Heating Projects”. In: *Applied Sciences* 9.15 (2019), p. 3142. ISSN: 2076-3417. DOI: 10.3390/app9153142.

[100] Heike Erhorn-Kluttig, Sarah Doster, and Hans Erhorn, eds. *Der energieeffiziente Universitätscampus: Pilotprojekte der Forschungsinitiative EnEff:Stadt*. EnEff. Stuttgart: Fraunhofer IRB Verlag, 2016. ISBN: 9783816796312.

[101] Silvia Coccolo, Jérôme Kaempf, and Jean-Louis Scartezzini. “The EPFL Campus in Lausanne: New Energy Strategies for 2050”. In: *Energy Procedia* 78 (2015), pp. 3174–3179. ISSN: 18766102. DOI: 10.1016/j.egypro.2015.11.776.

[102] Giorgio Pagliarini and Sara Rainieri. “Modeling of a thermal energy storage system coupled with combined heat and power generation for the heating requirements of a University Campus”. In: *Applied Thermal Engineering* 30.10 (2010), pp. 1255–1261. ISSN: 13594311. DOI: 10.1016/j.applthermaleng.2010.02.008.

[103] Johannes Oltmanns, Frank Dammel, and Peter Stephan. “Modeling the heat supply system of TU Darmstadt Campus Lichtwiese”. In: *Proceedings of ECOS 2017 - The International Conference on efficiency, cost, optimization, simulation and environmental impact of energy systems*.

[104] Astrid Ludwig, Uta Neubauer, Boris Hänßler, Hildegard Kaulen, Christian Meier, and Jutta Witte. *Technische Universität Darmstadt Fortschrittsbericht 2018*. Ed. by Technische Universität Darmstadt. Darmstadt, 2019. URL: https://www.tu-darmstadt.de/media/daa_responsives_design/01_die_universitaet_medien/aktuelles_6/publikationen_km/fortschrittsbericht/fortschrittsbericht_2018/Fortschritt_2018_deutsch_doppel.pdf (visited on Mar. 23, 2020).

[105] isoplus Fernwärmetechnik Vertriebsgesellschaft mbH. *Isoplus Planungshandbuch*. 2011. URL: https://www.isoplus.de/download/planungshandbuch.html (visited on July 8, 2020).

[106] Henrik Gadd and Sven Werner. “Heat load patterns in district heating substations”. In: *Applied Energy* 108 (2013), pp. 176–183. ISSN: 03062619. DOI: 10.1016/j.apenergy.2013.02.062.

[107] Dirk Vanhoudt. *TEMPO Project - Digitalisation in district heating networks*. 2019. URL: http://europeanenergyinnovation.eu/Latest-Research/Autumn-2019/TEMPO-Project-Digitalisation-in-district-heating-networks (visited on July 8, 2020).

[108] VDI-Gesellschaft Verfahrenstechnik und Chemieingenieurwesen. *VDI Heat Atlas: With 539 tables*. 2. ed. Springer reference. Heidelberg: Springer, 2010. ISBN: 9783540778769. URL: http://dx.doi.org/10.1007/978-3-540-77877-6.

[109] Badger Meter Europe GmbH. *Dynasonics TFX-5000: Transit Time Flow Meters*. 2020. URL: https://www.badgermeter.de/en/products-solutions/flow-measurement-technology/2626-dynasonicsr-tfx-5000/ (visited on May 26, 2020).

[110] Badger Meter Europe GmbH. *Dynasonics DXN: Portable transit-time flow and energy meter*. 2020. URL: https://www.badgermeter.de/en/products-solutions/flow-measurement-technology/102-dynasonicsr-dxn/ (visited on May 26, 2020).

[111] Karl Walter Bonfig. *Technische Durchflussmessung: Unter besonderer Berücksichtigung neuartiger Durchflussmeßverfahren*. 3. Aufl. Essen: Vulkan-Verl., 2002. ISBN: 380272190X.

[112] Deutsches Institut für Normung e.V. *Industrielle Platin-Widerstandsthermometer und Platin-Temperatursensoren (IEC 60751:2008)*. Berlin, 2009.

[113] Deutsches Institut für Normung e.V. *Thermische Energiemessgeräte – Teil 1: Allgemeine Anforderungen*. Berlin, 2019.

[114] Deutsches Institut für Normung e.V. *Energetische Bewertung von Gebäuden*. Berlin, 2011.

[115] Peter Stephan, Franz Mayinger, Karlheinz Schaber, and Karl Stephan. *Thermodynamik: Grundlagen und technische Anwendungen Band 1: Einstoffsysteme*. 17. Auflage. Springer-Lehrbuch. Berlin, Heidelberg: Springer-Verlag Berlin Heidelberg, 2007. ISBN: 9783540708131. DOI: 10.1007/978-3-540-70814-8.

[116] Herena Torío and Dietrich Schmidt. *Low Exergy Systems for High-Performance Buildings and Communities: Annex 49 Summary report*. Ed. by Fraunhofer IBP. Stuttgart, 2011. URL: https://www.annex49.info/download/summary_report.pdf (visited on Nov. 14, 2018).

[117] Paul Michael Falk. "Evaluation of community heating systems based on exergy analysis". Dissertation. Darmstadt: TU Darmstadt, 2018. URL: https://tuprints.ulb.tu-darmstadt.de/7372/ (visited on June 4, 2020).

[118] Jan Szargut, David R. Morris, and Frank R. Steward. *Exergy analysis of thermal, chemical and metallurgical processes*. New York: Hemisphere Publ. Corp, 1988. ISBN: 3540188649.

[119] Tymofii Tereshchenko and Natasa Nord. "Uncertainty of the allocation factors of heat and electricity production of combined cycle power plant". In: *Applied Thermal Engineering* 76 (2015), pp. 410–422. ISSN: 13594311. DOI: 10.1016/j.applthermaleng.2014.11.019.

[120] Marc A. Rosen. "Allocating carbon dioxide emissions from cogeneration systems: Descriptions of selected output-based methods". In: *Journal of Cleaner Production* 16.2 (2008), pp. 171–177. ISSN: 09596526. DOI: 10.1016/j.jclepro.2006.08.025.

[121] Wolfgang Mauch, Roger Corradini, Karin Wiesemeyer, and Marco Schwentzek. "Allokationsmethoden für spezifische CO2-Emissionen von Strom und Wärme aus KWK-Anlagen". In: *Energiewirtschaftliche Tagesfragen* 9 (2010).

[122] Luis Carr. *The Replacement Mix: Introduction of a Method for the Assessment of District Heat from CHP in the European Union Regarding Primary Eenrgy*. Ed. by FfE Forschungsstelle für Energiewirtschaft e.V. München, 2012.

[123] AGFW. *Arbeitsblatt AGFW FW 309 Teil 1*. Frankfurt am Main, Germany, 2014.

[124] Deutsches Institut für Normung e.V. *Energetische Bewertung von Gebäuden - Verfahren zur Berechnung der Energieanforderungen und Nutzungsgrade der Anlagen - Teil 4-5: Fernwärme und Fernkälte*. Berlin, 2017.

[125] Verein Deutscher Ingenieure. *Energiesysteme Kraft-Wärme-Kopplung Allokation und Bewertung*. Berlin, 2008.

[126] AGFW. *Arbeitsblatt AGFW FW 309 Teil 6*. Frankfurt am Main, Germany, 2016.

[127] Bundesamt für Wirtschaft und Ausfuhrkontrolle. *Merkblatt zu den CO2-Faktoren: Energieeffizienz in der Wirtschaft - Zuschuss und Kredit*. Ed. by Bundesamt für Wirtschaft und Ausfuhrkontrolle. Eschborn, 2019. URL: https://www.bafa.de/SharedDocs/Downloads/DE/Energie/eew_merkblatt_co2.pdf?__blob=publicationFile&v=2.

[128] Umweltbundesamt. *Entwicklung der spezifischen Kohlendioxid-Emissionen des deutschen Strommix in den Jahren 1990 - 2018*. Ed. by Umweltbundesamt. Dessau, 2019. URL: https://www.umweltbundesamt.de/sites/default/files/medien/1410/publikationen/2019-04-10_cc_10-2019_strommix_2019.pdf (visited on June 4, 2020).

[129] Marc Großklos. *Kumulierter Energieaufwand und CO2-Emissionsfaktoren verschiedener Energieträger und -versorgungen*. Ed. by Institut für Wohnen und Umwelt. Darmstadt, 2020. URL: http://www.iwu.de/fileadmin/user_upload/dateien/energie/werkzeuge/kea.pdf (visited on Mar. 12, 2020).

[130] Verein Deutscher Ingenieure. *Economic efficiency of building installations*. Berlin, 2012.

[131] European Central Bank. *The definition of price stability*. 2019. URL: https://www.ecb.europa.eu/mopo/strategy/pricestab/html/index.en.html (visited on June 4, 2020).

[132] J. Rogelj et al. *Mitigation Pathways Compatible with 1.5°C in the Context of Sustainable Development: : Global Warming of 1.5°C. An IPCC Special Report on the impacts of global warming of 1.5°C above pre-industrial levels and related global greenhouse gas emission pathways, in the context of strengthening the global response to the threat of climate change, sustainable development, and efforts to eradicate pove*. 2018. URL: https://www.ipcc.ch/site/assets/uploads/sites/2/2019/02/SR15_Chapter2_Low_Res.pdf (visited on June 4, 2020).

[133] Statistisches Bundesamt. *Daten zur Energiepreisentwicklung: Lange Reihen von Januar 2005 bis Oktober 2019*. Ed. by Statistisches Bundesamt. Wiesbaden, 2019. URL: https://www.destatis.de/DE/Themen/Wirtschaft/Preise/Publikationen/Energiepreise/energiepreisentwicklung-pdf-5619001.pdf?__blob=publicationFile (visited on June 5, 2020).

[134] e-netz Südhessen AG. *Netzentgelte Gas der e-netz Südhessen AG*. Darmstadt, 2019. URL: https://www.e-netz-suedhessen.de/fileadmin/user_upload/download/preisblatt_gas.pdf (visited on Mar. 12, 2020).

[135] e-netz Südhessen. *Netzentgelte Strom der e-netz Südhessen*. 2019. URL: https://www.e-netz-suedhessen.de/fileadmin/user_upload/download/preisblatt_strom.pdf (visited on Mar. 12, 2020).

[136] Wolfgang Suttor. *Blockheizkraftwerke: Ein Leitfaden für den Anwender*. 8., überarb. Aufl. BINE-Fachbuch. Stuttgart: Fraunhofer IRB-Verl., 2014. ISBN: 9783816793038.

[137] Harry Wirth. *Aktuelle Fakten zur Photovoltaik in Deutschland*. Freiburg, 2019. URL: https://www.ise.fraunhofer.de/content/dam/ise/de/documents/publications/studies/aktuelle-fakten-zur-photovoltaik-in-deutschland.pdf (visited on Nov. 21, 2019).

[138] Thorsten Urbaneck, Ulf Uhlig, Bernd Platzer, Ulrich Schirmer, Thomas Göschel, and Dieter Zimmermann. *Machbarkeitsuntersuchung zur Stärkung der Kraft-Wärme-Kopplung durch den Einsatz von Kältespeichern in großen Versorgungssystemen*. Ed. by Technische Universität Chemnitz. Chemnitz, 2006. URL: https://monarch.qucosa.de/api/qucosa%3A18477/attachment/ATT-0/ (visited on Mar. 12, 2020).

[139] The MathWorks. *MATLAB*. Natick, MA, 2018. URL: https://de.mathworks.com/?s_tid=gn_logo (visited on May 22, 2020).

[140] Solar-Institute Juelich of the FH Aachen. *CARNOT Toolbox Version 6.3*. 2018.

[141] Deutscher Wetterdienst. *Ortsgenaue Testreferenzjahre von Deutschland für mittlere, extreme und zukünftige Witterungsverhältnisse*. Ed. by Bundesamt für Bauwesen und Raumordnung. Offenbach, 2017. URL: http://www.bbsr.bund.de/BBSR/DE/FP/ZB/Auftragsforschung/5EnergieKlimaBauen/2013/testreferenzjahre/try-handbuch.pdf (visited on June 5, 2020).

[142] R Core Team. *R: A language and environment for statistical computing*. Wien, 2013. URL: http://www.R-project.org/ (visited on June 10, 2020).

[143] Sven E. Werner. *The heat load in district heating systems*. Vol. 496. Doktorsavhandlingar vid Chalmers Tekniska Högskola. N.S. Göteborg: Department of Energy Conversion Univ, 1984. ISBN: 9170321450.

[144] Josef Puhani. *Statistik: Einführung mit praktischen Beispielen*. 13th ed. 2020. 2020. ISBN: 978-3-658-28955-3. URL: https://doi.org/10.1007/978-3-658-28955-3.

[145] DWD Climate Data Center. *Historical hourly station observations of 2m air temperature and humidity for Germany, Version v006*. Ed. by Deutscher Wetterdienst. Offenbach, 2019. URL: ftp://ftp-cdc.dwd.de/climate_environment/CDC/observations_germany/climate/hourly/air_temperature/ (visited on Aug. 5, 2020).

[146] Nataliia Fedorova, Pegah Aziziyanesfahani, Vojislav Jovicic, Ana Zbogar-Rasic, Muhammad Jehanzaib Khan, and Antonio Delgado. "Investigation of the Concepts to Increase the Dew Point Temperature for Thermal Energy Recovery from Flue Gas, Using Aspen®". In: *Energies* 12.9 (2019), p. 1585. ISSN: 1996-1073. DOI: 10.3390/en12091585.

[147] Meryem Terhan and Kemal Comakli. "Design and economic analysis of a flue gas condenser to recover latent heat from exhaust flue gas". In: *Applied Thermal Engineering* 100 (2016), pp. 1007–1015. ISSN: 13594311. DOI: 10.1016/j.applthermaleng.2015.12.122.

[148] Deutsches Institut für Normung e.V. *Energetische Bewertung heiz- und raumlufttechnischer Anlagen*. Berlin, 2003.

[149] Johnson Controls-Hitachi Air Conditioning Technology. *York Absorption Chiller YHAU-CH400EXET*. Hong Kong, 2017.

[150] Kun Sang Lee. *Underground thermal energy storage*. Green energy and technology. London: Springer, 2013. ISBN: 9781447142737.

[151] Werner Dub. *Hybridnetze und ihre Relevanz für einen Energieversorger*. Ed. by MVV Energie. Mannheim, 2013. URL: https://www.wik.org/fileadmin/Konferenzbeitraege/netconomica/2013/Dub_MVV_Energie.pdf (visited on June 5, 2020).

[152] AGFW. *Arbeitsblatt AGFW FW 313*. Frankfurt am Main, Germany, 2015.

[153] Bundesministerium für Wirtschaft und Energie and Bundesministerium für Umwelt, Naturschutz, Bau und Reaktorsicherheit. *Bekanntmachung der Regeln für Energieverbrauchswerte und der Vergleichswerte im Nichtwohngebäudebestand*. 2015. URL: http://www.coaching-kommunaler-klimaschutz.de/fileadmin/inhalte/Dokumente/StarterSet/BMVBS_Energieverbrauchskennwerte_und_der_Vergleichswerte_im_Nichtwohngeb%C3%A4udebestand.pdf (visited on June 5, 2020).

[154] Jonathan G. Koomey. *Growth in Data Center Electricity Use 2005 to 2010*. Ed. by Analytics Press. Stanford, 2011. URL: https://www.missioncriticalmagazine.com/ext/resources/MC/Home/Files/PDFs/Koomey_Data_Center.pdf (visited on June 5, 2020).

[155] Fred Pierce. *Energy Hogs: Can World's Huge Data Centers Be Made More Efficient?* 2018. URL: https://e360.yale.edu/features/energy-hogs-can-huge-data-centers-be-made-more-efficient (visited on June 5, 2020).

[156] James Keirstead, Mark Jennings, and Aruna Sivakumar. "A review of urban energy system models: Approaches, challenges and opportunities". In: *Renewable and Sustainable Energy Reviews* 16.6 (2012), pp. 3847–3866. ISSN: 13640321. DOI: 10.1016/j.rser.2012.02.047.

[157] Eduard Oró, Victor Depoorter, Albert Garcia, and Jaume Salom. "Energy efficiency and renewable energy integration in data centres. Strategies and modelling review". In: *Renewable and Sustainable Energy Reviews* 42 (2015), pp. 429–445. ISSN: 13640321. DOI: 10.1016/j.rser.2014.10.035.

[158] Ali Habibi Khalaj and Saman K. Halgamuge. "A Review on efficient thermal management of air- and liquid-cooled data centers: From chip to the cooling system". In: *Applied Energy* 205 (2017), pp. 1165–1188. ISSN: 03062619. DOI: 10.1016/j.apenergy.2017.08.037.

[159] American Society of Heating, Refrigerating and Air-Conditioning Engineers. *Datacom equipment power trends and cooling applications*. 2. ed. Vol. 2. ASHRAE datacom series. Atlanta, GA: ASHRAE, 2012. ISBN: 9781936504282.

[160] H. F. Hamann, J. A. Lacey, M. O'Boyle, R. R. Schmidt, and M. Iyengar. "Rapid Three-Dimensional Thermal Characterization of Large-Scale Computing Facilities". In: *IEEE Transactions on Components and Packaging Technologies* 31.2 (2008), pp. 444–448. ISSN: 1521-3331. DOI: 10.1109/TCAPT.2008.923629.

[161] Khosrow Ebrahimi, Gerard F. Jones, and Amy S. Fleischer. "A review of data center cooling technology, operating conditions and the corresponding low-grade waste heat recovery opportunities". In: *Renewable and Sustainable Energy Reviews* 31 (2014), pp. 622–638. ISSN: 13640321. DOI: 10.1016/j.rser.2013.12.007.

[162] American Society of Heating, Refrigerating and Air-Conditioning Engineers. *Thermal Guidelines for Data Processing Environments – Expanded Data Center Classes and Usage Guidance: Whitepaper prepared by ASHRAE Technical Committee (TC) 9.9 Mission Critical Facilities, Technology Spaces, and Electronic Equipment*. 2011. URL: https://ecoinfo.cnrs.fr/IMG/pdf/ashrae_2011_thermal_guidelines_data_center.pdf (visited on June 5, 2020).

[163] Jackson Braz Marcinichen, John Richard Thome, and Bruno Michel. "Cooling of microprocessors with micro-evaporation: A novel two-phase cooling cycle". In: *International Journal of Refrigeration* 33.7 (2010), pp. 1264–1276. ISSN: 01407007. DOI: 10.1016/j.ijrefrig.2010.06.008.

[164] Emad Samadiani, Hrishikesh Amur, Bhavani Krishnan, Yogendra Joshi, and Karsten Schwan. "Coordinated Optimization of Cooling and IT Power in Data Centers". In: *Journal of Electronic Packaging* 132.3 (2010), p. 031006. ISSN: 10437398. DOI: 10.1115/1.4001858.

[165] Chandrakant Patel. "A vision of energy aware computing from chips to data centers". In: *The International Symposium on Micro-Mechanical Engineering, December 1-3, 2003*. URL: https://www.researchgate.net/publication/245136250_A_VISION_OF_ENERGY_AWARE_COMPUTING_FROM_CHIPS_TO_DATA_CENTERS (visited on June 5, 2020).

[166] Alfonso Capozzoli and Giulio Primiceri. "Cooling Systems in Data Centers: State of Art and Emerging Technologies". In: *Energy Procedia* 83 (2015), pp. 484–493. ISSN: 18766102. DOI: 10.1016/j.egypro.2015.12.168.

[167] G. F. Davies, G. G. Maidment, and R. M. Tozer. "Using data centres for combined heating and cooling: An investigation for London". In: *Applied Thermal Engineering* 94 (2016), pp. 296–304. ISSN: 13594311. DOI: 10.1016/j.applthermaleng.2015.09.111.

[168] Roger R. Schmidt, Kailash C. Karki, Kanchan M. Kelkar, Amir Radmehr, and Suhas V. Pantakar. "Measurements and predictions of the flow distribution through perforated tiles in raised-floor data centers". In: *Proceedings of IPACK'01 The Pacific Rim/ASME International Electronic Packaging Technical Conference and Exhibition July 8-13, 2001, Kauai, Hawaii, USA*. URL: http://www.plenaform.com/mm/files/plenaform_measurementspredictions.pdf (visited on June 5, 2020).

[169] Suhas V. Patankar. "Airflow and Cooling in a Data Center". In: *Journal of Heat Transfer* 132.7 (2010), p. 073001. ISSN: 00221481. DOI: 10.1115/1.4000703.

[170] Zhiguang He, Zhongyang He, Xing Zhang, and Zhen Li. "Study of hot air recirculation and thermal management in data centers by using temperature rise distribution". In: *Building Simulation* 9.5 (2016), pp. 541–550. ISSN: 1996-3599. DOI: 10.1007/s12273-016-0282-7.

[171] M. M. Ohadi, S. V. Dessiatoun, K. Choo, M. Pecht, and John V. Lawler. "A comparison analysis of air, liquid, and two-phase cooling of data centers". In: *28th Annual IEEE Semiconductor Thermal Measurement and Management Symposium (SEMI-THERM), 2012*. Ed. by Herman Chu. Piscataway, NJ: IEEE, 2012, pp. 58–63. ISBN: 978-1-4673-1111-3. DOI: 10.1109/STHERM.2012.6188826.

[172] R. R. Schmidt, E. E. Cruz, and M. Iyengar. "Challenges of data center thermal management". In: *IBM Journal of Research and Development* 49.4.5 (2005), pp. 709–723. ISSN: 0018-8646. DOI: 10.1147/rd.494.0709.

[173] Wen-Xiao Chu and Chi-Chuan Wang. "A review on airflow management in data centers". In: *Applied Energy* 240 (2019), pp. 84–119. ISSN: 03062619. DOI: 10.1016/j.apenergy.2019.02.041.

[174] Victor Depoorter, Eduard Oró, and Jaume Salom. "The location as an energy efficiency and renewable energy supply measure for data centres in Europe". In: *Applied Energy* 140 (2015), pp. 338–349. ISSN: 03062619. DOI: 10.1016/j.apenergy.2014.11.067.

[175] Siddharth Bhopte, Dereje Agonafer, Roger Schmidt, and Bahgat Sammakia. "Optimization of Data Center Room Layout to Minimize Rack Inlet Air Temperature". In: *Journal of Electronic Packaging* 128.4 (2006), p. 380. ISSN: 10437398. DOI: 10.1115/1.2356866.

[176] Dustin W. Demetriou and H. Ezzat Khalifa. "Thermally Aware, Energy-Based Load Placement in Open-Aisle, Air-Cooled Data Centers". In: *Journal of Electronic Packaging* 135.3 (2013), p. 030906. ISSN: 10437398. DOI: 10.1115/1.4024946.

[177] Neil Rasmussen. *Cooling Strategies for Ultra-High Density Racks and Blade Servers: White Paper 46*. Ed. by Schneider Electric. 2010. URL: https://www.insight.com/content/dam/insight/en_US/pdfs/apc/apc-cooling-strategies-for-ultra-high-density-racks-blade-servers.pdf (visited on June 5, 2020).

[178] Jayantha Siriwardana, Saman K. Halgamuge, Thomas Scherer, and Wolfgang Schott. "Minimizing the thermal impact of computing equipment upgrades in data centers". In: *Energy and Buildings* 50 (2012), pp. 81–92. ISSN: 03787788. DOI: 10.1016/j.enbuild.2012.03.026.

[179] Sang-Woo Ham and Jae-Weon Jeong. "Impact of aisle containment on energy performance of a data center when using an integrated water-side economizer". In: *Applied Thermal Engineering* 105 (2016), pp. 372–384. ISSN: 13594311. DOI: 10.1016/j.applthermaleng.2015.05.069.

[180] John Niemann, Kevin Brown, and Victor Avelar. *Impact of Hot and Cold Aisle Containment on Data Center Temperature and Efficiency*. Ed. by Schneider Electric. 2019. URL: https://download.schneider-electric.com/files?p_enDocType=White+Paper&p_File_Name=DBOY-7EDLE8_R5_EN.pdf&p_Doc_Ref=APC_DBOY-7EDLE8_EN (visited on Feb. 10, 2019).

[181] G. F. Davies, G. G. Maidment, and R. M. Tozer. “Opportunities for Combined Heating and Cooling Using Data Centres”. In: *CIBSE Technical Symposium, London, UK16-17 April 2015*. URL: https://www.researchgate.net/profile/Graeme_Maidment/publication/282849071_Opportunities_for_Combined_Heating_and_Cooling_Using_Data_Centres/links/561e464908aef097132b3949.pdf (visited on June 5, 2020).

[182] Eduard Oró, Victor Depoorter, Noah Pflugradt, and Jaume Salom. “Overview of direct air free cooling and thermal energy storage potential energy savings in data centres”. In: *Applied Thermal Engineering* 85 (2015), pp. 100–110. ISSN: 13594311. DOI: 10.1016/j.applthermaleng.2015.03.001.

[183] Jackson Braz Marcinichen, Jonathan Albert Olivier, and John Richard Thome. “On-chip two-phase cooling of datacenters: Cooling system and energy recovery evaluation”. In: *Applied Thermal Engineering* 41 (2012), pp. 36–51. ISSN: 13594311. DOI: 10.1016/j.applthermaleng.2011.12.008.

[184] Steve Greenberg, Evan Mills, Bill Tschudi, Peter Rumsey, and Bruce Myatt. *Best Practices for Data Centers: Lessons Learned from Benchmarking 22 Data Centers*. Ed. by ACEEE. Berkeley, CA, 2006. URL: https://datacenters.lbl.gov/sites/default/files/aceee-datacenters.pdf (visited on Mar. 24, 2020).

[185] Michael J. Ellsworth and Madhusudan K. Iyengar. “Energy Efficiency Analyses and Comparison of Air and Water Cooled High Performance Servers”. In: *Proceedings of the ASME 2009 InterPACK Conference*, pp. 907–914. DOI: 10.1115/InterPACK2009-89248.

[186] Yong Quiang Chi, Jonathan Summers, Peter Hopton, Keith Deakin, Alan Real, Nik Kapur, and Harvey Thompson. “Case study of a data centre using enclosed, immersed, direct liquid-cooled servers”. In: *2014 30th Annual Semiconductor Thermal Measurement & Management Symposium (SEMI-THERM)*. Piscataway, NJ: IEEE, 2014, pp. 164–173. ISBN: 978-1-4799-4374-6. DOI: 10.1109/SEMI-THERM.2014.6892234.

[187] Henry Coles and Steve Greenberg. *Data Center Economizer Cooling with Tower Water: Demonstration of a Dual Heat Exchanger Rack Cooling Device*. Ed. by California Energy Commission. Berkeley, CA, 2013. URL: https://www.energy.ca.gov/2015publications/CEC-500-2015-039/CEC-500-2015-039.pdf (visited on Feb. 15, 2019).

[188] Khosrow Ebrahimi, Gerard F. Jones, and Amy S. Fleischer. “Thermo-economic analysis of steady state waste heat recovery in data centers using absorption refrigeration”. In: *Applied Energy* 139 (2015), pp. 384–397. ISSN: 03062619. DOI: 10.1016/j.apenergy.2014.10.067.

[189] Jie Liu, Michel Garaczko, Sean James, Christian Belady, Lu Jiakang, and Kamin Whitehouse. “The Data Furnace: Heating Up with Cloud Computing”. In: *Proceedings of 3rd USENIX Workshop on Hot Topics in Cloud Computing 2011*. URL: https://www.microsoft.com/en-us/research/wp-content/uploads/2016/02/heating.pdf (visited on Aug. 5, 2020).

[190] Frank Dammel, Johannes Oltmanns, and Peter Stephan. “Nutzung der Abwärme des Hochleistungsrechners am Campus Lichtwiese der TU Darmstadt”. In: *EuroHeat&Power* (2019).

[191] A. H. Beitelmal and D. Fabris. “Servers and data centers energy performance metrics”. In: *Energy and Buildings* 80 (2014), pp. 562–569. ISSN: 03787788. DOI: 10.1016/j.enbuild.2014.04.036.

[192] Babak Lajevardi, Karl Haapala, and Joseph Junker. “An Energy Efficiency Metric for Data Center Assessment”. In: *Proceedings of the 2014 Industrial and Systems Engineering Research Conference*.

[193] Nader Nada and Abusfian Elgelany. “Green Technology, Cloud Computing and Data Centers: the Need for Integrated Energy Efficiency Framework and Effective Metric”. In: *International Journal of Advanced Computer Science and Applications* 5 (2014).

[194] M. K. Patterson, W. Tschudi, O. VanGeet, and D. Azevedo. “Towards the Net-Zero Data Center: Development and Application of an Energy Reuse Metric”. In: *ASHRAE Transactions* (2011).

Appendix

Publications

Peer reviewed journal papers

Johannes Oltmanns, David Sauerwein, Frank Dammel, Peter Stephan and Christoph Kuhn. ”Potential for waste heat utilization of hot-water-cooled data centers: A case study”. In: *Energy Science & Engineering* 8.5 (2020).

Johannes Oltmanns, Martin Freystein, Frank Dammel and Peter Stephan. ”Improving the operation of a district heating and a district cooling network”. In: *Energy Procedia* 149 (2018).

Other publications

Johannes Oltmanns, Frank Dammel, Peter Stephan. ”Decreasing the temperature of an existing district heating network”. *5th Smart Energy Systems and 4DH conference*, Copenhagen, Denmark, September 10-11, 2019.

Frank Dammel, **Johannes Oltmanns**, Peter Stephan. ”Nutzung der Abwärme des Hochleistungsrechners am Campus Lichtwiese der TU Darmstadt”. In: *EuroHeat&Power* (2019).

Johannes Oltmanns, Frank Dammel and Peter Stephan. ”Modeling the heat supply system of TU Darmstadt Campus Lichtwiese”. In: *Proceedings of ECOS 2017 – The 30th International Conference on Efficiency, Cost, Optimization, Simulation and Environmental Impact of Energy Systems*, San Diego, California, USA, July 2-6, 2017.

Student work contributing to this thesis

Franziska Ehmer, ”Entwicklung einer Fernwärme-Betriebsstrategie unter Berücksichtigung der Flexibilitätspotentiale von Gebäuden und Netzen”, *Master Thesis*, TU Darmstadt, 2020.

Niklas Stäter, ”Energieeffizienz für den Campus Lichtwiese an der Schnittstelle zwischen Gebäuden und thermischen Netzen”, *Master Thesis*, TU Darmstadt, 2019.

Johannes Hinrichs, ”Optimierung des Kraftwerksbetriebs am Campus Lichtwiese durch Ausnutzung der Speicherkapazitäten des Fernwärmenetzes”, *Master Thesis*, TU Darmstadt, 2018.

Peter Warsow, ”Entwicklung einer Regelstrategie für den intelligenten Betrieb der Wärme- und Kälteversorgung am Campus Lichtwiese”, *Master Thesis*, TU Darmstadt, 2018.

Thomas Beutner, ”Bewertung einer Absenkung der Temperaturen im Fernwärmenetz am Campus Lichtwiese”, *Master Thesis*, TU Darmstadt, 2017.

Fabian Hofmeister, ”Steuerung eines Fernwärmenetzes unter Ausnutzung von Wärmespeicherung im Netz”, *Master Thesis*, TU Darmstadt, 2017.

Johannes Full, ”Modellierung eines Kältenetzes für den Campus Lichtwiese der TU Darmstadt”, *Master Thesis*, TU Darmstadt, 2017.

Sebastian Zentgraf, ”Steuerung eines Fernwärmenetzes: Lastprognosen und Potential der Wärmespeicherung im Netz”, *Master Thesis*, TU Darmstadt, 2017.

Philipp Heiß, ”Modellierung der Wärmeversorgung der TU Darmstadt mit einem saisonalen Wärmespeicher”, *Master Thesis*, TU Darmstadt, 2016.

Simon Schild von Spannenberg, ”Saisonaler Wärmespeicher auf dem Campus Lichtwiese der TU Darmstadt”, *Bachelor Thesis*, TU Darmstadt, 2016.

Secondary side heat meter calibration certificate

Calibration certificate of the ultrasonic heat meter Dynasonics TFX-5000 used for secondary side heat metering.

Badger Meter

8635 Washington Ave
Racine, WI 53406
262-639-6770 | 800-876-3837
www.badgermeter.com

Calibration Certificate

Customer Information:

Customer Name:	BADGER METER EUROPE GMBH CS
Customer Order #:	614953
Customer PO #:	72595

Lab Information:

Calibration Tech:	HDA
Test Stand #:	7
Calibration Date:	12/19/2019
Cal. Liquid:	Water - Tap
Lab Temperature (°F):	71.23 °F
Lab Rel Humidity (%RH):	12.51 %RH
Pipe Size:	1.88

Unit Under Test (UUT) Information:

Catalog Number:	DR-G-UZ-R-S-AF-WW-C-AK-C-XX-T-P-R-F
Serial Number:	10000654
Meter Rev:	NA
Software Version:	02.01.452
Scale:	0.925
Supply Voltage:	100-240VAC
Re-Calibration Interval:	Annual

Comments:

NA Standard Units

UUT Calibration Results (As Left)

English Units

Master	UUT	
Flow Rate	Flow Rate	Error
GPM	GPM	(% Rate)
15.34	15.30	0.25%
37.49	37.77	-0.74%
74.78	75.49	-0.95%
93.82	94.36	-0.57%
113.60	112.84	0.66%

Metric Units

Master	UUT	
Flow Rate	Flow Rate	Error
LPM	LPM	(% Rate)
58.07	57.93	0.25%
141.89	142.95	-0.74%
283.03	285.72	-0.95%
355.13	357.16	-0.57%
429.96	427.11	0.66%

Status:	PASS
Meter Accuracy (% of Rate):	1% +/- 0.03 ft/s

Certified By:

Master Meter Information:

Test Stand	Pipe	QA #	Model #	Serial #	Uncertainty	Re-Cal Date
7	Stainless 316	TFM-1981	Optiflux 4000	A11P00767	0.25%	03/04/2020

The calibration is performed using standards traceable to the National Institute of Standards and Technology, NIST. The equipment and calibration procedure complies with ISO 9001:2015. All certifications are conducted with tap water at 70° F (21° C) and 1.0 cSt. calibrations for alternate fluids have been mathematically corrected and are not traceable to NIST. This calibration report may not be reproduced, except in full, without the written approval from Badger Meter Inc.

QS 258
Rev. A
'02/15
Page 1/1